TUSCIA UNIVERSITY OF VITERBO
-ITALY-

DEPARTMENT OF TECHNOLOGY, ENGINEERING AND ENVIRONMENT AND FOREST SCIENCES (DAF)

PHD IN SCIENCES AND TECHNOLOGIES FOR THE FOREST AND ENVIRONMENTAL MANAGEMENT- XXII CYCLE

SCIENTIFIC SECTOR- DISCIPLINARY AGR/10
RURAL CONSTRUCTION AND FORESTRY LAND

PhD Thesis

Presented by

Aziz Abouabdillah

HYDROLOGICAL MODELING IN A DATA-POOR MEDITERRANEAN CATCHMENT (MERGUELLIL, TUNISIA). ASSESSING SCENARIOS OF LAND MANAGEMENT AND CLIMATE CHANGE.

Coordinator
Prof. Gianluca Piovesan

Supervisors
Dr. Antonio Lo Porto
Prof. Nicoletta Ripa

2006-2009

This thesis is submitted in fulfillment of the requirements for the Degree of Doctor of Philosophy.

UNIVERSITÀ DEGLI STUDI DELLA TUSCIA
-VITERBO-

DIPARTIMENTO DI TECNOLOGIE, INGENERIA E SCIENZE DELL'AMBIENTE E DELLE FORESTE

CORSO DI DOTTORATO DI RICERCA IN SCIENZE E TECNOLOGIE PER LA GESTIONE FORESTALE ED AMBIENTALE-XXII CICLO

SETTORE SCIENTIFICO-DISCIPLINARE AGR/10
COSTRUZIONE RURALI E TERRITORIO AGROFORESTALE

Tesi di Dottorato di Ricerca

Dottorando

Aziz Abouabdillah

HYDROLOGICAL MODELING IN A DATA-POOR MEDITERRANEAN CATCHMENT (MERGUELLIL, TUNISIA). ASSESSING SCENARIOS OF LAND MANAGEMENT AND CLIMATE CHANGE.

Cordinatore
Prof. Gianluca Piovesan

Tutors
Dr. Antonio Lo Porto
Prof. Nicoletta Ripa

2006-2009

ACKNOWLEDGEMENTS

***I** am greatly indebted to the Water Research Institute (CNR-IRSA) for their financial support through a grant from the European project "Aquastress"*

***I** would like to express my profound gratitude to Dr. Antonio Lo Porto for his invaluable contribution through supervision of this PhD research. He had a Paramount input into this research through his guidance from initial proposition to its completion and brought out the best of me. Thank you.*

***T**here is a person I need to mentioned especially, Dr. Anna Maria De Girolamo, I owe her my sincere gratitude for her kindness, her useful contributions and support at various stages of this work.*

***T**hanks also go to Prof. Nicoletta Ripa for her supervision, help and assistance particularly during my stay in Viterbo.*

***T**o those in the Water Research Institute (IRSA-Bari), I would like to thank with all my heart for making my study so memorable and pleasurable. Thanks also to the Tuscia University of Viterbo (Italy) for the opportunity provided to me to achieve this academic goal.*

***I**'d like to convey my heartfelt thanks to Dr. Jeff Arnold, Dr. Mike white and Professor Raghavan Srinivasan for their efforts and assistance, during my PhD training in the Texas A & M University and the ARS-USDA in Temple.*

***I** wish also to thank Prof. Wesley Wess Wallender for his scientific support, as well as his kind help and assistance during my PhD training in the University of California Davis.*

***I** wish to express my sincere gratitude to the INAT (Institute National Agronomique de Tunis), and in particular to Prof. Lili Zohra Chaabana and Mr. Aymen Lazrek for their significance help and data providing; the IRD (Institut de Recherche et de Development) in particular Dr. Christian Leduc as well as to all other data providers not explicitly mentioned above.*

***I** would like to express my most sincere gratitude to Prof. Ahmen Bamouh and Prof, Benasser Alaoui from my home Institute (IAV-Hassan II) for their significant help and encouragement.*

***T**hanks also to the examiners who provided valuable feedback, Prof. Roberto Mercurio, Prof. Enrico Marchi, and Prof. Carmelo Riccardo Fichera.*

***I** would also like to express my sincere thanks to the numerous colleagues who have supported me along the way.*

DEDICATION

This thesis is dedicated to

***M**y Father who has raised me to be the person I am today. You have been with me every step of the way, through good times and bad. Thank you for all the unconditional love, guidance, and support that you have always given me, and helping me to succeed. Thank you for everything. I love you.*

***M**y mother, who has been a source of inspiration to me throughout my life. Thanks for your support encouragement, and constant love that have sustained me throughout my life. I love you.*

***M**y sister Chadia, for her never ending moral support and prayers. Thanks for your love and encouragement, I give my deepest expression of love and appreciation for the encouragement to you and your husband Si'Mohammed.*

***M**y brother Moulay Ahmed, thanks for your advices and support. I m very proud of your success. I wish to express my sincere gratitude to you and your wife Zineb.*

***M**y sister Siham, who proffered me unconditional love and support. Thanks to be my friend and my confidant, you have been a great source of inspiration and motivation throughout the years. Thanks Sima.*

***M**y lovely nephews Ali, Omar, Mehdi and Ghali. The happiness of the family. Thanks for giving me your love and support, and most importantly were often the source of much loved distraction.*

***T**he Memory of my dear grandmother who passed away during the first months of this thesis. May God bless you Oumi.*

***O**ns, for always being here for me. Thank you for your continual love, support, and patience. I could not have made it through without you by my side.*

***L**oving thanks to my childhood friends Charif, Hatim, Younes, Noureddine and Mehdi who knowingly and unknowingly- led me to an understanding of some of the more subtle challenges to our ability to thrive important roles.*

***M**y friends, Yassine, Soufinae, Otman, Meryem,Houda,Taha, Mounia, Hamid, Hind, Youssef, Radhouan, Nadia, Farachichou, Moez, Khaoula. They played such important roles along the journey, as we mutually engaged in making sense of the various challenges we faced and in providing encouragement to each other at those times when it seemed impossible to continue. Thanks for always being there for me.*

***M**y most sincere appreciation goes to all my friends, at IRSA, without whom these three years would have been insufferable. I especially want to show my gratitude to Rita, Manola, Ramona, Gerardina, Daria, Delia, Valeria, Emanuele, Giuseppe, Domenico, Lorenzo, Carlo, Angelo and Vito. You have all made it a memorable time of my life.*

Yours sincerely

Aziz

ABSTRACT

Title: Hydrological modeling in a data-poor Mediterranean catchment (Merguellil, Tunisia).
Assessing scenarios of land management and climate change.

In the Mediterranean regions, hydrologic processes are quite specific due to the temporal variability of precipitation characterized by a succession of drought and flash-flood periods. These processes may also have changed due to a range of human activities such as land use changes, dams building, soil and water conservations works. The Merguellil catchment (Central Tunisia) is a typical Mediterranean semi-arid basin which suffers regular water shortage aggravated by current drought. It extends on an area of about 1200 km² upstream of the El Houareb dam which presents its outlet. This semi-arid zone is exposed to a high variability of rainfall in time and space. Annual means vary between 300 mm in the plain and 500 mm in the highest parts. During the recent decades the continuous construction of small and large dams and Soil and Water Conservation Works (SWCW) (ie. Counter ridges) has taken place within the watershed. These practices, that currently cover nearly ¼ of the basin surface, are classified in two categories: the practices on basin slopes constituted essentially by contour ridges (200 Km²) and the practices on the hydrographical network by implantation of small hilly dams draining about 170 Km. These water harvesting systems may intercept runoff at the upstream part of the catchment, thus depriving potential downstream users of their share of the resources. However, little is known about the effect of these water harvesting systems on the water balance components of arid watersheds.

In such a vulnerable situation of water resources availability, it can be expected that the impact of climate change will further worsen the situation.

The work presented here attempts to simulate the actual water and nutrient balance using the integrated hydrological model "Soil and Water Assessment Tool" (SWAT 2005). The simulation results revealed that evapotranspiration is the major component of the hydrological balance. Hydrological Calibration (1992-1994) and validation (1998) have been carried out referring to daily flow data at the Hafouz and Skhira flow-gauges. The model performance was satisfactory and the Nash-Sutcliffe Efficiency coefficient ranges from 0.6 to 0.7.

The model was rather successful in reproducing water flow. However the low sampling frequency and the lack of detailed water quality measurement data did not allow an in-depth

evaluation of the SWAT performance in predicting nutrient and sediment. Some scenarios were further generated. The first one regards the removal of contour ridges to assess their impact to water and sediment load. The results show that the contour ridges contribute to the retention of high quantity of sediment. These regulations reduce the surface runoff by 32 %. Planting the olive trees between contours could improve its yield. The second scenario consists in the reduction of the applied fertilizers. By reducing 20% in the applied fertilizers no change was detected in the olive yield, while a small change was noted for durum wheat yield's (-2%). Whereas a net decrease in nutrient load was observed at the outlet. This reduction ranges, from 3 to 10% for nitrates, from 2.5 to 8% for total nitrogen and from 13 to 16.5 % for total phosphorus.

Finally, the SWAT model was used to study the impact of future climate on water resources of this Mediterranean catchment. Future climate scenarios for periods of 2010-2039 and 2070-2099 were generated from the Canadian Global Coupled model (CGCM 3.1) for scenarios A1B, B1, and A2. These CGCMs data were then statistically downscaled to generate future possible local meteorological data of precipitation and temperature in the study area. SWAT model was run first under current climate (1986-2005) and then for the future climate period to analyze the potential impact of climate change on flow, evapotranspiration, and soil moisture across this catchment. Finally, Richter et al.'s Indicators of Hydrologic Alteration (IHA) were used to analyze the flow regime alterations under changing climate. The main results indicate that this catchment would suffer a combination of increased temperature and reduced rainfall that will reduce water resources in this area. Consequently, summer droughts would be intensified. Different spatial responses to climate change were observed in the catchment for near future simulations. Higher altitude regions would experience an increase of the total water yield, while a reduction is foreseen for lower parts. For far future, a noticeable decrease would affect water resources in all part of the catchment.

RIASSUNTO

Titolo: Applicazione di un modello idrologico ad un bacino Mediterraneo (Merguellil, Tunisia) in condizione di scarsezza di dati. Valutazione degli scenari connessi all'uso del suolo e ai cambiamenti climatici.

Nelle regioni del Mediterraneo, i processi idrologici sono caratterizzati dalla variabilità temporale delle precipitazioni che si manifesta attraverso la successione di periodi di siccità e allagamenti.

L'alterazione dei processi idrologici nell'area del Mediterraneo è attribuibile, oltre che alle alterazioni climatiche globali, anche alla pressione antropica sul territorio attraverso la modificazione dell'uso del suolo, la costruzione di sbarramenti fluviali e le opere di protezione idraulica e del suolo.

Il bacino idrografico di Merguellil (nella Tunisia centrale) è un tipico bacino semi arido del Mediterraneo caratterizzato da un deficit idrico aggravato dagli attuali eventi siccitosi. L'area è contraddistinta da un'elevata variabilità delle precipitazioni nello spazio e nel tempo. In particolare, la media annuale di precipitazione varia tra 300 mm nelle aree di pianura e 500 mm in quelle più alte. Nel corso degli ultimi decenni il bacino è stato interessato dalla costruzione di dighe e le opere di protezione idraulica e del suolo. Queste pratiche, che attualmente ricoprono il 25% della superficie del bacino, si distinguono in due categorie di interventi: quelle che interessano i versanti del bacino, essenzialmente fossi di guardia e terrazzamenti (200 km^2), e quelle che insistono sul reticolo idrografico attraverso la costruzione di sbarramenti (170 km). Questi sistemi di raccolta dell'acqua intercettano il ruscellamento superficiale della parte più elevata del bacino, privando la parte bassa di una cospicua aliquota d'acqua. Tuttavia, l'effetto di questi interventi di sistemazione idraulica sulle componenti del bilancio idrico dei bacino aridi è poco conosciuto.

In tale situazione di vulnerabilità delle risorse idriche, ci si attende che l'impatto dei cambiamenti climatici peggiori la situazione. Il presente lavoro ha lo scopo di modellare le risorse idriche attuali e il bilancio dei nutrienti nel bacino di Merguellil utilizzando il modello idrologico integrato "*Soil and Water Assessment Tool*" (SWAT, 2005). I risultati delle simulazioni rivelano che l'evapotraspirazione è la principale componente del bilancio idrologico.

La calibrazione idrologica (1992-1994) e la validazione (1998) è stata condotta riferendosi ai dati giornalieri di portata delle stazioni idrolometriche di Hafouz e Skhira.

La performance del modello è stata soddisfacente ottenendo un coefficiente di efficienza di Nash-Sutcliffe che varia tra 0.6 e 0.7. Il modello ha riprodotto correttamente le portate. Tuttavia la bassa frequenza di campionamento e la carenza di misure dettagliate di qualità dell'acqua non hanno permesso di valutare approfonditamente le performance di SWAT nel simulare il carico di nutrienti e sedimenti.

Sono stati generati alcuni scenari. Il primo scenario riguarda la rimozione dei fossi di guardi per valutare il loro impatto sul carico idraulico e dei sedimenti. Queste regolazioni riducono il ruscellamento superficiale del 32%. La piantumazione di alberi di ulivo tra i fossi di guardia potrebbe migliorare la resa.. Il secondo scenario consiste nella riduzione dei fertilizzanti utilizzati. Attraverso la riduzione del 20% del quantitativo dei fertilizzanti nessun cambiamento della resa degli ulivi è stato osservato, mentre un ridotto cambiamento è stato osservato nella resa del grano duro (-2%). Invece una netta diminuzione nel carico di nutrienti è stata osservata all'uscita. Questa riduzione varia dal 3% al 10% per i nitrati, dal 2.5% all'8% per l'azoto e dal 13% al 16.5% per il fosforo totale.

Infine, il modello SWAT è stato utilizzato per lo studio di impatto del clima futuro sulle risorse idriche del bacino idrografico. Gli scenari climatici futuri per il periodo 2010-2039 e 2070-2099 sono stati generati dal modello accoppiato globale canadese CGCM 3.1 per gli scenari di emissione A1B, B1, e A2. I dati del modello climatico CGCM sono stati sottoposti ad una procedura di *downscaling* statistico per generare scenari locali di precipitazione e temperatura dell'area di studio. Il modello SWAT è stato fatto girare prima in condizioni climatiche attuali (1986-2005) e poi in condizioni di cambiamento climatico futuro per analizzare l'impatto potenziale dei cambiamenti climatici sulla portata, evapotraspirazione ed umidità del suolo del bacino in esame. Infine, per analizzare le alterazioni del regime di portata sono stati utilizzati gli indicatori dell'alterazione idrologica (*Indicators of Hydrologic Alteration –IHA*) di Richter *et al*.

I risultati principali indicano che nel bacino studiato, l'azione combinata dell' incremento di temperatura e riduzione della precipitazione, porterà alla riduzione delle risorse idriche. Gli effetti del cambiamento climatico sulle risorse idriche del bacino non sono univoci per tutta l'area, ma si differenziano in base alle caratteristiche topologiche del territorio. Le regioni ad alte altitudine subiscono un incremento del tasso totale d’acqua, mentre per le parti basse si prospetta una riduzione. Per l’ultimo trentennio del secolo, invece una pesante diminuzione delle risorse idriche influenzerà tutte le parti del bacino.

RESUMÉ

Titre: Modélisation hydrologique au niveau d'un bassin versant Méditerranéen (Merguellil, Tunisie) pauvre en données. Evaluation des scenarios de gestion des terres et du changement climatique

Dans les régions méditerranéennes les processus hydrologiques sont assez particuliers à cause de la variabilité temporaire des précipitations qui sont caractérisées par une succession de périodes sèches et humides. Ces processus sont aussi susceptibles à des changements de type anthropique à l'exemple du changement de l'occupation du sol, de la construction des barrages et des travaux de conservation des eaux et des sols. Le bassin versant de Merguellil (Tunisie centrale) est un bassin Méditerranéen, semi-aride qui souffre fréquemment de la rareté de la ressource eau aggravé par les sécheresses actuelles. Au niveau du barrage El Houareb, il draine une aire de 1200 km^2. Comme tous les milieux méditerranéens et semi-arides, le bassin de Merguellil est caractérisé par une très forte variabilité spatiale et temporelle des précipitations. Les moyennes annuelles varient entre 300 mm sur les plaines et 500 mm sur sa partie amont relativement montagneuse. Au cours des dernières décennies, le bassin du Merguellil a été l'objet de nombreux aménagements hydro-agricoles tel que la construction des petits et grands barrages collinaires, et les travaux de conservation des eaux et des sols (CES) (ex. Banquettes). Ces aménagements, qui s'étendent actuellement sur ¼ de la surface du bassin, peuvent être classifiés en deux catégories. La première concerne les aménagements des versants par la construction des banquettes. Ces derniers couvrent une surface de 200 Km^2. La deuxième consiste à la construction des petits barrages collinaires sur le réseau hydrographique. La surface drainée par ces derniers est estimée à 170 Km^2. Ces aménagements qui interceptent le ruissellement à l'amont du bassin, privent par conséquent les usagers à l'aval de partager la ressource en eau. Par ailleurs, l'impact de ces systèmes de collecte d'eau sur les composantes du bilan hydrologique dans les bassins versant arides est encore peu étudié. D'autre part, dans ce cadre où les ressources en eau sont très vulnérables, il a été prédit que les changements climatiques vont aggraver de plus la situation. Le travail présenté ici tend à simuler le bilan hydrique et des nutriments en utilisant un model hydrologique intégré "Soil and Water Assessment Tool" (SWAT 2005). Les résultats de simulation montrent que l'evapotranspiration est une composante majeure du bilan hydrologique. La calibration (1992-1994) et la validation (1998) du modèle

sont effectuées en utilisant les séries journalières de débit au niveau des stations hydrométriques de Hafouz et Skhira. La performance du modèle est satisfaisante et le coefficient d'efficience de Nash- Sutcliffe varie entre 0.6 et 0.7. Le modèle était assez réussi dans la simulation de l'écoulement. Par contre, la faible fréquence échantillonnage et le manque de mesures détaillées de qualité de l'eau n'a pas permis une évaluation plus profonde de la performance du modèle SWAT dans la simulation des nutriments et des sédiments. Quelques scénarios d'aménagement ont été aussi générés. Le premier concerne l'enlèvement des banquettes pour évaluer leur impact sur les écoulements et les sédiments arrivants à l'exutoire. Les résultats montrent que les banquettes contribuent à la rétention d'une grande quantité de sédiment et à la réduction du ruissèlement de 32%. Par ailleurs la plantation des oliviers dans l'espace entre-banquettes pourrait augmenter le rendement. Le deuxième scénario consiste en la réduction des fertilisants de 20%. Le résultat de ce scénario montre qu'il n'y a pas eu de changement dans le rendement de l'olive alors qu'une faible diminution (-2%) a été notée dans le rendement du blé dur. L'impact le plus net de la réduction des fertilisants consiste dans la diminution de la concentration des nutriments à l'exutoire. Cette diminution varie entre 3 et 10% pour les nitrates, entre 2.5 et 8% pour le nitrogène total et entre 13 et 16.5% pour le phosphore total.

Finalement, le modèle SWAT a été utilisé pour étudier l'impact du changement climatique sur les ressources en eau au niveau de ce bassin Méditerranéen. Les futures scénarios climatiques pour la période 2010-2039 et 2070-2099 ont été générés à partir du model '*Canadian Global Coupled model (CGCM 3.1)*' pour les scénarios A1B, B1, and A2.

Ces dernières données dérivées à partir des CGCM ont subis par la suite une réduction statistique d'échelle en utilisant la technique de 'statistical downscalling' pour prédire à la fin les variables météorologiques de température et de précipitation à l'échelle locale de la zone d'étude. Pour analyser les éventuels impacts du changement climatique sur l'écoulement, l'évapotranspiration et l'humidité du sol, le modèle SWAT a été appliqué en deux temps : le premier considérant le climat actuel (1986-2005) et le second considérant le futur climat. Finalement, les indicateurs d'altération hydrologique de Richter et al. (IHA) ont été calculé pour les deux périodes (actuelle et future) pour évaluer l'altération du régime hydrologique causé par le changement climatique. Il a été noté que dans le futur le bassin sera sujet d'une augmentation de température et diminution de précipitation qui vont réduire les ressources en eaux. Par conséquent les sécheresses estivales seront intensifiées. D'autre part une nette différence spatiale a été observée quand à l'impact du changement climatique sur le bassin versant et ce pour le proche future. En effet durant cette période les régions à haute altitude pourraient subir une augmentation des ressources en eau alors qu'au contraire une diminution a été prédite au niveau de plaines. Pour le loin future, une nette diminution des ressources en eau affecterait toutes les régions du bassin versant.

TABLE OF CONTENTS

LIST OF FIGURES

LIST OF TABLES

LIST OF PHOTOS

LIST OF APPENDICES

ABBREVIATIONS AND ACRONYMS

AI	Aridity Index
AIM	Mediterranean Isoclimatic Area
ARS	Agricultural Research Service
EEA	European Environment Agency
BD	Bulk Density
BF	Baseflow Index,
CES	Conservation Des Eaux Et Du Sol.
CGCM	Generation Of The Canadian Global Coupled Model
CO2	Carbon Dioxide
DCV	Daily Variation Coefficient
DEM	Digital Elevation Model
DGF	Direction Générale Des Forêts
DGRE	Direction Générale Des Ressources En Eaux
ET	Evapotranspiration
GIS	Geographic Information System
GLUE	Generalised Likelihood Uncertainty Estimation
GTZ	Technische Zusammenarbeit Gmbh
HEC1	Hydrologic Engineering Center
HOF	Hortonian Overland Flow
HU	Heat Unit
HRUS	Hydrologic Response Units
IHA	Indicators Of Hydrologic Alteration
IPCC	Intergovernmental Panel On Climate Change
NERC	Natural Environment Research Council
PPM.	Parts Per Million
PRMS	Precipitation-Runoff Modeling System
R-B	Index Richards-Baker Flashiness Index
R-R	Rainfall Runoff
RSA	Regional Sensitivity Analysis
SCS	Soil Conservation Service
SOF	Saturated Overland Flow
SWAT	Soil And Water Assessment Tool
UK	United Kingdom
USA	United State Of America
USDA	United States Department Of Agriculture
USEPA	United State Environmental Protection Agency
USGS	United States Geological Survey
WMO	World Meteorological Organization
WSCW	Water And Soil Conservation Works
LAI	Leaf Area Index
PHU	Plant Heat Units
PET	Potential EvapoTranspiration
MUSLE	Modified Universal Soil Loss Equation
ESRI	Environmental Systems Research Institute

RUE	Radiation-Use Efficiency
SCS-CN	Soil Conservation Service-Curve Number
IGNF	Institut Géographique National Français
IRD	Institut De Recherche Pour Le Développement
TP	Total Porosity
FC	Field Capacity
WP	Wilting Point
AWC	Available Water Capacity
INM	Natural Resource Conservation Service
NRCS	Institut National De Météorologie
UTM	Universal Transverse Mercator
MARS	Monitoring Of Agriculture With Remote Sensing,
AVFA	Agence De Vulgarisation Et Formation Agricole
NSE	Nash-Sutcliffe Model Efficiency
R^2	Coefficient Of Determination
FAO	Food And Agriculture Organization
NWP	Numerical Weather Prediction
LM	Linear Model
NLM	Non Linear Models
AET	Actual Evapotranspiration

LIST OF SYMBOLS

%	Percentage
mm/day	Millimeter per day
°C	Degree Celsius
Mkm^2	Million square kilometer
m	Meter
°N	North
Mm	Millimeter
°E	East
m^3/cm yr	Cubic meter per centimeter per year
bm^3	Billion cubic meter
Mm^3	Million cubic meter
g/l	Gramm per liter
ΔS	Changes in storage
Q	Streamflow
km^2	Square kilometer
km	Kilometer
m^3/s	Cubic meter per second
mm	Millimeter
$<$	Less than
$>$	Greater than
mm m^{-1}	Millimeter per meter
M^3	Cubic meter
mm/year	Millimeter per year
Tmax	Maximum daily temperature
Tmin	Minimum daily temperature
Δbio	Potential increase in total plant biomass on a given day
kg/ha	Kilogram per hectare
MJ/m^2	Mega joule per meter square
MJ	Mega joule
Hphosyn	Intercepted photosynthetically active radiation
mm/ha	Millimeter per hectare
P	Precipitation
T	Temperature
Sr	Solar radiation
Ws	Wind speed
T/day	Tons per day
kg/day	Kilogram per day
Mg/l	Milligram per liter
NO3	Nitrate
NH4	Ammonium
MNP	Mineral phosphorus
TWY	Total water yield

AQR	Aquifer recharge
GWQ	Groundwater flow
RES	Reservoir
PCP	Precipitation
SON	September October November
DJF	December January February
MAM	March April may
JJA	June July august

.

CHAPTER 1. INTRODUCTION

1.1 PROBLEM STATEMENT

There is a growing consensus in Earth systems sciences that global temperatures are increasing and will continue to increase during the next century, leading to changes in global climate patterns (IPCC, 2002). Different regions of the globe are expected to respond differently to global warming; the Mediterranean region has been identified as one of the Earth's primary 'hot-spot' for climate change, due to the magnitude of expected changes to temperature and rainfall patterns (Giorgi, 2006).

Surprisingly, the issue of climatic change in the Mediterranean region has rather sparsely been addressed in studies performed more than 5–10 years ago. The region has recently received increasing scientific interest. In fact, the Mediterranean has some particular characteristics that demand to put it high on the research agenda. There is a high confidence that many semi-arid and arid areas (e.g., the Mediterranean Basin, western USA, southern Africa and northeastern Brazil) are particularly exposed to the impacts of climate due to climate change (IPCC, 2007). These changes in the climate regime can influence natural processes of a watershed ecosystem (Band et al. 1996; IPCC, 2001; Stone et al. 2001) and have long-term implications on economic and ecological processes (USEPA, 2004).

In the Mediterranean climatic zone, also labeled as semi-arid or sub-humid (Piñol et al., 1991), hydrological processes are largely variable both in time and space due to the high variability of rainfall regime, in addition to the influence of topography and the spatial distribution of geology, soil and land-use (Kosmas et al., 1997; Pilgrim et al., 1988; Thornes et al., 1996). The arid and semi-arid regions of the world are experiencing the most intense water scarcity. In North Africa water scarcity is intensified with populations grow and economies develop. Like the most countries in this region, Tunisia exemplifies the general water scarcity problem.

Water management is the most critical issue in dry areas as it impacts the livelihood of people and the productivity of the land and the society in general. For thousands of years, inhabitants of the dry areas have constructed water-harvesting systems that helped them to cope with water scarcity (El Amami, 1984; Boers, 1994; Oweis et al., 2004). These systems were built to capture surface runoff from sparsely covered, rocky mountain slopes or to divert occasional wadi flow to fields for crop production. Despite the long and successful history of these systems, little is known about their effect on the hydrological processes in these dry areas.

The Tunisian government has put considerable efforts into Water and Soil Conservation Works (WSCW) through physical, institutional, and legislative measures for the past three decades. The Ministry of Agriculture enacted a national strategy for soil and water conservation for the decade 1991–2000, based on managing slope stability, gradients and shapes, and transferring surface water for agricultural development. A program was then initiated to construct 1000 hill dams, 4000 structures for flood control and groundwater recharge, to protect 600000 hectares by implementing conservation measures. The implementation of these actions was coupled with regional planning covering a number of governorates.

Generally, Water and Soil Conservation Works (WSCW) are built in uplands to face erosion and water scarcity problems. They consist of hill slope works reducing surface runoff and increasing local infiltration, and of small dams collecting headwater flow and providing supplemental water for irrigation. With the fast growth of WSCW-equipped areas, it becomes necessary to investigate hydrological impacts and manage resources at larger scales, especially where conflicts between upstream and downstream water users increase. In fact, water harvesting systems may intercept runoff at the upstream part of the catchment, thus depriving potential downstream users of their share of the resources (Oweis et al., 1999). An example is the wadi bed system in the Matruh area in northwest Egypt, where the introduction of water harvesting techniques negatively affected water users downstream of the system (Moustafa, 1994). Nasri (2007) demonstrates that a cascade of bench terraces built on a 14.48 ha hill slope do significantly reduce sediment transport on the Ousseltia region of central Tunisia. Nasri et al. (2006) studied the hydrological impact of contour ridges in an 18.1 km^2 catchment and on 0.11km^2 hill slopes respectively. In both cases, introduction of contour ridges resulted in a runoff decrease varying between 50% and 90% for rainfall below 60-70 mm/day.

Studies on impacts of WSCW are extremely rare in large catchments as heterogeneity and data scarcity increase with catchment size. Despite the critical importance of water in arid and semi-arid areas, hydrological data have historically been severely limited. It has been widely stated that the major limitation of the development of arid-zone hydrology is the lack of high quality observations (McMahon, 1979; Nemec and Rodier, 1979; Pilgrim et al., 1988). Many reasons are behind this data limitation. Populations are usually sparse and economic resources limited; in addition, the climate is harsh and hydrological events infrequent, but damaging (Wheater et al., 2007).

Since limited hydrological information is available in semi arid watersheds, adequate hydrological assessment tools should be flexible to deal with poor quantity and quality input data (Lange and Singh, 2003). One approach to assisting sustainable water resource development and management within river basins is the use of mathematical modeling of watershed hydrology (Singh and Woolhiser 2002). Numerical models of groundwater and surface water resources systems have been used to simulate the behavior of catchment systems since the 1960s (Zoppou, 2001). However, increasing computer speed and the development of new mathematical representations of physical processes has allowed the science of computer simulation to pass from being of academic interest only to a practical engineering procedure (Viessman & Lewis, 2003). The use of hydrological modeling tools to address a wide spectrum of environmental and water resources problems is now commonplace.

1.2 PROJECT HOLDER

This research work is part of a European project “Aquastress project” (6th EU framework program) about Mitigation of Water Stress through new Approaches to Integrating Management, Technical, Economic and Institutional Instruments.

The overall goal of this project is to improve the availability of high quality water at catchment scale by assessing different schemes of land use pattern and management. The task has the objective to define a modeling framework to assess sustainability of land uses in water limited environments and to allow the selection of a list of suitable Best Management Practices (both based on non-structural/management and structural approach) that allow that water quality goals discussed and decided with stakeholders are met.

1.3 RESEARCH OBJECTIVES

In this thesis, a study on the Merguellil catchment, a Mediterranean semi-arid area with a limited data set in central Tunisia, is presented. Soil and Water Assessment Tool (SWAT) model was used to simulate the water balance and nutrient balance and to assess the impact of land use and land cover activities on the hydrology. Some scenarios were further generated. The first one regards the removal of contour ridges to assess their impact to water and sediment load and crop yield. The second scenario consists in the reduction of the applied fertilizers in order to increase the availability of a god quality of the water in the downstream area.

In such a vulnerable situation of water resources availability, it can be expected that the impact of climate change will further worsen the situation.

In this study we report therefore on the result of investigating the impact of climate change on water resources in the Merguellil catchment (central Tunisia) for the near (2010-2049) and far (2050-2099) future. We used the Soil and Water Assessment Tool Model (SWAT 2005) to study the effect of climate change at subbasin level. We used the output of the third Generation of the Canadian Global Coupled Model (CGCM 3.1) version T63. We specifically looked at the changes in various components of the water balance including precipitation, evapotranspiration, total water yield, soil moisture and river discharge. In addition the impact of climate change on olive and wheat yield was also investigated. Finally, we analyze the flow regime alterations under changing climate using the Richter et al.'s (1996) Indicators of Hydrologic Alteration (IHA).

1.4 SCHEMATIC PRESENTATION OF THE THESIS

This work is presented in five chapters. In the first one, after a brief introduction of the problem statement, the research objectives were presented. In the second one, the literature review presents the Mediterranean climate, Problems of water resources in this region with special focus on Tunisia. In addition, Water balance Components are explained as well as the hydrologic modeling approaches. Another part points out the problem of data scarcity in semi-arid areas. Finally, the last part of this chapter highlights the impact of climate change on Mediterranean water resources.

In the Third chapter, the study area was presented, as well as the available data base such as the DEM, soils, land uses, climatic characteristics, and Water and Soil Conservation Works (WSCW). In addition, we carried out a study on the temporal and spatial repartition of precipitation in the catchment. We report also some results about the hydrologic regime in the study area. In a second part, we describe the SWAT model and the required input data indicating the different equations used and the different procedure of the simulation. Another part is devoted to the preparation and the adjustment of the input data and how we model the different WSCW presented in the catchment. In the last part of this chapter, we describe the different steps of the SWAT model setup.

A Summary of the results obtained from the SWAT model simulation is the subject of chapter 4. These results include the sensitivity analysis conducted, the calibration and validation of the model comparing the measured and simulated flow in different flow gauges. Afterward, the water balance in the Merguellil catchment is presented as well as the nutrient quality simulation. The evaluation of sediment and nutrient was also outlined. Finally the impact of soils and land use on hydrologic and nutrient balances are highlighted in the end of this chapter.

In the firths and last chapter, we try to take into account all the stresses (climatic and anthropogenic) that the Merguellil catchment is facing. In view of this, some scenarios were generated. First one consists on in the removal of contour ridges from the upstream area the in order to assess the impact of these regulation on the on the hydrological regime, sediment retention and crop yield. Second one consists on the reduction of the applied fertilizers in order to improve water quality.

In the Last part of this study, we report on the result of the investigation of the impact of climate change on water resource of the Merguellil catchment. We used the output of the third Generation of the Canadian Global Coupled Model (CGCM 3.1) version T63.

In addition the impact of climate change on olive and wheat yield was also investigated. Finally, we analyze the flow regime alterations under changing climate using the Richter et al.'s (1996) Indicators of Hydrologic Alteration (IHA).

The application of the SWAT model for the Merguellil catchment confirms that SWAT is a useful tool that can already be used to make preliminary assessment of the water and land management of the basin.

CHAPTER 2. LITERATURE REVIEW

2.1 MEDITERRANEAN CONTEXT

The Mediterranean basin is a transition area covering the Mediterranean Sea as such and land encompassing it, limited by deserts to the south and temperate areas to the north (Figure 2.1). The Mediterranean type of climate spread not only on the Mediterranean basin but cover also areas in South Africa, Chile, Mexico, USA, and South Australia. The connotation of ‘‘Mediterranean climate’’ is included in the qualitative classification of the different types of climate on Earth (e.g. Köppen, 1936) and it has been used to define the climate of other (generally smaller) regions besides that of the Mediterranean basin itself. It includes a range from arid, through semi-arid to sub-humid conditions. According to the Köppen scheme (Figure 2.2) most areas of the Mediterranean fit into the dry or warm, temperate climate zones. However, it has been demonstrated that the boundaries produced by the Köppen scheme are highly sensitive to the data set used to define it. Emberger proposed simple boundaries to the climate region using an index calculated by dividing the summer rainfall in mm by the average maximum temperature of the warmest month in degrees Celsius. A value of five delimited the Mediterranean climate zone, with seven being the boundary of the sub-Mediterranean zone. Although this scheme works well for the northern part of the basin, it is completely inappropriate for the south, delimiting the limits of the Mediterranean zone in the middle of the Sahara. Daget (1980) defined a compromise based on the ratio of warm-season to cold-season precipitation and the summer concentration of temperatures. The ‘Mediterranean Isoclimatic Area’ (AIM in French) is thus defined, providing better fit to the region as a whole, including the semi-arid zones of North Africa. However, although this is probably the best definition of the Mediterranean climate, there is still a feeling that it is derived empirically, rather than being based on any good a priori reasons. A typical’ Mediterranean vegetation is often used as a definition of the Mediterranean region. The olive is very commonly used as an indicator species, but, its distribution is also very strongly controlled by human activity in the past and present. Other authors have chosen to use country boundaries or other political or administrative boundaries. Such a definition is also somewhat artificial. If the smallest administrative level is chosen, large areas of the hinterland that are vital to Mediterranean socioeconomic systems are cut off. These levels also differ from country to country. If the country level is chosen, then clearly some areas are included that clearly do not share Mediterranean characteristics of any sort – northern France and the south of Libya and Egypt being the clearest examples here. The administrative units also differ vastly according to the country chosen (reflecting in part the different population densities and their spatial distributions).

In summary, none of these simple definitions of the region are really satisfactory. All include important elements and exclude others. None so far has included Portugal, for example, despite the fact that it shares a number of common traits with the rest of Iberia and the region. The Mediterranean has been a cross-roads, both physically and socially. It has marked a place where plate boundaries have met, air masses mixed, plants combined from different regions and evolved into endemic species, and people have developed new ways of life and spread them to Europe and beyond. Subsequently, the interactions with the wider world have had significant impacts on the peoples and environments of the region. As noted above, it is partly because of this rich and varied heritage that the Mediterranean is an interesting and useful environment to study.

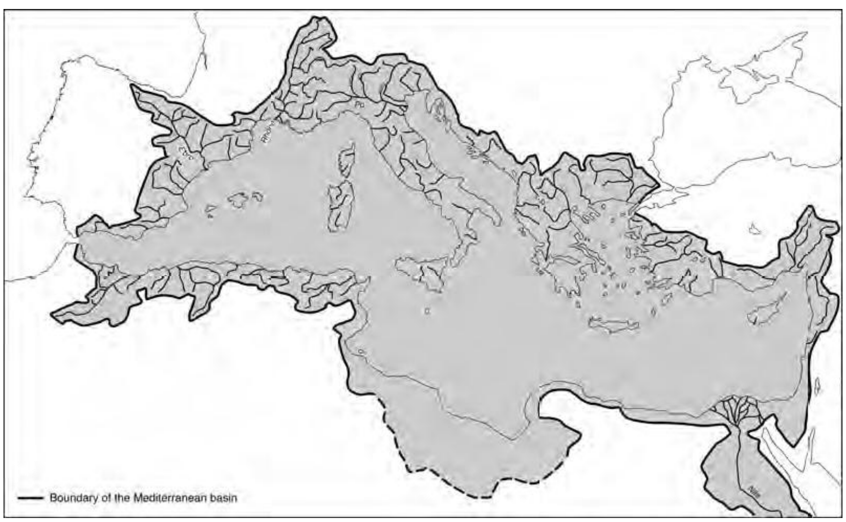

Figure 2.1 The catchment of the Mediterranean Basin (Source: Reproduced in Grenon and Batisse (1989)).

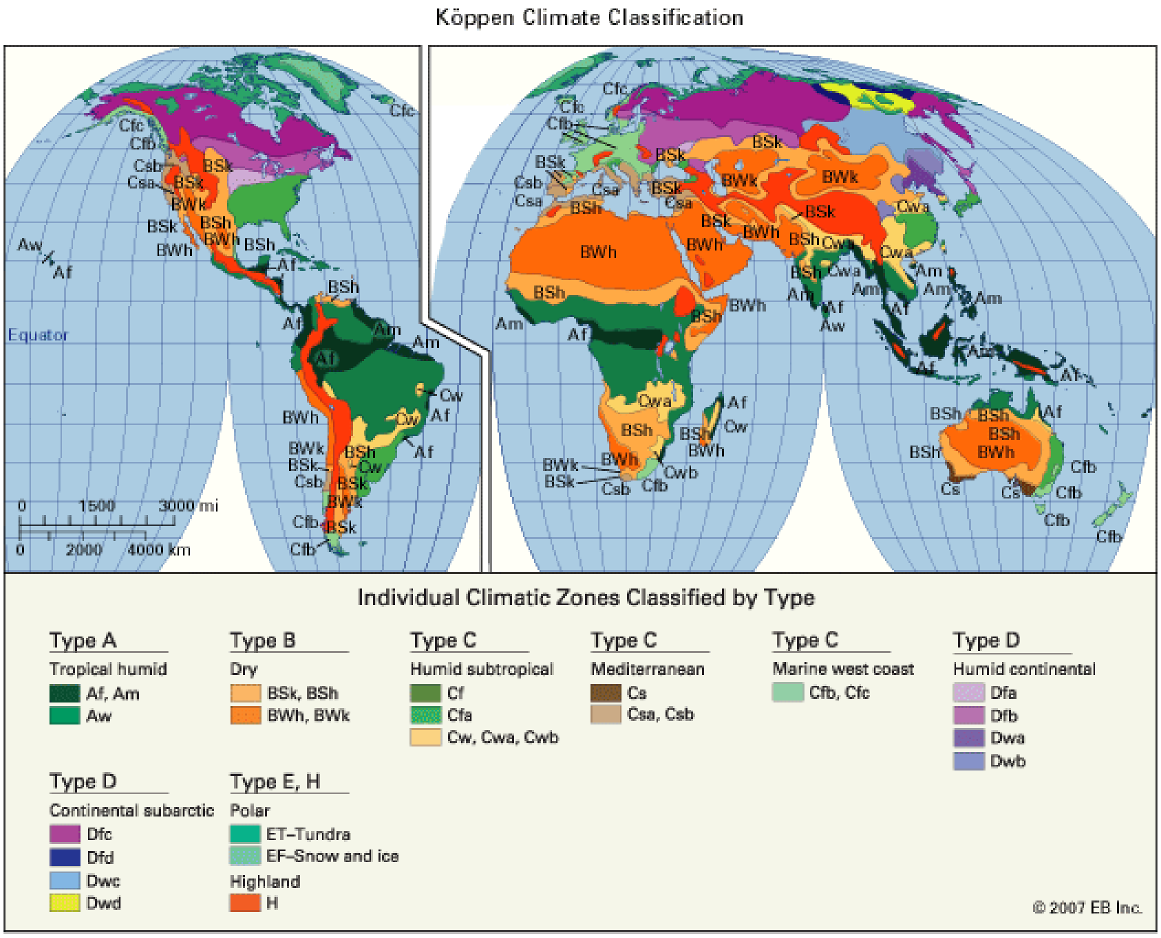

Figure 2.2 Köppen climate classification

The Mediterranean type of climate is characterized by contrasting variations in temperature and precipitation between winter and summer, and prone to extremes. Winters are cool and relatively wet. While summers are warm and dry with a strong soil water deficit. The average temperature of the hottest month can be >22 °C. In the Mediterranean region the strong difference between the wet winters and the dry summers is caused by the seasonal alternation of the dominance of cyclonic storms in winter and subtropical high pressure cells over the adjacent ocean in summer with subsiding maritime tropical air causing dry conditions in summer. The Mediterranean climate in most regions is confined to narrow coastal belts. Only in the European/African/Near East area, because of the Mediterranean Sea, it covers about 10 Mkm^2 reaching from Portugal to south of the Caspian Sea with a core area that stretches over 46 degrees longitude and covers about 6 Mkm^2. Of this area $2.496 * 10^6$ km^2 belong to the Mediterranean Sea surface. If the

Black and Marmara Seas are counted as well, the sea surface covers 3.1 *10^6 km^2. The general temperature and precipitation distribution in the European/African Mediterranean basin is presented in Table 2.1.

Table 2.1 Mean surface air temperature and precipitation regime of the Mediterranean basin according to the European Climate Support Network (1995). Reference period 1960-1990

Quantity	Season	European lowlands	European highlands	North African coastal zone	Sea
	winter	7.5 ± 2.5	2.5 ± 2.5	12.5±2.5	15 ±5
Temperature	spring	12.5 ±2.5	7.5 ± 2.5	17.5 ±5	15 ±5
(°C)	summer	22.5 ± 2.5	15 ±5	32.5 ± 10	22.5 ± 5
	autumn	17.5 ±2.5	10 ±5	20 ±5	20 ±5
	winter	1-3	3-10	0.25 - 2	2 - 10
Precipitation	spring	1 -3	3 - 10	0-2	0-2
(mm/day)	summer	0- 1	1 -3	0 - 0.5	0-1
	autumn	1 - 5	2-10	0-2	0.5 - 5

The climate gradient across the Mediterranean basin is extreme. It ranges from the cold mountainous areas of the Alps with annual mean temperatures below zero (-2 °C at 2500 m elevation) to the hot plains of Africa with annual mean temperatures up to about 22 °C even near the coast and 32.5 °C inland (25.5 °N) (Bolle, 2003). Inland the annual maximum temperatures are reached in July while at the coast it is delayed to August which indicates the effect of the sea on the climate (Bolle, 2003).

The amplitude of the temperature wave is larger at the dry inland stations as compared to Mediterranean coastal sites and the differences between the stations are larger in summer than in winter. The Mediterranean basin also contains the sites with highest European annual precipitation of much above 1000 mm at the eastern Adriatic coast and its hinterland (4600 mm near 42.8 °N, 22.3 °E) and less than 100 mm in North Africa at 32 °N (Bolle, 2003).

In Figure 2.3, the annual course of average rainfall across Tunisia is presented. It shows the gradient from the highest winter precipitation at the northwestern coast to the eastern coast and the inland. Remarkable is that at the more southern stations often the winter precipitation maximum is not in December or January but in October and March. The spatial variability of the

Mediterranean climate is high even at relatively small spatial scales.

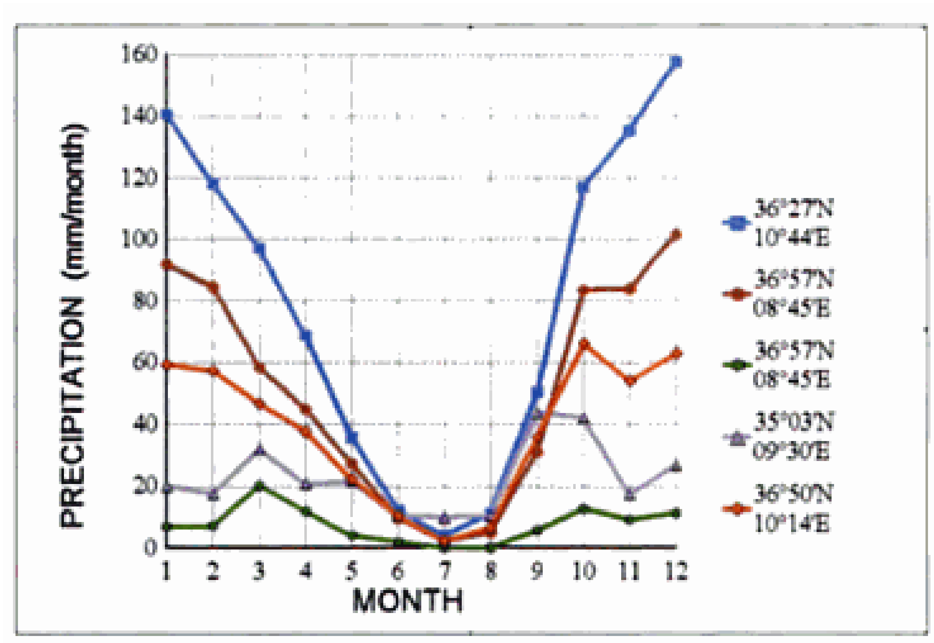

Figure 2.3 Annual course of precipitation at some stations in Tunisia after WMO (1999)

2.2 WATER RESOURCES IN THE MEDITERRANEAN: MAJOR PROBLEM FACETS

Water resources are a huge topic and a very important one, because water impinges on virtually every aspect of daily life. Most of the Mediterranean regions are water poor and prone to water shortages. The Mediterranean climate is considered the main source of water scarcity in these regions. In fact, with long periods of hydrologic deficit and high levels of inter-annual variability in rainfall, in addition to long periods of over-exploitation, the issue of water shortage is exacerbated. During the last decades, fresh water is becoming scarcer and more unequally distributed in the Mediterranean basin countries (Wainwright and Thornes, 2004).

Climate change, the growing demand for water in agricultural and urban development, as well as the expanding tourism industry, have further increased the pressure on water resources and hence aggravated the water stress on the region. Population growth in many southern Mediterranean countries is the major factor affecting water resources, reducing the water availability per capita. Urbanization increases urban demands, which are of high-priority and intensifies conflicts among users. Tourist population in the Mediterranean is very significant, and tourist water consumption is about three times higher than local demands (EEA, 2000).

These rapid social and environmental changes will have negative implications towards current and future sustainability. Pressures and impacts of water scarcity often result in conflicts among users and with an apparent lack of policy response towards sustainable management, due to the complex institutional structure and legislation (Garrote et al. 2005; Iglesias and Moneo 2005; Garrido and Llamas 2006). UN projections (UN Population Division, 1994) show that four Mediterranean countries already have less than the minimum required water availability to sustain their own food production (295 m^3/cm yr). By 2025, eight countries will be in virtually the same situation. These countries are essentially all on the Southern rim of the Mediterranean basin.

In the Mediterranean region, agriculture is considered to be the sector where the largest volume of water can be saved. Agriculture accounts for some 80 % of total demand and large amounts of water are poorly used. In many areas, agriculture is impossible without irrigation (Papadopoulos, 1995). Consequently the conventional water resources will be insufficient to even meet the domestic water demand at the beginning of the next century and the need for alternative water resources such as reuse of waste water is unavoidable.

Towards acute water shortage in the Mediterranean basin, water experts and politicians agreed that water management problems must be addressed immediately and they not an exclusive matter of water quantity but also of water quality. In recent years water pollution has become a high priority issue for the protection of the quantity and the quality of the surface water and groundwater resources. Degradation of the groundwater quality is a common problem in the Mediterranean region due to multiple pressures on the aquifers: excessive pumping in relation to average natural recharge, return flow from irrigation water with intense use of agrochemicals, leakage from urban areas, landfills, septic tanks, sewers, mine tailings, among others (Barraque 1998; Fornes et al. 2005). Also irrigated agriculture in semi-arid regions, although increases crop productivity and economic stability, however, it is one of the major diffuse source contributors to the contamination of surface and groundwater bodies, mainly from pesticides and fertilizers.

Control of pesticides and optimization of fertilization with crop uptake are essential management strategies for better control of irrigated agriculture. Drought episodes also contribute to the degradation of groundwater quality (Iglesias and Moneo 2005) as a result of the overuse of aquifers. An important number of Mediterranean wetlands are affected by irrigation activities since their ecosystems depend to a significant degree on the sustainability of agro-ecosystems. Habitats' conservation and agriculture have in many cases irreconcilable interests (Hellegers and van Ierland 2003). Many aquifer systems that naturally contain vast quantities of brackish water, have limited possibilities for exploitation for human or agricultural uses, imposing so, additional demand stress to neighboring aquifers with higher water quality. Also saline intrusion is an important concern in aquifers, especially in the Mediterranean region, where as a result of the high seasonal water demand, mainly for tourism, they have been over pumped.

2.3 WATER RESOURCES IN TUNISIA

2.3.1 RAINFALL AND SURFACE WATER POTENTIAL

Surface water resources in Tunisia are characterized by problems of quantity and quality. These resources are limited because of the semi-arid to arid climate found in most of the country, with episodic droughts, and a natural deterioration of water quality because of the salty types of rocks found within the country (Benabdellah, 2007).

Tunisia receives on average 230 mm/year of rainfall; that is 36 billion cubic meters (bm^3) of rainfall. However, this volume varies between $11bm^3$ during a drought year and 90 bm^3 during a very wet year.

The variability of the climate under the Mediterranean influence in the north and under the Saharan influence in the south makes rainfall at the same time scarce and unequally distributed in space and time. The annual precipitation is on average 594 mm in the north, 289 mm in the center and only about 150 mm in the south. The ratio between the highest observed values and the lowest observed values of precipitation vary from 4.4 in the north to 15.8 in the south, illustrating the temporal irregularity and variability of rainfall. The decade beginning in 1990 had 4 dry years, one very wet year (1995-96), three relatively wet years and two average rainy years.

In the southern part of the country, this decade was rather a dry one. Rainfall information has been collected and stored since 1900. Over the last decade, records show that Tunisia experienced 12 important flood periods alternated with 17 dry periods.

Droughts appear two to three times every 10 years and can last two, three or even four successive years. Surface water resources are estimated at 2700 million cubic meters (Mm^3) distributed per year over three natural areas distinguished by their climatic and hydrological conditions as well as by rather homogeneous geomorphologic and geological aspects.

The north provides relatively regular contributions evaluated to 2190 Mm^3, thus representing 82% of the total surface water potential while covering only 16% of the country. The center part, covering 22% of the area, is characterized by irregular resources. It provides 12% of the total surface water potential. The southern part of the country which accounts for approximately 62% of the total area is the poorest in surface water, providing very irregular resources evaluated at 190 Mm^3 which represents 6% of the country's total potential of water. The quality of surface water, evaluated by its degree of salinity, varies according to the origin of the resource. Considering that a salinity of less than 1.5g/l is acceptable, and then approximately 72% of the surface resources may be considered of good quality. Water quality also varies across the country with 82% of the water resources in the north considered good quality, 48% of that in the center and only 3% in the south (Benabdellah, 2007).

These inequalities in quantities and quality make water management more difficult and explain the need to transfer surface water from the north to the Sahel and the south in order to improve the drinking water supply and insure equity between regions.

2.3.2 GROUNDWATER POTENTIAL

The groundwater resource is estimated at 2000 Mm^3, confined within 212 shallow aquifers containing 719 Mm^3 and 267 deep aquifers. It is estimated that 650 Mm^3 of this resource, located mainly in the south, is nonrenewable.

Like surface water, groundwater is characterized by unequal allocation and variable quality in terms of salinity. Groundwater is distributed as follows:

- The north has 55% of the shallow groundwater resources and only 18% of the deep groundwater resources
- The center provides 30% of the shallow resources and 24% of the deep resources

- The south provides 15% of the shallow resources and has 58% of the deep resources.

Good quality groundwater is found in only 8% of shallow water and 20% of deep aquifers. If one accepts that salty water up to 3g/l can be used in the agricultural sector and for the production of drinking water, then approximately 36% of groundwater resources are not suited for these two sectors which are in increasing demand.
Another phenomenon, which highly affects the quality of water, is drought. In periods of drought, the salinity of the water stored in shallow aquifers can reach 3.5 g/l due to overdraft as resources are drawn down for both drinking and irrigation.

2.3.3 TOTAL WATER RESOURCES POTENTIAL

Water resources in Tunisia are estimated at 4700 Mm^3 including 650 Mm^3 of nonrenewable resources or 13.8% of the total water resources. Groundwater resources represent 42.5% of the total potential. Thus, the per capita endowment is at about 450 Mm^3 per year. This ratio will reach 315 Mm^3 per capita per year in 2030. This ratio is higher in other Mediterranean countries such as Morocco with a ratio of about 1083 or Algeria, with a ratio of 655 (Benabdellah, 2007).

2.3.4 WATER BALANCE

Meeting the increasing demand for water while accounting for the space and time imbalance of water quantity and quality makes water scarcity one of the most urgent problems of the country.
From the information given above, it can be easily derived that the water balance will be negative in the near future. The projected volumes for the year 2030 show a strong water stress warning by comparing exploitable water volume of 2732 Mm^3 to the water demand volume of 2760 Mm^3. The use of the reclaimed water becomes necessary to fill the water deficit of 389Mcm (Benabdellah, 2007).
The exploitation index of renewable resources, the degree to which renewable natural water is exploited, and the vulnerability of the country as regards cyclical shortages is estimated at 57 % for the period of 1990 to 1997 (Blue Plan, 2000). Above 50%, this index reveals high pressure on renewable fresh water resources and indicates the need for rationalizing the management of water uses and demands. It highlights the need for Tunisia to adjust policy on water availability

and demand.

2.4 HYDROLOGY OVERVIEW

This chapter provides a brief overview of the hydrologic cycle and discusses the role of hydrology, not only in the global contexts of weather and climate but also in the local and regional contexts of weather as it affects water resources management. This chapter contains a description of the hydrologic cycle and the identification of its specific reservoirs and fluxes.

2.4.1 THE HYDROLOGIC CYCLE

Figure 2.4 represents a conceptual model of the hydrologic cycle and shows Earth's water movement between the ocean, land, and atmosphere. As with all cycles, it is ongoing and continuous, and there is no specific start or end point.

Precipitation is water released from the atmosphere in the form of rain, snow, sleet or hail. During precipitation, some of the moisture is evaporated back into the atmosphere before ever reaching the ground. Some precipitation is intercepted by plants, a portion infiltrates the ground, and the remainder flows off the land into lakes, rivers, or oceans. An important difference between the roles of snow and rain is that runoff occurs relatively quickly following the rain event, whereas snow usually melts much more slowly over days, weeks, or months. The subsequent surge of snowmelt runoff can provide seasonal recharge to groundwater resources but can also trigger flood conditions if the snowmelt occurs too rapidly and in excessive amounts. In addition, the solid snow or ice may change directly into a gas, skipping the liquid state, in the process called sublimation. When precipitation is intercepted by plants, it is eventually evaporated back to the atmosphere. When it infiltrates the ground, it can be taken up by roots and transpired by plants, it can be evaporated from the soil, or it may recharge an aquifer.

The water in an aquifer is called groundwater, and its rate of flow in the subsurface is such that water can reside in aquifers for days to centuries before discharging to a surface body of water (e.g., river, lake, and ocean). Once groundwater has discharged into a river, lake, or ocean, the surface of the water body is exposed for evaporation, causing moisture to collect and concentrate in the atmosphere, eventually returning to the earth as precipitation as the cycle begins again. In addition to natural discharge, groundwater can more rapidly discharge when an aquifer is pumped. With the advent of motorized pumps, the rapid removal of groundwater from aquifers is a relatively recent phenomenon that has greatly affected the depletion of the aquifers and the water balance of many catchments (Potter et al., 2003).

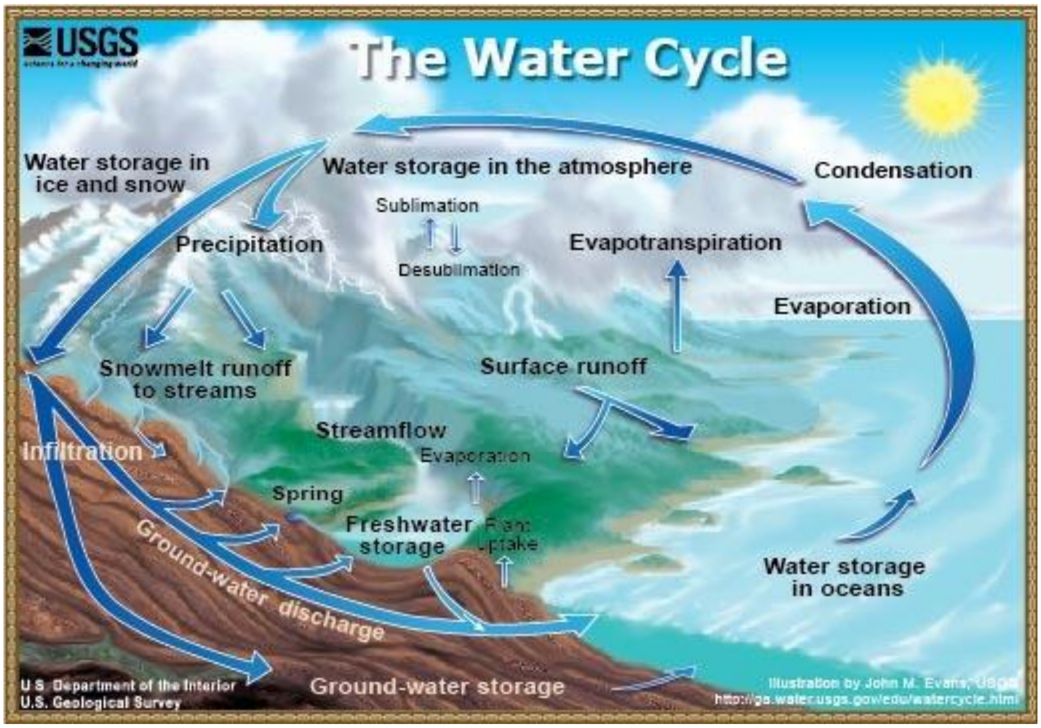

Figure 2.4 Schematic representation of the hydrologic cycle. (USGS)

While the hydrological cycle is a continuous process, it is by no means uniform throughout the globe: the residence time of water varies often dramatically among different portions of the cycle. For example, water is continuously evaporated from the surfaces of water bodies (such as oceans, lakes, and rivers). Similarly, precipitation that is intercepted by plants and other surfaces is often evaporated within a matter of hours. Once evaporated, it takes an average of 10 days for a water molecule to cycle through the atmosphere, but if it infiltrates to the water table, or if the precipitation occurs in a polar region, it may reside for hundreds of years before transferring to another step in the hydrologic cycle. In addition to variable residence times, the processes associated with the hydrologic cycle are not evenly distributed over the globe; they vary by climatic region (Potter et al., 2003). For example, evapotranspiration occurs readily in semi-arid and arid regions, but subsequent precipitation may not occur within the same basin or region. The dramatic differences in how the cycle operates are especially evident when one evaluates the hydrologic cycle at the catchment scale.

2.4.1.1 RESERVOIRS

On a global scale, the important reservoirs in the hydrologic cycle are the ocean, atmosphere, polar ice, groundwater, and moisture from land surfaces. At the global scale, water is transferred between reservoirs via four fluxes: precipitation, evapotranspiration, sublimation, and runoff. On a catchment scale, the availability of fresh water is the focus. Critical reservoirs on this scale are the atmosphere, lakes, rivers, and groundwater. Oceans and polar ice are typically irrelevant at the catchment scale, although seasonal snowmelt can contribute significantly (or destructively, in the case of floods) to a basin's water resources. Fluxes within a catchment are more strongly weighted toward the recharge and withdrawal of potable groundwater, as well as the occurrence of surface water flows. Fresh water comprises only 2.5% of the world's total water supply. Of this scant freshwater supply, 69.6% is immobilized in ice and snow, primarily in the polar regions; no saline groundwater accounts for 30.1%; and the remainder of fresh water (0.3%) is distributed among lakes, rivers, wetlands, atmospheric water, and biological water found in plants and animals. While groundwater is Earth's second largest source of fresh water, on the average it accounts for less than 1% of the earth's total water supply; however freshwater availability varies greatly on a regional basis (Potter et al., 2003).

2.4.1.2 FLUXES

The major fluxes within the hydrologic cycle are described below, and their role in the global- and/or catchment-scale hydrologic cycle is addressed.

2.4.1.2.1 PRECIPITATION

Precipitation is the process by which liquid and solid-phase aqueous particles, such as rain, snow, sleet, and hail, fall from the atmosphere to Earth's surface. The occurrence of precipitation over land is typically cited as the driving force of the hydrologic cycle, since it triggers the commencement of other fluxes (evapotranspiration, runoff, infiltration) by providing a new source of moisture to the system. The intensity and frequency of precipitation vary considerably both spatially and temporally, and the effects of precipitation can be both welcome (e.g., during droughts) or undesirable if it occurs in excess and causes subsequent flooding. In some regions, where dry air dominates the weather conditions, precipitation may fall from the clouds but evaporate before ever reaching the ground; this is a phenomenon known as virga. Measurements and estimates of precipitation (volume and intensity) are critical to any study or modeling effort involving the hydrologic cycle. Rain-gages have been the primary mechanisms for observation, but their sparse distributions and other limitations do not provide the spatial and temporal resolution needed for various modeling and research efforts. Recent advances are rapidly improving the situation by merging satellite and radar with gage information.

2.4.1.2.2 EVAPOTRANSPIRATION

Evaporation is defined as "the rate of liquid water transformation to vapor from open water, bare soil or vegetation with soil beneath" (Shuttleworth, 1993), and transpiration is the rate of water added to the atmosphere as it moves from soil through the stomata of vegetation. Evapotranspiration (ET) is thus a compound term that describes the collective effect of evaporation of water and transpiration of plants. It is the primary process that moves moisture from Earth's surface to the atmosphere. The only other natural means by which water is transferred from the earth to the atmosphere is the process of sublimation, where solid phases of water (e.g., snow and ice) transition directly to atmospheric vapor in the absence of melting. Sublimation typically occurs in regions of cool temperatures and low relative humidity. Evapotranspiration is often an elusive variable to quantify, as it varies diurnally, seasonally, and with changes in precipitation events.

2.4.1.2.3 RUNOFF

Runoff is generally thought of as the movement of excess rainfall across the land surface into rivers, lakes, or the ocean. It occurs when the rate of precipitation exceeds the rate of infiltration at the soil surface, or when soil is saturated. Runoff is a particularly important process at the catchment scale, since it can recharge reservoirs and replenish rivers that may subsequently recharge the groundwater; runoff can also cause soil erosion, and excess runoff can lead to flooding.

To understand the runoff generation, we can imagine the soil as represented by a tank with a perforated lid and an outlet at the bottom (Figure 2.5). The storage capacity (C) of the tank depends on its depth and porosity. Deep soils with a high porosity have good storage capacity. Rain falling on the perforated lid passes through the surface as infiltration at a rate in mm h^{-1} and moves down through the unsaturated soil to the saturated zone. If the rainfall intensity (mm h^{-1}) is higher than the infiltration rate, then the rainfall runs off. This process is called Hortonian overland flow (HOF). After time, the spare capacity in the tank (C-S) reduces as more infiltration occurs until (C-S)=0. Spare capacity approaches zero and this slows down the entrance of water into the soil. When all the storage is filled, the arrival of more water causes saturated overland flow (SOF). The relative role of these two mechanisms varies down slope because throughflow, if it occurs at all in Mediterranean soils, brings the lower parts of the slope to saturation earlier. This is called the partial contributing-area concept.

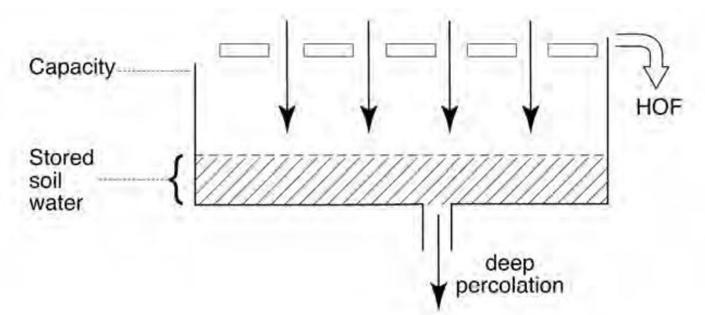

Figure 2.5 Tank model of soil hydrology

Since the proportion of rainfall lost as runoff rises significantly as the percentage of vegetation cover falls below about 30 %, bare soils produce a large runoff coefficient. Moreover, soils in the Mediterranean often have low infiltration capacities because the soils dry out in the summer, following the winter moisture. Fine surface ‘seals’ develop, perhaps only 1–2mm thick, and these increase the runoff rates. Sometimes evaporation leads to chemical as well as mechanical seals (often of calcium carbonate) that again reduce the infiltration rates very dramatically.

Mediterranean soils with high erosion rates also often have stones exposed at the surface. In this position, the stony soils create higher runoff rates and lower infiltration rates, whereas soils with a large proportion of buried stones may have higher infiltration rates (Poesen and Lavee, 1994).

2.4.1.2.4 GROUNDWATER

Natural groundwater fluxes are typically slow; water may reside in an aquifer for as little as a few hours or for hundreds of years. Accordingly, groundwater itself is often perceived, on the average, as a relatively slow-moving reservoir in the global hydrologic cycle. At the catchment scale, however, where stream - aquifer interactions are relatively rapid and substantial, the average groundwater fluxes are relatively fast moving. They comprise: (1) the natural flow of water between watersheds, (2) the water pumped from an aquifer, (3) mountain- front recharge (seasonal infiltration of snowmelt at the base of mountain ranges), (4) event-based infiltration (infiltration from precipitation and subsequent rises in surface water levels, especially rivers), and (5) artificial recharge via anthropogenic conservation projects.

2.4.2 THE WATER BALANCE: GLOBAL TO CATCHMENT SCALE

The water balance simply refers to the volumes of water that flow through various components of the hydrologic cycle. More specifically, it is another useful conceptual model in which the components of the hydrologic cycle are evaluated as storage units that are affected by various inputs and outputs. If the various components of the cycle can be quantified or at least estimated, it is possible to gain an understanding of how alteration of a component might affect the balance of the hydrologic cycle. The most simplistic formulation of a water balance is denoted by the elementary continuity equation that conveys the notion that "input to a hydrologic system (I) equals the output from the system (O), plus or minus any changes in storage ΔS ":

$$I = O \pm \Delta S$$

Where, for a given domain, I is the total inflow, comprised of surface runoff (into the domain), groundwater inflow and precipitation; O is the outflow of evapotranspiration, surface runoff (out of the domain), and groundwater; and ΔS is the change in storage, whose variables are determined by the scale of the domain. The concept of a water balance is useful at both global and regional scales. At the basin or watershed scale, where groundwater and surface water interactions might encompass the primary focus, precipitation and groundwater inflow would be a model's input, while overland flow, groundwater outflow, and evapotranspiration would be its outputs.

2.5 HYDROLOGIC MODELING

Modeling methods have been widely used for over 40 years for a variety of purposes, but almost all modeling tools have been primarily developed for humid area applications. Arid and semi-arid areas have particular challenges that have received little attention.

The development of models has gone hand-in-hand with developments in computing power. While event-based models originated in the 1930s and could be used with hand calculation, the first hydrological models for continuous simulation of rainfall-runoff processes emerged in the 1960s, when computing power was sufficient to represent all of the land-phase processes in a simplified, “conceptual” way. Later, in the 1970s and 1980s, increases in power enabled “physically based” hydrological models to be developed, solving a coupled set of partial differential equations to represent overland, in-stream, and subsurface flow and transport processes, together with evaporation from land and water surfaces.

And currently, global climate models are able to represent the global hydrological cycle with simplified physics-based models. In parallel, recent developments in computer power provide the ability to use increasingly powerful methods for the analysis of model performance and to specify the uncertainty associated with hydrological simulations.

The relationship between models and data is fundamental to the modeling task. Current technology and computing power can provide powerful pre- and post-processors for hydrological models through Geographic Information Systems, linking with digital data sets to provide a user-friendly modeling environment. Global developments in remote sensing, coupled with modeling and data assimilation, are providing new sources of information. For example, precipitation estimates for mid-latitudes are now available in near real-time; remote sensing of water body elevation is approaching the point where resolution is useful for real-time hydrological modeling limitations.

2.5.1 RAINFALL-RUNOFF MODELING

A model is a simplified representation of a real-world system, and consists of a set of simultaneous equations or a logical set of operations contained within a computer program. Models have parameters, which are numerical measures of a property or characteristics that are constant under specified conditions. A lumped model is one in which the parameters, inputs, and outputs are spatially averaged and take a single value for the entire catchment. A distributed model is one in which parameters, inputs, and outputs vary spatially. A semi-distributed model may adopt a lumped representation for individual sub-catchments. A model is deterministic if a set of input values will always produce exactly the same output values, and stochastic if, because of random components, a set of input values need not produce the same output values. An event-based model produces output only for specific time periods, whereas a continuous model produces continuous output. The tasks for which rainfall-runoff models are used are diverse, and the scale of applications ranges from small catchments, of the order of a few hectares, to that of global models. Typical tasks for hydrological simulation models include:

- modeling existing catchments for which input–output data exist, e.g., extension of data series for flood design of water resource evaluation, operational flood forecasting, or water resource management;
- runoff estimation on ungauged basins;
- prediction of effects of catchment change, e.g., land use change, climate change;
- coupled hydrology and geochemistry, e.g., nutrients, acid Rain;
- coupled hydrology and meteorology, e.g., Global Climate Models.

Clearly, the modeling approach adopted will, in general, depend on the required scale of the problem (space-scale and time-scale), the type of catchment, and the modeling task. Some of the tasks pose major challenges, and it is helpful to consider a basic classification of model types, after Wheater et al. (1993), and their strengths and weaknesses.

2.5.1.1 METRIC MODELS

At the simplest level, all that is required to reproduce the catchment-scale relationship between storm rainfall and stream response to climatic inputs, is a volumetric loss, to account for processes such as evaporation, soil moisture storage, and groundwater recharge, and a time-distribution function, to represent the various dynamic modes of catchment response. This is the basis of the unit hydrograph method, developed in the 1930s, which, in its basic form, represents the stream response to individual storm events by a non-linear loss function and linear transfer function. The simplicity of the method provides a powerful tool for data analysis. Once a set of assumptions has been adopted; (separating fast and slow components of the streamflow hydrograph and allocating rainfall losses), rainfall and streamflow data can be readily analyzed, and a unique model determined. This analytic capability has been widely used in regional analysis. In the UK, for example, the 1975 Flood Studies Report (NERC, 1975) used data from 138 UK catchments to define regression relationships between the model parameters, and storm and catchment characteristics for the rainfall loss and transfer functions. This lumped, event-based model provides the basic tool for current UK flood design, and, through the regional regression relationships, a capability to model flow on ungauged catchments (the regional relationships were updated in the 1999 Flood Estimation Handbook (Institute of Hydrology, 1999) through the replacement of manual by digital map-based characteristics). The unit hydrograph is also widely adopted internationally in the form of the US Soil Conservation Service model, available within the US Corps of Engineers HEC1 model. Synthetic unit hydrographs can readily be generated based on default model parameters, which is particularly helpful in data scarce situations. However, relatively little work has been done to evaluate the associated uncertainty with these estimates. This data-based approach to hydrological modeling has been defined as metric modeling (Wheater et al., 1993). The essential characteristic of metric models is that they are based primarily on observations and seek to characterize system response from those data. In principle, such models are limited to the range of observed data, and effects such as catchment change cannot be directly represented. In practice, the analytical power of the method has enabled some effects of change to be quantified; the UK regional analysis found the degree of urban development to be an important explanatory variable, and this is used in design to mitigate impacts of urbanization. The unit hydrograph is a simple, event, model with limited performance capability. However methods of time-series analysis can be used to identify more complex model structures for event or continuous simulation. These are typically based on parallel linear stores, and provide a capability to represent both fast- and slow-flow components of a streamflow hydrograph. These provide a powerful set of tools for use, with updating techniques, in real-time flood forecasting.

2.5.1.2 CONCEPTUAL MODELS

The most common class of hydrological model in general application incorporates prior information in the form of a conceptual representation of the processes perceived to be important. The model form originated in the 1960s, when computing power allowed, for the first time, integrated representation of the terrestrial phase of the hydrological cycle, albeit using simplified relationships, to generate continuous flow sequences. These conceptual models are characterized by parameters that usually have no direct, physically measurable identity. The Stanford Watershed Model (Crawford and Linsley, 1966) is one of the earliest examples, and, with some 16–24 parameters, one of the more complexes. To apply these models to a particular catchment, the model must be calibrated, i.e., fitted to an observed data set to obtain an appropriate set of parameter values, using either a manual or automatic procedure. The problem arises with this type of model that the information content of the available data is limited, particularly if a single performance criterion (objective function) is used (Kleissen et al. 1990) and hence in calibration the problem of non-identifiability arises, defined by Beven (1993) as "equifinality." For a given model, many combinations of parameter values may give similar performance (for a given performance criterion), as indeed may different model structures. This has given rise to two major limitations. If parameters cannot be uniquely identified, then they cannot be linked to catchment characteristics, and there is a major problem in application to ungauged catchments. Similarly, it is difficult to represent catchment change if the physical significance of parameters is ambiguous. Developments in computing power, linked to an improved understanding of modeling limitations, have led to some important theoretical and practical developments for conceptual modeling.

Firstly, recognizing the problem of parameter ambiguity, appropriate methods to analyze and represent this have been developed. The concept of generalized sensitivity analysis was introduced (Spear and Hornberger, 1980), in which the search for a unique best fit parameter set for a given data set is abandoned; parameter sets are classified as either "behavioral" (consistent with the observed data) or "non-behavioral" according to a defined performance criterion. An extension of this is the generalized likelihood uncertainty estimation (GLUE) procedure (Freer et al., 1996).

The current generation of stochastic analysis tools allows detailed investigation of model structure and parameter uncertainty, leading to parameter-efficient models that seek to extract the maximum information from the available data. They also allow formal recognition of uncertainty in model parameters, and provide the capability to produce confidence limits on model simulations (Wheater et al., 2007).

2.5.1.3 PHYSICS-BASED MODELING

An alternative approach to hydrological modeling is to seek to develop "physics-based models," i.e., models explicitly based on the best available understanding of the physics of hydrological processes. Such models are based on a continuum representation of catchment processes and the equations of motion of the constituent processes are solved numerically using a grid, of course discretized relatively crudely in catchment-scale applications. They first became feasible in the 1970s when computing power became sufficient to solve the relevant coupled partial differential equations (Freeze and Harlan, 1969; Freeze, 1972).

The models are thus characterized by parameters that are, in principle, measurable and have a direct physical significance. An important theoretical advantage is that if the physical parameters can be determined a priori, such models can be applied to ungauged catchments, and the effects of catchment change can be explicitly represented.

In practice two fundamental problems arise with such models. The underlying physics has been (necessarily) derived from small scale, mainly laboratory-based, process observations. Hence, firstly, the processes may not apply under field conditions and at field-scales of interest. There is, for example, numerical evidence that the effects of small-scale heterogeneity may not be captured by effective, spatially aggregated, properties (Binley and Beven, 1989). Secondly, although the parameters may be measurable at small-scale, they may not be measurable at the scales of interest for application. An obvious example of both is the representation of soil water flow at hillslope-scale.

There is, therefore, a need for fundamental research to address issues such as the appropriate process representation and parameterization at a given scale. For groundwater flow and transport, significant progress has been made; new theoretical approaches to the representation of heterogeneity have been developed (Dagan, 1986), and stochastic numerical methods have been developed to represent explicitly the uncertainty associated with heterogeneous properties and to incorporate conditioning on field observations. Extension to the more complex problems of field-scale hydrology is urgently needed, but severely constrained by data availability. Most of the complexity of physically based models, and the associated problems discussed above, arise from the representation of subsurface flows, and the inherent lack of observability of subsurface properties.

The situation often met in arid areas is that overland flow is the dominant runoff mechanism, and surface properties are, in principle, much more readily obtained. It was therefore argued by Woolhiser (1971), that it is in this environment that physics-based models are most likely to be successful.

2.5.2 LOCAL MODELING PROCEDURES

Various modeling procedures for the use of conceptual rainfall-runoff models have been suggested (e.g., Beck, 1981a; Anderson and Burt, 1985). Local procedures vary with the particular circumstances of each case. However, a number of steps can commonly be found in most modeling procedures when applying a rainfall-runoff model to a particular catchment: these are model structure selection, sensitivity analysis, calibration, validation and prediction (Figure 2.6).

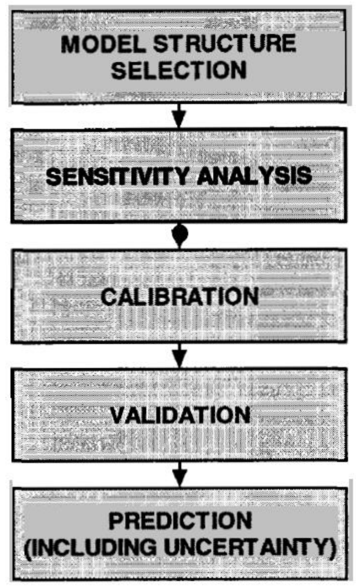

Figure 2.6 Conventional (simplified) procedure for local rainfall-runoff modeling

2.5.2.1 MODEL STRUCTURE SELECTION

A model structure appropriate for the envisaged modeling purpose, the given catchment characteristics and (time-series) data has to be selected (Wagener, 1998). The modeling purpose defines aspects such as which hydrological processes need to be considered and what modeling time step is required. The available data enable a certain degree of causality of process description to be used and allow a particular minimum temporal resolution. The catchment characteristics (and the hydrologist’s perception of the hydrological system) are important criteria to determine what type of process description is suitable. However, subjective criteria such as the availability and experience with a particular modeling code, i.e., a set of mathematical equations implemented in a piece of software, or the cost to purchase or develop a code might be of equal importance in the decision making process.

2.5.2.2 SENSITIVITY ANALYSIS

Sensitivity analysis is an investigation of how sensitive the model output is to changes in the parameter values. It can also be used to test the influence of other aspects such as initial or boundary conditions. The analysis can take place at two different stages within the modeling process. First, it can be placed before the calibration step to identify the most important parameters, and therefore model components, with respect to Rainfall-Runoff Modeling - Conventional (simplified) procedure for local rainfall-runoff modeling the model's performance. Insensitive parameters can then be fixed to a suitable value to decrease the dimensionality of the calibration problem (e.g., Abdulla et al., 1999; Bastidas et al., 1999). The model performance will often only decrease marginally when this step of complexity reduction is performed sensibly, i.e., when parameter interaction is considered (Bastidas et al., 1999; Wagener et al., 1999). Osidele and Beck (2001) put this approach into a formal framework of hypothesis testing for model structure identification.

The second option is to perform a sensitivity analysis after the calibration step to estimate whether the parameters are identified well or poorly, which is indicated by the response surface slope (Clarke, 1973). The response surface is the topographic surface defined in the n + 1-dimensional space by a criterion of model performance (objective function), plotted with respect to the n model parameters. The common weakness of all these approaches is that they assume independence between parameters, an assumption rarely justified in RR modeling. The approaches to sensitivity analysis most often applied to RR models are probably the perturbation and the Regional Sensitivity Analysis (RSA) methods. In the first approach, individual parameters are perturbed over their feasible range using a particular step size, while the remaining parameters are kept fixed at optimal values.

2.5.2.3 CALIBRATION

As noted earlier, one criterion for a model structure to be classified as conceptual is the requirement that some of its parameters must be estimated through calibration against observed system output. This can be achieved in a single step in cases where the parameters enter the model linearly, i.e., Q = BM(I) where Q is the streamflow (or any other system output), B is the parameter vector, M is the model structure (i e . , a collection of functions which can be linear or non-linear), and I is the model input (e.g., precipitation). Solutions can be derived using for example Single Value Decomposition (Gershenfeld, 1999).

However, in most RR model structures, the parameters appear inside the constituent functions, i.e., they enter non-linearly, Q = M (B, I). The consequence is that an iterative solution is required and it is not possible to determine with certainty whether the best solution has been found (Gershenfeld, 1999).

A large number of calibration procedures to find such a solution in an iterative fashion have been tested over almost four decades probably starting with (Dawdy and ODonnell, 1965). While varying greatly in detail, they generally consist of the following four components: objective function, calibration data, adjustment strategy, termination criterion. Objective function Visual inspection of calculated and observed hydrographs is a very important tool in any calibration procedure. However, for longer periods of manual calibration and for automatic calibration in general, one must specify an aggregated measure of the model performance, a so-called objective function (also sometimes called loss function). The Nash and Sutcliffe (1970) efficiency (NSE) (Nash and Sutcliffe (1970), allows for example, comparison of a model's performance over different catchments (Legates and McCabe, 1999).

The nonlinear relationship between the parameters and outputs of R-R models makes the linear regression solution methods impractical to use, thus reliance on iterative or sequential (recursive) procedures to attain an acceptable solution is required. Iterative schemes work by repeatedly computing the model accuracy based on the guessed model parameters and all available data. Iterative methods are necessarily restricted to off-line applications, where a batch of data has been previously collected for processing. In contrast, in sequential procedures, one uses each measurement (real system output) as soon as it becomes available to update the model parameters and model states which result in improved model outputs (Thiemann et al., 2001; Moradkhani et al., 2005) This attribute makes such approaches practical in either on-line or off-line applications. Since the advent of digital computers, automatic model calibration through optimization methods has been used extensively to calibrate the conceptual R-R model parameters.

In automatic calibration, the problem is formulated as an optimization problem through objective function or sometimes called loss or cost function (Figure 2.7). This is a measure of the ability of the model to replicate the observed system response.

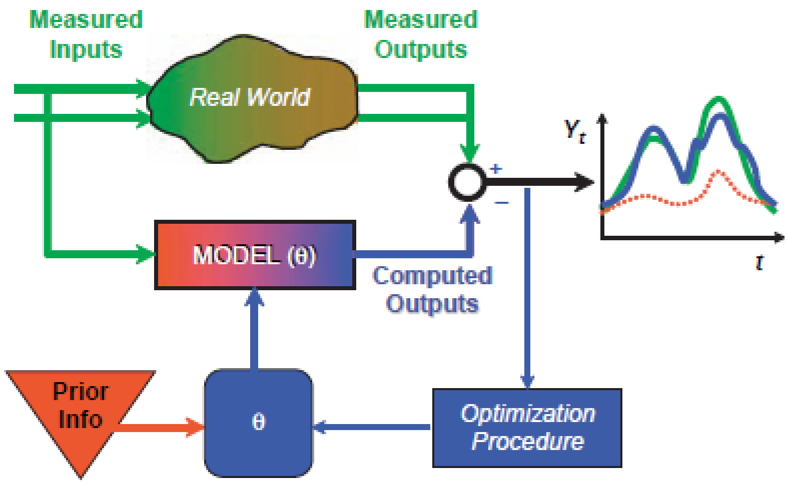

Figure 2.7 The concept of model calibration as an optimization problem

The success of any model calibration depends on the observed data, model structure, calibration conditions and optimization procedure. Gupta et al. (2005) list the necessary conditions for a realistic hydrologic simulation by effectively estimating the model parameters called a well-calibrated model. These conditions are: (1) consistency of model structure and its behavior with current understanding of hydrologic processes, (2) consistency between input-state-output behavior of the model and measurements of watershed behavior, (3) accuracy (unbiasedness) and precision (small uncertainty) of model predictions

The Problem of Model Calibration (Parameter Estimation)

In general terms, hydrologic models are defined by state or prognostic variables which define the dynamics of a system, and also parameters as quantities characterizing the system. Parameters may be classified into physical and process parameters (Sorooshian and Gupta, 1995). Physical parameters are those which can be measured directly independent of the observable river basin responses, such as, watershed area, impervious area in a watershed, local permeability obtained using core samples, fraction of vegetated area, and areal percentage of water bodies. The process parameters, on the other hand, are those which cannot be measured directly and needs to be inferred by indirect means (Gupta et al., 1998), such as, effective depth of soil moisture storage, effective lateral interflow, rate of drainage for hypothetical lumped storages, mean hydraulic conductivity, and surface runoff coefficient. Although these parameters cannot be expected to have physical interpretations, they are assumed to be related to inherent properties having physical relevance in hydrologic systems.

In order for a model to closely and consistently simulate the observed response (dynamic behavior) of a river basin over some historical period for which forcing data (precipitation) and system output (e.g., streamflow) are available, the model parameters need to be tuned or calibrated. The linkage between data, model and parameters are shown schematically in Figure 2.8. A variety of model calibration techniques have been developed and implemented to ensure conformity between the model simulations of system behavior and observations. A basic approach to obtain the parameter values is the trial and error procedure, the so called manual calibration. The model knowledge and large number of model performance measures defined by objective functions accompanied by visual inspection of the agreement and differences between model predictions and the observation, and above all, the human judgment are all taken to guide the adjustments to the best guess for model parameters (Boyle et al., 2000; Duan, 2003).

There are 3 levels associated with manual calibration (Boyle et al., 2000). In level zero, the watershed data are examined and a priori estimates of the likely values of parameter sets developed. This provides the initial uncertainty of the estimates by defining the feasible parameter ranges using the estimates from similar adjacent watersheds, look-up tables, etc. In level one, the analysis of some segments of streamflow hydrograph that are most relevant to specific parameter/s is made followed by the parameter adjustment. In this step, the parameter interaction is generally disregarded. Finally, in level two, the most difficult step, while examining the watershed hydrograph the parameter interaction is taken into account and adjustment of the parameters is made accordingly.

The process of manual calibration is less affected by noises in calibration data; however, the multitude of nonlinearly interacting parameters in hydrologic models makes this procedure very labor-intensive requiring extensive training. This expertise is not only difficult to gain, but also hard to transfer from one hydrologist to another (Sorooshian et al. 2008)

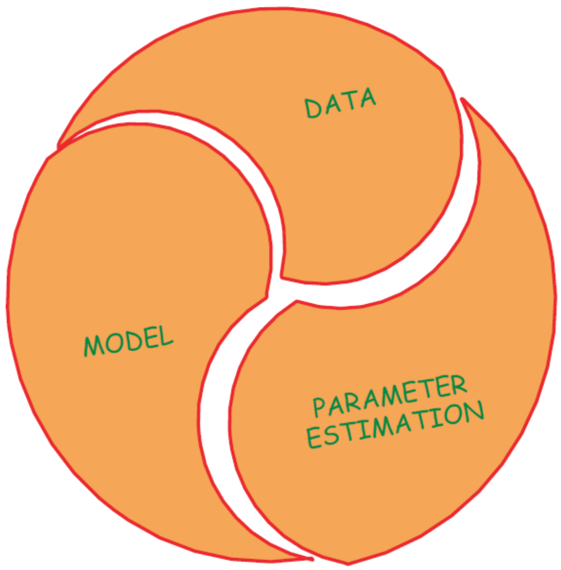

Figure 2.8 Linkage of data, model and parameter estimation (calibration) (Sorooshian et al. 2008)

2.5.2.4 VALIDATION

A step often included in modeling procedures is validation or verification (Beven, 20004). However, the definitions of what this step actually represents vary considerably (Anderson and Bates, 2001). Very often, validation is taken to mean testing the model on a data set independent from the one used for calibrating the model structure, commonly in the form of a split-sampling test where a data set is divided into two periods. This is however sometimes considered a minimum requirement for the suitability of a model. KlemeS (1986) proposed a more thorough, hierarchical scheme of model validation. It contains four stages in which the model's performance to predict streamflow is tested:

(1) a simple split sample test as described earlier; (2) a proxy-busin test, testing the capability of the model to predict flow in a hydrological similar catchment; (3) a differential split sampling test, where the two data periods selected have different hydrological characteristics (e.g., a dry and a wet period); and (4) a proxy-basin differential split sampling test, combining tests (2) and (3). The idea is to test the ability of a model to perform a specific task, not to check its

hydrological soundness (KlemeS, 1986). Applications of this type of validation using only streamflow (e.g. Mroczkowski et al., 1997; Seibert, 1999) have shown that it is often not very discriminative since different models or even model structures pass when using the same type of data. Mroczkowski et al. (1997) subsequently added another stage by testing the performance with respect to additional output variables (stream chloride and groundwater). In one case they found that all three variables were required to objectively show that a model failed the validation. A slightly different approach is the analysis of the residual properties, assuming the hydrological model behaves like a regression model. The choice of a particular error model, made implicitly when selecting an OF, often allows analysis of the residuals in order to establish whether they conform to the assumptions made.

The detection of a correlation between residuals and a forcing variable might for example indicate that not all the information in the data is used and another model component could be identified (Beck, 1981). The validation approaches described have, however, a scientific basis that is dubious if the idea is to show that a particular model is correct. Oreskes et al. (1994) argue that this idea is ill posed and should be replaced by mere model evaluation, leading to the rejection of all those models which are unsuitable. Different hydrologists have adopted the idea of a more Popperian approach (Popper, 2000) in order to derive a more scientific basis for hydrological modeling (eg, Wagener et al., 2003b). Popper (2000) suggested scrutinizing theories (models) using all available means and rejecting those that fail. However, verification or validation of a theory as the true one is logically not possible.

2.5.2.5 PREDICTION - INCLUDING UNCERTAINTY

Uncertainty is unfortunately an integral part of any hydrological modeling undertaken. It is therefore important to analyze this uncertainty and its effect on the predicted output variable. The uncertainty in the modeling process has four major components (e.g., Bastidas *et al.,* 1999; McIntyre *et al.,* 2002):
Data uncertainty, i.e., errors introduced by the measurement itself, by the temporal and spatial discretization of measurements (e.g., the use of point measurements to estimate areal average values of a variable) or by data pre-processing; Model structural uncertainty, i.e., simplifications

and/or inadequacies in the description of real world processes. The unavoidable deficiencies in the model structure often result in the problem that different parameter sets, *(i.e.,* different models) fit one mode of system response at the expense of other response modes that are reproduced less accurately (Gupta et al., 1998); Model specification uncertainty, i.e., the inability to converge to a single best model using the information provided by the available data. This uncertainty results mainly from data and model structure uncertainties (Melching, 1995) since (a) the calibration procedure propagates data uncertainty into the model parameters leading to similar model performance with erroneous data and parameters as with true data and parameter values (e.g., Melching *et al.,* 1991); and (b) characteristics of the model structure such as thresholds and interacting parameters result in multiple regions of attraction in the model space and in multiple local optima within those regions, making it difficult to identify the globally optimum model (Duan *et al.*, 1994).

Uncertainty due to unknown initial conditions, i.e., the states of the model (e.g., moisture content of stores) is usually unknown at the beginning of any calibration or simulation period. However, this uncertainty can often be minimized by either calibrating the initial conditions or using a warming-up period, which allows the internal states to adjust. Additionally, one has to keep in mind that even if those uncertainties could be removed, there would still be randomness in the natural processes themselves (Melching *et al.,* 1990). This randomness introduces uncertainty that cannot be reduced. It is assumed here that this uncertainty can be associated with data uncertainties if sufficiently long data records are used.

2.6 HYDROLOGICAL PROCESSES IN ARID AREAS

2.6.1 DATA SCARCITY IN ARID AND SEMI ARID AREAS

Despite the critical importance of water in arid and semi-arid areas, hydrological data have historically been severely limited. It has been widely stated that the major limitation of the development of arid-zone hydrology is the lack of high quality observations (Nemec and Rodier, 1979; Pilgrim et al., 1988). There are many good reasons for this. Populations are usually sparse and economic resources limited; in addition, the climate is harsh and hydrological events infrequent, but damaging. However, in the general absence of reliable long-term data and experimental research, there has been a tendency to rely on humid-zone experience and modeling tools, and data from other regions. At best, such results will be highly inaccurate. At worst, there is a real danger of adopting inappropriate management solutions which ignore the specific features of dry land response. Despite the general data limitations, there has been some substantial and significant progress in development of national data networks and experimental research. This has given new insights and we can now see with greater clarity the unique features of arid zone hydrological systems and the nature of the dominant hydrological processes. This provides an important opportunity to develop methodologies for flood and water-resource management which are appropriate to the specific hydrological characteristics of arid areas and the associated management needs, and hence to define priorities for research and hydrological data (Wheater et al., 2007).

2.6.2 HYDROLOGICAL REGIME IN ARID AND SEMI ARID-AREA

Arid and semi-arid regions are defined as areas where water is at its most scarce. The hydrological regime in these areas is extreme and highly variable, where flash floods from a single large storm can exceed the total runoff from a sequence of years. Globally, these areas face the greatest pressures to deliver and manage freshwater resources. Problems are further exacerbated by population growth, increasing domestic water use, expansion of agriculture, pollution, and the threat of climate change (Wheater et al., 2007). However, there is little guidance on the hydrology of arid areas, and none on the decision support tools that are needed to underpin flood and water resource management.

2.6.3 PRESSURE IN ARID AND SEMI-ARID ENVIRONMENT

In the arid and semi-arid regions of the world, water resources are limited, and under severe and increasing pressure due to expanding populations, increasing per capita water use and irrigation. Point and diffuse pollution, increasing volumes of industrial and domestic waste, and over-abstraction of groundwater provide a major threat to those scarce resources. Floods are infrequent, but extremely damaging, and the threat from floods to lives and infrastructure is increasing, due to urban development. Ecosystems are fragile, and under threat from groundwater abstractions and the management of surface flows. Added to these pressures is the uncertain threat of climate change. Clearly, effective water management is essential, and this requires appropriate decision support systems, including modeling tools.

2.7 CLIMATE CHANGE

Fossil fuel consumption has caused an increase in anthropogenic emissions of carbon dioxide (CO2) and other greenhouse gases (IPCC, 2007). Due to higher concentrations of these gases in the atmosphere, the proportion of solar radiation hitting the Earth that is reflected back into space is reduced, leading to a net warming of the planet (Kalnay and Cai, 2003). Based on the range of emission scenarios presented to the Intergovernmental Panel on Climate Change (IPCC, 2007), CO2 concentrations are expected to increase from the present day concentration of approximately 330 pm to between approximately 550 and 970 ppm. The magnitude of this increase will depend on future human activities, as well as technological and economic development.

For all IPCC scenarios, however, General Circulation Models (GCMs) predict that increases in atmospheric greenhouse gas concentrations will raise surface temperatures. These changes will likely affect the hydrologic cycle. Among the GCMs and emission scenarios used by the IPCC, temperatures in 2100 are expected to be between 1.1 and 6.4 °C higher than temperatures in 1900, accompanied by changes in rainfall intensity and amount (IPCC, 2007). Possible changes in regional and seasonal patterns of temperature and precipitation and their implications for the hydrologic cycle are as yet poorly understood. An increase of atmospheric CO2 will directly affect plant transpiration and growth which are inherently tied to the hydrologic cycle. Experimental evidence indicates that stomatal conductance of some plants will decline as atmospheric CO2 increases, resulting in a reduction of transpiration (e.g., Wand et al., 1999; Medlyn et al., 2001; Wullschleger et al., 2002). Research has also shown that total leaf area of many plant types may increase with increased atmospheric CO2 concentrations (e.g., Wand et al., 1999; Pritchard et al., 1999; Saxe et al., 1998), potentially offsetting the reduction of stomatal conductance.

Much research has been done to elucidate the effects that climate change and increased atmospheric CO2 concentration will have on watershed processes. Studies have reported that an increase in CO2 while holding temperature and precipitation constant will cause increases in water yield (e.g., Aber et al., 1995; Fontaine et al., 2001; Chaplot, 2007). Using present day precipitation patterns, studies have shown that higher temperatures lead to increased evaporation rates, reductions in streamflow, and increased frequency of droughts (e.g., Rind et al., 1990; Nash and Gleick, 1993; Abbaspour et al., 2009). Labat et al. (2004) demonstrated that a temperature increase by 1 °C may lead to a global runoff increase by 4% due to increased oceanic evaporation. Kamga (2001) used WatBal, a hydrologic water balance model (Yates, 1996), to show that a 1 and 3°C temperature increase and a 4– 13% change in rainfall intensity would result in variations in annual river fluxes of - 3% to +18% in Cameroon. In Africa, Legesse et al. (2003) used the Precipitation-Runoff Modeling System (PRMS) model (Leavesley, 1983) to simulate runoff, predicting a runoff decrease by 30% in response to a 10% decrease in precipitation amount. A 1.5 °C increase in air temperature resulted in a runoff decrease of 15%.

In a study of climate change effects on the Missouri River in the USA, Lettenmaier et al. (1999) used output from three transient GCMs and one double CO2 GCM to evaluate potential effects of climate change on water resources. They estimated that the Missouri River would experience a reduction in streamflow between 6% and 34%, which would greatly impact economic infrastructure along the river. All of these studies indicate that watershed processes may be very sensitive to changes in precipitation, temperature and increased atmospheric CO2 concentrations. Despite many studies on the effects of climate change, up-to-date quantitative information on the effects of changes in precipitation and temperature on soil and water resources is still scarce.

2.7.1 CLIMATE CHANGE AND ITS IMPACTS ON MEDITERRANEAN WATER RESOURCES

Water is one of the most important elements for the sustainability of life on earth. Impacts of climate change in water resources as well as worldwide problems like scarcity, conservation, sanitation and management of water resources have placed the water related issues on top of the international agenda.

In the Mediterranean basin, the consequences of climate change are forecasted to be particularly severe, increasing the already existing water stress in the region, including in Southern and Southeastern Europe, North Africa and the Middle East. Phenomena such as recurrent and persistent droughts, high variability in precipitation, serious decrease of soil moisture, river flow decrease, extreme weather events, desertification, etc. are expected to increase significantly in the region and will impact on freshwater availability in terms of quantity and quality. Other serious effects of warming in the Mediterranean could be sea level rise resulting inter alia in land erosion and salt water intrusion in coastal areas, thus in the loss of inhabitable and arable land as well as serious alterations of natural habitats and damages in important ecosystems.

Water resources being already scarce throughout the whole region, in combination with increased water demand due to demographic pressure and urbanization, tourism and development needs in general, climate change is likely to lead to further environmental degradation jeopardizing directly or indirectly social cohesion, well being and quality of life as well as security in the immediate future.

CHAPTER 3: METHODOLOGY

3.1 PREAMBLE

This chapter details the various steps taken in the implementation of the research work. Modeling results largely depend on the quality of the input data; as such a lot of time was spent in ensuring the integrity of the input data such as rainfall, climatic and soils data.
A range of few models have been developed over the past 10 years as a part of a number of national and UE project. Mathematical models can offer a valid support to study watershed problems; in particular distributed models are able to identify pollution sources and to quantify the impact of human activities (point and diffuse sources) on water resources. In addition these models offer the possibilities to simulate different scenarios and to analyse related problems.

The Soil Water Assessment Tool (SWAT) was chosen as one of the models as it had been extensively used in related studies that had similar objectives of finding the impact of water harvesting system, impact of non point source and impact of climate change, among other things. Most of the input data needed to run the model was available, although in an unprocessed format.

3.2 STUDY AREA

The Merguellil basin is located in Kairouan, center of Tunisia (Figure 3.1) between the parallels 39G 60N and 39G 78 N and the Meridian 7G 55E and 8 G 35 E (Kallel et al., 1975). It is bounded by the Bellouta and Serdj mountains in the North, by El Ala plateau, Touilla and Trozza mountaims in the South, by Barbrou mountains and Kesra plateau in the West, while the basin outlet is eastward along the Kairouan valley.
The Merguellil catchment is characterized by a semi-arid climate. It extends on an area of about 1200 km² upstream of the El Houareb dam (Figure 3.1). The river network has an overall length of around 158 km. It is an intermittent river with a mean annual discharge of 0.6 m^3/s measured at Haffouz flow-gauge.

This watershed presents a hilly topography (altitude between 200 and 1200 m with a mean elevation value of 500 m) and has diversified condition of geology, morphology, vegetation and land-use. This semi-arid zone is exposed to a high variability of rainfall in time and space. Annual means vary between 300 mm in the plain and 500 mm in the highest parts. The annual mean temperature is 19.6 °C, with a maximum of 48 °C in August and minimum of -2 °C in January and the mean annual potential evapotranspiration is 1430 mm/year with a maximum of 1600 mm/year, decreasing with altitude. Half of the catchment area is cultivated with annual crops (wheat) and trees (olive and almond). Grazing lands cover 30%, forest 19%, and urban areas 1%. The population in the Merguellil catchment remains very low (1%) concentrated in the Haffouz and Zebess regions.

The water stress situation within the Merguellil catchment can be summarized as a limited resource facing an increasing water demand. Additionally, since four decades the Merguellil river basin is experiencing continuous change in its hydrologic system due to the construction of 44 hill ponds (Figure 3.1), 5 hill reservoirs (Figure 3.1), around 250 km^2 of contour ridges, and the large El Haoureb dam (Photo 3.1) at the outlet since1989. This later has a capacity of storage equal to 95 million cubic meters (Mm^3) at its principal spillway and is strongly connected to Kairouan plain aquifer. Over 60% of the inflow collected by the El Houareb dam infiltrate and recharge the aquifer (Kingumbi et al., 2004; Leduc el al., 2007). This aquifer is equipped with numerous wells having diverse purposes. Even this aquifer is over-exploited however it is easily restored.

After the floods of the Kairouan city in 1969, which caused severe human and material damages to the city, the large El Houareb dam was established with the main objective of protection of the city. However, besides reducing floods this dam served also to develop irrigated areas and to supply the city with potable water.

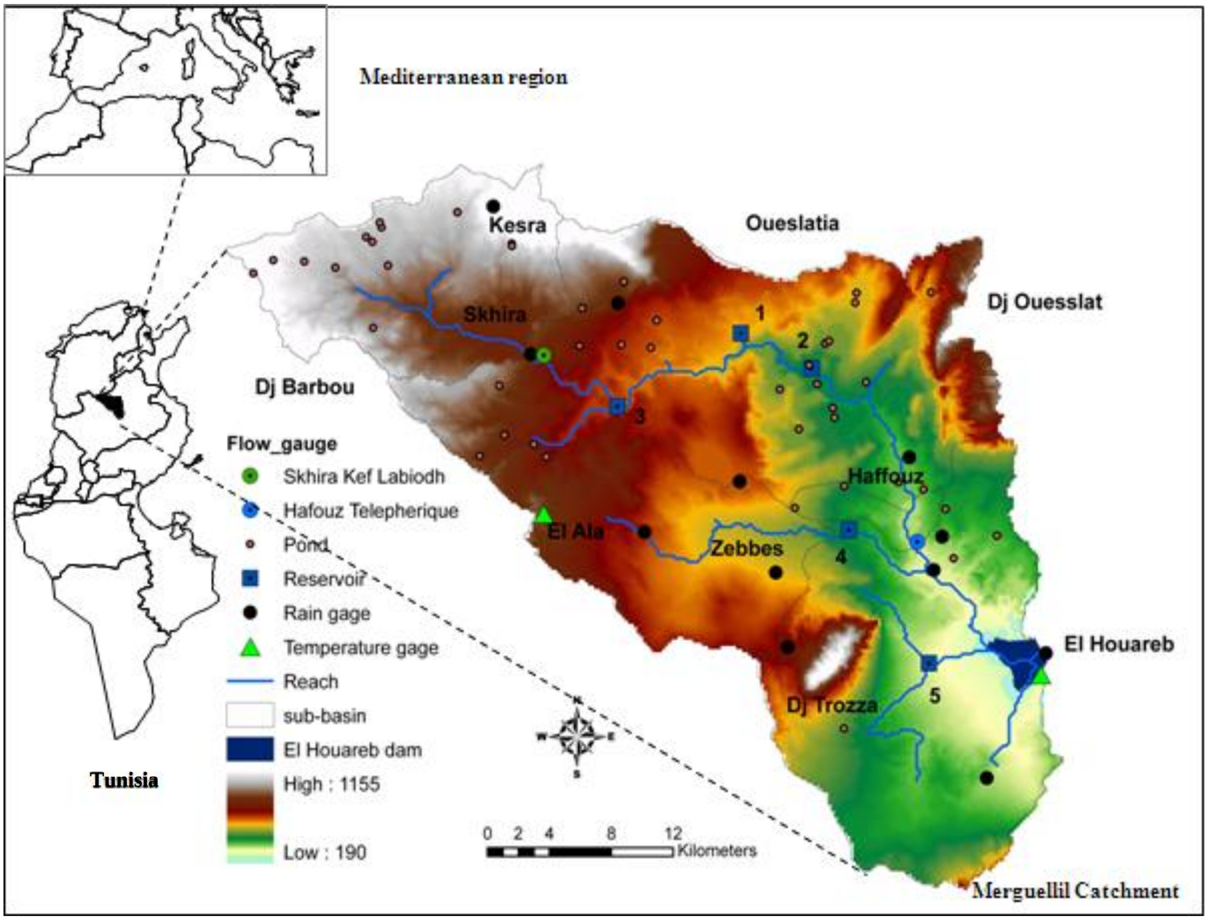

Figure 3.1 Location of the study area

Photo 3.1 El Houareb Dam on May 2007 (left) and on May 2008 (right)

3.2.1 MERGUELLIL ENVIRONMENT

The Merguellil catchment presents two contrasting aspects: an hilly upstream (1200 km^2), with an altitude between 200 and 1200 m, and a very flat downstream, part of the Kairouan plain that extends over more than 3000 km^2.

The Merguellil catchment is endorheic and river flow is not perennial, but sometimes very violent: about 80 % of the annual flow is produced in 12 days. Before the construction of the big El Houareb dam, at the border between the upstream part and the Kairouan plain, the largest floods of Wadi Merguellil reached the Sebkha el Kelbia, a large salt lake often dried up and smaller floods vanished in the Kairouan plain by both evaporation and infiltration to the aquifer. For the period 1989-2005, the mean annual flow of Wadi Merguellil calculated at the entry of the El Houareb dam was 17 Mm^3 (extremes of 2.5 and 37.6 Mm^3). The exceptional flood of the 1969 autumn were estimated at about 175 Mm^3, with a peak flow over 3000 m^3/s, which resulted in the inundation of the Kairouan plain, high human and material losses. Groundwater resources may complement the surface water resource but they are not evenly distributed: 3 small aquifers cover the lower part of the upstream catchment; the thick and large aquifer in the Kairouan plain alluvium is the most important of central Tunisia.

3.2.2 IMPACT OF HUMAN ACTIVITIES

Water has been a constant concern for the local people and the first visible works for saving water date back to the Roman Empire. Before the 20^{th} century, the little population, mainly nomadic, exploited the region as an extensive grazing area. Deep changes occurred in the last century, with a spectacular demographic growth and a rapid development of agriculture, in response to local and national incitements. Irrigation is now widely spread all over the Kairouan plain and depends on groundwater, leading to the overexploitation of the plain aquifer. In the upstream, crops are more various and irrigation less present.

In 1989, the big El Houareb dam was built for preventing catastrophic floods. In fact, the major part of the dam water infiltrates (and recharges groundwater) or evaporates. The reservoir has often dried up. Dam releases are very exceptional.

The numerous works for water and soil conservation in the upstream catchment result in a significant decrease in the river flow, and completely modify the regional water balance. Moreover they do not represent a new reliable local water resource. Water is also taken from aquifers for providing drinking water to inhabitants of the catchment but also to remote areas, along the coast where population and tourism activities are much denser.

3.2.3 PEDOLOGY

Since Tunisia is at the same time a Mediterranean and a Saharan country the soils show all the signs of this climatic, morphological and geological diversity. According to the French system of soil classification the soils of Tunisia are classified as podzols, vertisoils, red Mediterranean soils, calcic-magnesic soils (dominant soils), brown and isohumic soils, saline and hydromorphic soils and also poorly evolved soils. Their distribution is based on the catena system (Mtimet, 2000).

In the Merguellil catchment, soil texture varies from clay to coarse sand textured. The upper basin contains shallow soil over a limestone crust rigid, the rest of the basin is composed of deep sand on sandstone.

The soil map of the Merguellil catchment (Figure 3.2) presents four main units: poorly evolved soils, Carbonate soils (calci-magnesic), Iso-humic soils, and mineral soils resulting from erosion (association).

- **Poorly evolved soils**, either wind borne or flu-vial, form the best agricultural lands of south west (oasis or Ségui soils). In fact, they are deep (>1.50 m) and have silty-loam to sandy texture. Organic matter can barely exceed 0.5%. Gypsum accumulations could be present at medium depths of 40 - 60cm and gypsum borne crust is therefore present almost everywhere at the boundaries of garaâts and chotts. Of course, salinity appears from bottom to upper layers. Its content varies according to the cultivation patterns. In most cases, these soils show spots of water logging and salinity as found in Ne-fzaoua, Gherib, Jerid, Gafsa regions (Mtimet, 2000; Mtimet, 1999, Raspic, 1999).
- **Iso-Humic soils** are brown soils with dominantly coarse texture. They are rather deep with an organic matter content ranging from 0.5% to 1.5%. On the plateau of Sidi

M'hedeb and Sfax, they have calcareous crusting, which allows them to be associated to calcicmagnesic soils. Which due to their erosion residues (high sand content) have a moderate retention capacity (60-80 mm m^{-1}) (Mtimet et al, 1996, 1997; Mtimet, 2000).

- **Carbonate soils (calcic-magnesic)** cover the north-west part of the basin where irrigation is poorly developed. Characteristically they possess a low field capacity (30-60 mm m^{-1}). They regularly cover calcareous parent materials. Their thickness is variable following the general ground morphology. They exhibit crusted horizons or contain coarse calcareous elements (Mtimet, 2000; Mtimet, 1999).
- **Mineral soils resulting from erosion (association).** The valleys and the slopes are generally covered with calcareous or gypsum nodule-soils. This Soil type is more presented in Mountains, where the calcimagnesic soil formed a continuous cover formerly balances with a good forest cover. The outcrop of the bed rock is due to important erosion started by the degradation of the vegetation. This degradation is more visible on the broad marly outcrops located at the south of Makthar.

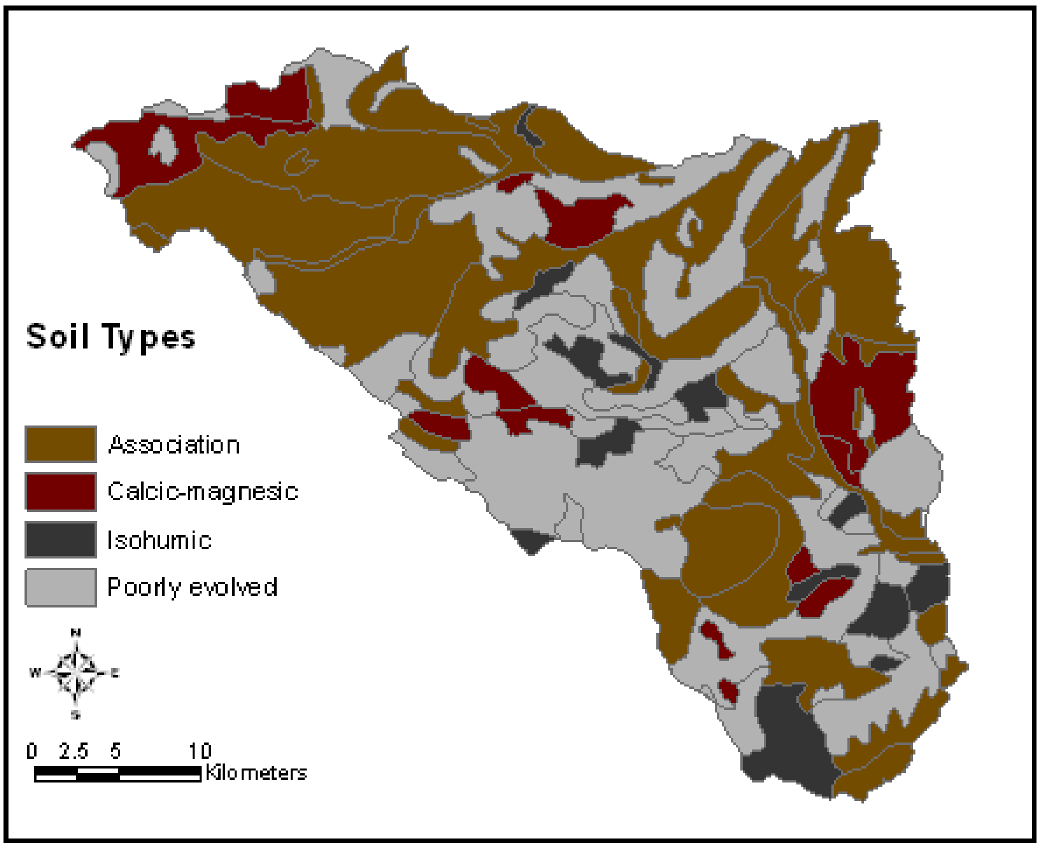

Figure 3.2 Soil map of the Merguellil catchment

3.2.4 LAND USE

The Vegetation cover decreases from upstream to downstream. The upper part of the basin is covered by forest, which accounts for 18.5 % of the total basin area; pasture for another 21.5%, mainly in the central region, an urban area is concentrated in the small cities of Haffouz, el Ala and Kesra and presents (0.5%), water bodies (2.5%) while crops cover the remaining 57%, chiefly in the south east and north (kingumbi 1999) (Figure 3.3).

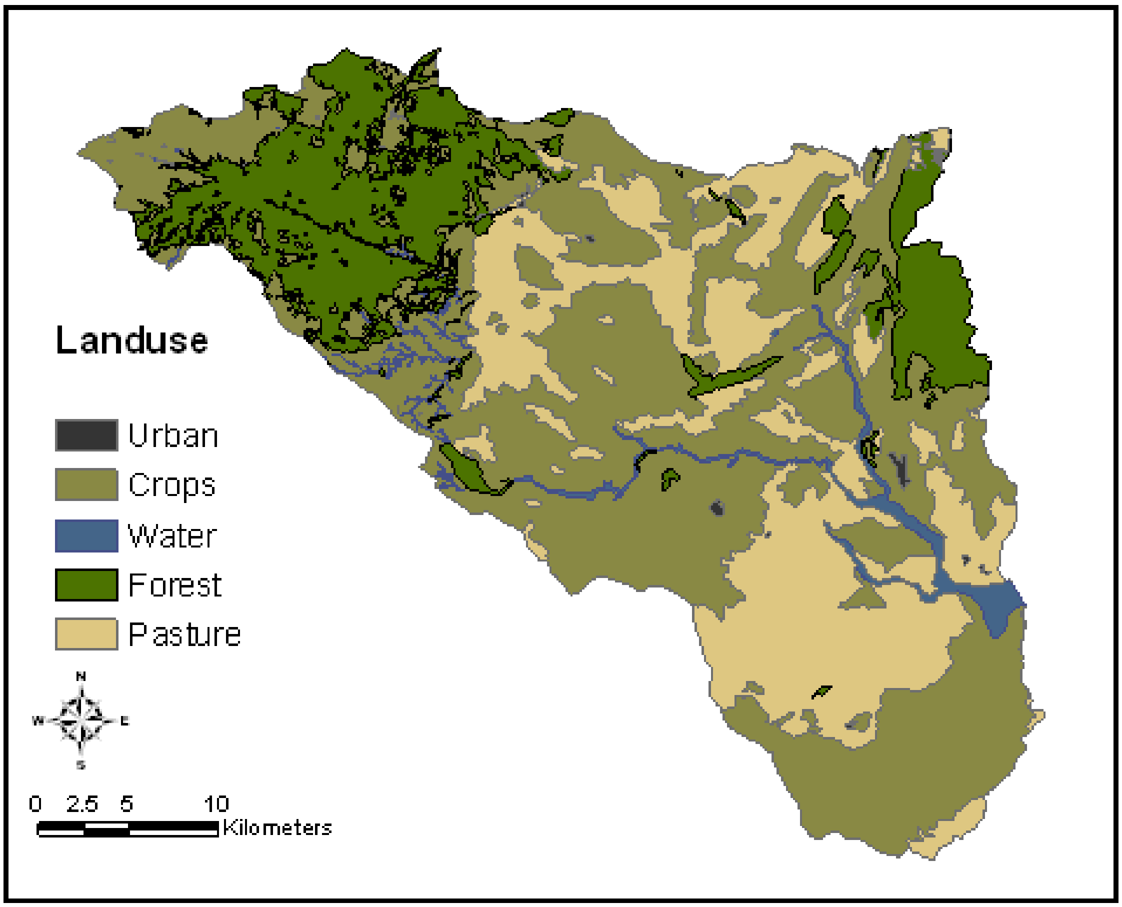

Figure 3.3 Land use map of the Merguellil catchment (Direction Générale des Forêts, 1996)

The upper catchment is underlain by sedimentary deposits, mainly limestone, with alluvium along the larger valleys. In the lower catchment the Kairouan plain is a collapsed basin filled with a laterally and vertically heterogeneous sequence of Pliocene - Quaternary flood deposits bought down by the Zeroud and Merguellil rivers; these deposits are up to 700 m thick.

2.3.5 PRECIPITATION

The climate of central Tunisia is characterized by rains not very abundant, rare, but sometimes stormy and often brutal, distributed over all the year with a maximum in autumn and in spring. The irregularity and variability are the typical characteristics of this zone on all the scales (annual, monthly and daily). Generally the North-western slopes receive more rains than the South-eastern slopes. Moreover, rains of autumn prevail on the rains of spring. The catchment area of Merguellil belongs to low rainy zone with annual precipitation from 200 to 400 mm distributed out of 40 to 70 days of rain. According to the Emberger classification, The North western part of the Merguellil catchment is situated in the superior and inferior semi-arid boundaries, while the rest of the basin like Kesra, Trozza and Djbel Oueslat belong to the inferior Semi-arid boundary (CES, 1986).

3.2.5.1 SPATIAL DISTRIBUTION OF PRECIPITATION IN THE MERGUELLIL CATCHEMENT

Precipitation decreases from the upstream to the downstream; the highest values are recorded at the Kesra.F and Skhira stations in the upstream of the catchment, while the lowest value is at EL Houareb rain-gage. Precipitation varies with altitude; indeed the highest values are observed on the plate level such as that of Makthar and El Alaa, land on mountains which form the relief of the basin like Djebel Trozza. Generally, the North-western part of the catchment receives more rains than the South-eastern part (Figure 3.4).

Mean monthly precipitation over a period of 10 years (1990-2005) on the totality of the Merguellil catchment is presented in Figure 3.5. We note that most rainy months are September (50mm) and January (41mm). From May, monthly precipitations decrease until reaching the lowest values in July.

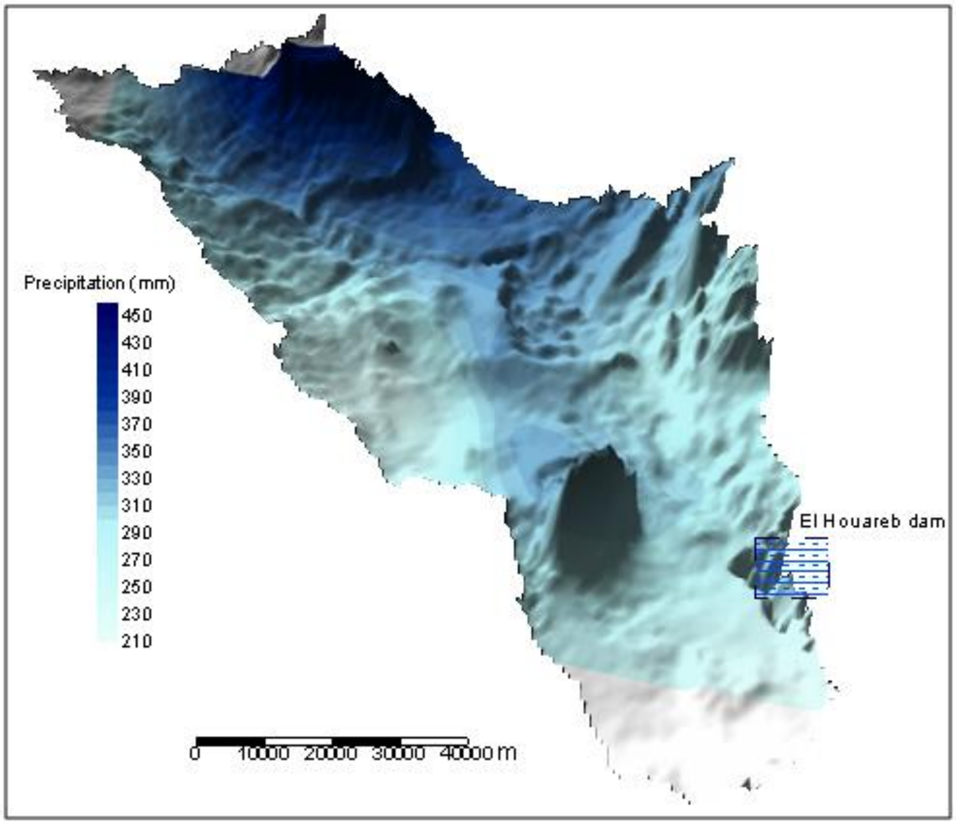

Figure 3.4 Spatial distribution of precipitation in the Merguellil catchment

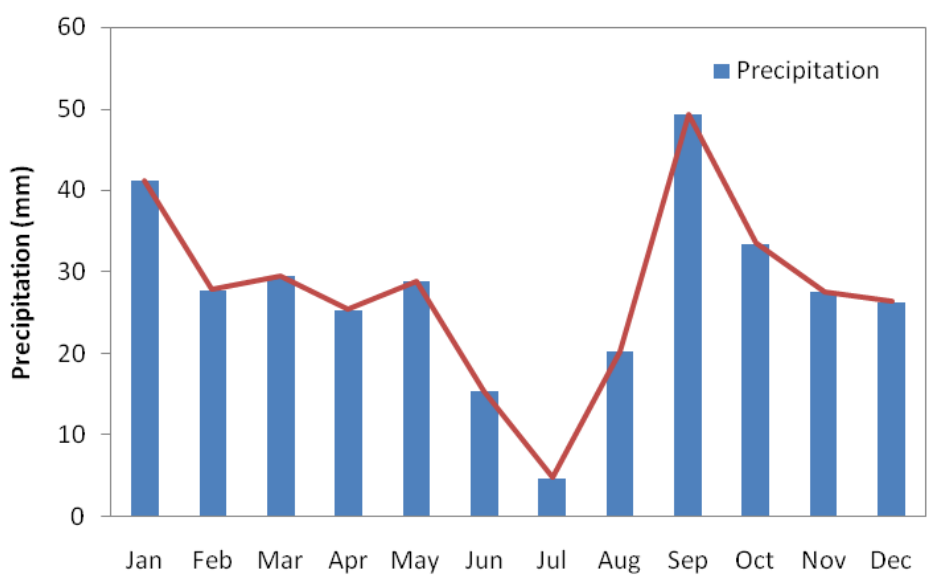

Figure 3.5 Mean monthly precipitations in the Merguellil catchment based on measured data in all rain-gages from 1990 to 2005

3.2.6 TEMPERATURE

No temperature gages were located within the watershed, and even the available stations in the proximity of the basin [Kairouan (1901-1979), Makthar (1901-1979) and Sbiba (1964-1982)] have records that do not cover the simulation period (1986-2005).

The mean monthly temperatures within the Merguellil catchment fall below 10 ° C during December, January and February. They are between 10 and 20 °C during October and November and during April and May.

The hottest months in the basin Merguellil are July and August. In these months, the monthly mean maximum temperatures exceeded 10 °C, but they stay below 35°C. The coldest period of the year is the winter months from December to February, with average monthly minimum below 5 ° C. They remain below 10 ° C during November, March and April and exceed this threshold, the rest of the year.

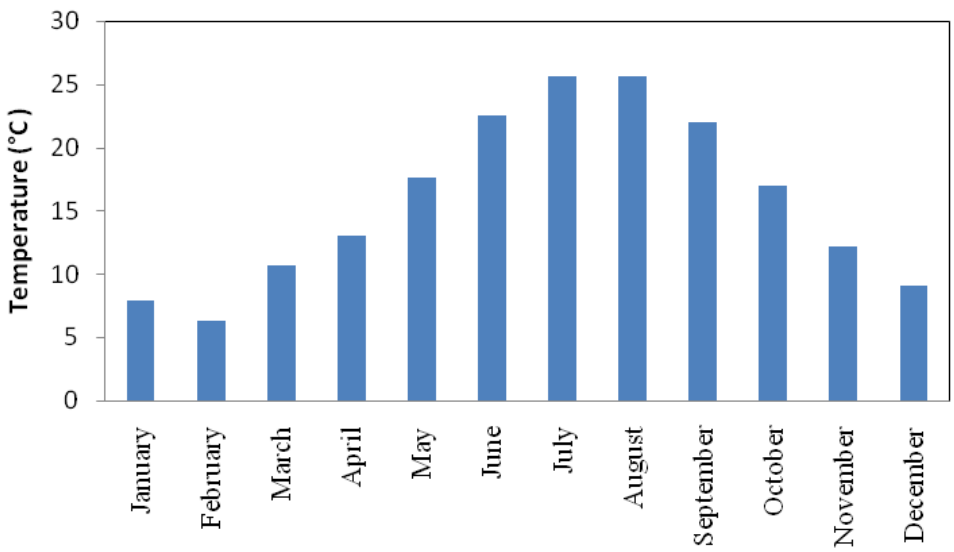

Figure 3.6 Mean monthly temperatures in the Merguellil catchment based on measured data in Sbiba, Makther and kairouan stations from 1972 to1982

3.2.7 HUMIDITY

Relative humidity is the ratio between the amount of water vapor in the air and maximum absorption capacity of the air at a given temperature. The mean monthly value oscillates between 55% and 70% during the cold season and between 40% and 55% during the warm season.

The climate is moderately dry from September to April and very dry from May to August. Relative humidity increases in the presence of thunderstorms and lowered during sirocco (hot wind). In Kairouan, it is high during October (65%), November (61%), December (64%), January (65%) and low in June and July (48%), August (50%).

3.2.8 EVAPOTRANSPIRATION

The average annual actual evaporation over the basin, measured at lakes Fidh Ali,Fidh Ben Naceur and El Morra by the Colorado method (IRD and CES, 1998), is approximately 1600 to 2000 mm close to that measured in Kairouan (2100 mm).

3.2.9 STREAMFLOW

The major function of the streamflow data is to compare and calibrate simulated runoff; hence its integrity is important. Calibration is done using the longest uninterrupted time series (Chapter 4.1.2 calibration and validation).

There are a total of 2 gauging stations within the catchment with daily discharge data obtained from DGRE kairouan. The data from the gauge stations are summarized in Table 3.1.

Table 3.1 Summary of streamflow gauging stations

Station ID	Station name	Start year	End year	Missing data
1486100340	Skhira Kef labiodh	1974	2003	10 months
1486100170	Haffouz telepherique	1984	2003	16 months

The locations of the Skhira Kef Labiodh and Haffouz flow-gauges used for the project are also shown in Figure 3.1.

De Girolamo el al, (2008) analysed the flow change rate at the Skhira Kef Labiodh station using the Richards-Baker (Baker et al., 2004) Flashiness Index. This index measures streamflow variations in response to rainfall events, per daily unit discharge.

$$R-B\,Index=\frac{\sum_{i=1}^{n}\left|q_{i-1}-q_i\right|}{\sum_{i=1}^{n}qi}$$

In which i is the day number, q_i and q_{i-1} are the discharges on day i and day i-1, respectively.

A high degree of flashiness indicates that a river is quick to respond to the rainfall events. This behavior is typical for basins characterized by steeper or rolling topography, often with a low degree of soil permeability, or with a significant impervious area. Conversely, low values of R-B Index are typical for basins with flat terrain, whose soils are often highly permeable, and with a high degree of shallow groundwater recharge.

The high value of the flashiness index at the Skhira station (1.46) explains that the river has a flashy character. The river has a quick response to the rainfall event. Other indices in the same river were calculated are shown in Table 3.2.

Table 3.2 Overview of Indices results and some characteristics of the Merguellil catchment on the Skhira Kef labiodh flow-gauge (De Girolamo et al., 2008)

R_B: Richards-Baker Flashiness Index, DCV: Daily Variation Coefficient, BF: Baseflow Index, And AI: Aridity Index.

Stream	State	Area (Km^2)	R-B Index	AI Index	DCV Index	BF Index	Q max (mm)	Q min (mm)	Annual discharge 10^6 m^3
Skhira	TN	180	1.46	0.22	768	0.09	55.10	0.00	6.94

Comparing R-B index trends between 1970 and 1998, it can be observed that in the Skhira subbasin (180 km^2) there was an increase in the index over time (Skhira, Triolo, Celone). Considering only data recorded in the decade 1985-1995, it appears that the R-B Index trend line slopes can change. It can be observed from Figure 3.7, showing the trends in R-B Index values reported for the Skhira show a greater variability, ranging between 0.98 and 1.90. This can be attributed to its greater variability in annual discharge.

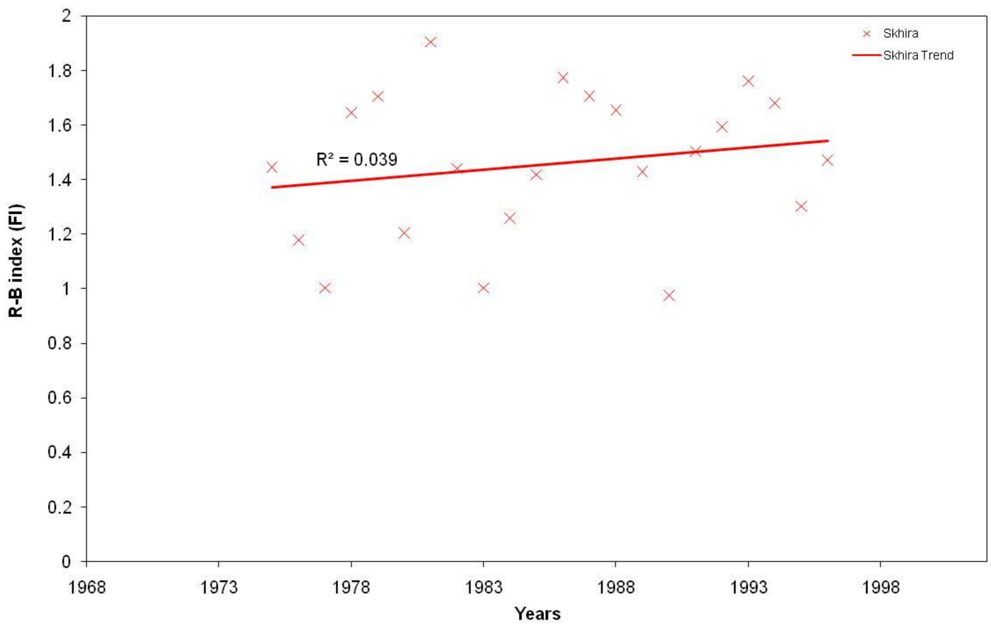

Figure 3.7 Trends in R-B Index at the Skhira basin (De Giorlamo et al., 2008)

3.2.8 SOIL AND WATER CONSERVATION WORKS

In the 1990's, the Tunisian government and international donors have subsidized the construction of WSCW (contour ridges and small dams) to reduce gully formation and allow supplemental irrigation in the Merguellil catchment (Figure 3.8). Between 1989 and 2005, 44 small dams were built, collecting runoff from 128 km^2. Contour ridges were constructed over 234 km^2 of lands, 12% of which located within the catchments of the small dams. As of 2005, WSCW collects runoff from 28% of the Merguellil catchment surface area. 97% of WSCW-controlled areas are located outside the Merguellil headwater catchment in the downstream part of the Merguellil catchment where they control 32% of the surface area. The forest in the upper sub-catchment probably explains why WSCW are almost absent from this area.

Three kind of water harvesting techniques are presented in the study area: Five large reservoirs (Figure 3.8) located on the main channel network; they receive the water from all subbasins upstream from of the water body; 44 small dams (Figure 3.8) collecting headwater flow and providing supplemental water for irrigation; and Contour ridges were constructed over 234 km^2 of lands, 12% of which located within the catchments of the small dams.

3.2.8.1 SMALL AND LARGE DAMS

Hill ponds are small compacted earth dams with a height of the dam varies between 5 and 8m and length from 100 to 300 m and the average capacity is 0.1 million m^3. They are equipped with floodway for 1 or 2 m from the coast to the crest and an underground fighter and sampling which crosses the dam. Largest dams are called hill reservoirs. Their heights are 8 to 12 m and can store over 1 million m^3 (Ghola, 1993).

These structures (Hill ponds and hill reservoirs) have a relatively high cost compared to volume stored water: The dams are generally designed to improve local agriculture. They have an important role on the retention of sediment and protect big reservoirs from silting and water recharge groundwater (DGF and GTZ, 1994).

In the absence of other techniques of water transfer, ponds are the best way to initiate a process of local development. The sites chosen are not only dictated by the characteristics of the physical environment, but also depend on the willingness of people to participate in development project of territory (Selmi and Talineau, 1995).

The hill ponds have different size: 37% of these ponds were built in the sixteen's within an American project for the development of watershed Merguellil. They are totally or partially silted as a result of the exceptional flood of 1969 (Photo 3.2). The ponds built after 1969 are partly clogged by 10% to 80%: these are the ponds that have more water resources. The ponds were built primarily to protect the reservoirs against silting (Ben Mansour et al., 1994). In the 90s the construction of large hill reservoirs that contain more important water. (Photo 3.3) The biggest reservoir is El Kharroub (1.27 million m^3). Data about the hill ponds reservoirs were provided from the CES Kairouan (Direction de Conservation des Eaux et des Sols).

According to some statistics collected by the Office of the Ministry of Agriculture showed that the speed of construction of these ponds is much higher than the rate of exploitation (Bouzid, 1998). The analysis of the diversity of crop management systems around the ponds made in 1996 shows that 50% of farmers have not introduced the Irrigation and retains their traditional production, 28% begin to use the water in their agricultural production function, and 22% are engaged in small irrigation (Albergel and Rejeb, 1997).

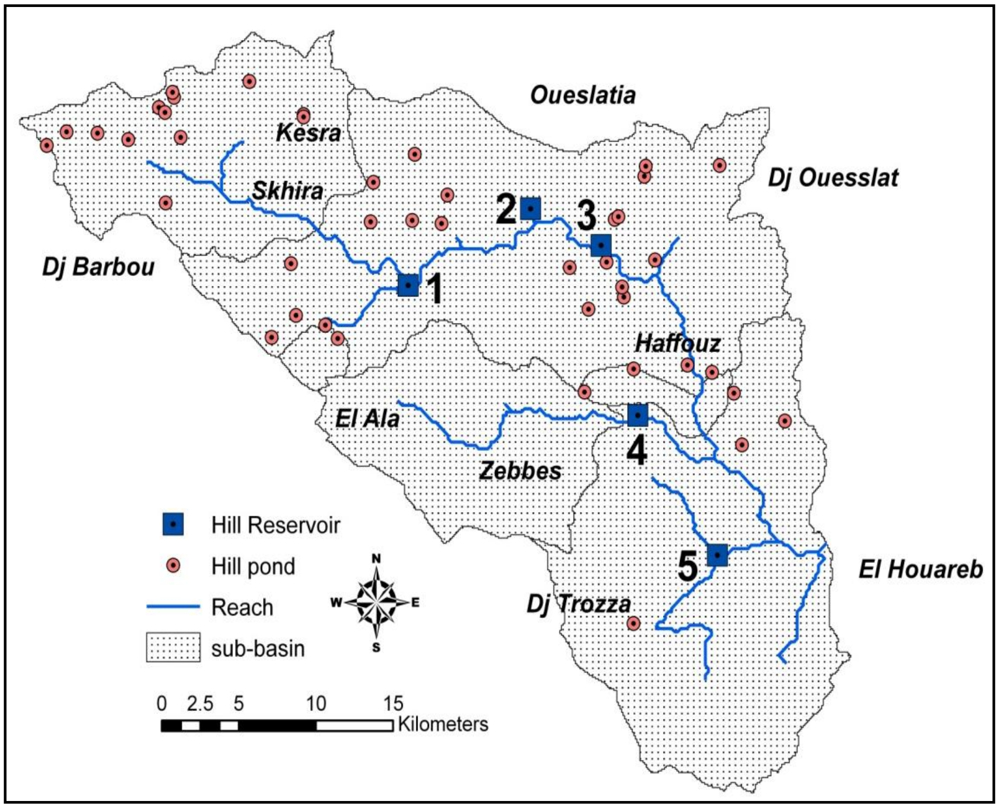

Figure 3.8 Large and small dams (hill pond and hill reservoir) in the Merguellil catchment

Photo 3.2 Siltation of El Maiz pond

Photo 3.3 El Morra reservoir

3.2.8.2 CONTOUR RIDGES

The Contour ridges have been used in many parts of the world as a soil and water conservation technology. There has been a forceful adoption of this technology through many countries' legislation as the example of Tunisia where since the 1990's, the Tunisian government has started to subsidize the construction of Water and Soil Conservation Works (WSCWs).

In the Merguellil catchment contour ridges were constructed over 230 km^2 of lands. Contour ridges are small earth structures constructed across the curve levels (Photo 3.4). The main objective for their construction is to reduce the erosive power of surface runoff resulting in the reduction of soil erosion and to increase local infiltration (Photo 3.5).

Soil conservation implies also indirectly water conservation. In fact, since the water conservation capacity of a soil depends on the soil depth, thus when a soil profile is conserved by minimizing erosion its depth remains large and with it water holding capacity. In the Merguellil catchment, besides increasing the amount of water added to the soil profile, contour ridges intent also to protect downstream reservoirs against silting (Achour and Viertman, 1993 ; CES et al., 1995) as they constitute a good sediment traps. In addition these contours are adopted to familiarize the farmers to plant along the curve levels. The design of the ridges is done in a manner to prevent overtopping by runoff. Ridges follow the contour at a spacing of usually 1 to 2 meters. Runoff is collected from the uncultivated strip between ridges and stored in a furrow just above the ridges (Critchley and Klaus 1991).

Crops are planted on both sides of the furrow. The length of contour ridges is variable since they can be interrupted by any obstruction making difficult their alignment. In the Merguellil watershed the spacing between ridges ranges from 5 m (at El Ala and Haffouz) and 8 m (at El Hammam). Contours ridges induce considerable terrain loss; considering a contour ridges spaced of 6.5 m with a length varying from 200 to 500 m, the terrain loss per hectare oscillates between 13 and 32 % which is not negligible particularly in cultivated lands.

According to CES et al., (1995), it is more suitable to construct the contour ridges under the following conditions:

- Rainfall: 300 - 400 mm/year,
- Low rainfall intensity. This is not the case of semi arid climate ,
- Slopes: 4 – 6 %,
- Soils: fertile and quite deep soils (at least 80 cm) with a suitable infiltration rate.

Photo 3.4 Contour ridges in the Merguellil catchment Photo 3.5 water retention by contour ridges

The surface converted into contour ridges spread over time is presented in Table 3.3. Until 1970, the contour ridges were located mainly in the center of the basin. During the last decade, they were gradually extended to the entire basin (Figure 3.9).

Table 3.3 Surface area converted to contour ridges in the Merguellil catchment from 1970 to 1998

Year	Area with contour Ridges (Ha)
1970	1600
1980	2310
990	9743
1998	19600

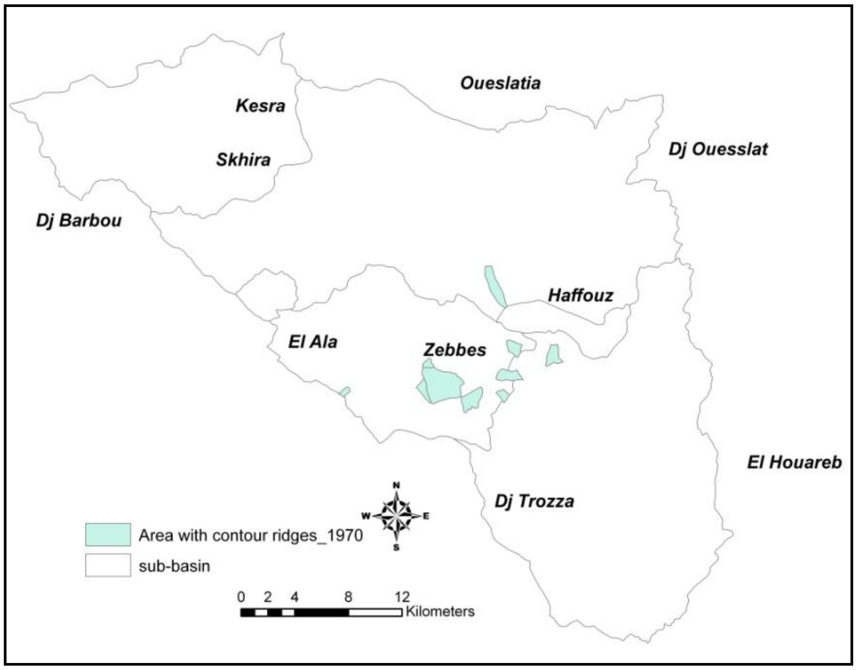
Oueslatia
Kesra
Skhira
Dj Ouesslat
Dj Barbou
Haffouz
El Ala
Zebbes
El Houareb
Dj Trozza
N
W
E
S
Area with contour ridges_1970
sub-basin
0 2 4 8 12
Kilometers

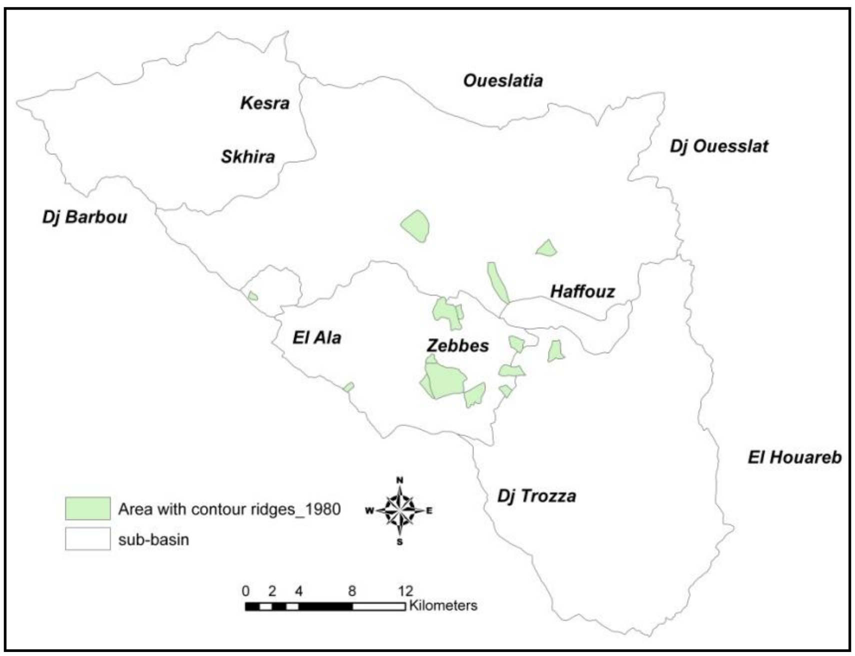
Oueslatia
Kesra
Skhira
Dj Ouesslat
Dj Barbou
Haffouz
El Ala
Zebbes
El Houareb
Dj Trozza
N
W
E
S
Area with contour ridges_1980
sub-basin
0 2 4 8 12
Kilometers

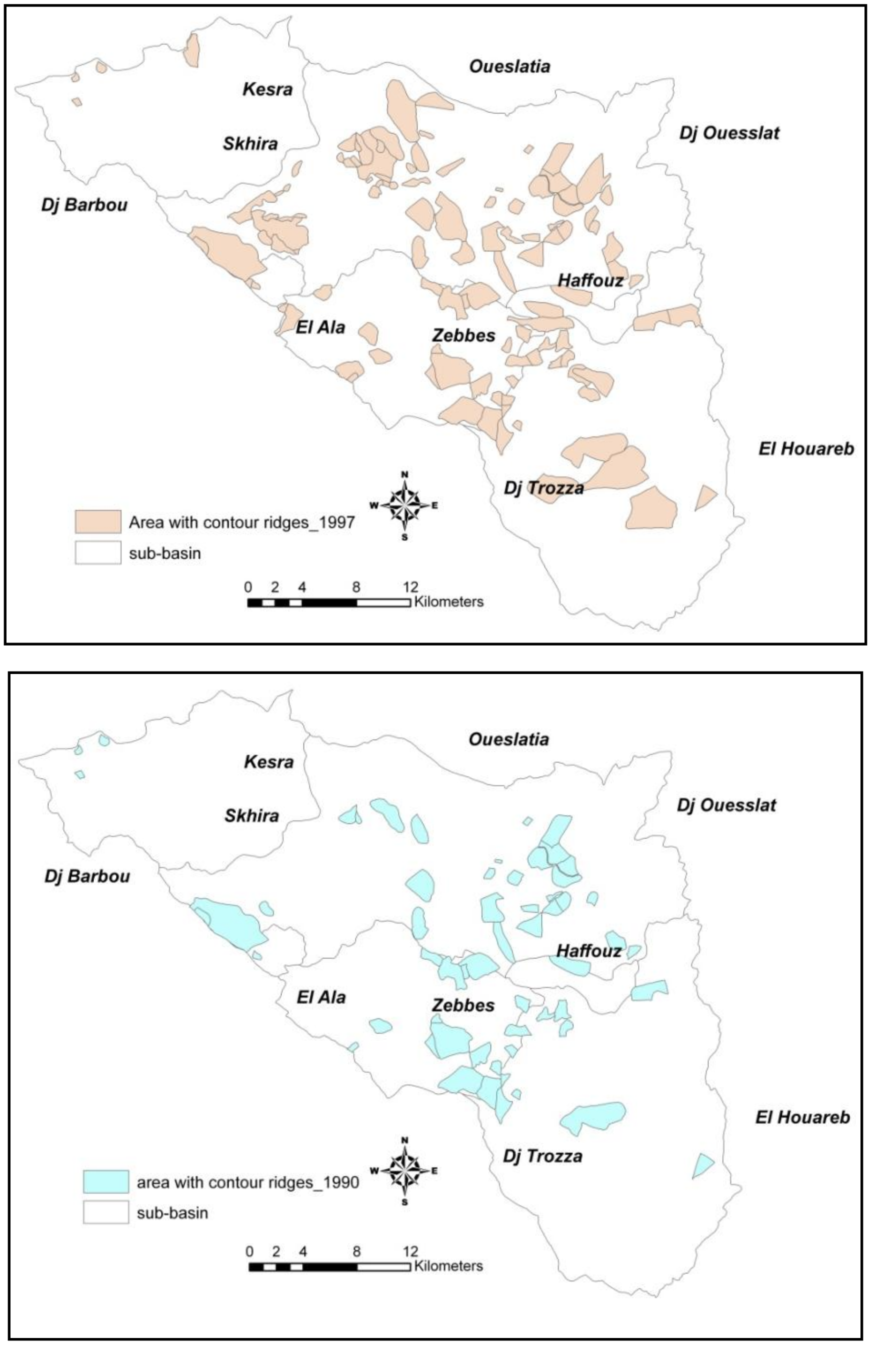

Figure 3.9 Evolution of the area converted to contour ridges in the Merguellil catchment

3.3 THE HYDROLOGIC SIMULATOR (SWAT)

SWAT is a basin scale, continuous time model that operates at either a sub daily or daily time step and is designed to predict the impact of management on water, sediment, and agricultural chemical yields in un-gauged basins (Arnold et al., 1998). The model was developed by the United State Department of Agriculture, Agricultural Research Service (USDA-ARS) to assist water resource managers in assessing water supplies and nonpoint source pollution on watersheds and large river basins (Arnold et al., 1994).

The model is physically based and therefore requires specific information about weather, soil properties, topography, vegetation, and land management practices occurring in the watershed.

SWAT simulates physical processes of plant growth, hydrology, erosion and pesticide transport using soils, land use, climate and topography as primary inputs. SWAT can run at either a sub daily or daily time step.

3.3.1 MODELING APPROACH AND STRUCTURE

The conceptual framework for SWAT consists of a two stage modeling approach; the first is constituent generation (runoff, sediments, nutrients, pesticides) and the second is transportation (or routing) of the constituents through a stream network.

The SWAT Arcgis interface is used to partition a catchment into a number of sub-catchments using an inputted digital elevation model (DEM). This is an automated process with a model user defining the minimum area threshold for sub-catchment delineation (Neitsch *et al.*, 2001). Sub-catchments are linked by a network of nodes and channels to represent a stream network for a catchment area. Within each sub-catchment there can be one or many hydrologic response units (HRUs), which represent a unique combination of land use, soil type, and slope.

The user may chose to have every HRU combination that occurs represented in the model, or may chose to set a minimum area threshold to limit the number HRUs to be modeled. Computational efficiencies are gained by selecting a threshold to minimize the number of HRUs. All matching HRU combinations within a single sub-catchment are considered as a lumped area in the model.

Runoff and other constituents are generated at HRU scale. Agricultural practices such as tillage type, irrigation, and fertilizer application rates and methods, can be explicitly described and simulated for each HRU.

SWAT can be described as a semi-distributed model, with each sub-catchment distributed spatially and matching HRU lumped within a sub-catchment. Unlike a fully distributed model no interactions and no fluxes occur across boundaries of HRUs within the model (Chen and Mackay, 2004). Instead, streamflow and pollutant loads generated at HRU scale within a sub-catchment are summed on an area weighted basis and used as input to the sub-catchment channel reach. SWAT then models constituent routing (including losses and transformations) through channel sections to the catchment outlet.

No matter what type of problem studied with SWAT, water balance is the driving force behind everything that happens in the watershed. To accurately predict the movement of pesticides, sediments or nutrients, the hydrologic cycle as simulated by the model must conform to what is happening in the watershed. (Neitsch *et al.*, 2001).

The hydrologic cycle, as it applies to water held in a soil, simulated by SWAT is based on the water balance equation:

$$SWt = SW0 + (Rday - Qsurf - Ea - Wseep - Qgw)$$

Where;

SW_t is the final soil water content (mm H_2O),

SW_0 is the initial soil water content on day *i* (mm H_2O),

t is the time (days),

R_{day} is the amount of precipitation on day *i* (mm H_2O),

Q_{surf} is the amount of surface runoff on day *i* (mm H_2O),

E_a is the amount of evapotranspiration on day *i* (mm H_2O),

w_{seep} is the amount of water entering the vadose zone from the soil profile on day *i* (mm H_2O), and

Q_{gw} is the amount of return flow on day *i* (mm H_2O).

Soil water is updated on a daily basis by any rainfall exceeding daily runoff volume. Infiltration is partitioned into a soil profile from the surface, filling subsequent layers to total porosity. When a soil profile layer is above its defined field capacity, soil water redistribution occurs. Downward movement of water can be limited by the saturated hydraulic conductivity of individual soil layers. Redistribution from the lowest profile layer is assumed lost to the system as deep drainage. Water can be lost from the soil profile as transpiration and soil evaporation.

SWAT models rainfall-runoff partitioning processes using the Soil Conservation Service curve number method (SCS, 1972). Rainfall may be intercepted and held in the vegetation canopy or fall to the soil surface. Water on the soil surface can infiltrate into the soil profile or flow off as runoff. Infiltrated water is held in the soil profile until it is evaporated or transpired. Water in excess of the soils water holding capacity drains through to recharge aquifer systems or flows laterally to intersect the surface again and contributes to runoff. The potential pathways of water movement simulated by SWAT in a HRU are illustrated in Figure 3.10.

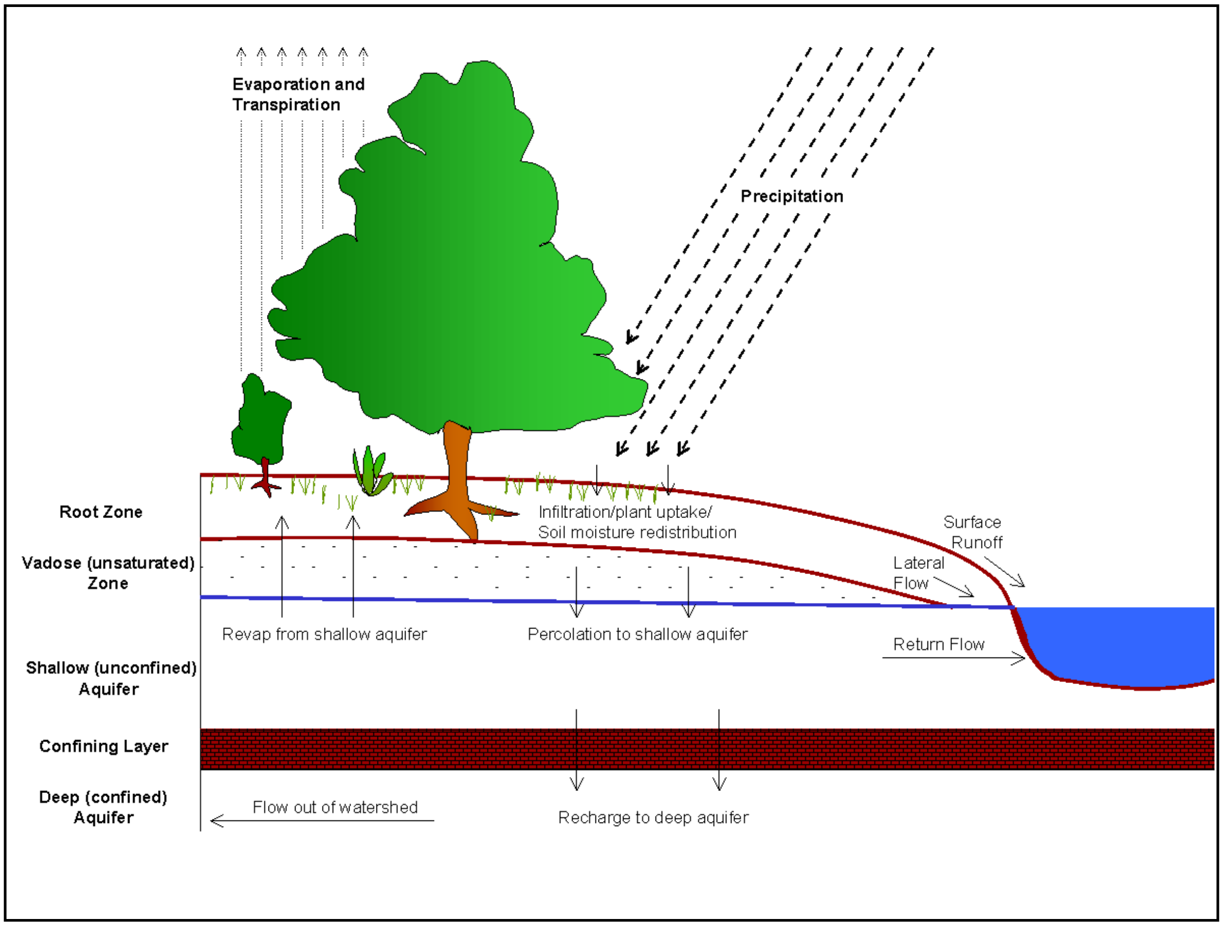

Figure 3.10 Schematic representation of a HRU hydrologic cycle (Source: Neitsch et al., 2001)

Surface runoff is routed through the channel system using the Muskingum routing method. The Muskingum routing method represents the storage volume in a channel reach as a conceptual combination of wedge and prism storages. When a flood wave moves through a reach segment, inflow initially exceeds outflow and a wedge of storage is produced. As the flood wave recedes outflow exceeds inflow and a negative wedge is produced. In addition to wedge storage, a reach segment contains a prism of storage formed by a volume of constant cross-section along a reach length.

3.3.2 PLANT GROWTH

SWAT uses a plant growth model based on heat unit (HU) and leaf area index (LAI) method of Watson (1947). A HU is defined as each 1 degree above a specified minimum value for a particular crop accumulated on a daily basis, and plant heat units (PHU) are the total accumulated heat units required for a plant to reach maturity. Leaf area development follows an optimal curve under non-limiting conditions, and LAI achieved is controlled by accumulation of HU's. Root length development, important to characterize plant access to soil water supply, is similarly controlled by HU accumulation. SWAT also models nutrient cycling and plant development can be limited by availability of either nitrogen or phosphorus. Once the maximum leaf area and root depth are attained they remain constant until plant death.

Potential evapotranspiration (PET) of a plant can be calculated in SWAT using the Hargreaves (1985) method. The Hargreaves method is given in the following Equation

$$\lambda E0 = 0.0023 . H0 . (Tmax - Tmin)0.5 . (Tav + 17.8)$$

Where;

λ is the latent heat of vaporization (MJ kg^{-1}),

E_o is the potential evapotranspiration (mm d^{-1}),

H_0 is the extraterrestrial radiation (MJ m^{-2} d^{-1}),

T_{max} is the maximum air temperature for a given day (°C),

T_{min} is the minimum air temperature for a given day (°C), and

T_{av} is the mean air temperature for a given day (°C)

While SWAT provides other options to calculate PET, the Hargreaves (1985) method was chosen for use in this project because the necessary data were readily available. This method requires daily maximum and minimum temperature and radiation values as a minimum data set. Other options to calculate PET in SWAT require data such as relative humidity and wind speed, which were not available for the study area.

Actual evapotranspiration, which includes both transpiration and evaporation, is calculated on a daily basis as a function of PET. It incorporates extent to which leaf area has developed which controls transpiration (E_t) and the level of soil covered by crop residues and leaf area which controls soil evaporation (E_s).

$$Et = E0.LAI\ 0\ /3.0 \quad 0 \leq LAI \leq 3.0$$

$$Et = E0 \quad LAI > 3.0$$

$$Es = E0.covsol$$

Where;

Eo is the PET (mm d^{-1})

LAI is the leaf area index, and

covsol is the soil cover index.

Crop biomass is modeled as a function of leaf area development and light interception. Intercepted sunlight is converted into biomass using radiation use efficiency for each plant species. Default values are provided in SWAT but can be defined by a model user. The maximum increase in biomass on a given day is estimated from intercepted photosynthetically active radiation (Monteith, 1977):

$$\Delta bio = RUE.Hphosyn$$

Where;

Δbio is the potential increase in total plant biomass on a given day (kg/ha),

RUE is the radiation-use efficiency of the plant (kg/ha $(MJ/m^2)^{-1}$ or 10^{-1} g/MJ), and

Hphosyn is the amount of intercepted photosynthetically active radiation on a given day (MJm^{-2}).

The amount of daily solar radiation intercepted by leaf area of the plant is calculated from Beer's law:

$$H\ phosyn = 0.5.Hday.(1.exp(Kl.LAI =))$$

Where;

Hday is the incident total solar (MJ m^{-2}),

K_l is the light extinction coefficient, and

LAI is the leaf area index.

Upon maturity of annual crops a percentage of biomass is removed as crop yield and the remainder converted to stubble residue. Stubble residue mass is reduced at a constant percentage per day to simulate decay.

3.3.3 EROSION AND SEDIMENT TRANSPORT

Sediment yield is estimated for each HRU by the Modified Universal Soil Loss Equation (MUSLE) as described by Williams (1975) as:

$$Sed = 11.8.(Qsurf \, . q \, peak \, . area \, hru)0.56. K_{\text{USLE}}. C_{\text{USLE}}. P_{\text{USLE}}. PS_{\text{USLE}}. CFRG$$

Where;

sed is the sediment yield on a given day (metric tons),

Q_{surf} is the surface runoff volume (mm/ha),

q_{peak} is the peak runoff rate ($m^3 \, s^{-1}$),

$area_{hru}$ is the area of the HRU (ha),

K_{USLE} is the USLE soil erodibility factor (0.013 metric ton m^2 hr/(m^3-metric ton cm)),

C_{USLE} is the USLE cover and management factor,

P_{USLE} is the USLE support practice factor,

LS_{USLE} is the USLE topographic factor, and

CFRG is the coarse fragment factor.

The Universal Soil Loss Equation (USLE) uses rainfall as an indicator of erosive energy to estimate long term average erosion whereas MUSLE uses daily runoff amount and peak runoff rate to simulate daily erosion and sediment yield. The peak runoff rate is an indicator of the erosive power of a storm and so can be used to predict sediment loss (Neitsch *et al.*, 2001).

Calculation of runoff volume has been described earlier and SWAT calculates the peak runoff rate with a modified rational method. The peak runoff rate is the maximum runoff flow rate that occurs with a given rainfall event.

The amount of sediment that is transported from a reach segment per day is calculated by multiplying streamflow and sediment concentration, where the sediment concentration is calculated as:

$$Conc_{\text{sed,ch,mx}} = C_{\text{sp}} \,.\, V_{\text{ch.pk}}^{spexp}$$

Where;

Conc $_{\text{sed,ch,mx}}$ is the maximum concentration of sediment that can be transported by the water (ton m^3 or kg L^{-1}),

c_{sp} is a coefficient defined by the user,

$V_{ch.pk}$ is the peak channel velocity (m s^{-1}), and

spexp is an exponent defined by the user. The exponent, spexp, normally takes a value of 1.5 (Neitsch *et al.*, 2001).

The peak channel velocity, $v_{ch,pk}$, is calculated from the discharge equation:

$$Vch,pk = \frac{q_{\text{ch,Pk}}}{A_{\text{ch}}}$$

Where;

$Q_{ch,pk}$ is the peak flow rate (m^3 s^{-1}), and

A_{ch} is the cross-sectional area of flow in the channel (m^2). The peak flow rate is defined as:

$$Q_{\text{ch,pK}} = prf \,.\, q_{\text{ch}}$$

Where;

prf is the peak rate adjustment factor, and

q_{ch} is the average rate of flow ($m^3 s^{-1}$).

3.4 SWAT SETUP

Despite the perceived data intensiveness of the model, it has been possible to apply it to an area with limited data.

3.4.1 MODEL INPUT

The SWAT model interface uses Arcgis 9.2 as the platform for inputting spatial data sets. The interface required a number of input layers and parameter sets, including a digital elevation model (DEM), a soil map and list of soil parameters, a land use map, and climate data. The DEM must be an ESRI Grid; however soils and land use may be either in ESRI grid, shape file, or geodatabase feature class. Climate data is entered as point data and any number of climate data points can be entered to allow for spatial variation of climate across a catchment.
The most important input data for the model are listed in Figure 3.11

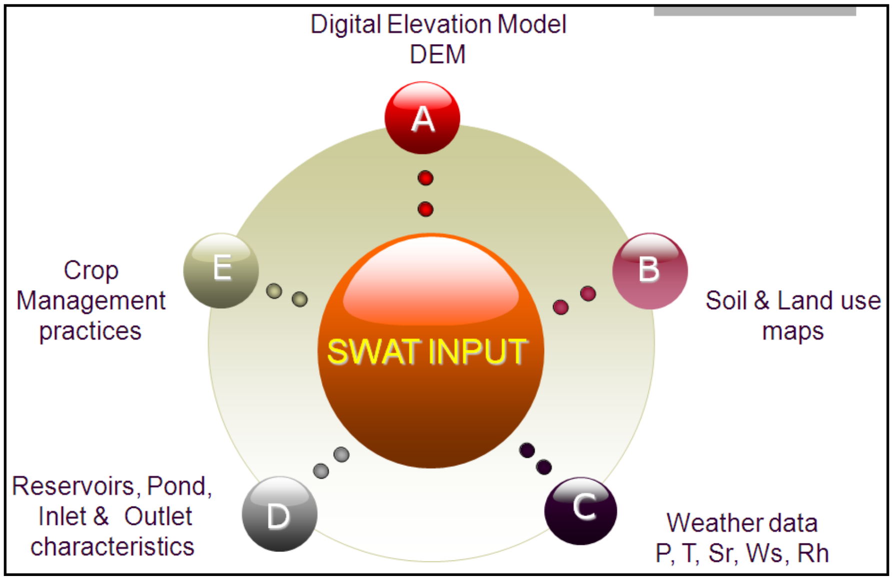

Figure 3.11 SWAT model Input

3.4.1.1 DIGITAL ELEVATION MODEL

The DEM is used to define sub-catchment boundaries and a stream network. Land use and soil are entered simultaneously and HRU defined on the basis of intersected layers. During the process of intersecting the land use and soil data, the user can define a threshold area (% of the sub catchment area) that any unique combination must achieve to be included as a HRU.

The SWAT 2005 interface has an ArcGis script that automates the process to define sub-catchment boundaries, stream network and slope factors. The ArcGis script also defines stream section dimensions (stream width, depth and bed slope) for each of stream reaches in a catchment. SWAT uses these dimensions in algorithms to route of water and sediment.

The DEM (Figure 3.12) was generated from contour lines provided form the Major State maps (1/50000) (IGNF, 1957) with an equidistance of 10 meters.

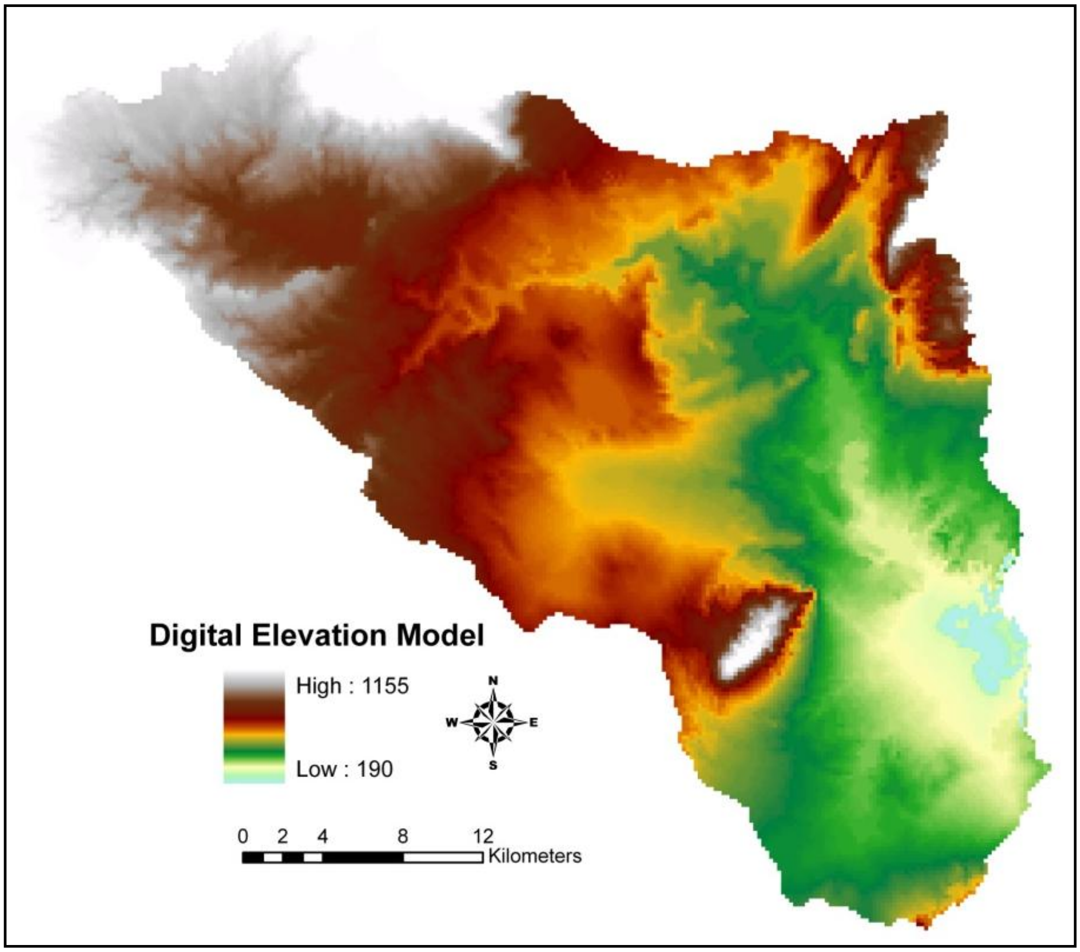

Figure 3.12 Digital Elevation Model of the Merguellil catchment

3.4.1.2 HYDROGRAPHIC NETWORK

In order to improve hydrographic, segmentation and sub-watershed boundary delineation, we Burn in a stream network of the catchment provided form GIS MErgamant (Monat, 2000). A stream network dataset can be superimposed onto the DEM to define the location of the stream network. This feature is most useful in situations where the DEM does not provide enough detail to allow the interface to accurately predict the location of the stream network.

The stream network of the Merguellil catchment provided by the IRD was elaborated for the Merguise project from topographic maps (1/50000) (Figure 3.13).

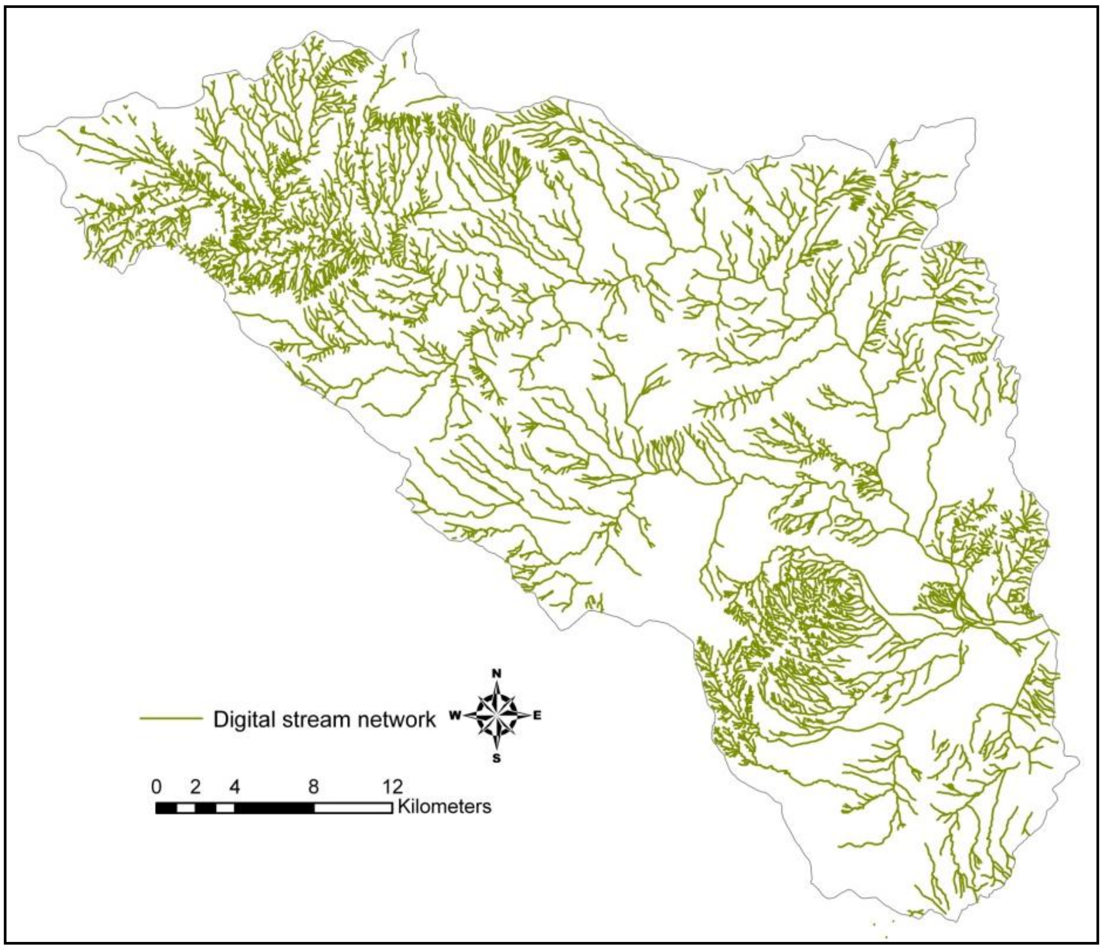

Figure 3.13 Hydrographic network of the Merguellil catchment (Monat, 2000)

3.4.1.3 LAND USE AND SOIL MAPS

The land-use and soil maps (Scale 1/200 000) in the basin were provided by the IRD (L'Institut de Recherche et Développement). These maps were developed using previous studies done on this area (Barbery and Mohdi, 1987; Mizouri et al.1990).

3.4.1.3.1 LAND USE MAP

The land-use map presents five different types: forest (18.5%), pasture (21.5 %), urban (0.5%), water bodies (2.5%) and crops (57%), whereas it does not indicate the crop type. In view of this, this map was modified using investigations done in 2007 in the study area. The new land-use map (Figure 3.14) shows the presence of Durum wheat (39.5%), olives (11.5%), almond (4%), apples (1%), Apricot (0.5%), Tomatoes (0.3%) and water melon (0.2%) highlighting that the irrigated crops present only 1.7% of the whole area of the watershed (Tomatoes, apples, and some areas with olive trees).

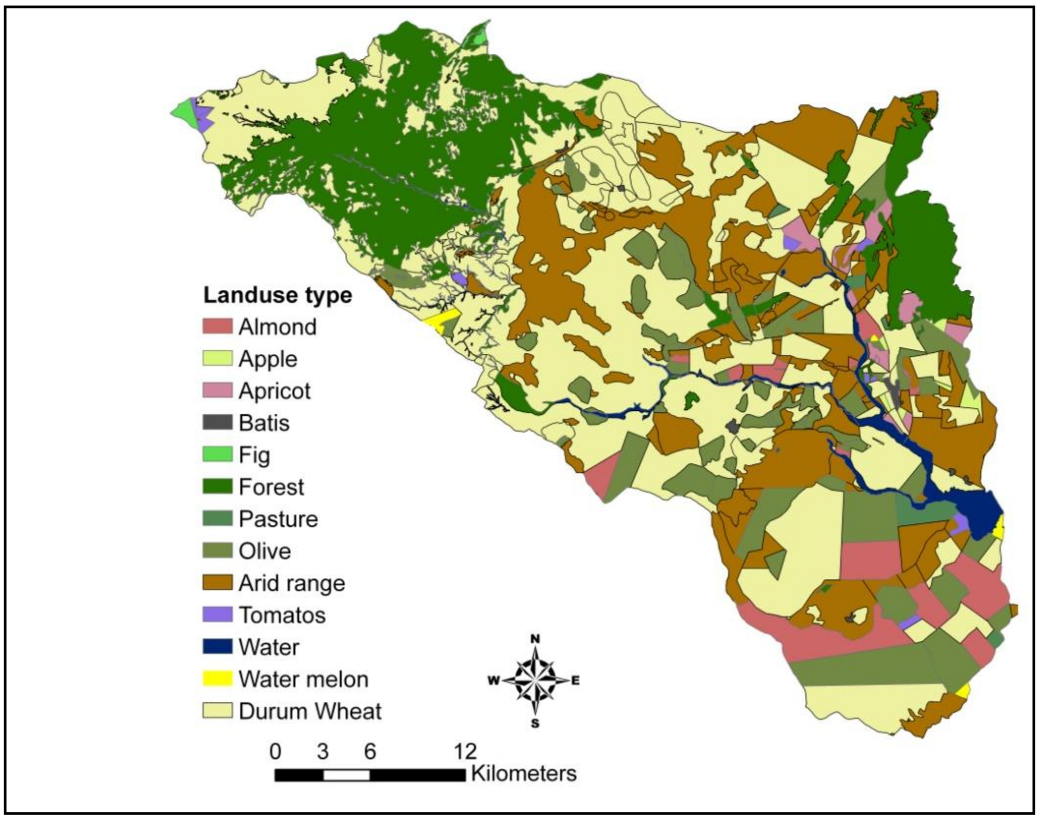

Figure 3.14 Updated land use map of the Merguellil catchment

3.4.1.3.2 SOIL MAP

The soil map presents four main units: poorly evolved soils, Carbonate soils (calci-magnesic), Iso-humic soils, and mineral soils resulting from erosion (association). Each unit groups several soil types. The information from the profiles was individually added to the soils database in SWAT from which the model incorporates parameter values defined spatially by the soils shape files. The identification of each soil type was done using some previous studies describing the soil profiles in the Merguellil catchment (Direction des sols 1963-1982) (Appendix 1). However these profiles do not cover all the area. Based on the analysis results of some soil samples done by Dridi (2000) (Appendix 2), the missing soil profiles were completed. The new soil map (Figure 3.15) presents 31 different soil types. For each soil type, proprieties not available in the dataset such as the available water content, the saturated hydraulic conductivity and the bulk density were calculated using the water characteristics calculator (Saxton and Rawls, 2006). All soil parameters are listed in the Appendix 3 for each soil type.

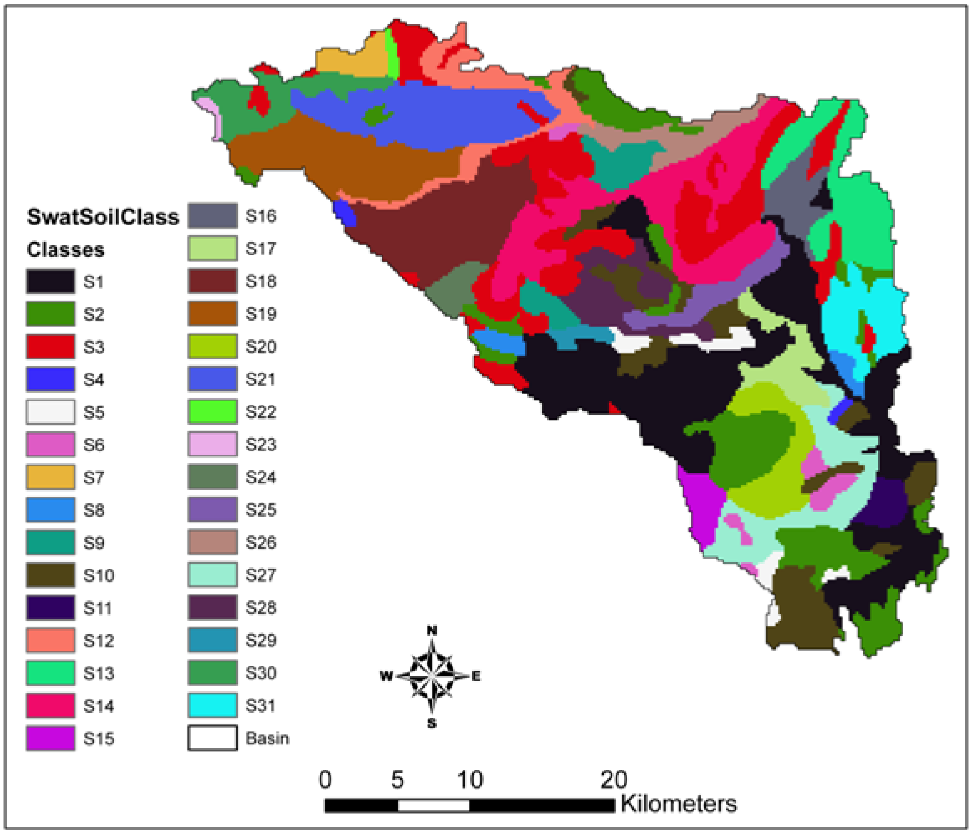

Figure 3.15 Updated Soil map of the Merguellil catchment

3.4.1.3.2.1 ADJUSTMENTS TO SOILS PARAMETERS

The water balance simulated by SWAT uses soil water store characteristics. As soil water store dynamics can be considered a primary factor in hydrology modeled by SWAT, it was imperative to define soil store reliably.

The water content of a soil can range from zero when the soil is oven dried to a maximum value corresponding to total porosity (TP) when the soil is saturated. For plant-soil interactions, two intermediate stages are recognized: field capacity (FC) and permanent wilting point (WP). FC is the water content found when a thoroughly wetted soil has drained for approximately two days. WP is the water content when plants growing in a soil wilt and do not recover if their leaves are kept in a humid atmosphere overnight.

In SWAT WP is calculated as a function of bulk density (BD) and clay content (%), FC is calculated as WP plus available water capacity (AWC) of the soil and TP is calculated as a function of bulk density. It was observed during setting up the model that soils data yielded results where field capacity FC exceeded TP, which is physically impossible.
Figure 3.16 shows the soil textures in the Merguellil catchment were classified according to the USDA textural triangle (Appendix 4). We note the dominance of a sandy loam texture (32 %) flowed by a Silty loam (22%), while the clay loam texture present 15 %.

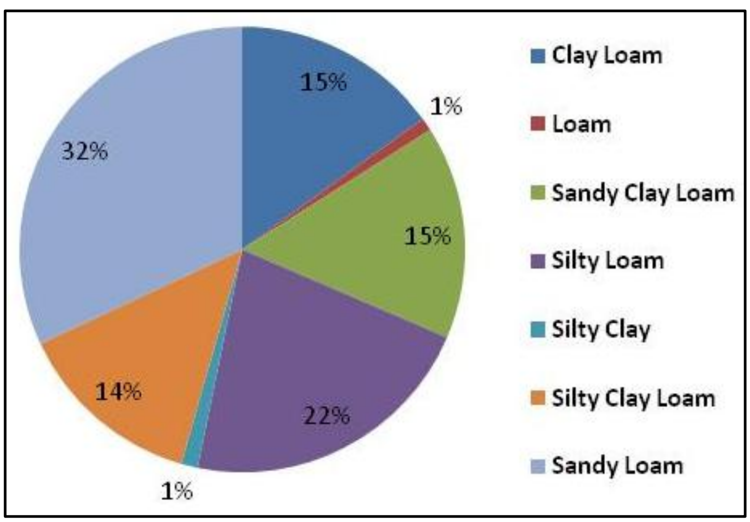

Figure 3.16 Soil texture in the Merguellil catchment

3.4.1.3.2.2 SOIL HYDROLOGIC GROUPS

The U.S. Natural Resource Conservation Service (NRCS) classifies soils into four hydrologic groups based on infiltration characteristics of the soils. NRCS Soil Survey Staff (1996) defines a hydrologic group as a group of soils having similar runoff potential under similar storm and cover conditions. Soil properties that influence runoff potential are those that impact the minimum rate of infiltration for a bare soil after prolonged wetting and when not frozen. These properties are depth to seasonally high water table, saturated hydraulic conductivity, and depth to a very slowly permeable layer. Soil may be placed in one of four groups, A, B, C, and D, or three dual classes, A/D, B/D, and C/D.

Definitions of the classes are:

A: (Low runoff potential). The soils have a high infiltration rate even when thoroughly wetted. They chiefly consist of deep, well drained to excessively drained sands or gravels. They have a high rate of water transmission.

B: The soils have a moderate infiltration rate when thoroughly wetted. They chiefly are moderately deep to deep, moderately well-drained to well-drained soils that have moderately fine to moderately coarse textures. They have a moderate rate of water transmission.

C: The soils have a slow infiltration rate when thoroughly wetted. They chiefly have a layer that impedes downward movement of water or have moderately fine to fine texture. They have a slow rate of water transmission.

D: (High runoff potential). The soils have a very slow infiltration rate when thoroughly wetted. They chiefly consist of clay soils that have high swelling potential, soils that have a permanent water table, soils that have a clay pan or clay layer at or near the surface, and shallow soils over nearly impervious material. They have a very slow rate of water transmission.

Based on these classes' definitions we classified the different soil types within the Merguellil catchment. Most of soil are grouped in the C Hydrologic group, the rest belong to Hydrologic group B (Table 3.4).

Table 3.4 Soil hydrological group

Hydrologic group	
Group B	Group C
S13, S15, S20, S21, S25, S26, S27, S28, S29, S31	S1, S2, S3,S4, S4, S5, S6, S7, S8, S9, S10, S11, S12, S14, S16, S17, S18, S19, S22, S23, S24, S30, S32

Because both soil hydraulic properties and soil erodibility were estimated exclusively based on texture, soils have been divided into groupings according to clay content to facilitate discussion and visualization (Figure 3.17). These groups correspond to soil hydrologic group mentioned above in section.

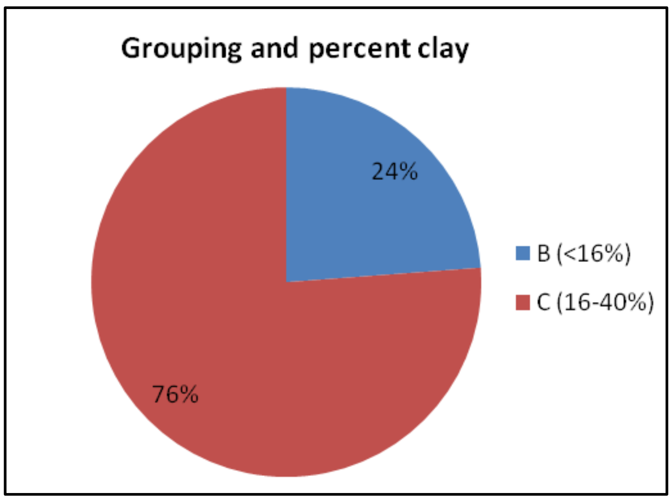

Figure 3.17 Percent area of soils in the Merguellil catchment. Soils are divided into groupings according to clay content, by percent weight

3.4.1.4 CLIMATIC DATA

3.4.1.4.1 RAINFALL GAGE

The recorded rainfall data were obtained from DGRE Kairouan (Direction Generale des Resources en Eaux) and INM (Institut National de Meteorologie).

There are a total of 32 rainfall stations within, or in close proximity to the study area, which are summarized in Table 3.5 and graphically in Figure 3.18 providing a visual assessment of discontinuities in the time series. Of these, only 18 have daily rainfall data for the period 1986-2005 were selected. The location of these stations is shown in Figure 3.19. They were chosen according to their locations (Table 3.5) to ensure a total cover of the study area, and according to the available time series Missing data in some stations were completed from the closest station (generally less than 5 km) according to Lo Presti et al., 2008.

Table 3.5 Rain-gages name and coordinate

Name Rain-gage	Longitude (UTM 32)	Latitude (UTM 32)	Longitude (Degree)	Latitude (Degree)	Altitude (m)
Ain Beidh	564144	3928283	9.7072	35.4960	277
Barage El Houareb	567965	3936106	9.7500	35.5663	86
El Ala EC	551312	3936486	9.5663	35.5707	456
El Ala GN	550541	3941166	9.5581	35.6130	459
Haffouz D	561269	3943421	9.6767	35.6327	291
Haffouz S	560730	3941322	9.6706	35.6138	250
Kesra B9	532888	3963143	9.3640	35.8119	1007
Kesra Foret	532319	3964126	9.3578	35.8207	1062
Majbar	520597	3955033	9.2278	35.7391	1050
Neggaz EC	543572	3940892	9.4811	35.6108	505
Ouled Amo	548204	3946877	9.5326	35.6646	541
Skhira B	534739	3954862	9.3842	35.7371	640
Tella	521207	3962521	9.2347	35.8066	875
Zebess Tele	551421	3943849	9.5679	35.6371	396
El Gueria	540364	3958060	9.4465	35.7658	605
Sidi Mbar	523319	3947214	9.2577	35.6685	780
Messiouta	542076	3943710	9.4647	35.6363	538
Bouhafna	559148	3948398	9.6536	35.6777	300
AIN GRAB	565615	3937352	9.7242	35.5776	
DJEBEL TROZZA	552785	3931906	9.5822	35.5294	
EL ALA CTV	550541	3941166	9.5580	35.6129	
MAKTAR PF	518436	3967382	9.2041	35.8504	
OUSLATIA INRAT	555266	3966180	9.6119	35.8382	
OUSLATIA FORET	553255	3966876	9.5897	35.8446	
ZBARA	566176	3932889	9.7300	35.5374	
BRAHMIA ECOLE	538563	3939072	9.4257	35.5946	
DJOUAMIA	535401	3943557	9.3909	35.6351	
BARRAGE MORRA	535958	3948797	9.3973	35.6824	
SIDI MBAREK	523319	3947214	9.2576	35.6685	
MOAZIL	553083	3949468	9.5866	35.6876	
OUSLATIA GN	553330	3966846	9.5905	35.8443	
SIDI BOUJDARIA	563369	3938167	9.6994	35.5851	
HOUAREB BLED SBITTA	569551	3936118	9.7675	35.5663	

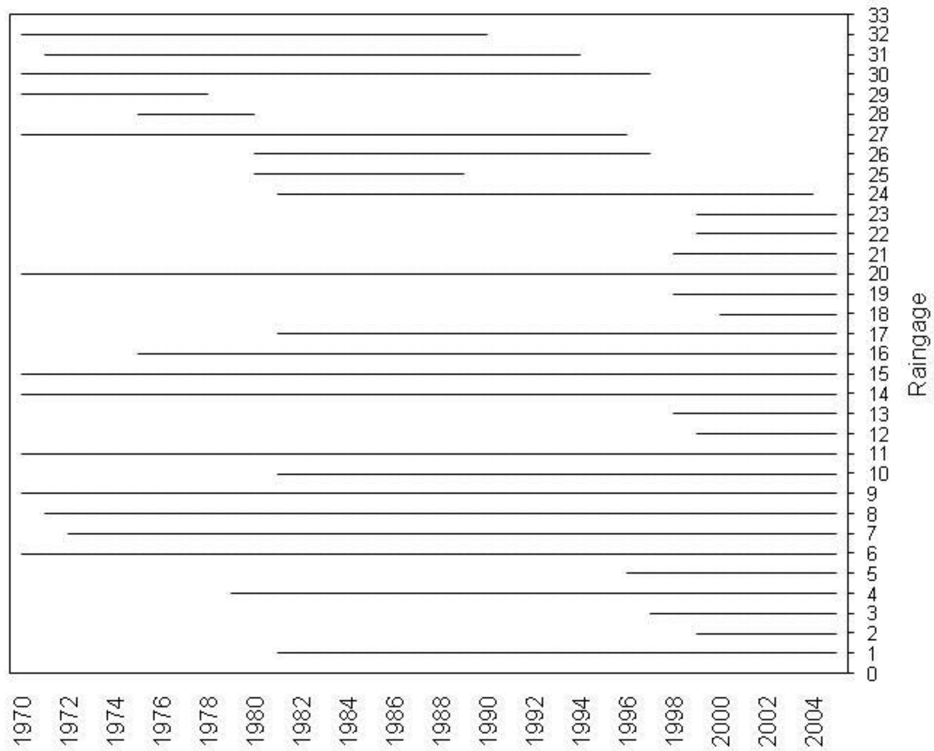

Figure 3.18 Discontinuities in daily rainfall

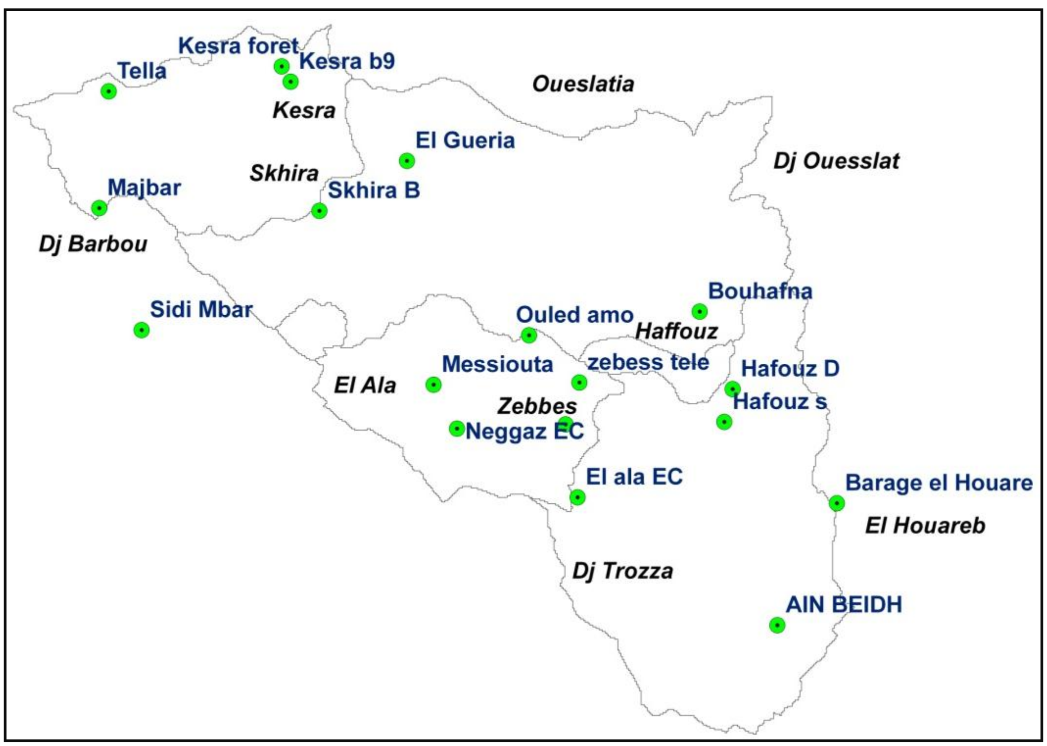

Figure 3.19 Location of the rain-gages in the Merguellil catchment

3.4.1.4.2 TEMPERATURE GAGE

No temperature gages were located within the watershed, and even the available stations in the proximity of the basin [Kairouan (1901-1979), Makthar (1901-1979) and Sbiba (1964-1982)] have records that do not cover the simulation period (1986-2005). Consequently, minimum and maximum interpolated daily temperatures were sourced from MARS/AGRIFISH, Unit of the Joint Research Center of the European Commission. These data were developed in the context of the "Crop Growth Monitoring System" (CGMS) project, (Micale and Genovese, 2004). They consist on an interpolation into 50 km square grid of measured data, obtained from existing meteorological stations across Europe and North Africa for the time period 1986-2005. The projection of the Merguellil catchment on the MARS grid map results into two grids, one covering the upstream and one the downstream of the watershed.

3.4.1.5 RESERVOIRS

A reservoir is an impoundment located on the main channel network of a watershed. The features of an impoundment are shown in Figure 3.20.

The water balance for a reservoir is:

$$V = V_{\text{stored}} + V_{\text{flowin}} - Vf_{\text{lowout}} + V_{\text{pcp}} - V_{\text{evap}} - V_{\text{seep}}$$

where V is the volume of water in the impoundment at the end of the day (m^3 H_2O), V_{stored} is the volume of water stored in the water body at the beginning of the day (m^3 H_2O), V_{flowin} is the volume of water entering the water body during the day (m^3 H_2O), $V_{flowout}$ is the volume of water flowing out of the water body during the day (m^3 H_2O), V_{pcp} is the volume of precipitation falling on the water body during the day (m^3 H_2O), V_{evap} is the volume of water removed from the water body by evaporation during the day (m^3 H_2O), and V_{seep} is the volume of water lost from the water body by seepage (m^3 H_2O).

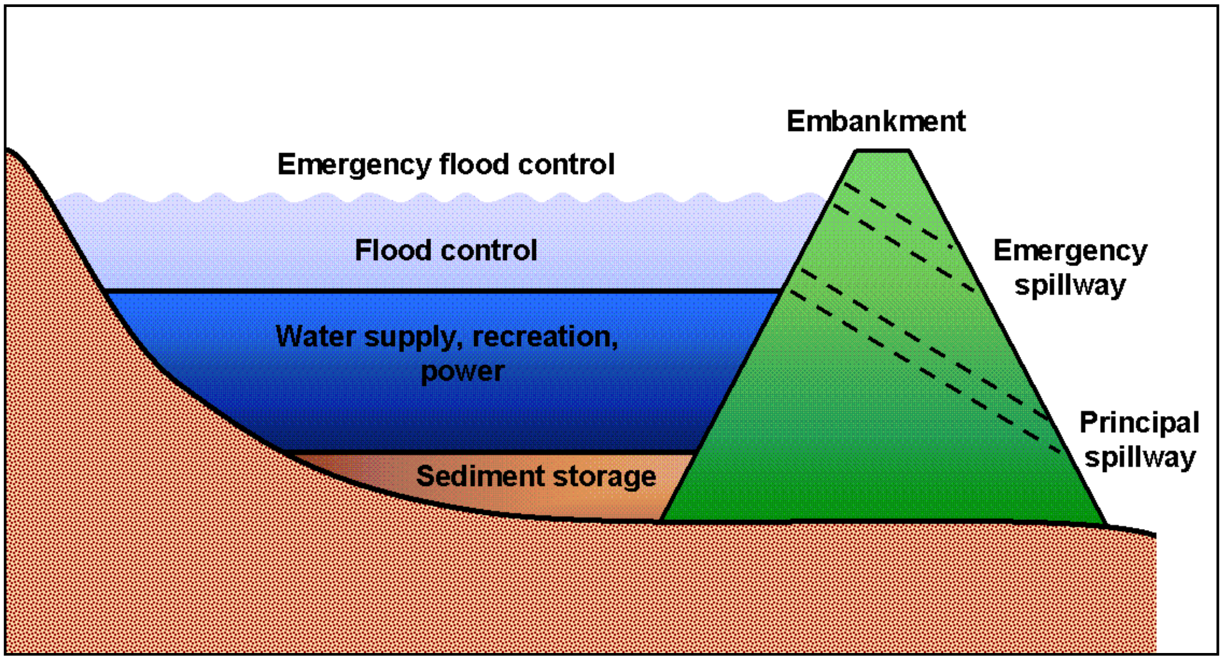

Figure 3.20 Components of a reservoir with flood water detention features (After Ward and Elliot, 1995).

The volume of outflow may be calculated using one of four different methods: measured daily outflow, measured monthly outflow, average annual release rate for uncontrolled reservoir, controlled outflow with target release.

We use the average annual release rate as the method to calculate reservoir outflow. The reservoir releases water whenever the reservoir volume exceeds the principal spillway volume, Vpr.

If the reservoir volume is greater than the principal spillway volume but less than the emergency spillway volume, the amount of reservoir outflow is calculated:

$$V_{\text{flowout}} = V - V_{\text{pr}} \qquad if \qquad V - V_{\text{pr}} < q_{\text{rel}}.86400$$

$$V_{\text{flowout}} = q_{\text{rel}}.86400 \qquad if \qquad V - V_{\text{pr}} > q_{\text{rel}}.86400$$

If the reservoir volume exceeds the emergency spillway volume, the amount of outflow is calculated:

$$V_{\text{flowout}} = (V - V_{\text{em}}) + (V_{\text{em}} - V_{\text{pr}}) \quad if \quad V_{\text{em}} - V_{\text{pr}} < q_{\text{rel}}$$

$$V_{\text{flowout}} = (V - V_{\text{em}}) + q_{\text{rel}}.86400\, if \quad if \quad V_{\text{em}} - V_{\text{pr}} > q_{\text{rel}}.86400$$

where $V_{flowout}$ is the volume of water flowing out of the water body during the day (m^3 H2O), V is the volume of water stored in the reservoir (m^3 H2O), Vpr is the volume of water held in the reservoir when filled to the principal spillway (m^3 H2O), Vem is the volume of water held in the reservoir when filled to the emergency spillway (m^3 H2O), and q_{rel} is the average daily principal spillway release rate (m^3/s).

Five large dams located on the stream network of the Merguellil catchment are modeled as reservoirs. These reservoirs receive water contributed to the channel network from all upstream subbasins. Table 3.6 provides a list of reservoirs on the Merguellil River that were included in the model.

Table 3.6 Characteristics of 5 large reservoirs included in the SWAT model

	Name	YEAR_RES	RES ESA (ha)	RES_EVOL ($10^4 m^3$)	RES_PSA (ha)	RES_PVOL ($10^4 m^3$)
Res 1	El Karrou	1997	17	127	15	100
Res 2	Enmel	1997	16	105	15	100
Res 3	El Morra	1996	11.9	76	11.5	70.5
Res 4	Smiti	2001	25	950	15	100
Res 5	El Hammam	2002	11	85	10	77

YEAR_RES: Year of the reservoir became operational. RES_ESA Reservoir surface area when the reservoir is filled to the emergency spillway. RES-EVOL volume of water needed to fill the reservoir to the emergency spillway. Res_PSA. Reservoir surface area when the reservoir is filled to the principal spillway
RES_PVOL volume of water needed to fill the reservoir to the principal spillway

3.4.1.6 PONDS

Ponds are water bodies located within subbasins that received inflow from a fraction of the subbasin area. The algorithms used to model this type of water bodies differ only in the options allowed for outflow calculation.
The water balance for a pond is:

$$V = V_{\text{stored}} + V_{\text{flowin}} - Vf_{\text{lowout}} + V_{\text{pcp}} - V_{\text{evap}} - V_{\text{seep}}$$

where V is the volume of water in the impoundment at the end of the day (m^3 H_2O), V_{stored} is the volume of water stored in the water body at the beginning of the day (m^3 H_2O), V_{flowin} is the volume of water entering the water body during the day (m^3 H_2O), $V_{flowout}$ is the volume of water flowing out of the water body during the day (m^3 H_2O), V_{pcp} is the volume of precipitation falling on the water body during the day (m^3 H_2O), V_{evap} is the volume of water removed from the water body by evaporation during the day (m^3 H_2O), and V_{seep} is the volume of water lost from the water body by seepage (m^3 H_2O).

Pond outflow is calculated as a function of target storage. The target storage varies based on flood season and soil water content. The target pond volume is calculated:

$$V\text{targ} = V\text{em} \quad if \quad mon_{\text{fld, beg}} < mon < mon_{\text{fld,end}}$$

$$V\ targ = V\ pr + \frac{(1 - min\left[\frac{sw}{FC}, 1\right])}{2} \,.(Vem - V\ pr)$$

where V_{targ} is the target pond volume for a given day (m^3 H_2O), V_{em} is the volume of water held in the pond when filled to the emergency spillway (m^3 H_2O), V_{pr} is the volume of water held in the pond when filled to the principal spillway (m^3 H_2O), SW is the average soil water content in the subbasin (mm H2O), FC is the water content of the subbasin soil at field capacity (mmH2O), mon is the month of the year, $mon_{fld,beg}$ is the beginning month of the flood season, and $mon_{fld,end}$ is the ending month of the flood season. Once the target storage is defined, the outflow is calculated:

$$V_{\text{flowout}} = \frac{V - V_{\text{targ}}}{ND_{\text{targ}}}$$

where $V_{flowout}$ is the volume of water flowing out of the water body during the day (m^3 H_2O), V is the volume of water stored in the pond (m^3 H_2O), V_{targ} is the target pond volume for a given day (m^3 H_2O), and ND_{targ} is the number of days required for the pond to reach target storage.

44 small dams (subbasin impoundment) are modeled as ponds (Figure 3.8). The catchment area of a pond is defined as a fraction of the total area of the subbasin. The water entering this impoundment is generated in the subbasin; they cannot receive water originating in other subbasins. Characteristics of these ponds are listed in the Appendix 5.

3.4.1.7 POTHOLES

Contour ridges referred to us as Pothole; each pothole can cover all the HRU area or a percentage of this area. The runoff generated within these HRUs flows to the lowest portion of the pothole rather than contributing to flow in the main channel. To define HRU as pothole, we input to SWAT the Fraction of HRU that drains into the pothole. This fraction was determined by overlapping the contour ridges shape file to the HRUs one. One pothole is located in one HRU for one subbasin where the contour ridges are built. If the area with the counter ridge is bigger than the HRU considered as pothole, the water entering the pothole may be contributed from other HRUs in the subbasin. We specify then the fraction of flow from upland HRUs that contributes to the pothole HRU, with the remainder flowing directly to the channel system. Figure 3.21 presents a schematic presentation of the HRU considered as pothole and the contribution of other HRUs with the water to this pothole. We count 23 potholes added to the Model. Another input is the Maximum volume of water stored in the pothole. We used the results obtained by Dridi (2000) when she calculates the maximum water storage capacity in different area set with the contour ridges within the Merguellil watershed. She takes into account some physical characteristics of the contour ridges such as the height, distance between contours, and slope.

Figure 3.22 points up the spatial repartition of the water storage capacity of these contour ridges. The mean storage capacity of areas with contour ridges is about 85 mm. Data about the HRUs considered as potholes and those drained into the pothole are listed in Appendix 6.

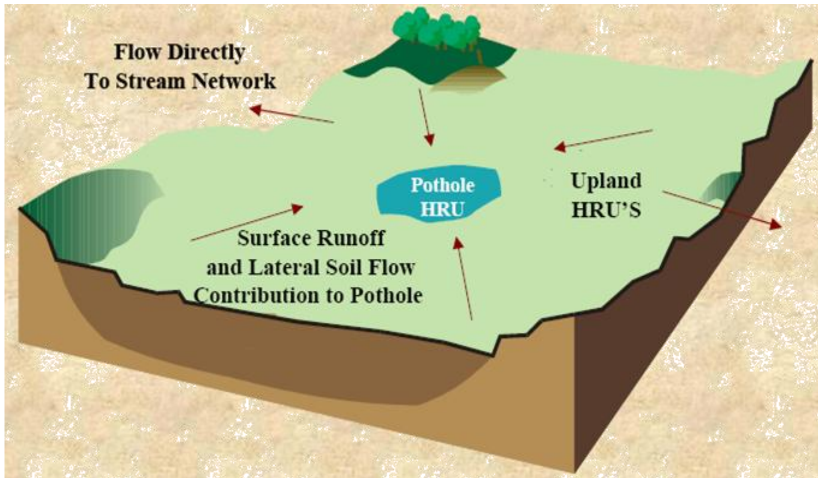

Figure 3.21 Location of pothole and hydrologic response Unit in the landscape (Du et al., 2005)

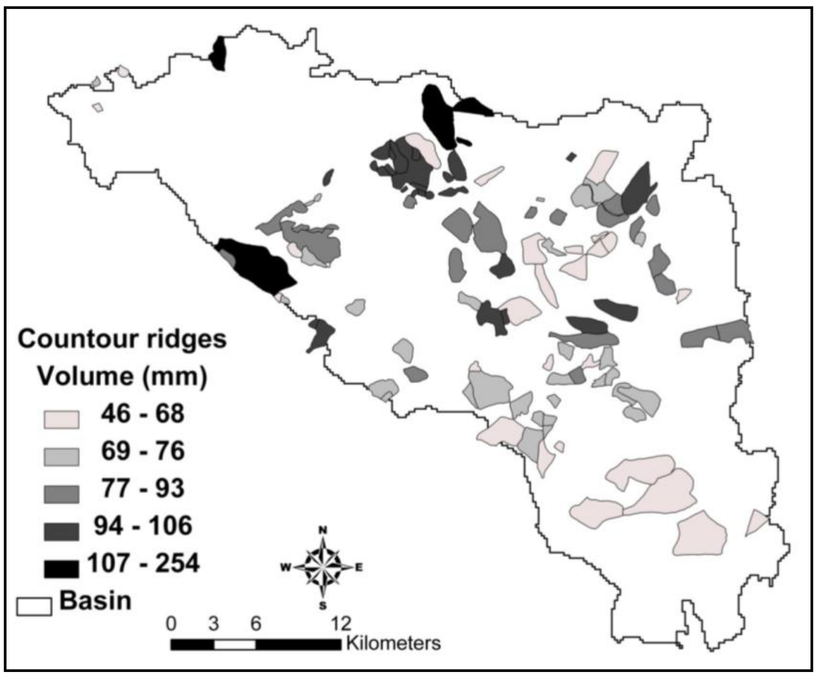

Figure 3.22 Spatial repartition of water storage capacity (mm) of the contour ridges in the Merguellil catchment

The water balance for a pothole is given as:

$$V = V_{\text{stored}} + V_{\text{flowin}} - Vf_{\text{lowout}} + V_{\text{pcp}} - V_{\text{evap}} - V_{\text{seep}}$$

Where V is the volume of water in the impoundment at the end of the day (m^3), V_{pcp} is the volume of precipitation falling on the water body during the day (m^3), V_{flowin} is surface runoff and lateral soil flow from upland HRUs in the subbasin during the day (m^3), V stored is the volume of the water stored in the water body at the beginning of the day (m^3), V_{evap} is the volume of water removed from the water body by evaporation during the day (m^3), V_{seep} is the volume of water lost from the water body by seepage (m^3), and $V_{flowout}$ is the volume of water flowing out the water body during the day (m^3).

3.4.1.8 CROP MANAGEMENT OPERATIONS

Land management practices, such as planting and harvest schedules, tillage practices, fertilizer applications etc., are required by SWAT when the effects of land management practices on physical processes is to be examined. Accurate simulation of these practices is important for studies that desire to simulate erosion and, if applicable, nutrient and agrochemical transport and water resource use. Land management practice data was procured from interviews (Appendix 7) (2007, unpublished) with some farmers in the study area representing approximately all regions in the Merguellil catchment. These data were completed from Agriculture recommendation of Tunisia (AVFA, 2007). Management practices incorporated into SWAT for different crops presented in the study area are listed in Appendix 8.

3.4.2 MODEL SETUP

3.4.2.1 SUBBASIN DELINEATION

The subbasin delineation may be obtained from sub-watershed boundaries that are defined by surface topography so that the entire area within a subbasin flows to the subbasin outlet.

The DEM was used as a basis for modeling process. The stream network (Figure 3.23) was generated by incorporating a hydrographic stream network map provided form GIS MErgamant (Monat, 2000).

The stream network and outlet configuration may be refined by the user. Sub watershed outlets may be added. Table 3.7 and Figure 3.23 show respectively the coordinate and the location of the outlets we added to the stream network. Sub-watershed outlets are the points in the drainage network of a sub-watershed where streamflow exits the sub-watershed area. Adding outlets at the location of monitoring stations is useful for comparison of measured and predicted flows and concentrations. Skhira and Haffouz Outlet are useful to compare the flow and quality, while the other outlets are useful for the quality comparison. The Sub-watershed delineation is completed when we define the outlet of the watershed which the el Houareb dam.

Table 3.7 Outlets coordinates

Name	Longitude (UTM 32)	Latitude (UTM 32)
Kissra	533030.97	3963363.76
Shkira	535581.38	3954800.07
Barrage Ennmal	553251.85	3954984.68
Haffouze	559658.79	3943090.88
Jabbes	555102.89	3944002.45
Boujdaria	562505.96	3939967.80
Kharoub	548574.00	3956234.00

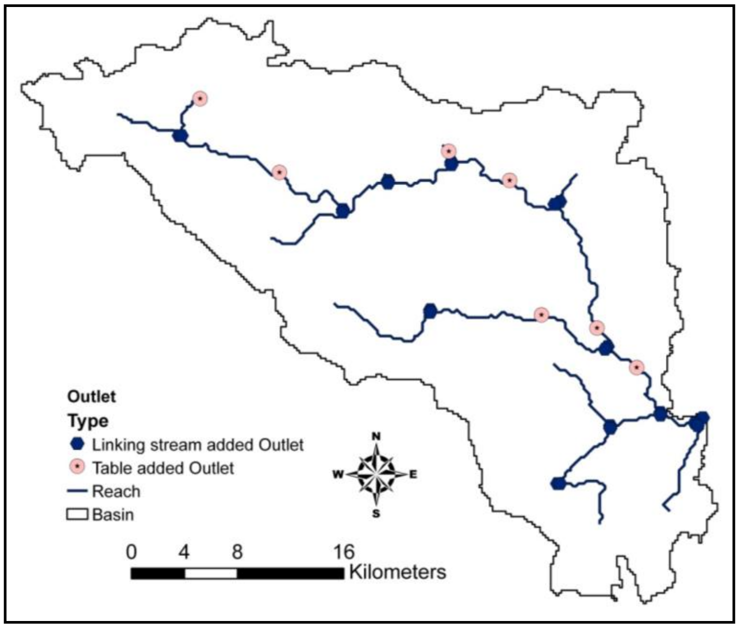

Figure 3.23 Main stream Network with the added outlet

The study area was divided into 30 subbasins, corresponding to a critical source area of 1085km^2 (Figure 3.24). After the delineation, A topographic report is generated provides a statistical summary and distribution of discrete land surface elevations in the watershed and all the sub watersheds.

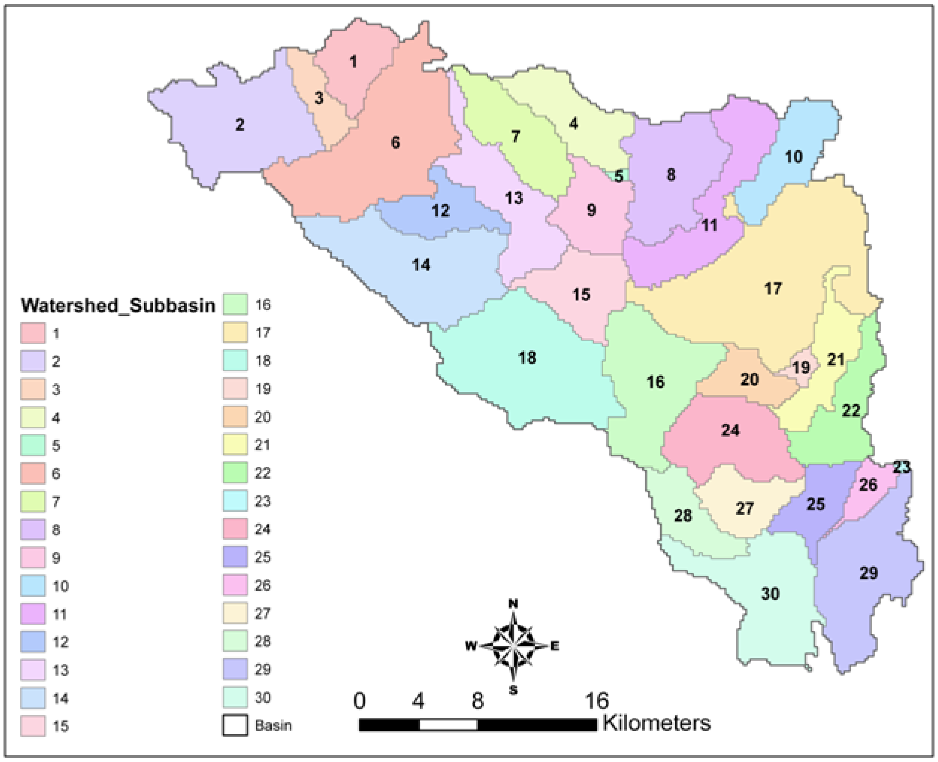

Figure 3.24 Subbasins delineation in the Merguellil catchment

3.4.2.2 LAND USE AND SOIL DEFINITION AND OVERLAY

Land use and soil data are required to determine the area and hydrologic parameters of each land/soil category to be simulated. These land/soil categories form the basis of the hydrological response units (HRUs) and terrain parameters are identical for all HRUs within a given subbasin, except for the channel length parameter used to compute the time of concentration, which varies depending on the size of the HRU.

We define SWAT Land Cover associated with land use layer categories. Table 3.8 shows the corresponding swat code for each land use layer.

Table 3.8 Corresponding name and code in SWAT for each land use type in the Merguellil catchment

Map	SWAT Crop name	SWAT code
Durum wheat	Durum wheat	DWHT
Olive	Olive	OLIV
Forest	Forest-Mixed	FRST
Arid range (Halfa or parcour)	Southwestern US(Arid) Range	SWRN
Tomatos	tomato	TOMA
Apple	Apple	APPL
Water	Water	WATR
Water melon	watermelon	WMEL
Pasture	pasture	PAST
Fig	Agricultural Land-Row Crops	AGRR
Almond	Almond	ALMD
Appricot	Orchard	ORCD
Batis	Residential-Low Density	URLD

Due to the lack of locally established values for the parameters, such as Soil Conservation Service-Curve Number (SCS-CN), the Leaf Area Index (LAI), etc, that describe the hydrological characteristics of the different land-use and soil types in the basin, a set of parameters was assigned considering their definition and allowable range (SWAT database) taking into account management practices (fertilizers application, tillage operation, irrigation), hydrological soil groups, land-use and climatic conditions. The data necessary to simulate growth is stored in the SWAT default crop growth database but does not include information on the olive tree which presents 12% of the cropping pattern.

Information necessary to simulate olive tree growth was, therefore, gathered from current literature according the criteria as outlined by Neitsch et al. (2002). All data used for olive tree plant growth simulations is summarized in Appendix 9.

3.4.2.3 HYDROLOGICAL RESPONSE UNITS

Subbasins can further be subdivided into hydrological response units (HRU), each of which represents a particular combination of soil, land-cover and slope within the subbasin. While the subbasins are delineated and located spatially, the further subdivision into HRUs is performed in a statistical way by considering a certain percentage of the subbasin area, without any specific location in the subbasin (Van Griensven et al., 2006).

The HRUs were defined by using the virtual approach which creates at least one HRU for each subbasin based on the given threshold values on percentage areas of land use soil and slope within the subbasin.

In order to eliminate minor land-uses, soils and slopes, a threshold level was selected in each subbasin of 10%, 10% and 10%, respectively. This means that if the percentage of the soil type or the land cover type or the slope is less than 10% of the subbasin area, it is considered negligible and is therefore not included in the ensuing analysis. Given these thresholds, 299HRUs (unique land-use/soil/slope combinations within subbasins) were created.

Table 3.9 provides a detailed description of the distribution of the land use, and soil classes in the watershed. Figure 3.25 outlines the land use percentage within the Merguellil catchment once the model applying the e threshold level of 10 %.

Table 3.9 SWAT Distribution of soil and land use classes in the Merguellil catchment

Land use	Area [ha]	%Watershed Area
Durum Wheat --> DWHT	46825.6234	43.71
Forest-Mixed --> FRST	20503.2184	19.14
Southwestern US (Arid) Range --> SWRN	24409.9019	22.79
OLIVE --> OLIV	10337.5525	9.65
Residential-Low Density --> URLD	59.3622	0.06
Water --> WATR	899.8148	0.84
Apple --> APPL	43.5323	0.04
Pasture --> PAST	444.7878	0.42
Almond ->ALMD	3502.3014	3.27
Tomato --> TOMA	102.8945	0.10

Soils	Area [ha]	% Watershed Area	Soils	Area [ha]	%Watershed Area
S21	6173.7954	5.76	S16	1598.7239	1.49
S3	10853.8861	10.13	S18	6369.1207	5.95
S7	952.9511	0.89	S24	895.2705	0.84
S22	235.9945	0.22	S28	1742.6965	1.63
S19	6024.114	5.62	S25	1960.9532	1.83
S30	2538.2342	2.37	S17	2625.6549	2.45
S2	7940.0171	7.41	S8	415.4243	0.39
S12	2911.1012	2.72	S31	1875.7145	1.75
S26	1857.1689	1.73	S27	3812.4566	3.56
S9	1448.2982	1.35	S20	2600.2092	2.43
S14	7353.5981	6.86	S6	919.8236	0.86
S1	20677.9494	19.3	S11	560.9054	0.52
S10	5453.2283	5.09	S15	1008.1358	0.94
S13	6044.7365	5.64	S5	278.8268	0.26

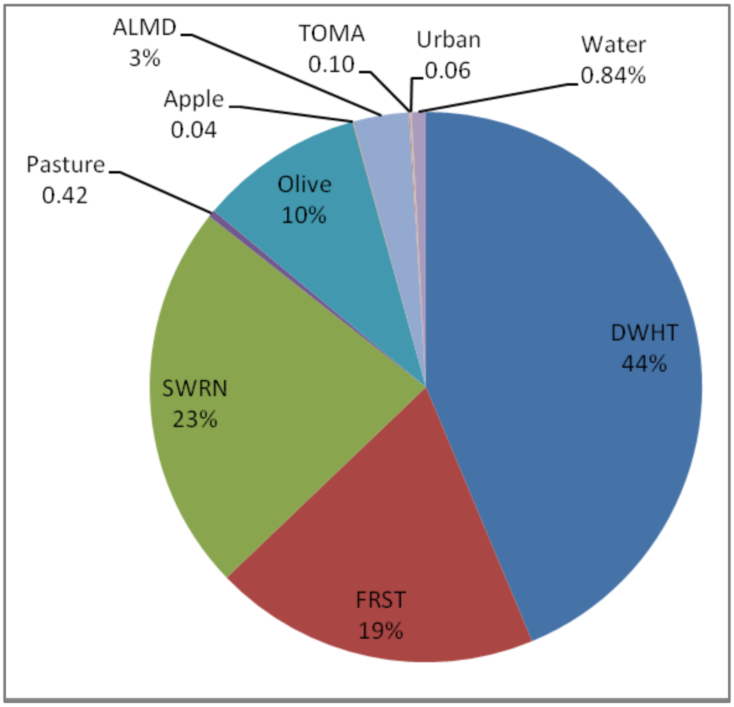

Figure 3.25 land use distribution within the Merguellil catchment after classification in SWAT

3.4.2.3 WEATHER DATA AND SIMULATION

The SWAT model was run on daily time step from January 1986 to December 2005. Weather data to be used in a watershed simulation is imported once the HRU distribution has been defined. SWAT uses the closest climate station to the centroid of a sub-catchment and applies this climate to all HRU's for that sub-catchment. 13 Rain-gages station was defined among those available (Figure 3.26). Kesrab9 Majbar sidi Mbar Negaz EC and Zebess Telepherique rain-gages were eliminated by the model.

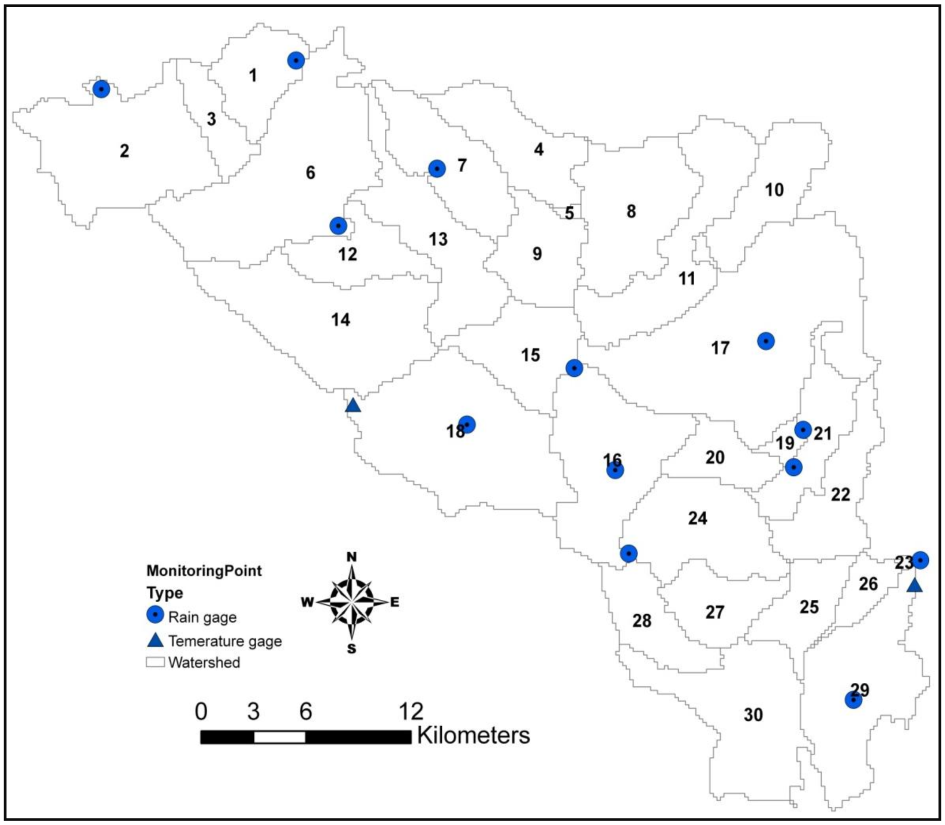

Figure 3.26 Selected Rain-gages and temperature gages that cover the 30 subbasins

The following chapter gives a summary of the results obtained from the SWAT model and the different scenarios considered.

CHAPTER 4 RESULT AND DISCUSSION

4.1 SWAT SIMULATION

Manual calibration is a complicated process in distributed models such as SWAT as over-parameterization is a well known problem (Box and Jenkins, 1976; Beven, 1989).
The important issue before calibration is to reduce the number of parameters that require fitting with input-output data by identifying parameters that have a significant influence on model simulations. This is done by performing a sensitivity analysis for the studied watershed. It should however be noted that sensitivity analysis results for hydrological models are not transferable between basins (Van Griensven et al., 2006).

The calibration for the current study was carried out during the period 01-01-1992 to 31/12/1994 with validation between 01/01/1996 to 31/12/1996. The period 01/01/1985 31/12/1989 was used as a warm up to help initialize the model prior to the start of the calibration period.

4.1.1 SENSITIVITY ANALYSIS

The SWAT model is a distributed-parameter model that has hundreds of parameters. Some of these parameters present initial or boundary conditions while others are forcing factors. Therefore, prior the calibration, a sensitivity analysis was conducted to assess the most sensitive parameters.
The analysis is done using predefined sets of input parameters that depend on what is being simulated as the model can simulate for flow, or flow in combination with sediments only or with water quality. In this case, only river flows were considered. The output of the sensitivity analysis is ranked based on observed flows and also independently of the observed flow values but from a mass balance of the model outputs.
The sensitivity analysis was done at the Haffouz station that covers 15 subbasins (675 km^2). The most sensitive parameters are identified in Table 4.1.

Table 4.1 Ranking of the six most sensitive parameters (1= most sensitive)

Parameter	Description	rank
CN2	Initial SCS CN II Value	1
SOL_AWC	Available soil water capacity	2
GW_Revap	Groundwater "revap" coefficient.	3
GWQMN	threshold depth of water in the shallow aquifer for return flow	4
ESCO	Soil evaporation compensation factor	5
EPCO	Plant uptake compensation factor	6

The description of the very important parameters (according to the above categorization) is given below:

CN2: Initial SCS runoff curve number for moisture condition. The SCS curve number is a function of the soil's permeability, land use and antecedent soil water conditions. Typical curve numbers for moisture conditions are listed in the Appendix 10 for various land covers and soil types done by the SCS Engineering Division (1986).

SOL_AWC: Available water capacity of the soil layer (mm H2O/mm soil). The plant available water, also referred to as the available water capacity, is calculated by subtracting the fraction of water present at permanent wilting point from that present at field capacity, AWC = FC − WP where AWC is the plant available water content, FC is the water content at field capacity, and WP is the water content at permanent wilting point.

GW_REVAP: As GW_REVAP approaches 0, movement of water from the shallow aquifer to the root zone is restricted. As GW_REVAP approaches 1, the rate of transfer from the shallow aquifer to the root zone approaches the rate of potential evapotranspiration. The value for GW_REVAP should be between 0.02 and 0.20.

GWQMN: Threshold depth of water in the shallow aquifer required for return flow to occur (mm H2O).

ESCO: Soil evaporation compensation factor. This coefficient has been incorporated to allow the user to modify the depth distribution used to meet the soil evaporative demand to account for the effect of capillary action, crusting and cracks. As the value for ESCO is reduced, the model is able to extract more of the evaporative demand from lower levels.

EPCO: Plant uptake compensation factor. The plant uptake compensation factor can range from 0.01 to 1.00. As EPCO approaches 1.0, the model allows more of the water uptake demand to be met by lower layers in the soil. As EPCO approaches 0.0, the model allows less variation from the original depth distribution to take place.

4.1.2 CALIBRATION AND VALIDATION

Masden (2000) noted that for modeling the rainfall-runoff process at the catchment scale, normally the only available information for evaluating the objective is the total catchment runoff. With this observation, he noted that the following objectives should be considered for proper evaluation of the calibrated model:

- A good agreement between the average simulated and observed catchment runoff volume (i.e. a good water balance).
- A good overall agreement of the shape of the hydrograph.
- A good agreement of the peaks with respect to timing, rate and volume.
- A good agreement for low flows.

However, Masden (2000) further observed that it can be difficult to achieve all of these objectives and that, in general, trade-offs exist between the different objectives, so that, for instance, one may find a set of input parameters that provide a very good simulation of peak flows but a poor simulation of low flows, and vice versa.

Based on the above sensitivity analysis, the hydrologic calibration procedure was carried out referring to daily flow data at Skhira Kef labiodh and Haffouz telepherique flow-gauges (Figure.3.1) over the period 1992-1994. In particular, the most sensitive input parameters were adjusted so that measured flow match values predicted by the model during this period. Measured daily flow at the same gauges for the year 1996 was used for the hydrological validation of the model. The statistical indicators used for the evaluation of model performance are the coefficient of determination (R^2) and the Nash-Sutcliffe model efficiency (NSE) (Nash et al., 1970)

The Nash–Sutcliffe model efficiency coefficient is used to assess the predictive power of hydrological models. It is defined as:

$$E = 1 - \frac{\sum_{t=1}^{T} \left(Q_o^t - Q_m^t\right)^2}{\sum_{t=1}^{T} \left(Q_o^t - \overline{Q_o}\right)^2}$$

where Qo is observed discharge, and Qm is modeled discharge. Q_o^t is observed discharge at time t (Nash et al., 1970).

Nash–Sutcliffe efficiencies can range from −∞ to 1. An efficiency of 1 (E = 1) corresponds to a perfect match of modeled discharge to the observed data. An efficiency of 0 (E = 0) indicates that the model predictions are as accurate as the mean of the observed data, whereas an efficiency less than zero (E < 0) occurs when the observed mean is a better predictor than the model or, in other words, when the residual variance (described by the nominator in the expression above), is larger than the data variance (described by the denominator).Essentially, the closer the model efficiency is to 1, the more accurate the model is. The Nash–Sutcliffe efficiencies have been reported in scientific literature for model simulations of discharge, and water quality constituents such as sediment, nitrogen, and phosphorus loadings. (Moriasi et al., 2007)

According to Van Liew et al. (2005), NSE value greater that 0.75 is considered “good”, value between 0.75 and 0.36 are considered “satisfactory” and values below 0.36 are considered “not satisfactory”. Henriksen et al. (2003) categorized NSE into five classes namely; excellent, very good, good, poor and very poor and defined the limits of the classes for each of the efficiency indexes. They proposed a limit of 0.5 for a result between good and poor performance. Liden and Harlin, (2000) and Andersen et al. (2001) also state that a good simulation should have an NSE between 0.5 and 0.95.

The r^2 coefficient of determination is calculated using the following equation:

$$r^2 = \left(\frac{\sum_{i=1}^{n} (O_i - \overline{O})(P_i - \overline{P})}{\sqrt{\sum_{i=1}^{n} (O_i - \overline{O})^2} \sqrt{\sum_{i=1}^{n} (P_i - \overline{P})^2}} \right)^2$$

Where Pi is the predicted value Oi is the observed value at time i, Ō is the mean observed value, and P is the mean predicted value for the entire time period i.

The ENS and R^2 coefficients were chosen for this study because they are recommended for use with SWAT (Neitsch et al., 2002). Using indicators of model performance that are consistent with current literature such as ENS and R2 also facilitates model comparison.

The results of the best parameters from the optimization runs are shown in Table 4.2. The parameter values of Table 4.2 were incorporated into the model for simulation for subbasins 1 to 14 and 17.

Table 4.2 Best parameter values

	DWHT		Frst_		Olive	SWRN		
Soil group	B	c	B	c	c	B	c	Definition
CN2	78	81	65	75	80	66	75	Initial SCS CN II value
All subbasins (1-14 and 17)								
AWC	-0.06							Available water content
CHK	5							Effective hydraulic conductivity [mm/hr]
Trans Rch	0.2							each transmission loss partitioning to deep aquifer
GWQMN	100							Threshold depth of water in the shallow aquifer required for return flow to occur [mm]
GWrevap	0.2							roundwater "revap" coefficient
RevapMiN	0.5							EVAPMN: Threshold depth of water in the shallow aquifer for "revap" to occur [mm]
GWalpha	0.048							ALPHA_BF : BAseflow alpha factor [days]
Esco	0.4							Soil evaporation compensation factor
Epco	1							plant water uptake compensation factor
EVLAI	10							Leaf area index at which no evaporation occurs from water surface [m^2/m^2]

Figure 4.1 compares simulated with measured stream flow at Skhira flow-gauge during the calibration (a) and validation (b) periods. For the calibration and validation periods the NSE is 0.62 and 0.68 respectively, while R2 is 0.77 and 0.82 respectively.

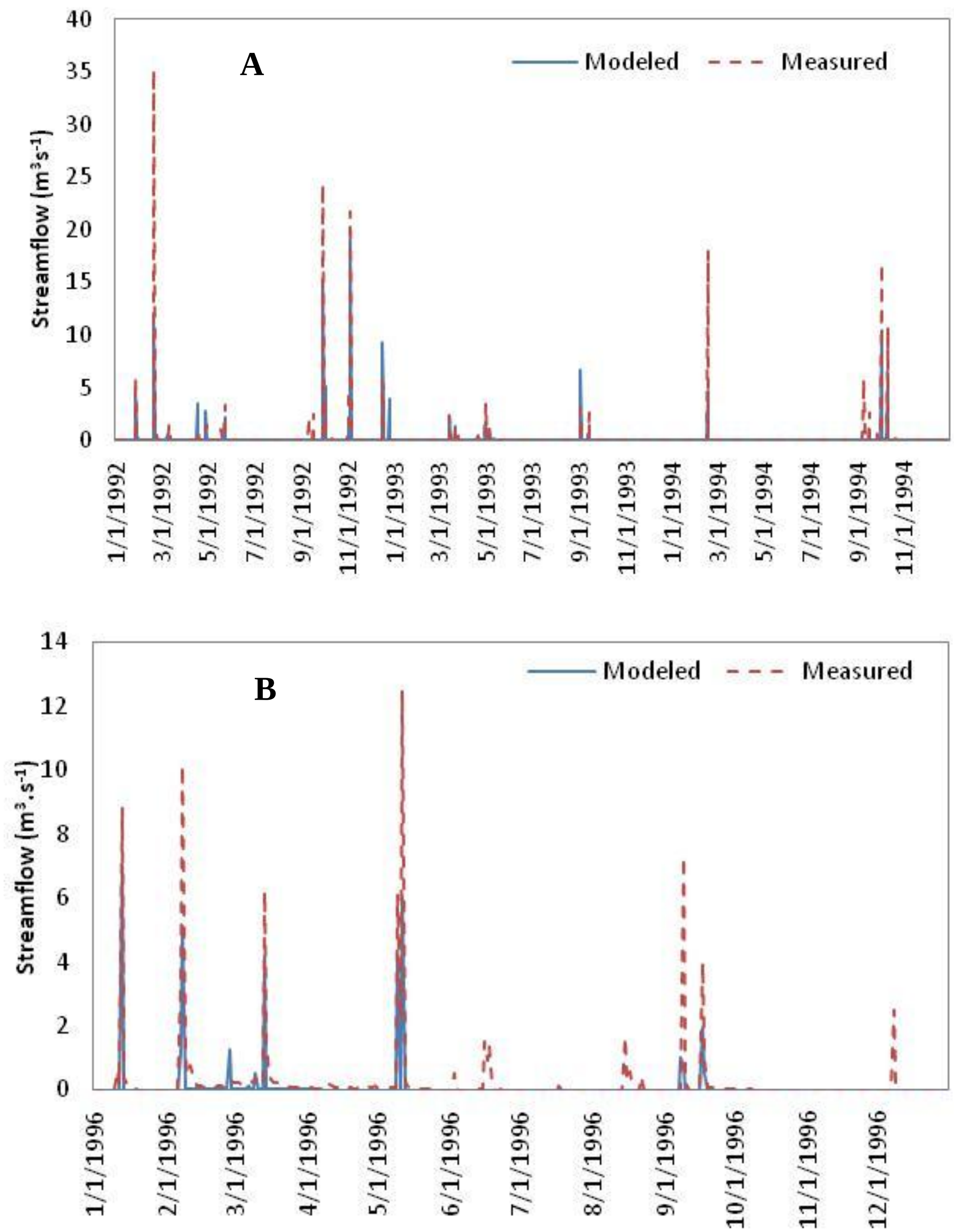

Figure 4.1Modeled (thick line) and observed (dashed line) stream-flow (m^3/s) during the calibration (a) and validation (b) periods at Skhira Kef Labiodh flow-gauge.

Figure 4.2 compares simulated with measured stream flow at Haffouz flow-gauge during the calibration (a) and validation (b) periods. For the calibration and validation periods the NSE is 0.6 and 0.7 respectively, while R2 is 0.7 and 0.8 respectively.

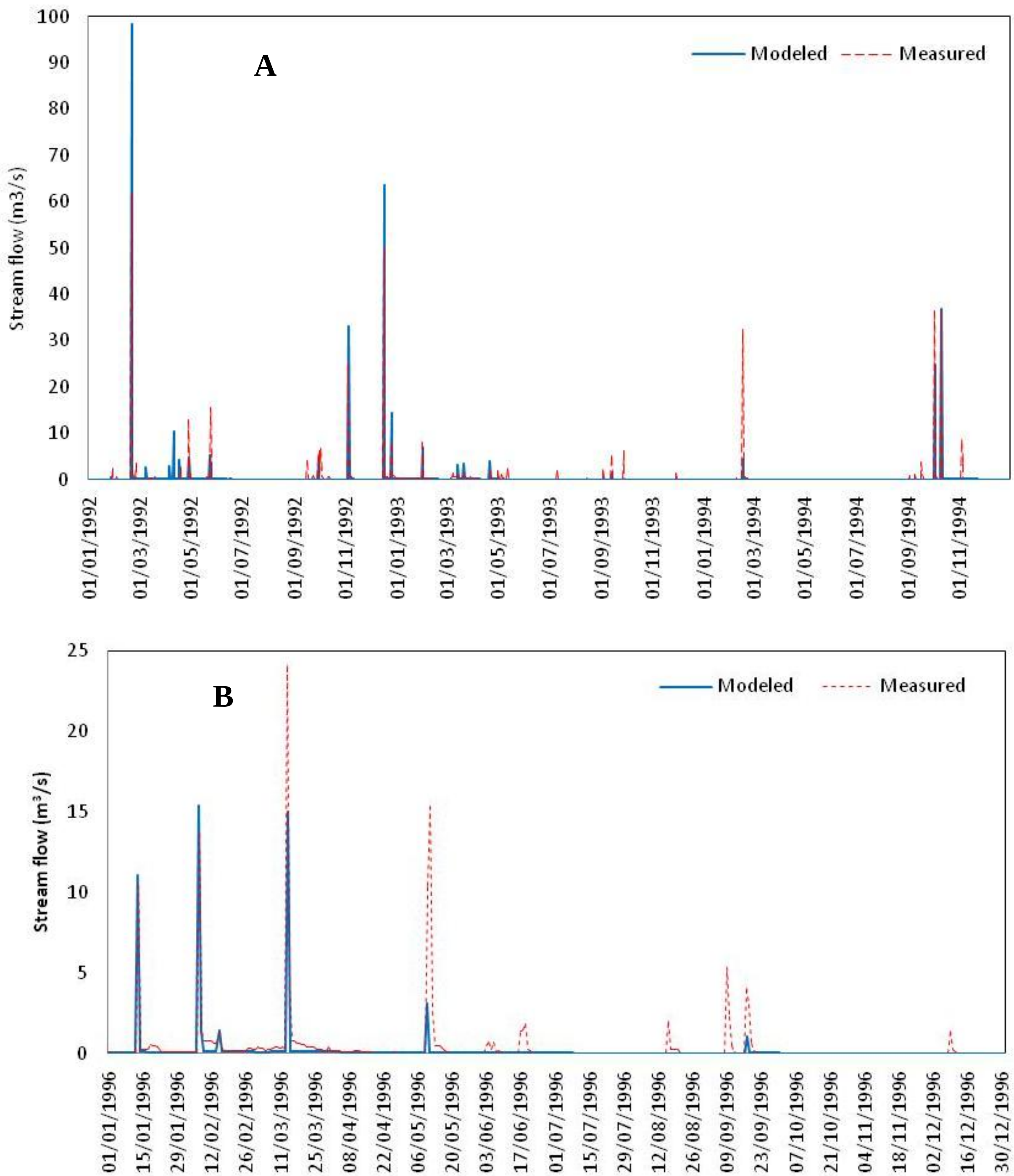

Figure 4.2 Modeled (thick line) and observed (dashed line) stream-flow (m^3/s) during the calibration (a) and validation (b) periods at Haffouz telepherique flow-gauge

Figure 4.3 indicates the correlation between observed and simulated stream flows for the Haffouz (a) and Skhira (b) flow-gauges at the calibration (right) and validation (left) period.

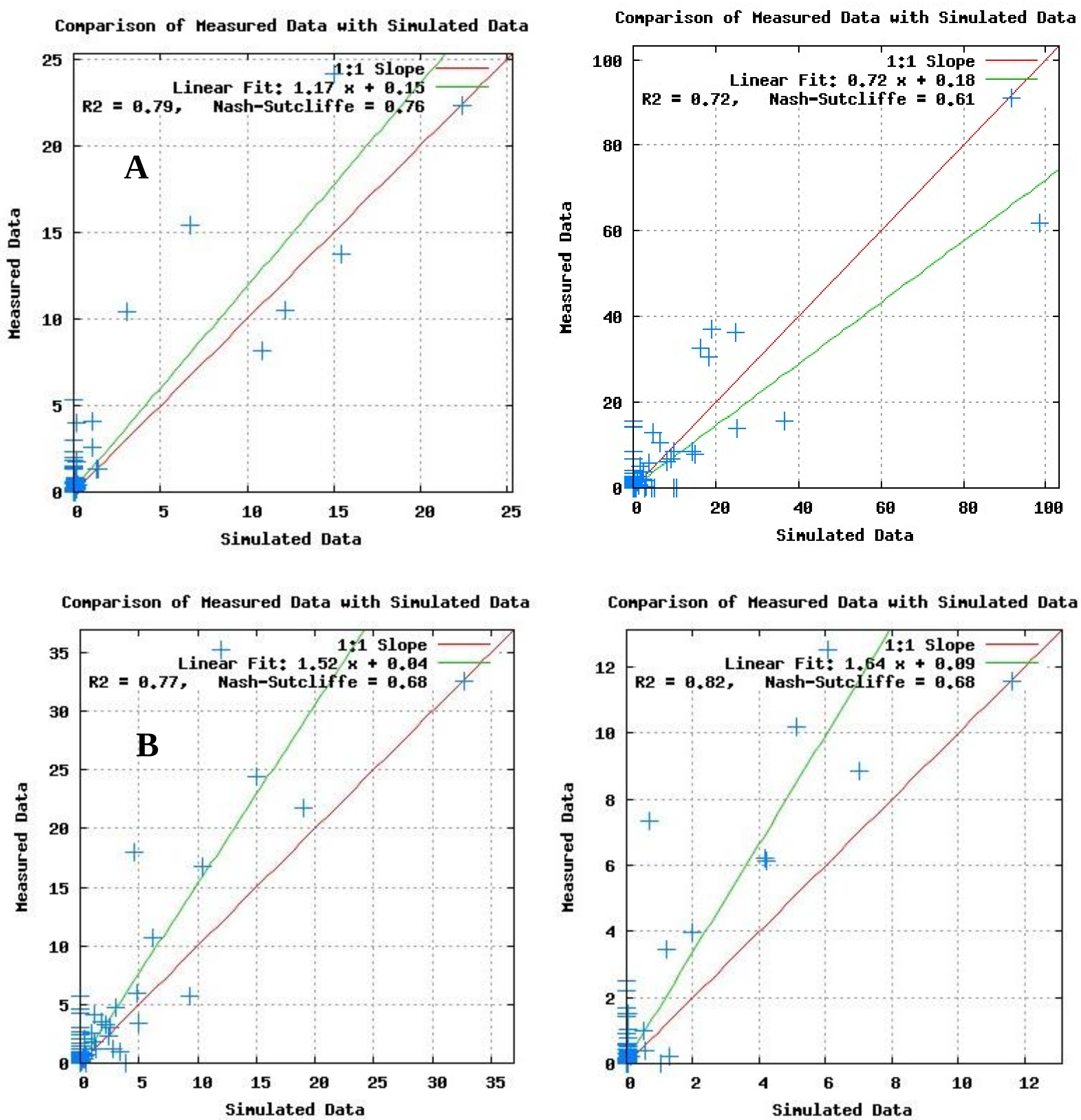

Figure 4.3 Correlation between measured and simulated stream flow at Skhira and Haffouz flow-gauges during the calibration and validation period.

Table 4.3 presents the annual NSE and R2 for the two stations. The NSE coefficient ranges between 1.2 for dry years (1993) and 0.76 for wet years (1996) for the Haffouz station. The inconsistencies in the differences between the simulated and the observed streamflow during the year 1992 could be an indication of the unreliability of the observed streamflow values. The model performance is satisfactory according to the criteria mentioned above.

Table 4.3 Annual values of NSE and R^2 for the two flow gauges.

		Skhira Kef Labiodh		Haffouz telépherique	
		NSE	R^2	NSE	R^2
Calibration	1992	0.69	0.77	0.58	0.83
	1993	0.64	0.69	0.12	0.05
	1994	0.610	0.79	0.68	0.68
Validation	1996	0.67	0.82	0.76	0.79

4.2 WATER BALANCE

The water balance at basin scale was calculated over the period 1990-2005. The monthly component and the mean annual values are summarized in Table 4.4. The simulation results show that the water balance is dominated by actual evapotranspiration (281 mm/year) that presents approximately 82% of annual rainfall and irrigation. Potential evapotranspiration (ETP) calculated with Hargraves-Samani method (1436 mm/year) falls in the range of the FAO methodology (FAO-56) (Allen et al., 1998) for estimating ETP in Tunisia. The surface runoff presents only 5.5% of the total annual rainfall, while the baseflow is very low (1.5%). This very small proportion of baseflow can be explained by the short duration and high intensity of rainfall events. In addition, in arid context, there is hardly any groundwater-generated baseflow since the water table is generally below of streambed (Shahin, 2007).

The average annual simulated water balance for the Merguellil basin is shown in Figure 4.4. The highest flows are observed from January to March. While during summer season, the river generally dried out due to a long drought period.

Table 4.4 Predicted water balance from 1990 to 2005 (SURF Q= surface runoff, ET= actual evapotranspiration, ETP= potential evapotranspiration)

MON	RAIN (MM)	SURF Q (MM)	LAT Q (MM)	TWY (MM)	ET (MM)	PET (MM)
1	41.15	3.96	0.17	4.28	12.43	45.48
2	27.75	3.28	0.13	3.92	16.15	58.86
3	29.5	2.66	0.14	3.44	26.68	92.07
4	25.35	1.08	0.1	1.9	45.5	120.09
5	28.79	0.5	0.1	1.27	53.86	169.49
6	15.38	0.14	0.08	0.73	31.52	200.91
7	4.75	0.04	0.04	0.43	14.47	220.49
8	20.19	0.38	0.06	0.65	16.15	197.98
9	49.28	0.7	0.13	0.98	22.31	134.78
10	33.47	0.97	0.13	1.28	18.62	96.13
11	27.54	0.74	0.09	1.06	12.7	57.07
12	26.33	1.85	0.1	2.22	11	43.08
Total	329.48	16.3	1.27	22.16	281.39	1436.43

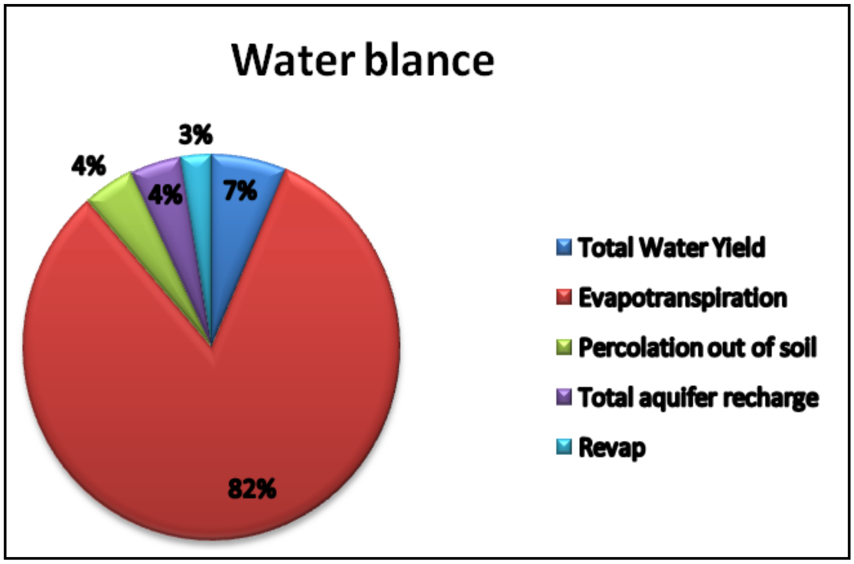

Figure 4.4 Water balance in the Merguellil catchment

4.3 WATER QUALITY SIMULATION

The sediment and nutrient of surface water were simulated form 1990 to 2005 with the SWAT model considering actual land-use and management practices (tillage operations, fertilizer application).

Mean monthly sediment and nutrient loads at the outlet are shown in Figure 4.5 All the parameters reach the maximum values in autumn and winter and the minimum during summer period. Sediment loads range between a maximum of 742 Tons per day (T/day) in March and a minimum of 0.09 T/day in July. The same behavior can be observed for Organic Nitrate and Phosphorus. The highest value of nitrate load (4044 kg/day) is predicted in March.

Finally, the low sampling frequency and the lack of detailed water quality measurement data did not allow an in-depth evaluation of the swat performance in predicting nutrient and sediment.

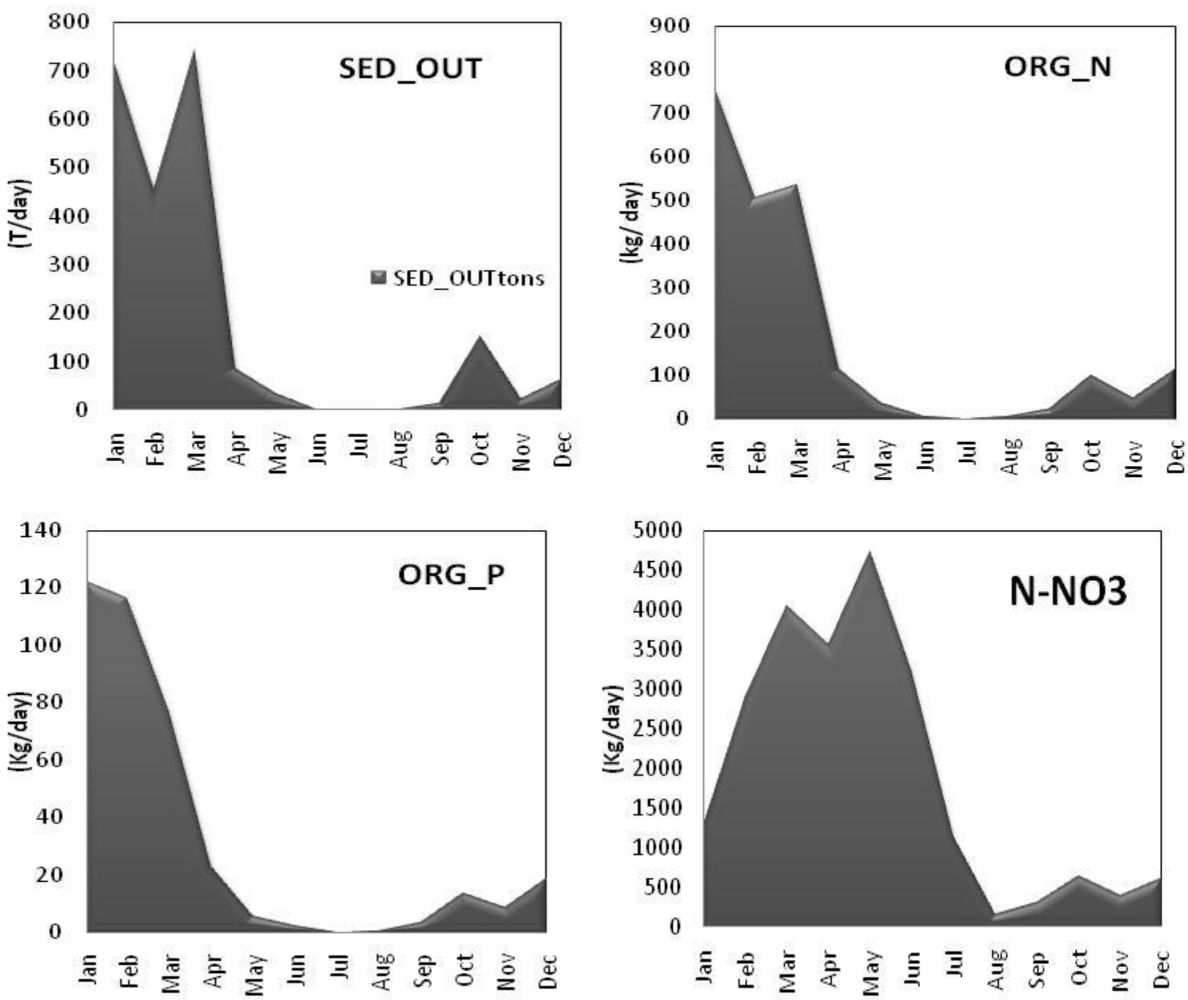

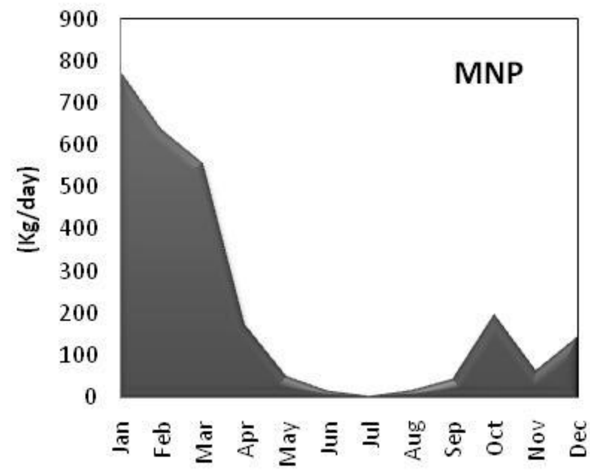

Figure 4.5 Average monthly loads simulated at the outlet for the period (1990-2005)

4.3.1 EVALUATION OF ANNUAL SEDIMENT

Figure 4.6 presents the yearly change in sediment load and concentration, simulated during the period 1990-2005 at the watershed outlet. The mean annual sediment load during the simulation period is 71430 T year^{-1} corresponding to 0.66 T ha^{-1} year^{-1}. Annual sediment loading reveal a high inter-annual variability that is dominated by changes in the annual flow amount (Figure 4.7). The highest sediment load was simulated in 1990 where we have recorded the highest flow. The sediment concentration does not follow the sediment load behavior. The highest concentration was simulated in 1994 (7317 mg/l) where the sediment load is relatively low. This high concentration value could be explained by the low flow value recorded in 1994 (0.16 m^{3}s^{-1}).

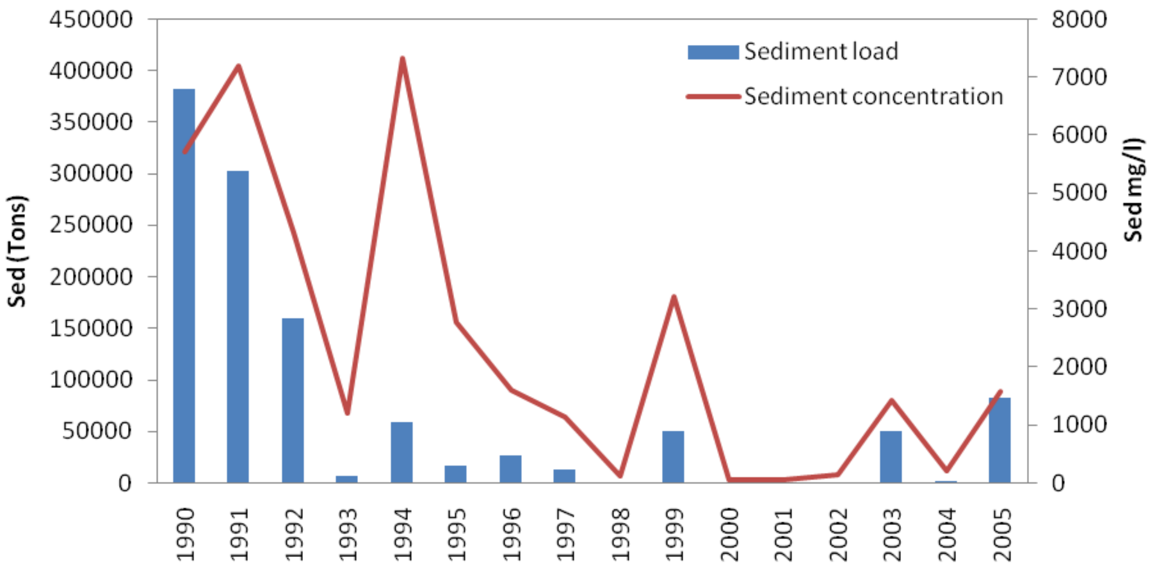

Figure 4.6 Annual variations of sediment load and concentration simulated at the outlet of the Merguellil catchment

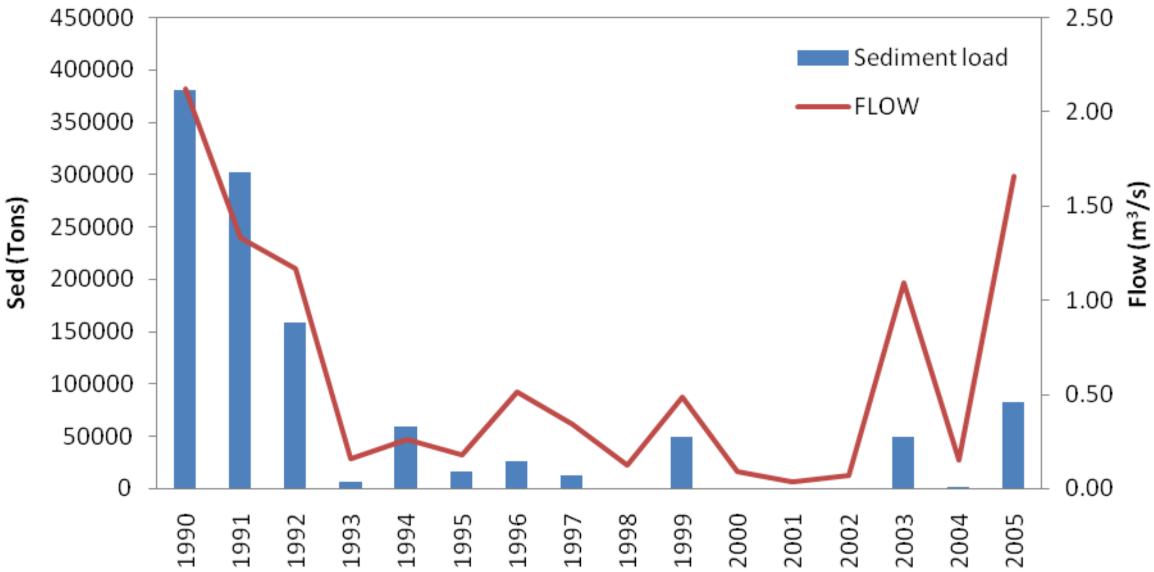

Figure 4.7 Annual variation of sediment load and flow simulated at the outlet of the Merguellil catchment

4.3.2 EVALUATION OF MONTHLY SEDIMENT

Figure 4.8 shows the intra-annual sediment load and concentration at the watershed outlet. The monthly values are presented in terms of means calculated on the simulated sediment load and concentration over the simulation period (1990-2005). The mean monthly sediment load at the outlet is 5952 T month^{-1} corresponding to 0.058T ha^{-1}month^{-1}. The sediment concentration curve follow the same tendency as the sediment load where the highest concentration is in January (7186 mg/l) and the lowest one is in July (15.26 mg/l) while the mean monthly concentration is 2262 mg/l.

We can notice a high intra-annual variability in sediment load and that it that is directly linked to monthly flow (Figure 4.9). The highest load was simulated in March (23016 T month^{-1} tons) where the highest flow is recorded (1.24 m^3/s) while the lowest load was simulated in July (2.8 T month^{-1}) corresponding to the lowest flow (0.07m^3/s). We can note also that the wet months (January, February and March) generate 83% of the total annual sediment load (59542 Tons).

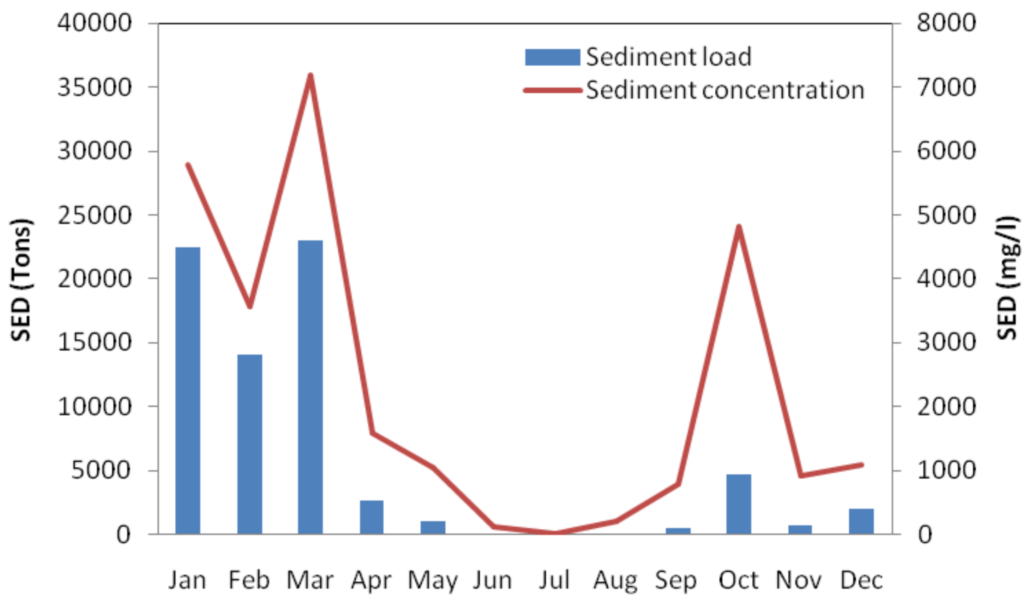

Figure 4.8 Monthly variation of sediment load and concentration simulated at the outlet of the Merguellil catchment

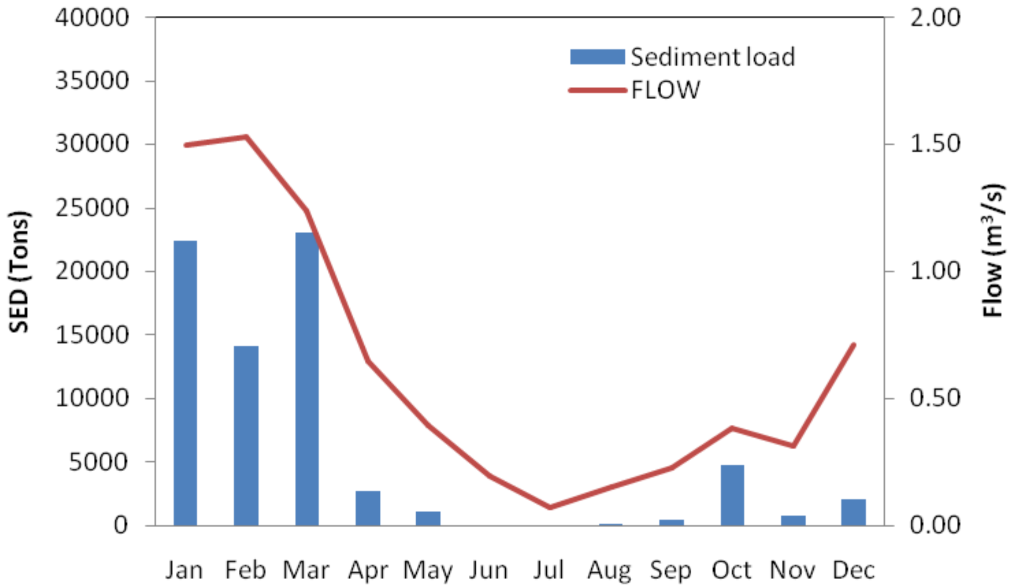

Figure 4.9 Monthly variation of sediment load and flow simulated at the outlet of the Merguellil catchment

4.3.3 EVALUATION OF ANNUAL ORGANIC NITRATE AND ORGANIC PHOSPHORUS

Figure 4.10 shows the yearly change in the simulated load of organic nitrate and organic phosphorus at the outlet of the Merguellil catchment. We observe the same behavior as for sediment. The mean annual organic nitrate and phosphorus loads during the simulation period are respectively 701430 kg year^{-1} (0.65 kg ha^{-1} year^{-1}) and 12130 kg year-^{1} (0.11 kg ha^{-1} year^{-1}). Annual Organic nitrate and phosphorus loading reveal a high inter-annual variability that is dominated by changes in the annual flow amount (Figure 4.11). The highest Organic nitrate and phosphorus loads were simulated in 1990 (359800 kg year^{-1} $^{\text{and}}$ 48260 kg year^{-1} respectively) where we have recorded the highest flow (2.12 m^{3} s^{-1}).

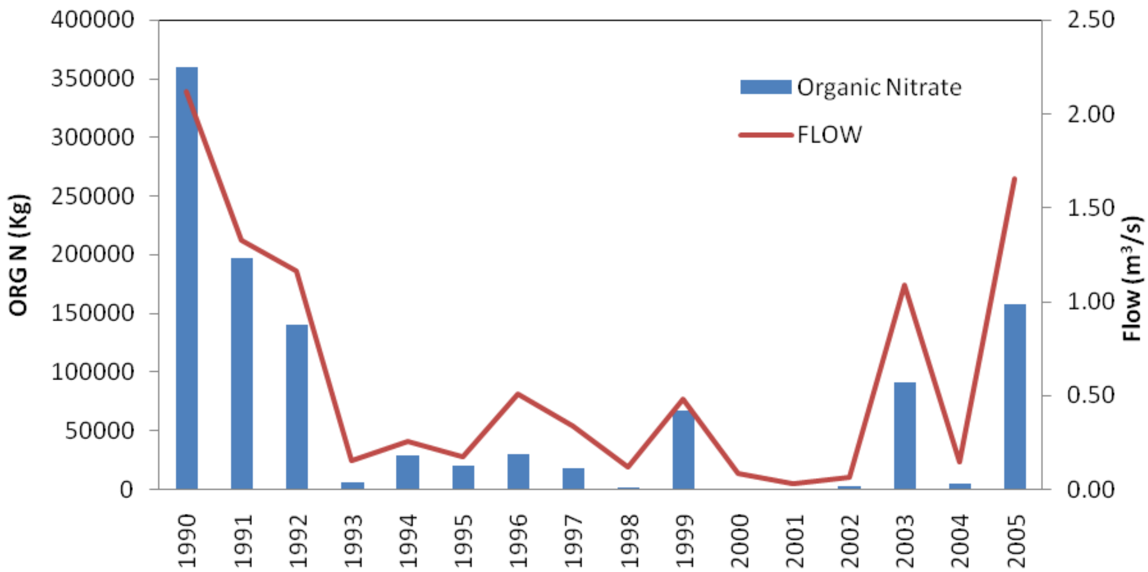

Figure 4.10 Annual variation of Organic nitrate load and flow simulated at the outlet of the Merguellil catchment

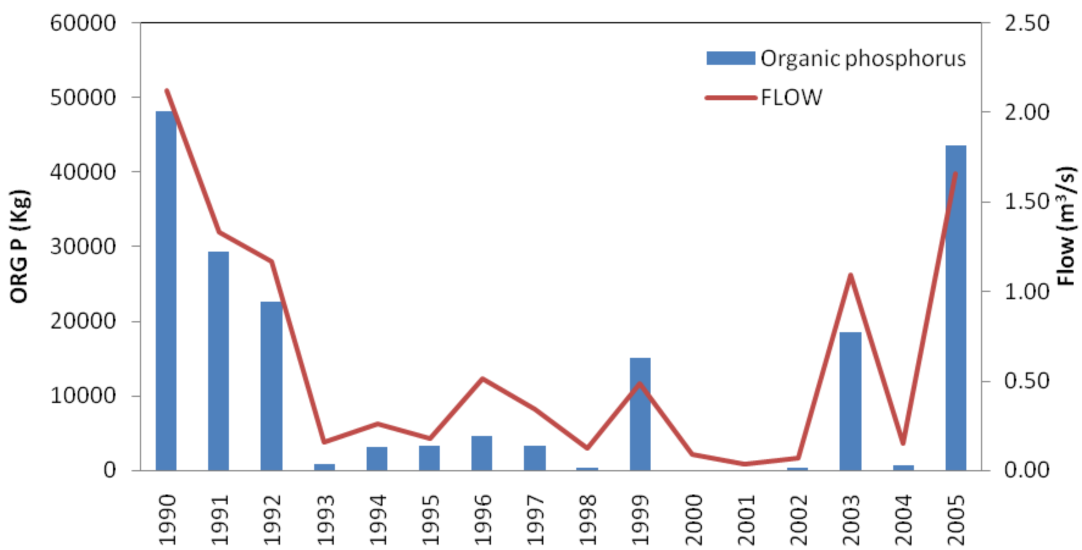

Figure 4.11 Annual variation of Organic Phosphorus load and flow simulated at the outlet of the Merguellil catchment

4.3.4 EVALUATION OF ANNUAL MINERAL NITRATE AND PHOSPHORUS

Figures 4.12 and 4.13 present the yearly change in loads of Mineral nitrate and phosphorus at the outlet. The annual average of mineral nitrate and phosphorus at the outlet of the catchment are respectively about 712400 kg year^{-1} (6.65 kg ha^{-1}) and 82710 kg year^{-1} (0.77 kg/ha).

Annual mineral nitrate and phosphorus loading reveal a high inter-annual variability that is dominated by changes in the annual flow amount (Figure 4.12). The highest mineral nitrate load was simulated in 2005 4800000 kg year^{-1}(44kg/ha) where we have recorded a high flow (1.66 m3 s^{-1}).

The highest mineral phosphorus load was simulated in 1990 312700 kg year^{-1}(2.19 kg ha^{-1}) where we have recorded a high flow (2.12 m^3 s^{-1}) (Figure 4.13).
The mineral nitrate concentration does follow the nitrate load behavior. The highest concentration was simulated in 2005 (91.9 mg/l) where the sediment load is high (Figure 4.14).

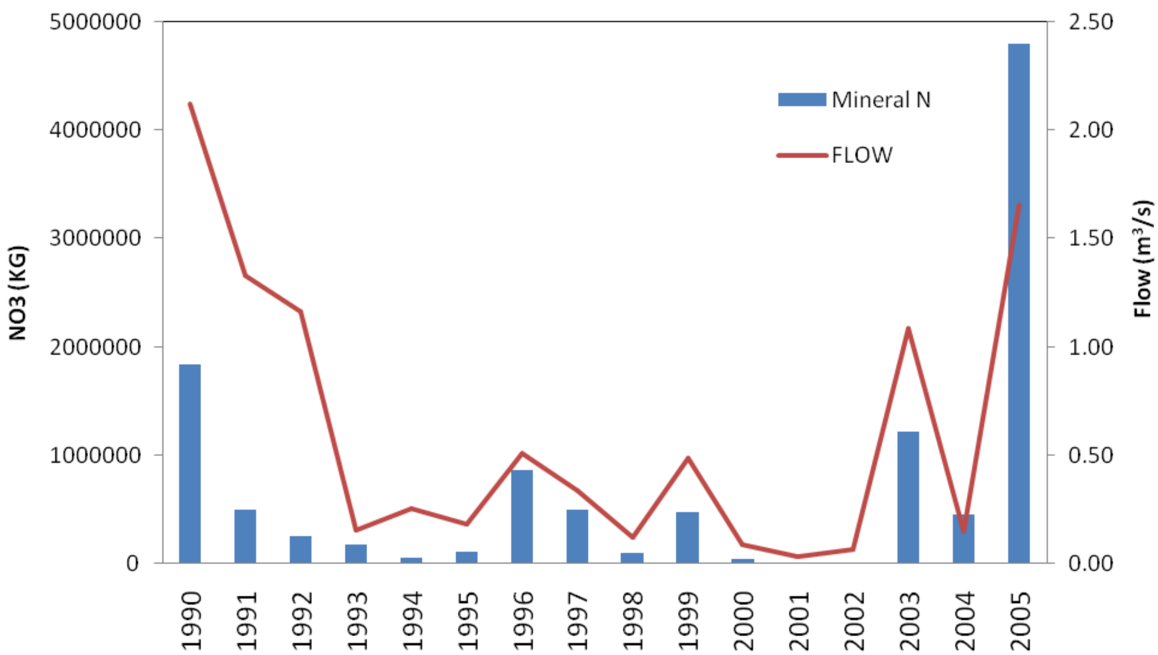

Figure 4.12 Annual variation of mineral nitrate load and flow simulated at the outlet of the Merguellil catchment

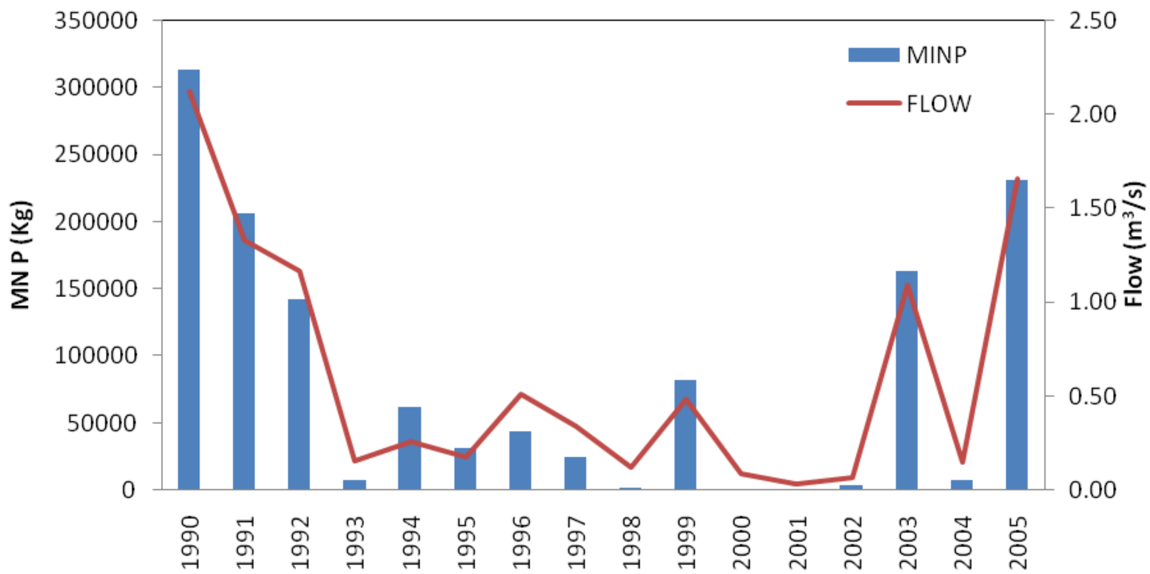

Figure 4.13 Annual variation of Mineral phosphorus load and flow simulated at the outlet of the Merguellil catchment

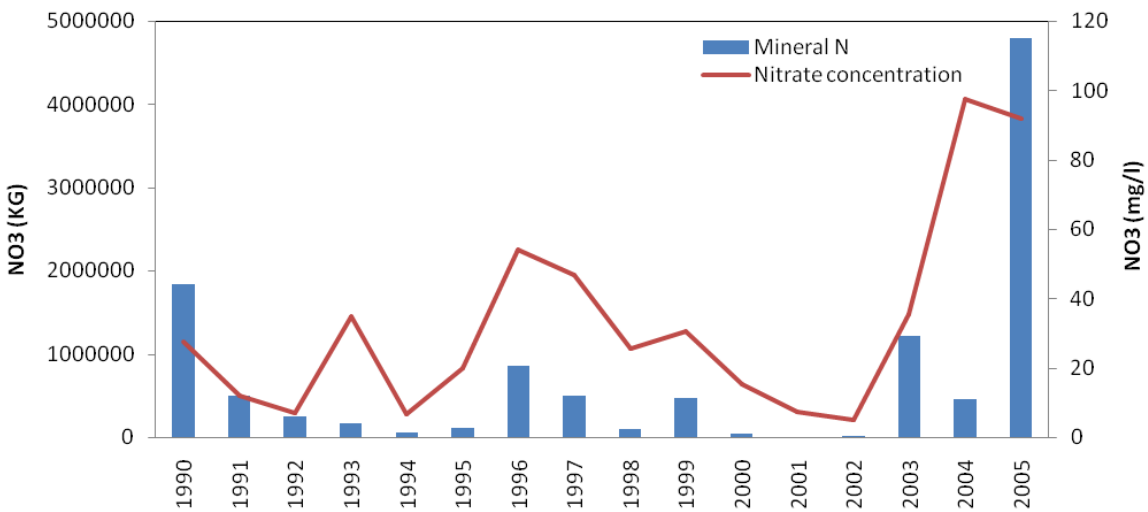

Figure 4.14 Annual variation of mineral nitrate load and concentration simulated at the outlet of the Merguellil catchment

4.5 MEASURED VIRUS SIMULATED NUTRIENTS

Since no water quality data were available during the simulation period (1986-2005), the model was not calibrated. Nevertheless, some analysis for nitrate (NO3), ammonium (NH4) and mineral phosphorus were done from January to June 2007 throughout the river network. The analysis results of these nutrients fall in the range of the predicted concentrations (Figure 4.15 and 4.16).

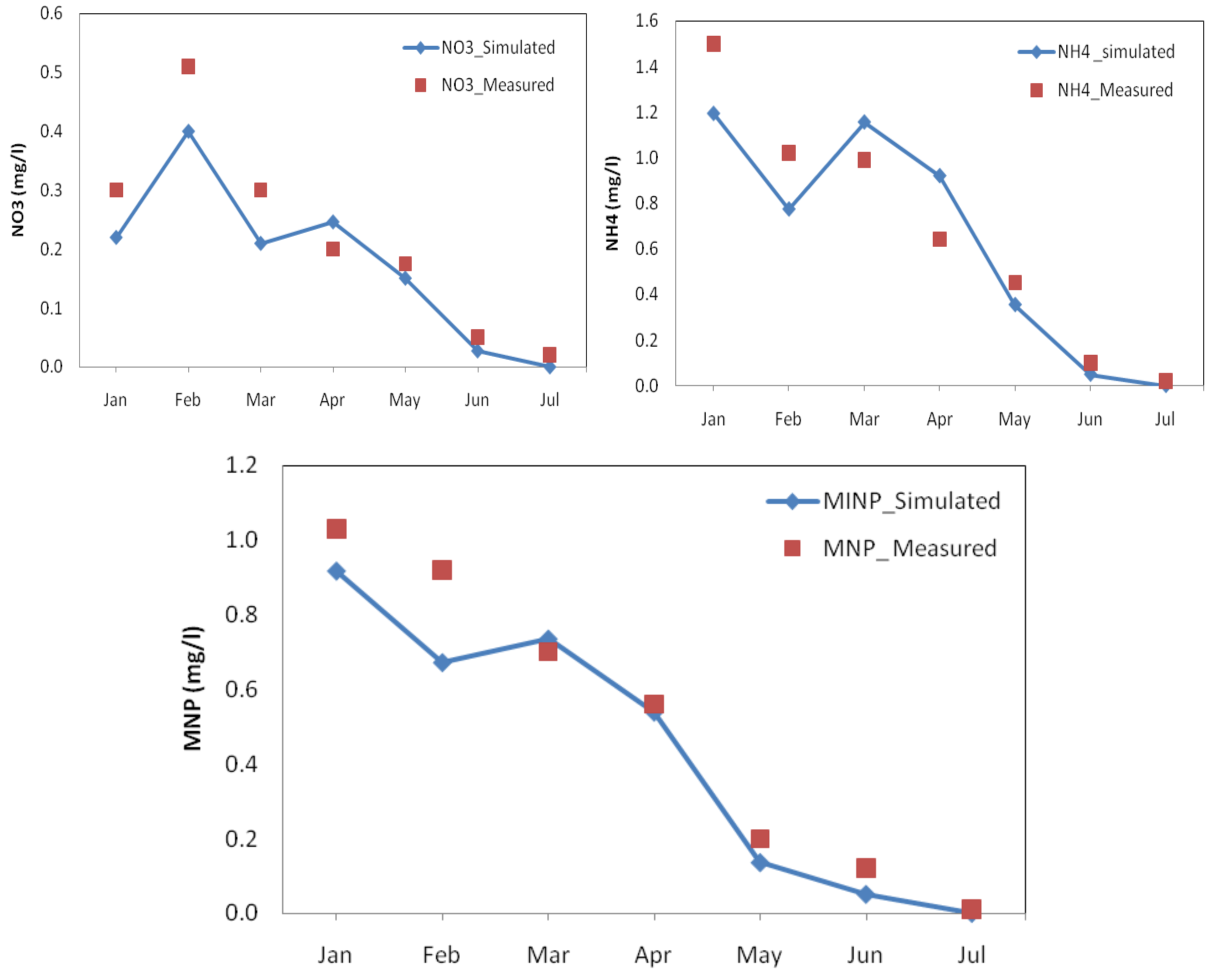

Figure 4.15 Measured virus simulated nutrients (mineral phosphorus, Ammonium and Nitrate) at the Skhira station

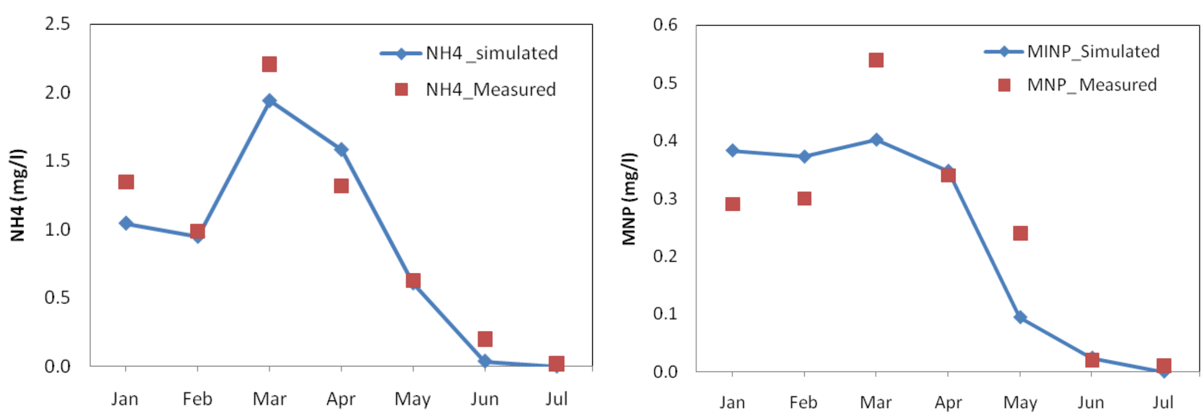

Figure 4.16 Measured virus simulated nutrients (Ammonium NH4 and mineral phosphorus MNP) at the Kissra station.

4.6 IMPACT OF SOILS

This section examines the components of the water cycle and sediment generation in relation to soil types. Group C with more clay content presents higher surface runoff and lower groundwater recharge comparing to group B. We note also that sediment yield for group C is lower than group B (Figure 4.17).

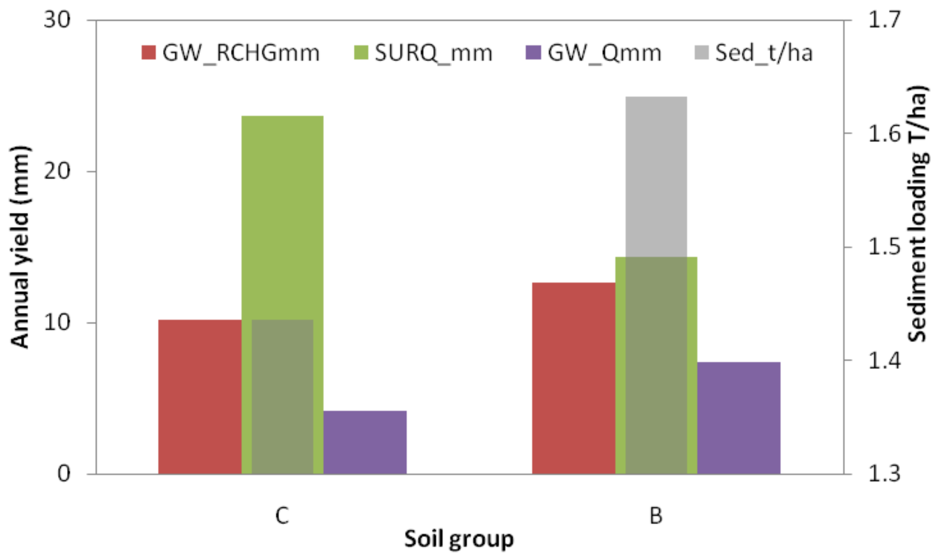

Figure 4.17 Average annual yields of the various components of the water balance according to clay content of soils.

4.7 IMPACT OF LAND-USE/LAND-COVER

Figure 4.18 illustrates shows that the variation of water balance components and sediment generation across soils is largely a factor of land cover.

SWAT simulates sediment loadings from Durum wheat, the principle land-cover in the Merguellil catchment basin, to be about 30% of total basin loadings (Figure 4.18). Without more quantitative data from the area, assessing the accuracy of simulated sediment loads from different land-covers cannot be assumed. Acquiring such data would most certainly allow fine tuning of the model and as a result improve basin-wide sediment yield simulations.

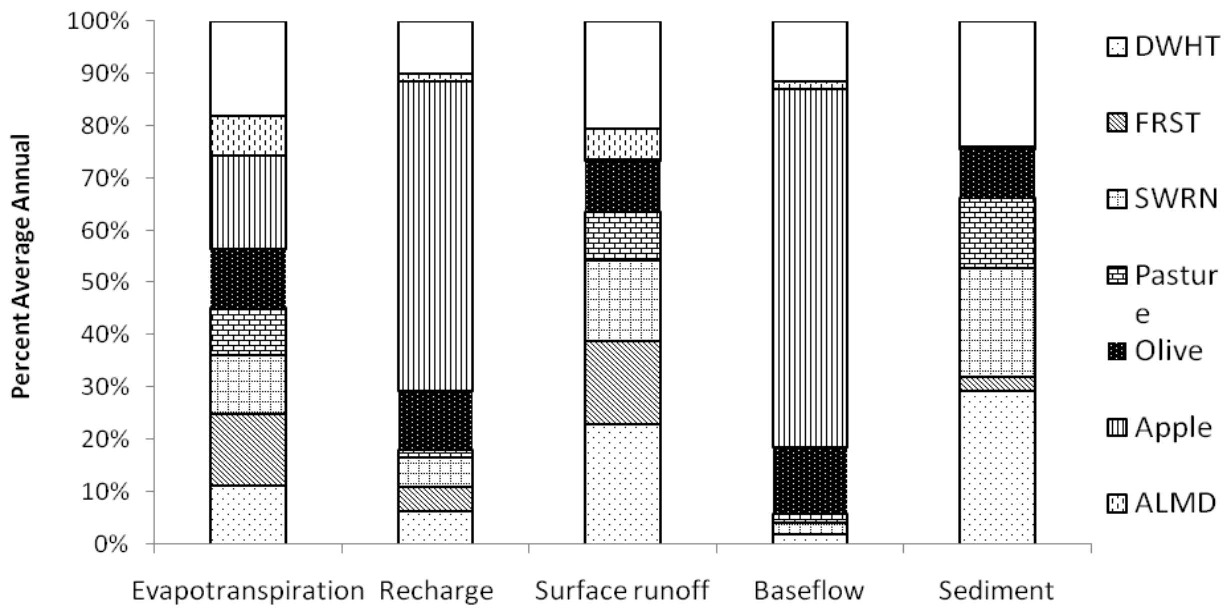

Figure 4.18 The portion contributed to the total annual yields by different land-cover

Table 4.5 presents the contribution of the land uses presented in the Merguellil catchment to different component of water and nutrient cycle. Land-cover, where relatively high quantity of mineral and organic nitrogen are produced, is principally durum wheat and urban (7.17 kg/ha and 10.17 kg/ha respectively). Durum wheat, the most abundant crop in the area (44%), contributes to the production of the highest value of sediment (2.21T/ha). This is due to the high surface runoff (27.21mm/year).

Table 4.5 Land use contribution to water and nutrient balance

	AREA km^2	PRECIP mm	SURQ mm	GWQ mm	ET mm	Sed t/ha	N kg/ha	ORGN kg/ha
DWHT	468.26	347.67	27.24	2.68	283.65	2.21	0.36	7.17
FRST	205.03	391.26	19.05	0.00	355.04	0.20	0.08	1.00
SWRN	244.10	329.79	18.16	3.39	282.36	1.56	0.06	2.35
Pasture	4.45	251.43	11.12	2.42	232.46	1.01	0.03	2.93
Olive	103.38	314.04	11.74	18.27	290.32	0.71	0.11	2.43
Apple	0.44	316.00	0.00	98.72	452.86	0.00	0.00	0.00
ALMD	35.02	238.25	7.15	2.15	196.47	0.04	0.03	0.29
TOMA	1.03	277.80	24.38	16.62	462.77	1.81	0.24	8.55
URBN	0.59	316.00	26.02	3.20	286.39	0.67	0.27	10.17

CHAPTER 5 ALTERNATIVE SCENARIOS

5.1 SCENARIO 1: REMOVING CONTOUR RIDGES

5.1. 1 IMPACT OF SWCW ON WATER BALANCE AND SEDIMENT LOADING

The Merguellil catchment suffers regular water shortage aggravated by current drought with different degrees of frequency, intensity and severity. In addition, the natural hydrological regime is continuously altered by the construction of 44 small dams (hill ponds) and 5 large dams (hill reservoirs) and contour ridges. These reservoirs are frequently completely dry especially during the summer period. However, they constitute good traps for sediment loading and protect then the outlet (El Houareb dam) against silting.

The simulation results show that since 1996, the hill reservoirs constructed within the watershed have contributed to the storage of big volume of water (about 6.43 million cubic meters per year (Mm^3/year), from 1996 to 2005). Nevertheless about 12% of these waters are loosed by evaporation. The model predicts that these reservoirs contribute to the retention of approximately 67 106 T/year of sediment.

The mean annual water volume stored in the hill ponds during the simulation period (1990-2005) is estimated to 1.70 Mm^3. The evaporation presents 3% of the water stored, while sediment loading is around 6635 T/year. The adding of contour ridges (potholes) within the watershed has contributed to the storage of a big volume of water. The average during the simulation period of the water inflowing in all the 23 potholes within the watershed is 335 mm/pothole/year. The storage period of the potholes does not exceed one day since all the water entering to the pothole is taken out either by evaporation or by infiltration to the aquifer. Evaporation Presents 10%, while the infiltration is 90 % respect of the water inflowing to potholes.

In order to assess the impact of these regulations on the hydrological regime and sediment retention, the option of removing these potholes from the upstream was simulated with the SWAT model.

The results (Table 5.1) show that during the simulation period, the potholes have reduced the runoff (Surface Q) by approximately 32 % and the total water yield (TWY) by 21 %, while the aquifer recharge (Total AQR) is increased by 50 %.

Table 5.1 Impact of potholes on water balance and sediment loading

	Surface Q (mm)	TWY (mm)	Total AQR (mm)	Volume ($10^6 m^3$)	Sediment (T/ha)
No pothole	23.93	27.94	10.19	26	96740
With Pothole	16.22	22.05	15.42	19	71430
Change (%)	- 32	- 21	+ 50	-25	-26

Figure 5.1 presents the change in annual surface runoff at the outlet caused by the potholes. We note that the potholes inhibit surface runoff during all years. As a consequence TWY is also reduced during all years except for 1998, 2000 and 2001 (Figure 5.2). This can be explained by the high increase of the total aquifer recharge during these years. As a consequence, the water volume at the outlet will decrease by 25% leading to a reduction of 26% in sediment load. This reduction in water volume varies from 5% in 2005 to 51% in 2002 corresponding respectively to wet and dry year (Figure 5.3).

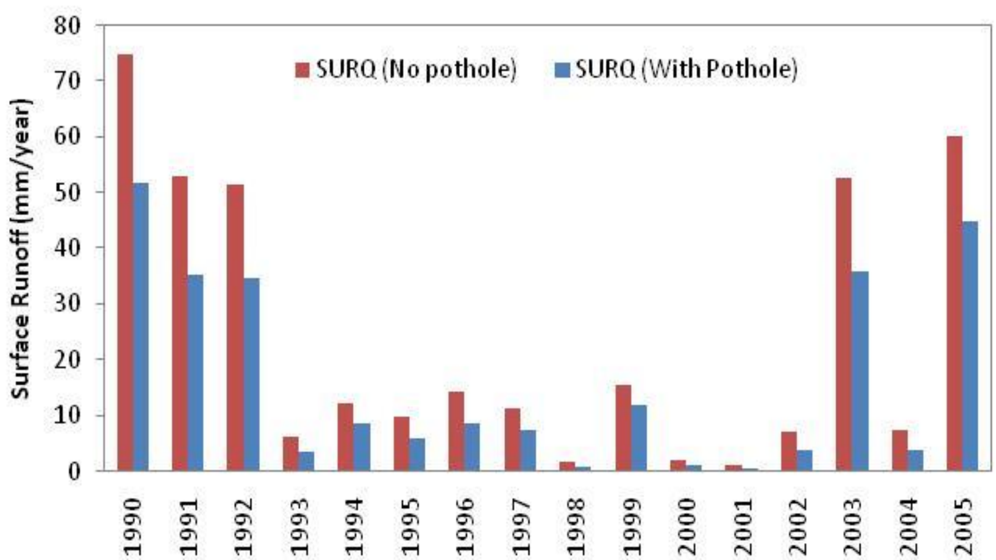

Figure 5.1 Impact of potholes on surface runoff

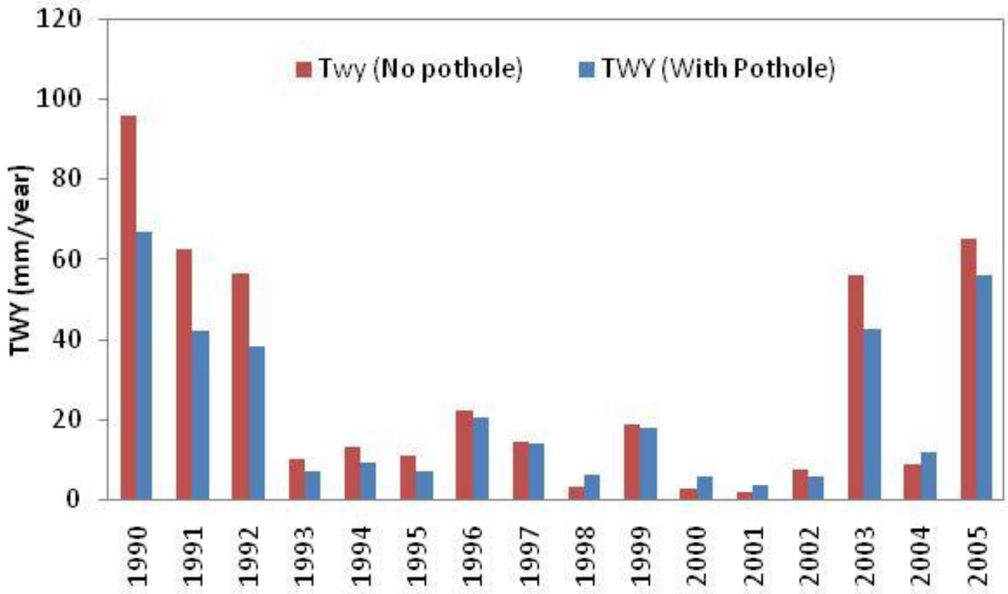

Figure 5.2 Impact of potholes on total water yield

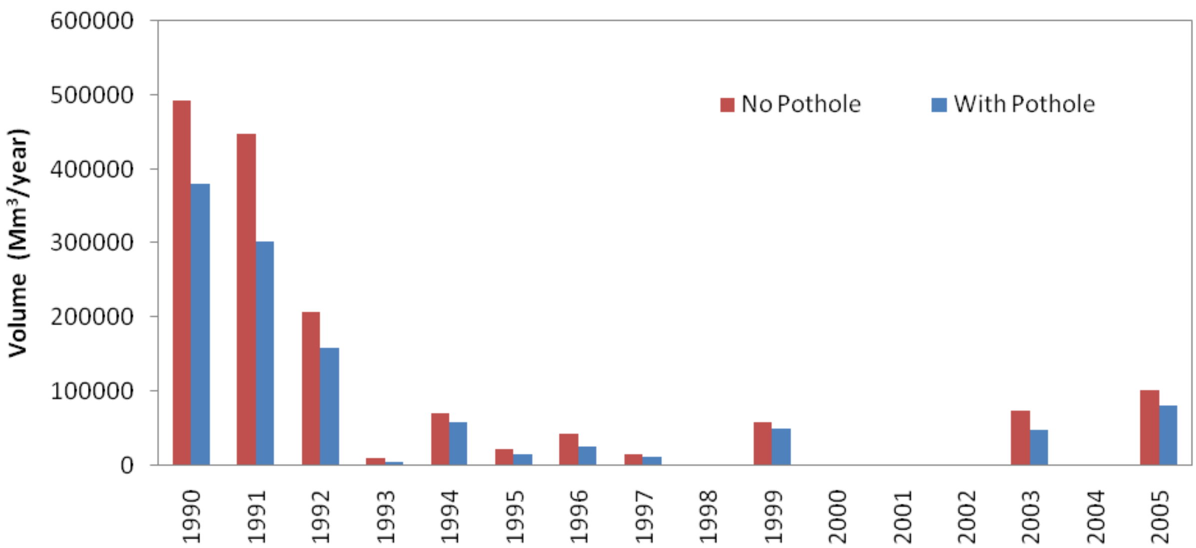

Figure 5.3 Impact of potholes Water volume at the outlet

As previously mentioned, the presence of pothole has reduced the surface runoff. Figure 5.4 shows the average values of surface runoff (SURQ) based on the historic data of 1990-2005 for each subbasin without potholes (a) as well as the anomaly graphs with potholes (b). All subbasins undergo a reduction in surface runoff. This decrease varies within the catchment based on the location (See Figure 3.8) and the volume of potholes (See Figure 3.21) upstream the subbasin. It is more emphasize (between 52 and 66 % of surface runoff reduction) in the mountain regions (Oueslati, el Ala, and Dj Bardou).

Figure 5.5 illustrates the average values of groundwater flow (GWQmm) based on the historic data of 1990-2005 for each subbasin without potholes (a) as well as with potholes (b). It should be pointed out that pothole increase the groundwater, however this increase in noted only subbasins 11, 12, 14 and 16. Subbasin 11 and 16 have potholes with water storage capacity higher than 100 mm receiving water from the HRU (considered as pothole) and additional contribution from other HRUs in the same subbasin. This leads to an increase in GWQ from 0 to 0.63 mm in subbasin 11 and from 9.5 mm to 53 mm in subbasin 16. Subbasin 14, with big pothole, is receiving water only from itself which explain the increase of the GWQ (from 0 to 4.36 mm).

In the upstream area of the Merguellil catchment some subbasins does not suffer any change in GWQ (subbasin 1 to 10). On the contrary, for the other subbasins, we note a decrease in GWQ due to surface runoff reduction upstream these areas. This reduction was more accentuate in the downstream area of the Merguellil catchment even if some subbasins are equipped with potholes. Figure 5.6 shows the average values of Total Water Yield (mm) based on the historic data of 1990-2005 for each subbasin without potholes (a) as well as the anomaly graphs with potholes (b). The results obtained show a reduction of the TWY in all the catchment except for subbasin 16. This is due to the fact that groundwater flow highly increases from 9.5 mm to 53 mm.

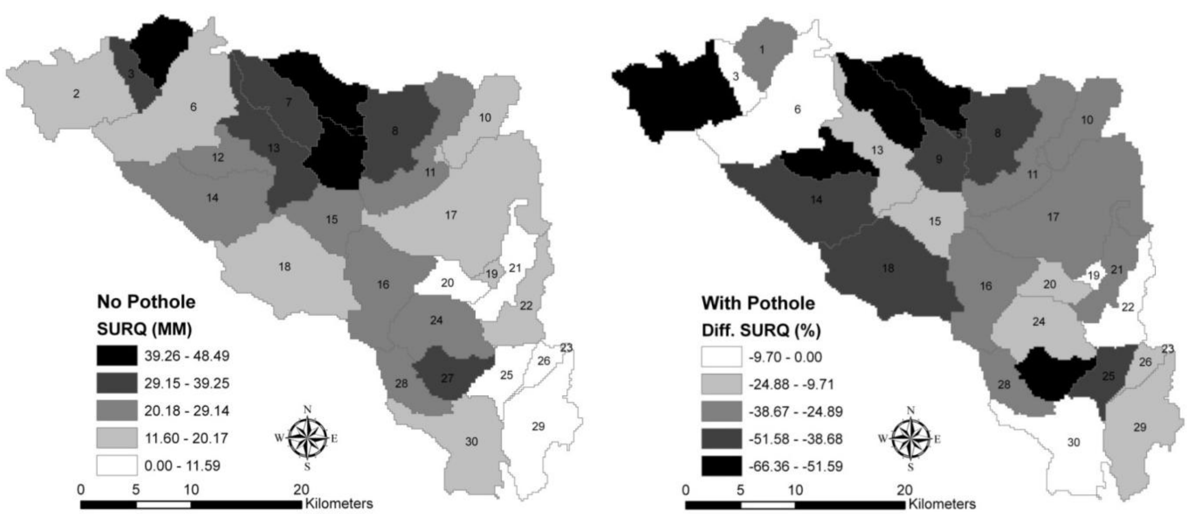

Figure 5.4 Impact of pothole on surface runoff reduction

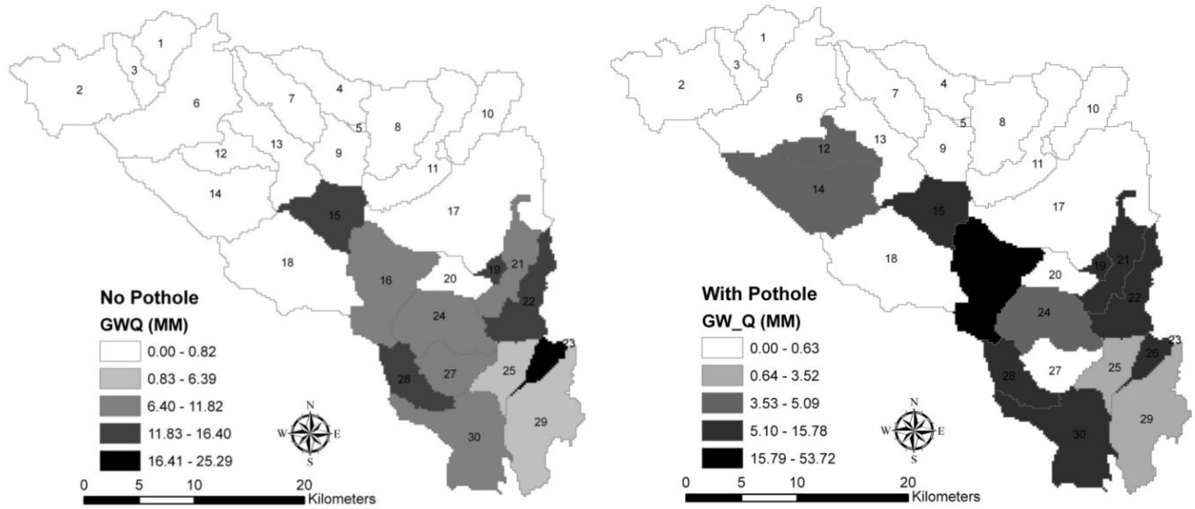

Figure 5.5 Impact of pothole on surface groundwater

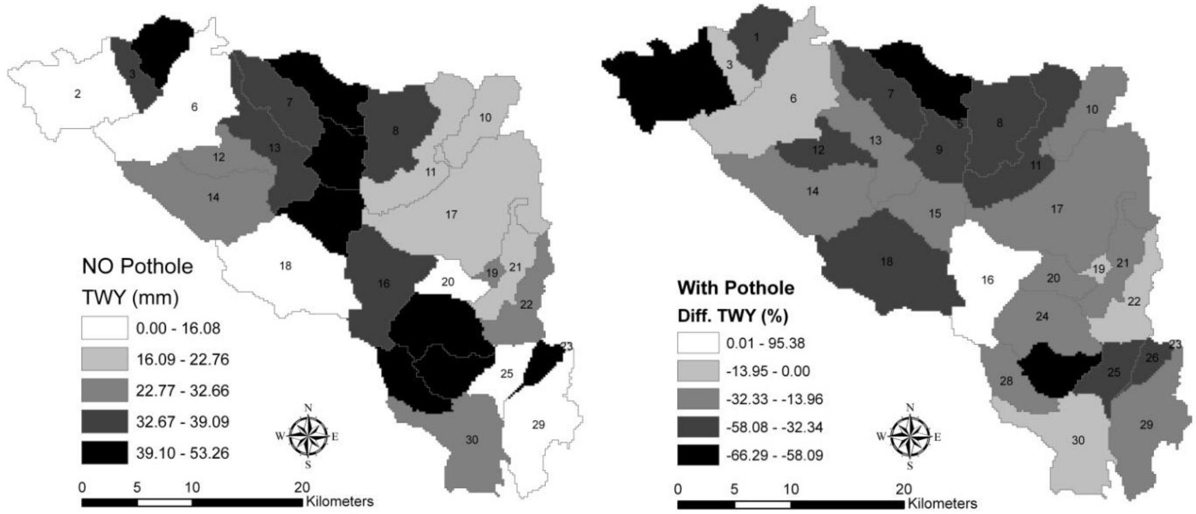

Figure 5.6 Impact of pothole on Total Water Yield

Figures 5.7, 5.8, and 5.9 show the average values of sediment yield, and organic nitrate and phosphorus respectively based on the historic data of 1990-2005 for each subbasin without potholes (left) as well as the anomaly graphs with potholes (right).

Potholes are considered as good traps of sediment and organic nutrient. We note reduction in all nutrient loads within the catchment. The reduction ranges between 0 and 71 % for sediment and 0 and 95% for organic nitrate and phosphorus.

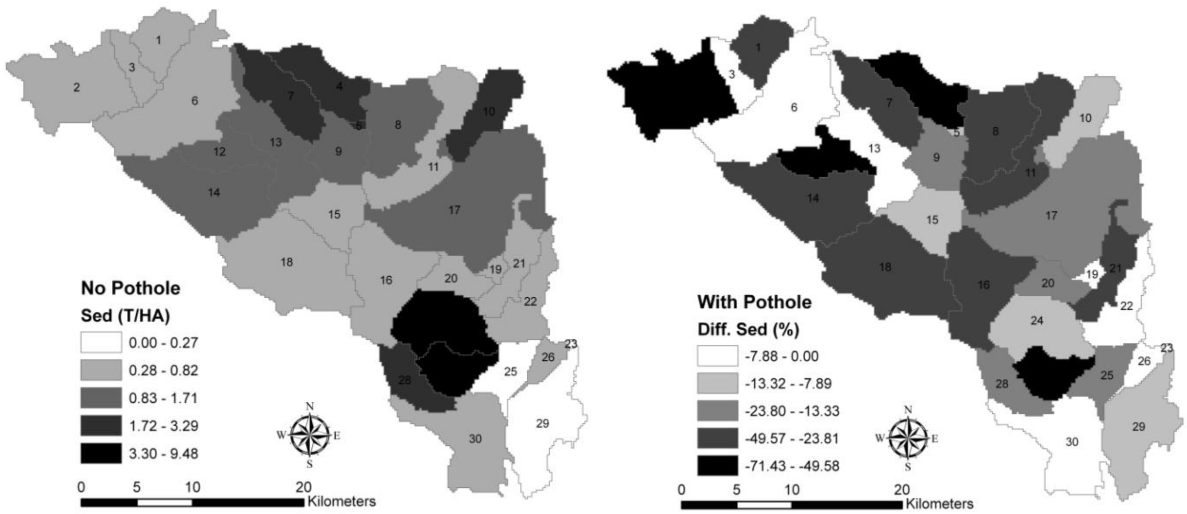

Figure 5.7 Impact of pothole on Sediment load

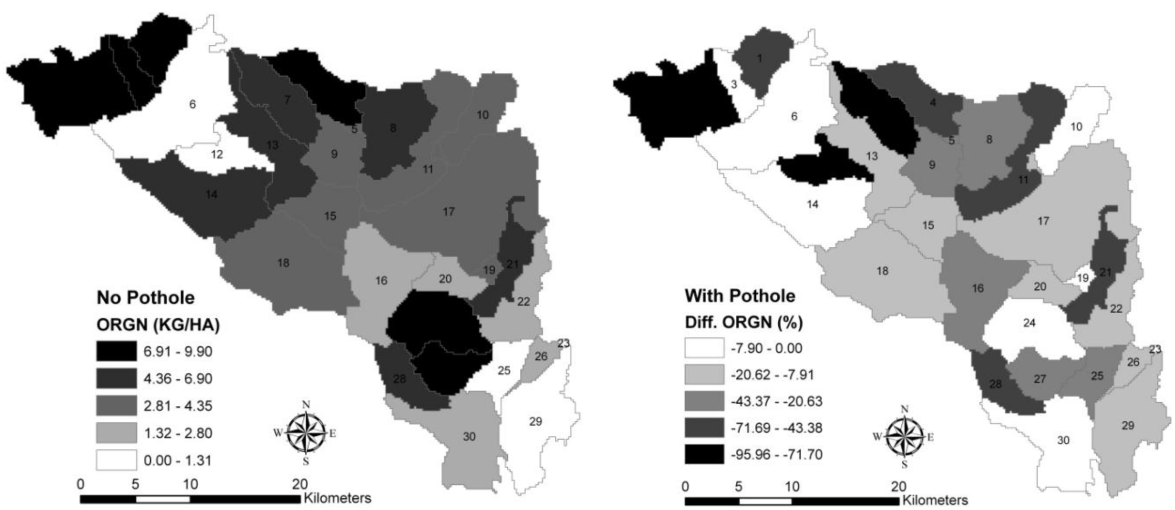

Figure 5.8 Impact of pothole on Organic Nitrate

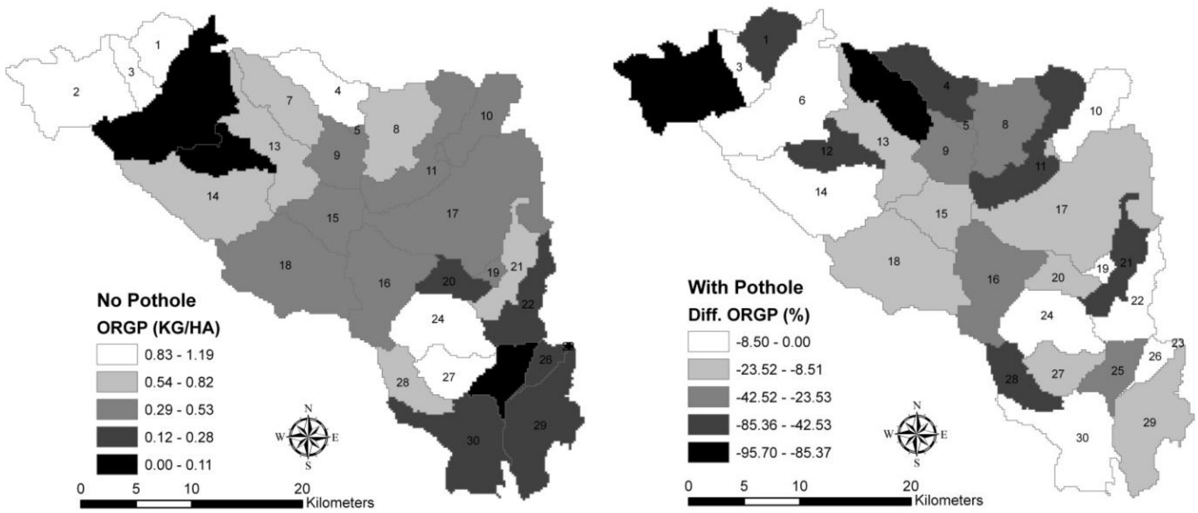

Figure 5.9 Impact of pothole on Organic Phosphorus

5.1.2 IMPACT OF CONTOUR RIDGES ON SEDIMENT RETENTION IN THE RESERVOIRS

The potholes constitute good traps for sediment loading and protect then the ponds and reservoirs against silting. Figure 5.10 presents the change in sediment loading in the 5 reservoirs within the catchment. The reduction is sediment retention in these reservoirs range between 12 % for El Hammam dam (RES 5) and 46 % for El Karrou dam (RES1).

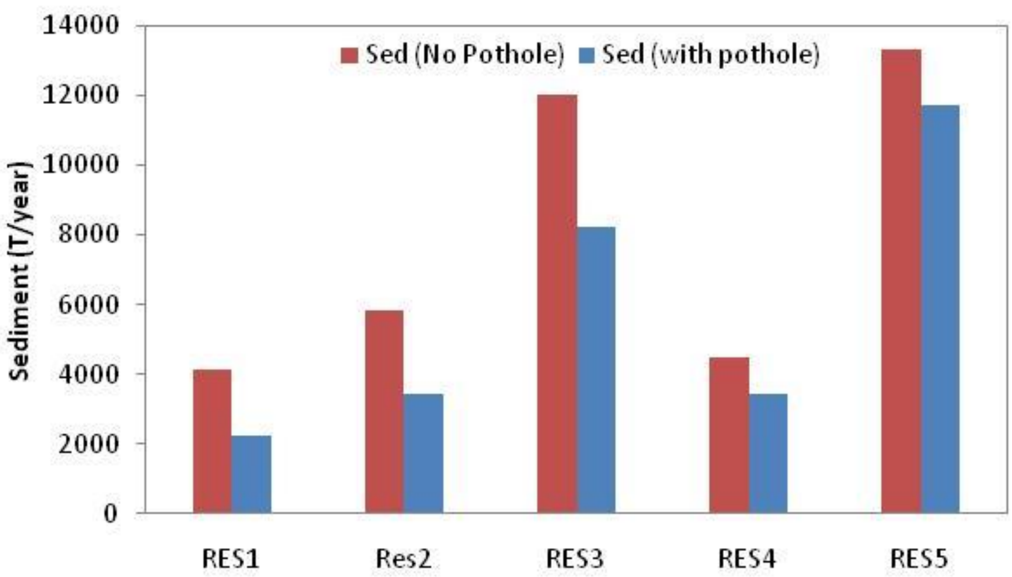

Figure 5.10 Impact of potholes on sediment retention in the five reservoirs within the watershed

5.1.3 IMPACT OF CONTOUR RIDGES ON CROP YIELD

To assess the impact of adding potholes on crop production, we have analyzed the change in the biomass and harvest dry yield of olive and durum in the HRUs considered as pothole (Table 5.2). Regarding the dry yield, a reduction of 5 % was noted for durum wheat when it is cultivated in potholes; whereas an important increase of about of 52% is noted for the olive. The biomass was also raised by 17 and 15% for Durum wheat and Olive respectively when they are cultivated in potholes.

Table 5.2 Impact of potholes on crop yield

	Durum Wheat		Olive	
	Harvest Yield (T/ha)	Biomass (T/ha)	Harvest yiled (T/ha)	Biomass (T/ha)
No pothole	3.09	9.6	2.08	118
In pothole	2.92	11.26	3.16	136
Change (%)	5%	+ 17	+ 52%	+ 15

Figure 5.11 illustrates the yield change for Durum wheat in different HRUs considered as potholes where these crops are cultivated. The reduction or the increase in the crop yield is owing to a variation in one or more stage of the crop growth cycle. The impact varies with space and variety.

We note a yield reduction in some HRUs_Pothole corresponding to subbasins (3, 5, 8, 10, 12, 14, 21, and 27). This reduction could be explained by the low soil water content in these HRUS considered as pothole and then a reduction of the potential water uptake by plant from the soil surface to any depth in the root zone.

These potholes are located in subbasin where the upstream is equipped by other potholes reducing the surface runoff (See Figure 5.4) and then soil water content. The yield reduction is more important in the pothole located in subbasin 14 which experience a decrease of 42 % of surface runoff leading to a decrease of 42 % in the yield. Same thing for the pothole number 12 which suffer a reduction of 37 % of total water yield leading to a decrease of 32 % of yield. The increase in Durum wheat yield is noted in potholes located in subbasins 1, 4, 7 and 11. It was more significant in subbasins 1 and 4 (36 % and 52 % respectively), located in north east boundary of the catchment. The contribution of water to these subbasins is generated from themselves. Potholes in subbasins 1 and 4 have a maximum water storage capacity of 100 mm receiving water from the HRUs where they are located and also from contribution of other Hrus in the same subbasin (only for subbasin 4, 50 % of water in HRU number 25 is drained in the pothole).

Figure 5.12 illustrates the Olive yield’s change in different HRUs considered as potholes. Conversely to durum wheat, Olive tree yield’s has increased in almost all the pothole_HRUs except in potholes located in subbasins 20 and 30. The increase is more relevant in subbasins 16 (70 %) due to the highly increase of groundwater recharge in these potholes (see chapter). Consequently the soil water content increases and then increases the potential water uptake by plant from the soil surface to any depth in the root zone.

It should be pointed out that the olive trees cultivated in subbasin 30 are irrigated. Furthermore the mean value presented with the red line in figure 5.12 illustrates only the non irrigated olive trees. We note a high yield as average of the simulation period (1990-2005). This yield decrease when the olive is cultivated in the pothole because of the reduction of the soil water content in this basin. In comparison, we simulated the yield cultivated in subbasin 30 without irrigation in both cases (with and without pothole), and the result showed that the yield decrease by 21 % with the presence of potholes.

Figure 5.13 illustrates the yearly change in the olive yield cultivated in the pothole located in subbasin 20. We can notice that the olive yield’s increase continuously and can be doubled for some years when it is cultivated in the potholes.

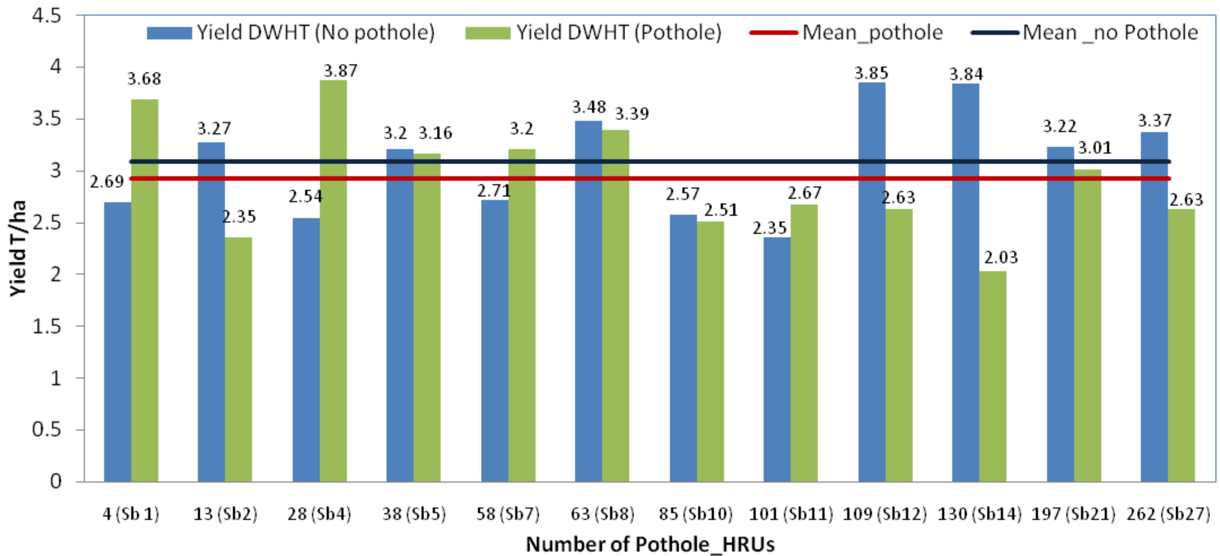

Figure 5.11 Impact of pothole on Durum wheat's yield

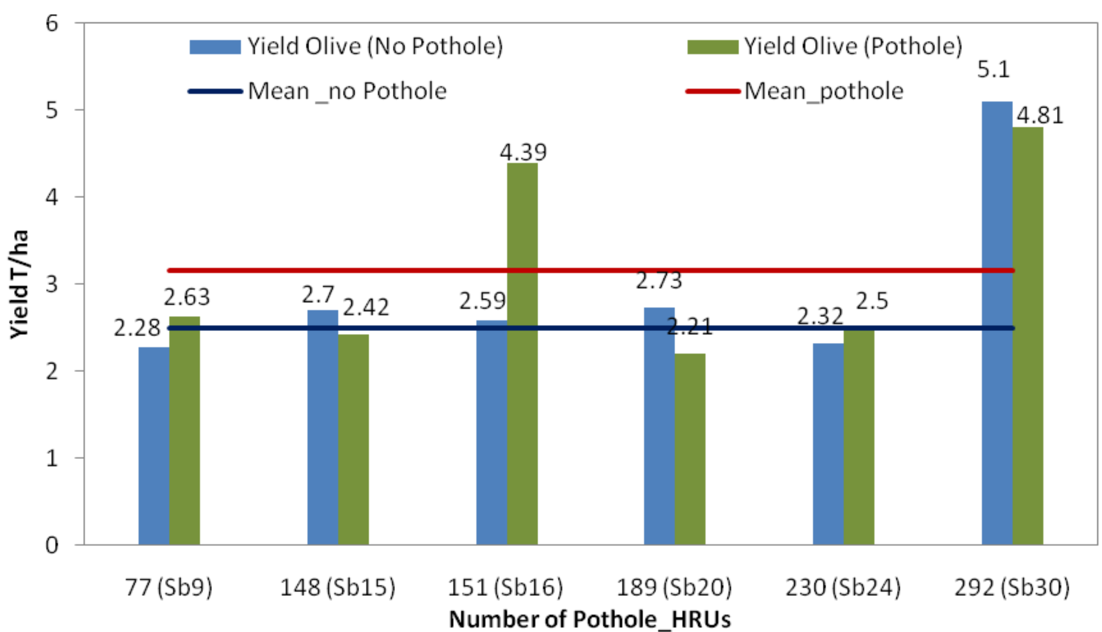

Figure5.12 Impact of pothole on Olive's yield

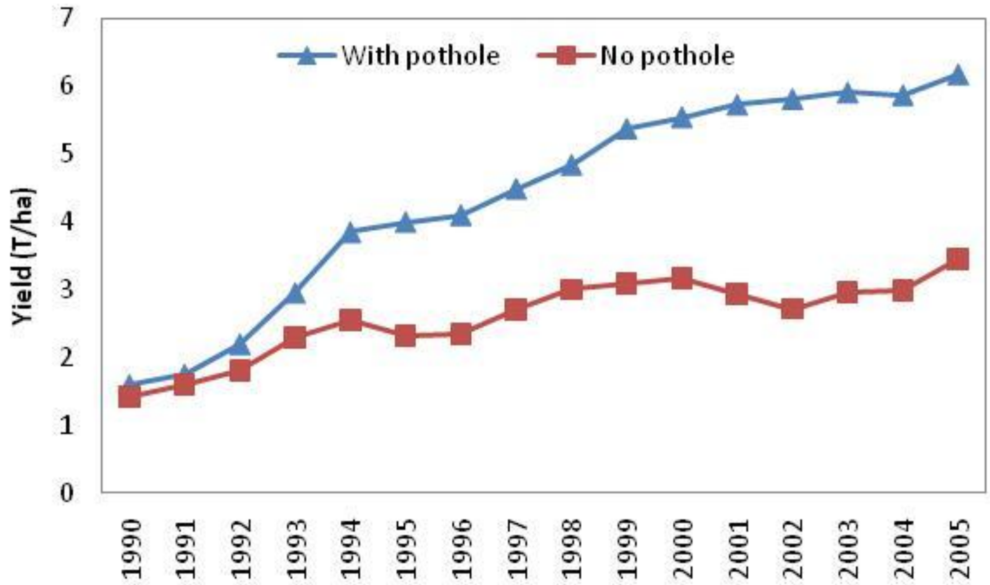

Figure 5.13 Impact of pothole on the olive yield in one of the potholes (Pot_HRU 151 Sb 20)

Most of the area considered as potholes are cultivated by durum wheat (70 %), the rest is olive trees (10%) and non-cultivated area (30 %). Since the introduction of potholes within some HRUs in the watershed has considerably increased the olive yield in these HRUs, Olive tree planting in pothole areas looks like an adequate solution to profit from these wet areas.

CONCLUSION 1

The hydrological model SWAT was applied to an arid watersheds with water-harvestings systems. The model was rather successful in reproducing water flow. However, the limited detailed temperature data availability and the lake of information about water quality measurement degraded the quality of the model results. The simulation results have clearly shown that contour ridges (considered as pothole in this study) within the watershed have an important role of the retention of sediment; whereas, they showed to have an impact on the hydrologic regime in the catchment by reducing the surface runoff by 32 %. In addition, planting the Olive tree between the contour ridges has shown an increase of the olive yield.

Since the cropping pattern in the upstream of El Houareb dam is dominated by non irrigated crops, and the irrigated areas extend over the downstream of El Houareb dam, then the water stored in the reservoirs and ponds serve mainly to recharge the aquifers. In fact, these water harvesting systems intercept runoff at the upstream part of the catchment, thus depriving potential downstream users of their share of the resources. It becomes necessary to manage resources at larger scales, especially where conflicts between upstream and downstream water users increase. Unfortunately, these water and soil conservation works are built in a water resource -limited area (low rainfall, high evaporation) and where the population badly controls the water resources. In addition, the main disadvantage of the use of rainwater harvesting systems in this area is that the system may be damaged during heavy rainstorms and need regular maintenance. Further studies should investigate the water management in these regulations.

5.2 SCENARIO 2: REDUCTION OF THE FERTILIZER AMOUNT

In order to achieve the high yields which drive modern agriculture, the farmers use to apply huge amount of nitrogen fertilizers. The application will continue to increase substantially as global population and food requirements grow. Unfortunately, while fertilizers are effective in driving crop yield improvements, they also frequently have a negative impact on the environment. In fact, since most plants are able to utilize only a part of the nitrogen fertilizer applied by growers, much of the remaining nitrogen fertilizer leaches into the aquifers and rivers which reduce dramatically the quality of water resources in this area. In addition the evaluation of the optimal plant requirement needs precise investigations on nutrients availability in the soil and nutrient management planning. In order to identify and simulate the positive impact of possible Best Management Practices, the SWAT model was used to generate a scenario with a reduction in fertilizer amount of 20%. This reduction was applied to durum wheat, olive, and almond. The objective of this study is to simulate the effects on water quality of the reduction in fertilizers use and to evaluate the impact of this reduction on crop yield. SWAT model was run considering actual land-uses, management practices and the amount and type of fertilizers adopted in the study area. All of input variables (weather, soils, land-use, and management conditions) are held constant in the two cases simulated, except for fertilizer application which varies according to policy scenario. The results of this scenario show a slight reduction of 2% in the durum wheat yield, 0.57% on the olive, while no change for the other crops was illustrated (Table 5.3).

Table 5.3 Estimated effects of reduction fertilizer application (20%) on the crop yield.

CROP	Yield (T/ha)		Yield reduction
	Baseline	Scenario 2	%
Durum wheat	2.56	2.51	2.09
Olive	3.33	3.31	0.57
Almond	0.23	0.23	0.00

The mean daily nutrient concentrations are lower for this scenario than those computed for the actual one. Therefore, on yearly scale and during the decade 1996–2005, it was noted a reduction in simulated loads for the reduced fertilizer scenario, compared to the actual scenario (Table 5.4). This reduction ranged, from 3 to 10% for nitrates, from 2.5 to 8% for total nitrogen and from 13 to 16.5 % for total phosphorus.

Table 5.4 Nutrient loads (T/year) at the outlet for the baseline and scenario 1 and the reduction percentage

	N-NO3 (T/year)			N total (T/year)			P total (T/year)		
	Baseline	Scenario1	%	Baseline	Scenario1	%	Baseline	Scenario1	%
1996	116	111	4	242	236	3	74	62	16
1997	183	176	4	361	352	3	85	74	13
1998	28	25	11	35	32	9	5	4	20
1999	167	157	6	364	353	3	109	94	14
2000	35	32	9	43	40	7	6.2	5.4	13
Mean	106	100	6	209	202	3	56	48	14

CONCLUSION 2

The results of this scenario suggests that a better use of the fertilizer, such as not over-applying it, could substantially reduce the amount of nutrients flowing down river without compromising crop yields. The results of this analysis will make good discussions on the impact of nitrogen control policies and will be of interest to government, farmers, fertilizer producers and environmental stakeholders.

The application of the SWAT model for the Merguellil catchment confirms that SWAT is a useful tool that can already be used to make preliminary assessment of the water and land management of the basin. These assessment will consequently be based on the best currently available knowledge for the study area under local conditions of data availability.

5.3 SCENARIO 3: CLIMATE CHANGE SCENARIO

5.3.1 FUTURE CLIMATE DATA AND MODEL SCENARIOS

Anticipating changes in the hydrologic cycle is particularly important for regions with limited water supplies such as the Merguellil catchment. In this chapter we report on the results of investigating the impact of climate change on water resources in this catchment for the near and far future. We specifically looked at the changes in various components of the water balance including precipitation, evapotranspiration, total water yield, soil moisture and river discharge.

A general circulation model (also known as a global climate model, both labels are abbreviated as GCM) uses the same equations of motion as a numerical weather prediction (NWP) model, but the purpose is to numerically simulate changes in climate as a result of slow changes in some boundary conditions (such as the solar constant) or physical parameters (such as the greenhouse gas concentration). GCMs are widely applied for weather forecasting, understanding the climate, and projecting climate change.

In order to best assess the expected climate change impacts on a species, ecosystem or natural resource in a region, climate variables and climate change scenarios must be developed on a regional or even site-specific scale (Wilby et al. 2001). To provide these values, projections of climate variables must be 'downscaled' from the GCM results, utilizing either dynamical or statistical methods (IPCC, 2001). The methods used to convert GCM outputs into local meteorological variables required for reliable hydrologic modeling are usually referred to as ‘downscaling’ techniques (Dibike and Coulibaly, 2005; Huntingford et al., 2006). Without downscaling, the climate is the same everywhere inside the grid box of the GCM. This is clearly not very realistic and does not give you confidence in the future climate projections at a specific location.

The most important and fundamental part of statistical downscaling is to create a realistic statistical model from observations. The main assumption of these techniques is that the statistical relationships identified for current climate will remain valid under changes in future conditions. Downscaling techniques may allow modelers to incorporate daily variability in future changes (e.g., Diaz- Nieto and Wilby, 2005) and to apply a probabilistic framework to produce information on future river flows for water resource planning (Wilby and Harris, 2006).

In this study we used the output of the third Generation of the Canadian Global Coupled Model (CGCM 3.1) version T63, which has a surface grid with spatial resolution of roughly 2.8 degree lat/long and 31 levels in the vertical. With this resolution, The Merguellil catchment fells inside one grid box of the CGCM. Future climate scenarios for periods of 2010-2039 and 2070-2099 were generated from (CGCM 3.1) for scenarios A1B, B1, and A2. These CGCMs data were then statistically downscaled to generate future possible local meteorological data of precipitation and temperature in the study area

Within the GCM we analyzed three commonly used scenarios: A1b, A2, and B1. The A1 scenarios are of a more integrated world. The A1 family of scenarios is characterized by a rapid economic growth, a global population that reaches 9 billion in 2050 and then gradually declines, a quick spread of new and efficient technologies. The A1B scenario in this family depicts a world with a balanced use of fossil and non-fossil fuel as a main energy source. The A2 scenarios are of a more divided world. This scenario describes a world of independently operating, self-reliant nations; continuously increasing population; regionally oriented economic development and slower and more fragmented technological changes and improvements to per capita income. The B1 scenario highlights a world with more integrated, and more ecologically friendly. This scenario is characterized by a rapid economic growth as in A1, but with rapid changes towards a service and information economy; population rising to 9 billion in 2050 and then declining in A1; reductions in material intensity and the introduction of clean and resource efficient technologies; an emphasis on global solutions to economic, social and environmental stability.

A key aspect of the climate change impact study is the spatial and temporal downscaling of the GCM results. In this study, the CGCM data were statistically downscaled for the period 1986-2000 using monthly linear regression model and monthly fourth degree non linear model from observation in different climate stations (13 rainfall and 2 temperature gages). These models were largely used in the literature (Wilby et al., 1998, Abbaspour et al., 2009). The parameters of the monthly linear and non linear regression are listed in Appendix 11 for all stations.

The SWAT model was run for the future climate period to analyze the potential impact of climate change on flow, evapotranspiration, and soil moisture across this catchment. Finally, Richter et al.'s Indicators of Hydrologic Alteration (IHA) were used to analyze the flow regime alterations under changing climate.

5.1.2 DOWNSCALING CLIMATE VARIABLE

The downscaled temperature data from the CGCM agreed quite well with the recorded historical data. The Regression coefficient R2 rages from 0.90 to 0.99 for the two temperature stations. Figure 5.14 shows the monthly calibration for the period (1990-2000) (a) and validation for the period (1986-1989) (b) for the downscaled temperature from CGCM on December and February in the station number 1 using the linear and non linear test (other figures for the calibration are listed in Appendix 12). The result of first degree linear and a fourth degree non linear model were similar except for low and high temperature.

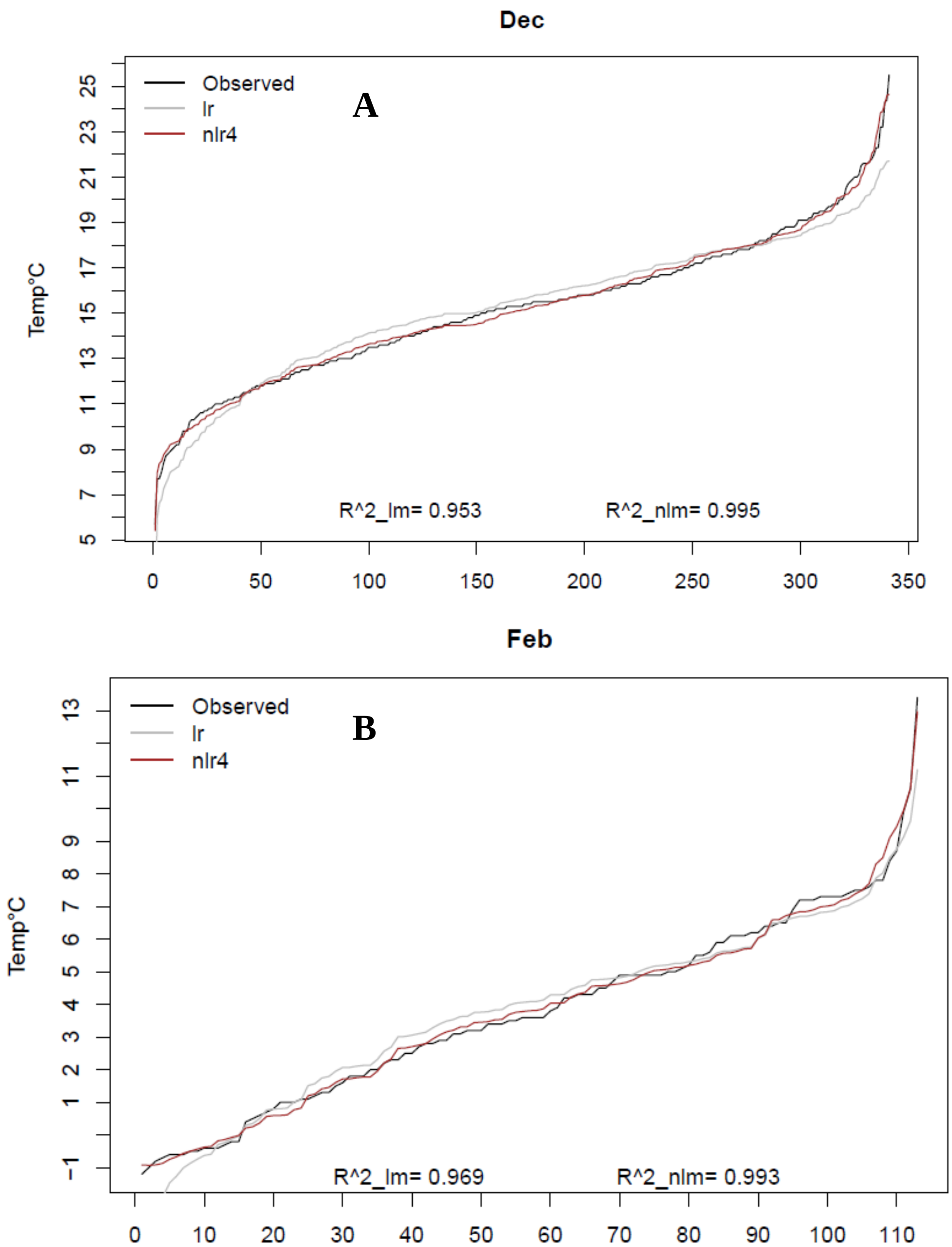

Figure 5.14. Tmax calibration on Decmber (a) and Tmin validation on February (b)

In order to select the most adequate regression model that fit better the observed data, statistical parameters such as median, min, max, 25% quantile, and 75% quantile were derived for observed and downscaled minimum and maximum temperature (from linear (lM) and non linear models (NLM)). The adequate model is the one that statistics fit well those derived from the observed data.

For example, Figure 5.15 shows the comparison between the statistical parameters mentioned above calculated for the minimum temperature at station 1 for the calibration period. In this figure, it is clear that non linear model fit better with the observed data than the linear model particularly in October. After confronting all the statistics for observed maximum and minimum temperature with those derived from the two downscaled models (LM and NLM), we opt for the non linear model.

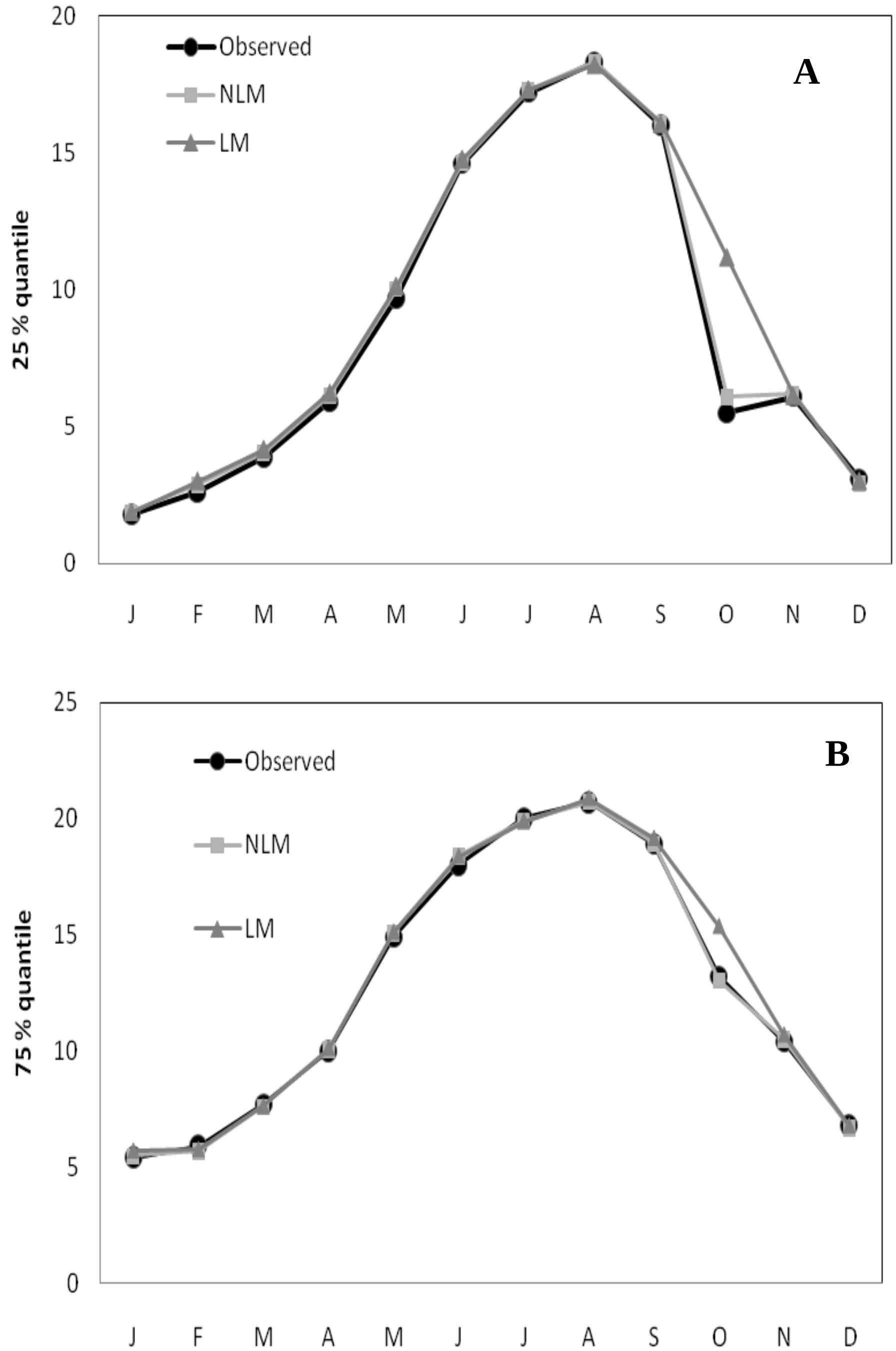

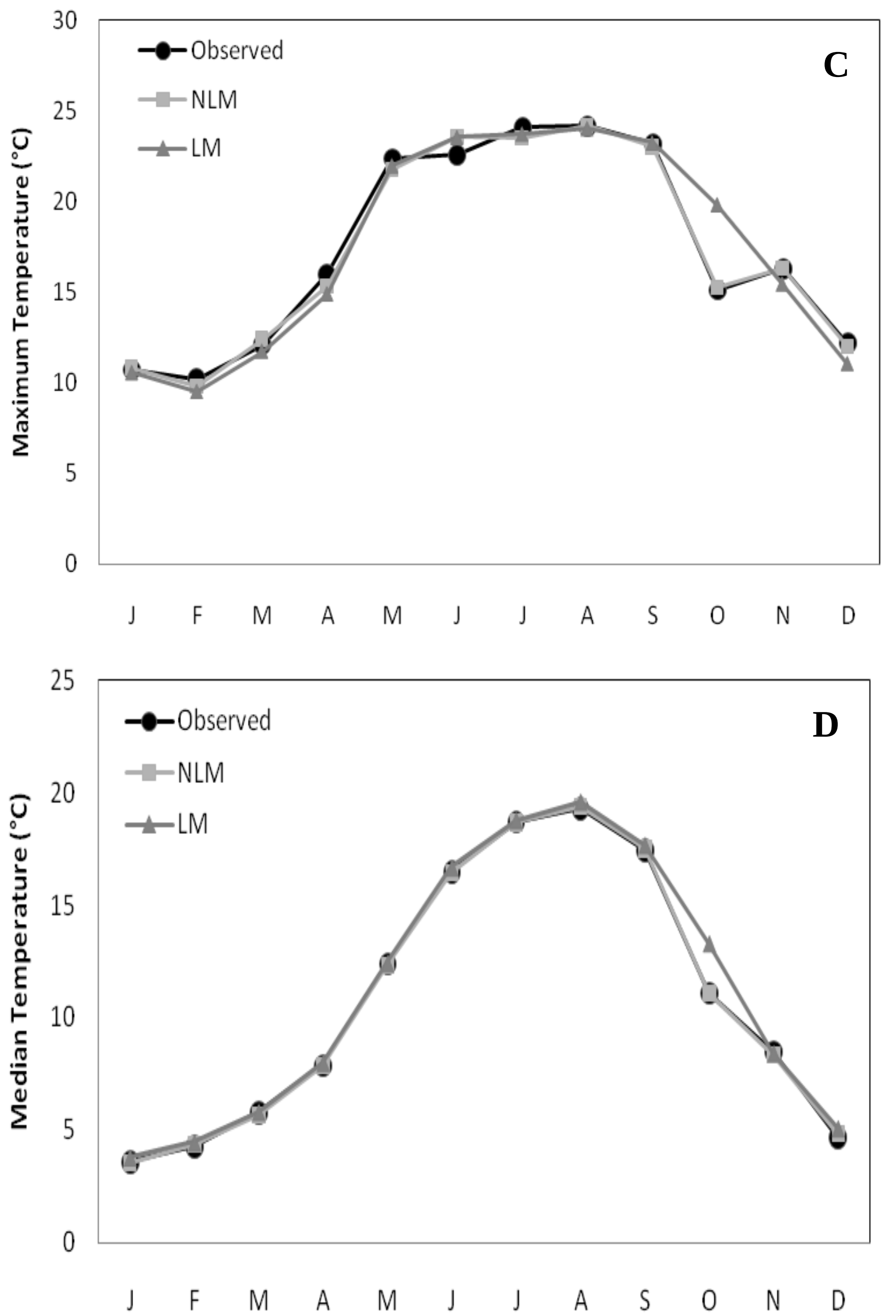

Figure 5.15 25% quantile (a), 75 % quantile (b), maximum temperature (c) and median temperature and (d) calculated for the minimum temperature at station 1 during the calibration period (1990-2000)

The fit of the downscaled rainfall data was also relatively good as compared with measured historical data. The Calibration and validation of the downscaled precipitation using first degree linear and a fourth degree non-linear are presented in figure 5.16 at El Houareb barrage rain gage on January (calibration) (a) and December (validation) (b).

The downscaled precipitation data from CGCM agreed quiet well with the recorded historical data. All the 13 stations had R2 values in the range of 0.70-0.97. The Same statistical parameters were calculated for precipitation as for temperature. These statistics show that non linear model fit better with the observed data. Hence we adopt for the non linear model.

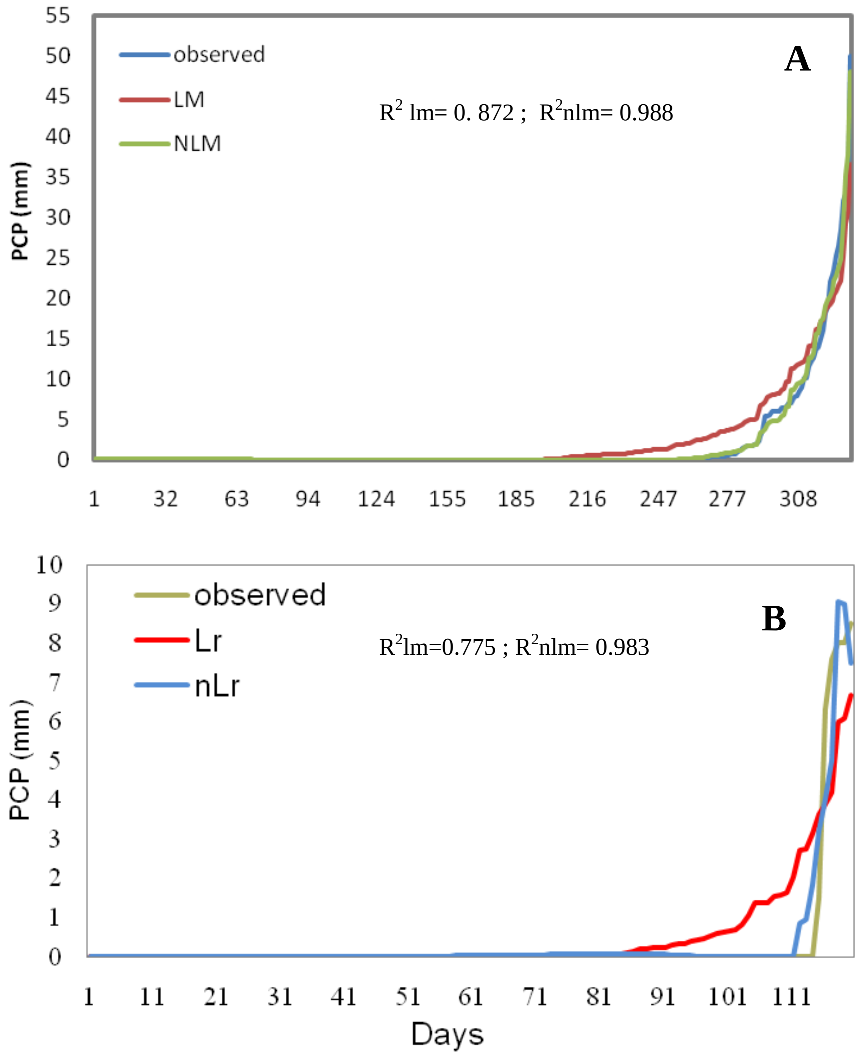

Figure 5.16 Calibration (a) of PCP downscaled on January (1990-2000) and validation (b) of PCP downscaled for September (1986-1989)

5.1.3 IMPACT OF CLIMATE CHANGE ON TEMPERATURE AND PRECIPITATION DISTRIBUTION

Future daily climatic data are generated by applying the non linear model to the future CGCMs data. Predicted long term average temperature max and min are compared with historical data for different scenarios in different time Period. During all periods, all scenarios show an increase in maximum and minimum temperature for both stations. Figures 5.17a,b and 5.17c,d show the average monthly changes in maximum temperature for station 1 and 2 respectively. Change in maximum temperature varies from 1 to 6 degree in different scenarios with the highest occurring in June for A2 scenario during the period 2070-2099.

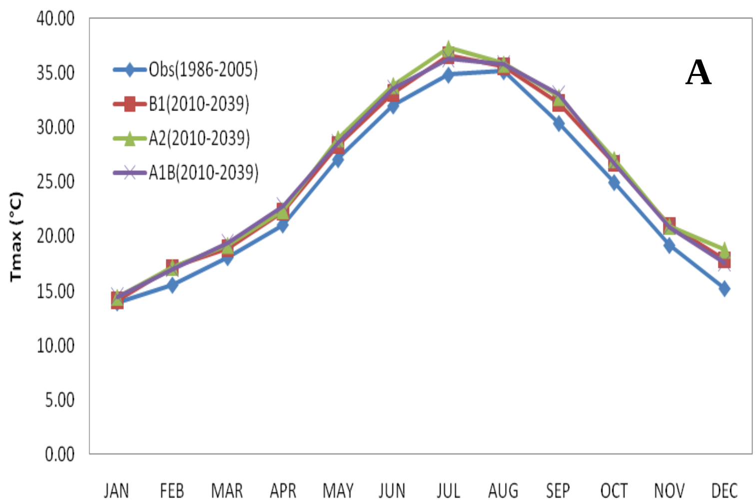

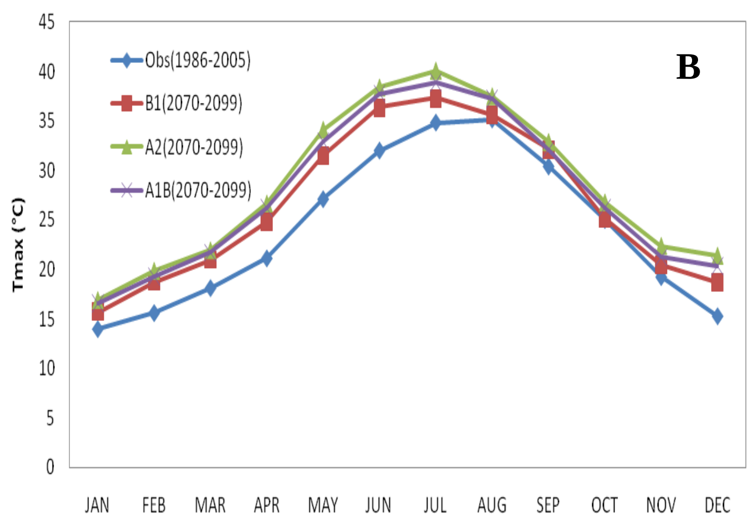

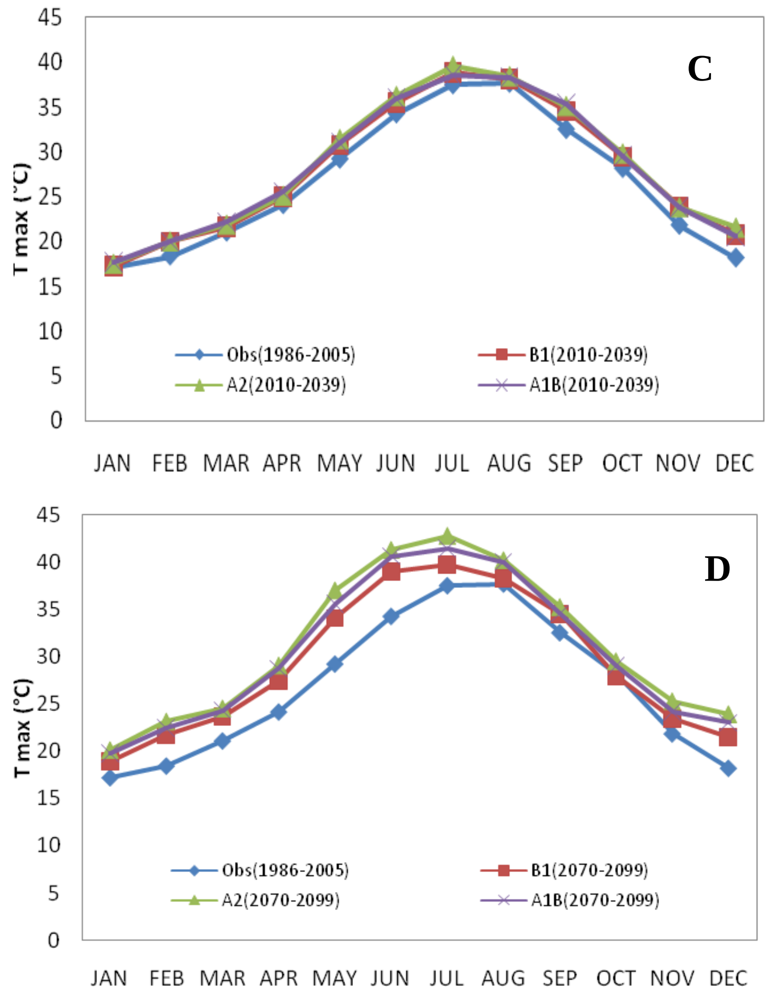

Figure 5.17 Mean monthly Tmax (°c) of the Merguellil catchment under current climate and downscaled GCM-generated Temperature for station 1 (a-near future and b-far future) and for station 2 (c- near future and d- far future)

Predicted long term average precipitations (mm day^{-1}) are compared with the historical data for different scenarios in different time period. Figure 5.18 shows the average monthly change on precipitation at "El Houareb barrage" rain rage. In general, all scenarios predict a decrease in almost all the months except in November for the near future. During this month, all scenarios predict an increase of about 0.1 mm day^{-1}for B1, 0.2mm day^{-1} for A2, and 0.5mm day^{-1} for A1B scenarios. The reduction in rainfall amount is notable in February and April with a decline of 0.4mmday^{-1} from the historical data 1986-2005.

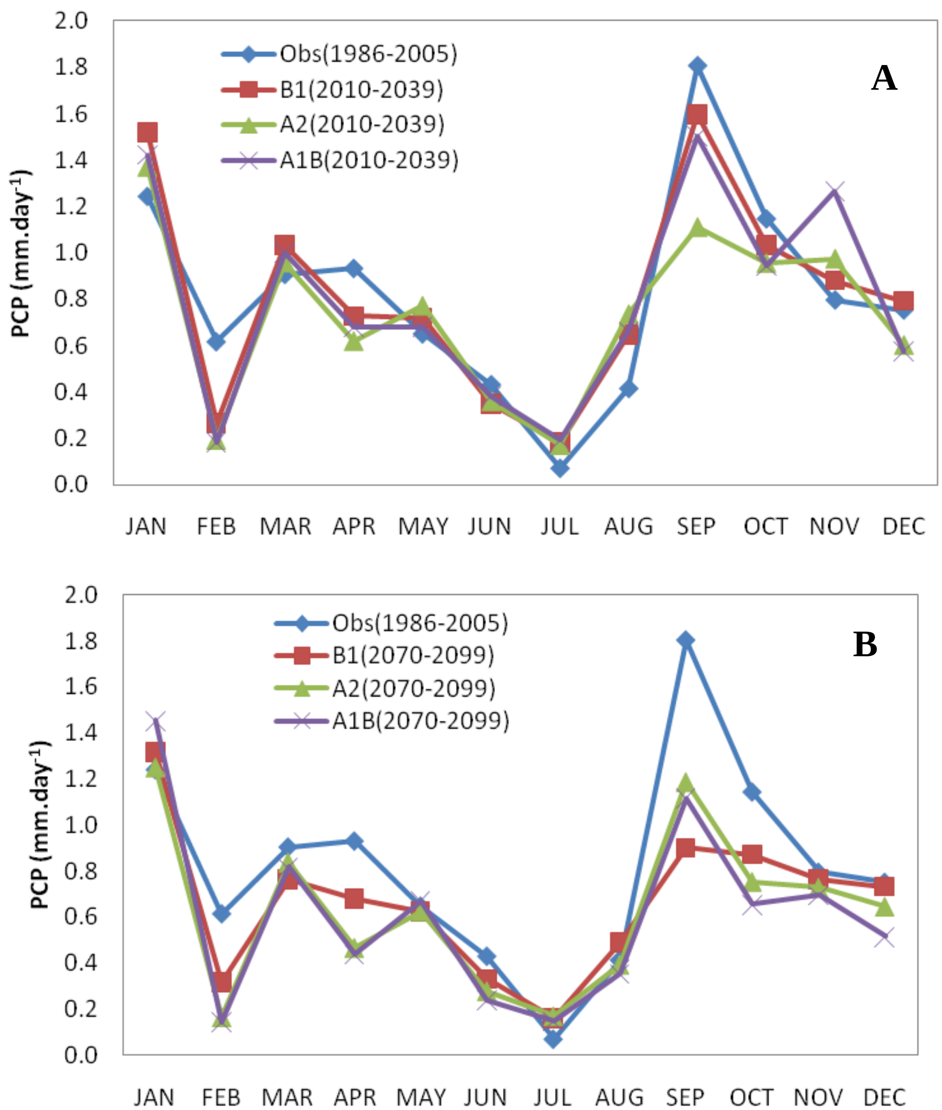

Figure 5.18 Mean monthly precipitations (mm day^{-1}) of the Merguellil catchment at El Houareb barrage station under current climate and downscaled GCM-generated precipitation for different scenarios (a-near future and b- far future).

Table 5.5 shows the seasonal average precipitation (mm month^{-1}) and temperature (°C) for four seasons: Autumn (SON), winter (DJF), spring (MAM) and summer (JJA) during the historical period (1986-2005). The seasonal change in precipitation and temperature on catchment scale are presented in Figure 5.19. For all scenarios, all seasons will experience an increase of temperature and a decrease in precipitation. Such changes will vary from season to another.

In autumn (SON) (Figure 5.19a), the decrease in precipitation is between 20% for A2 scenario and 28 % for A1B scenario. During this period rainfall would fall from 33 to 24 mm month^{-1}. In winter (DJF) (Figure 5.19b), the decrease in precipitation would reach 28 % for scenario A2 which will affect more the ecosystem of this already small water resource region. The increase in temperature is more severe in summer (JJA) for all scenarios and reaches 30 % for A2 (Figure 5.19d). Summer precipitation would also decrease especially for A2 and A1B scenarios (-50%). During this period, rainfall would fall from 13 to 6 mm month^{-1}. These significant changes in temperature and precipitation would intensify summer droughts.

Table 5.5 Seasonal average precipitation (mm month^{-1}) and temperature (°C) during the historical period (1986-2005) at catchment scale

Season	Months	PCP (mm.month^{-1})	Mean Temp (°c)
Winter	DJF	28	11
Spring	MAM	28	17
Summer	JJO	13	28
Autumn	SON	33	20

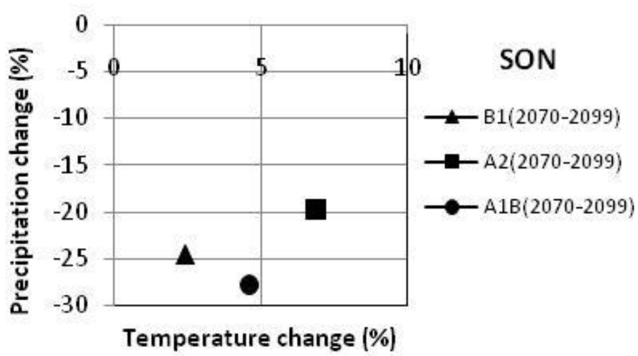

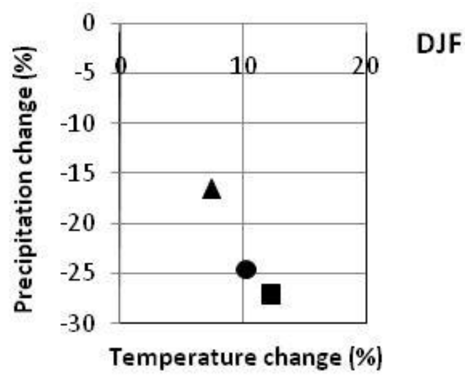

c) d)

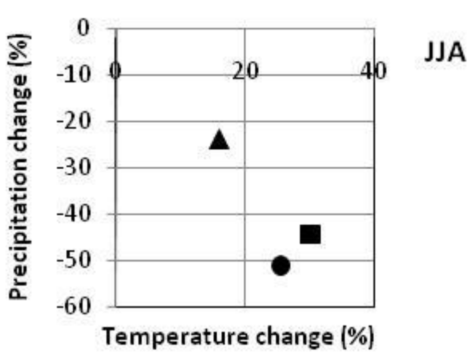

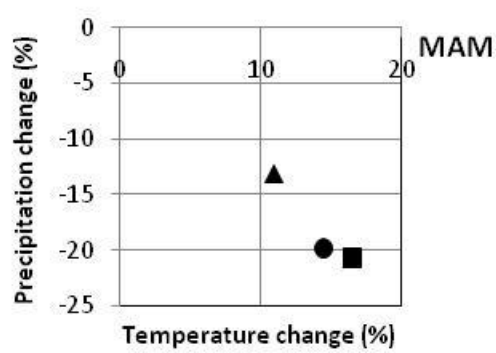

Figure 5.19 Seasonal changes in precipitation and temperature under future climate scenarios during the period (2070-2099). [a) SON = September October and November. b) DJF=

December, January and February. c) MAM= March, April and May. d) JJA = June, July and August.]

5.3.4 SWAT FUTURE SIMULATIONS

For future simulations, we used daily temperature and precipitation for each station from the downscaled GCM output (for scenarios A1B, A2, B1) for the year 2010- 2039, and 2070-2099. The 4 first years were skipped for model warm up. These data were then put into the SWAT model which modeled daily stream.

On catchment scale, all scenarios show a decrease in precipitation on near and far future (Table 5.6). This decrease would lead to a decrease in the TWY (which is river discharge plus groundwater recharge). As temperature increases, potential evapotranspiration is also expected to increase. Scenario A2 for the period 2074-2099 presents the extreme case with the highest PET of 1623 mm-year. Since the amount of water resources in expected to decrease in all scenarios, the actual evapotranspiration would also experience a decrease.

Table 5.6 Water balance component based on historical data of (1986-2005) and future climate scenarios.

Period	Scenario	PCP (mm)	TWY (mm)	PET (mm)	AET (mm)
1990-2005	Actual	329	28.69	1435	310
2014-2039	B1	290	19.38	1487	278
	A1B1	277	26.98	1456	254
	A2	266	13.45	1498	263
2074-2099	B1	248	13.19	1559	246
	A1B	219	8.26	1558	222
	A2	225	9.54	1623	228

Figure 5.20 shows the average values of the total water yield (TWY) based on the historic data of 1990-2005 as well as the anomaly graphs for scenarios B1, A1B and A2 for periods 2014-2039 and 2074-2099. Generally the total water yield decreases with the altitude. High values are noted in the mountain regions (Dj Trozza in the south, Kesra in the north), while low values are noted in the eastern part (Figure 5.20a). The near future simulations show an increase of the total water yield in the high altitude regions (Dj Barbou, El ala, and Dj Oueslat) of the catchment for all scenarios (Figures 5.20b,c,d). This increase is more noteworthy in El Ala region and reaches

200% for scenarios A1B and A2. While the south and the east part of the catchment would experience a reduction in the already small water resources. This reduction is more notable in Zebess. In the far future (Figure 5.20e, f, g), all scenarios show a decrease in water resources in all part of the catchment except the small increase in the western part for B1 and A2 scenarios.

It should be noted however that an increase of 200 % in the western part of the catchment amount to water resources of about 48 mm/year, which is still quite meager in water resource sense but could have a substantial impact on the ecosystem of this semi-arid region.

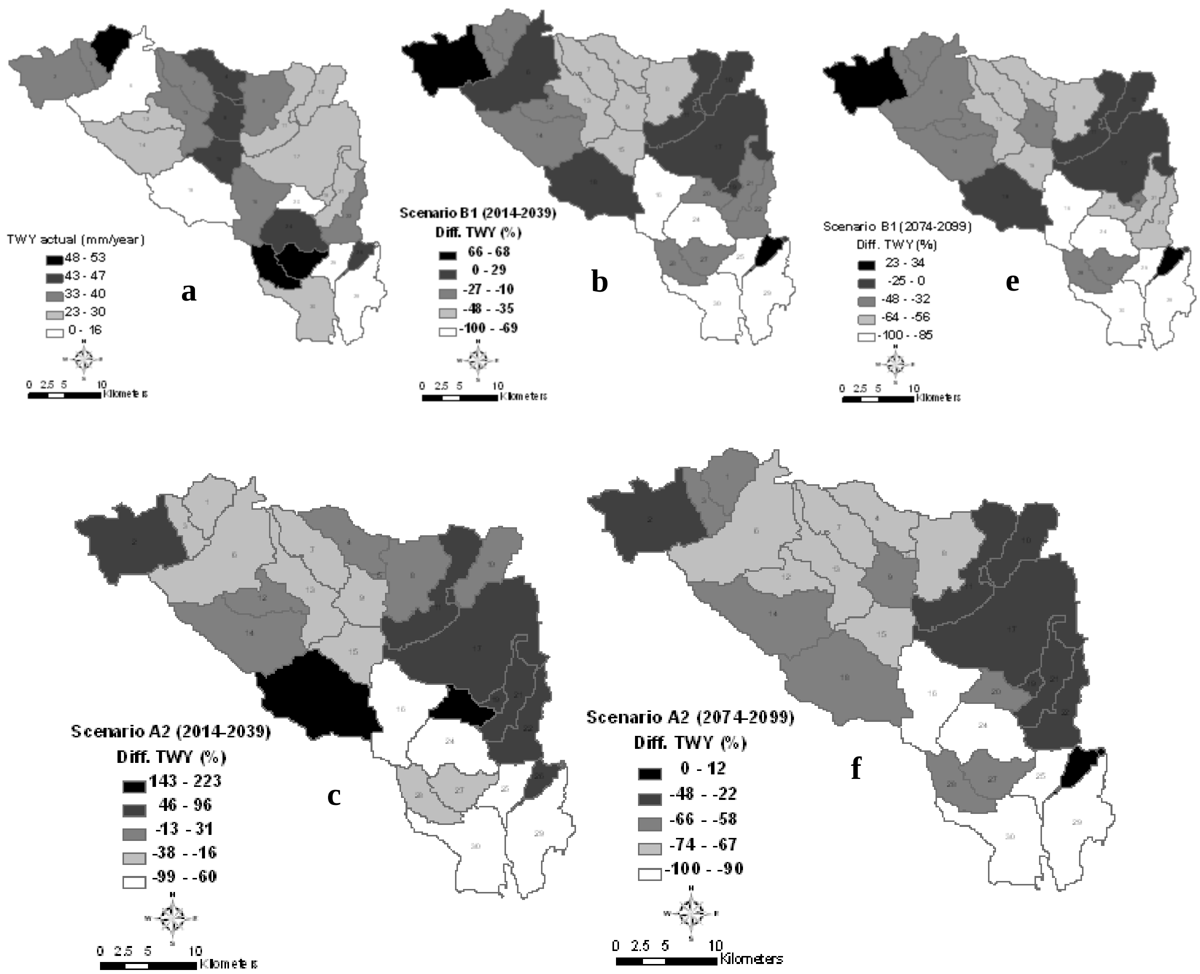

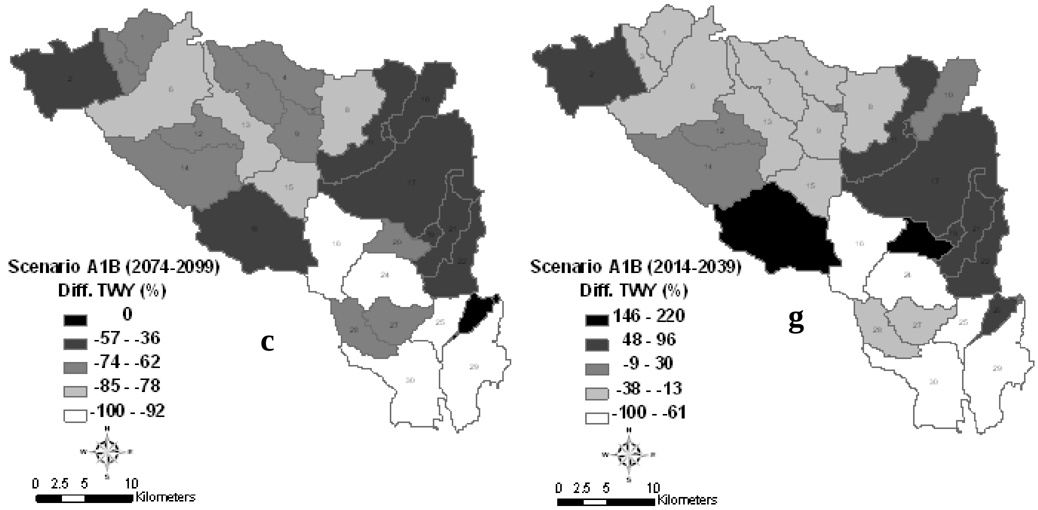

Figure 5.20 Average total water yield (mm/year) during the simulation period (1986-1990) (a) and the anomaly graphs for A1B, A2 and B1 scenarios for periods 2014-2039 and 2074-2099.

In the calculation of actual evapotranspiration, soil moisture and groundwater recharge, we assumed that the land cover in the future will stay the same as period of 1986-2005. Hence our results provide an indication of future changes rather than an actual scenario. As temperature increase, actual evapotranspiration is also expected to increase if there is enough water in the soil. Our calculations show AET decreasing in all the catchment because of the reduction in the soil water content except at El Ala region where AET increase due to the increase of the soil moisture.

Climate change is expected to have a profound influence on soil moisture. All scenarios predict a decrease in soil moisture for most region of the catchment. This decrease is more severe in the south in the near and far future for all scenarios. However, Scenario B1 (2014-2099) and scenario A2 (2014 and 2039) show an increase in the North West part of Skhira subbasin.

5.3.5 IMPACT OF CLIMATE CHANGE ON THE YIELD PRODUCTION

The durum wheat and olive trees are not irrigated crop, except few HRUs for the Olive trees. Climate change will have a significant negative impact on the wheat and olive production of the catchment as precipitation decreases. Table 5.7 shows the mean yearly dry yield for durum wheat, non irrigated and irrigated olive on catchment scale for the actual simulation (1990-2005) and the expected yield for different scenarios. We note a decrease in the crop yield for all scenarios during all periods.

In the far future, the scenario A1b presents an extreme case for the crop yield reduction. The durum wheat yield would decrease by 68 % and the olive yield by 73% (irrigated and rainfed). The reduction of yield for the rainfed crops is due to the reduction of precipitation. The impact of climate change on irrigated olive is more accentuated than on the non irrigated one because of the decrease of the total water yield which is river discharge plus groundwater recharge. The reduction of 73% on the yield of the non irrigated olive will result on a reduction of 4.11 T/ha.

Table 5.7 Impact of climate change on crop yield

Period	Scenario	Yield (T/ha)		
		Durum Wheat	non irrigated Olive	Irrigated Olive
1990-2005	Actual	2.71	2.35	5.62
2014-2039	B1	2.01	2.15	3.1
	A1B1	1.14	1.34	1.69
	A2	1.70	1.46	1.71
2074-2099	B1	1.63	1.52	2.4
	A1B	0.86	0.62	1.51
	A2	1.19	1.05	1.53

5.3.6 IMPACT OF CLIMATE CHANGE ON FLOW REGIME

5.3.6.1 INDICATORS OF HYDROLOGIC ALTERATION (IHA)

The quantity, timing and duration of river flow are critical components to water supply and water quality. The five components of flow regime (magnitude, frequency, duration, timing and rate of change) influence the ecological dynamics of river systems directly and indirectly through their effects on other primary regulators (Karr, 1991; Poff et al., 1997). Hence, climatic changes that create shifts in the timing and magnitude of low or high flow events or change the magnitude of river flow at monthly, seasonal, or yearly time scales could result in dramatically altered river systems (Gibson et al., 2005). The objective of this part is to examine the potential impacts of future climate scenarios on river flow regime at the catchment scale.

We evaluated current and predicted future flow regimes using Richter et al.'s (1996) Indicators of Hydrologic Alteration (IHA). IHA was designed to examine changes in flow regimes caused by dams, but its ability to compare flow regimes makes it an ideal tool for this study. This program takes daily streamflow values and characterizes flow regime in terms of five ecologically significant factors: magnitude, duration, frequency, timing, and rate of change. By dividing the streamflow record into a pre- and post-impact period, the program calculates the percentage change in several ecologically relevant statistics, including magnitude of monthly water conditions, magnitude and duration of annual extreme water conditions, timing of annual extreme water conditions, and frequency and duration of high and low pulses.

Since we were assessing the more subtle impact of climate on flow regime, we decided to focus on a specific subset of 37 statistics calculated by the program that were more likely to be sensitive to climate change. Specifically, we focused on mean monthly discharge for each month, magnitude of the 1-, 3-, 7-, 30- and 90-day maximum and minimum flows, timing of the 1-day maximum and minimum flows, and number of zero days. We assessed also the variability in monthly flows by calculating the coefficient of variation for each month over the period of record or the modeled periods.

5.3.6.2 FLOW REGIME ALTERATIONS UNDER CHANGING CLIMATE

We conducted IHA analysis on four sets of daily stream flow values. First, we calculated IHA hydrologic parameters for modeled daily stream flow under current climate from 1990 to 2005. Second, we calculated hydrologic parameters for the three future flows predicted by statistically downscaled GCMs corresponding to the three scenarios for the period 2074–2099. Finally, the coefficient of variation for the four datasets was calculated for each month.

To evaluate the impact of climate on flow regime, we compared the parameters calculated from the simulated data under current climate (1990–2005) to parameters calculated from the GCMs with predicted future climate (2074–2099).

The hydrographs under predicted climate for 2074–2099 differed markedly from the current conditions (Figure 5.21). Monthly flows decreased considerably compared to current conditions and did not exceed 1 m^3s^{-1}. Except for scenario B1 on September and November and scenario A2 on November where the discharge exceeds the current mean discharges.

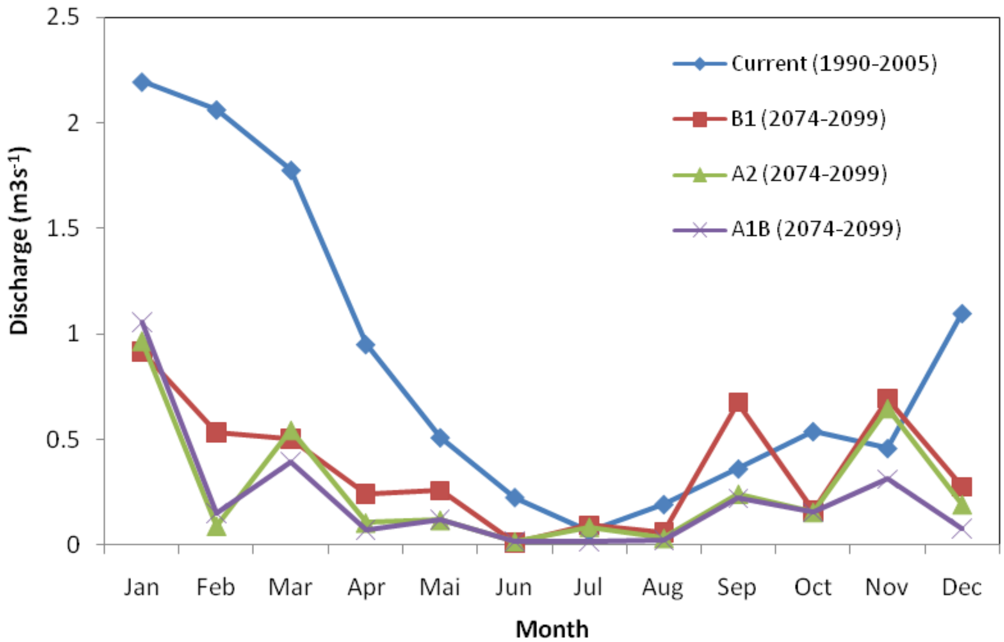

Figure 5.21 Mean monthly flow of the Merguellil River using simulated flows under current climate and downscaled GCM-generated stream flow.

Timing of the 1-day minimum was about 45 days earlier under future climate scenarios (24 January for B1 and A1B and 31 January for A2) compared to current conditions (11 March) (Figure 5.22), but the 1-day maximum was almost 35 days later under future climate scenarios (4 March for B1 and A1B and 14 March for A2) compared to current conditions (1 February) (Figure 5.23). In addition, the flow regime under predicted future climate scenarios will have an extended period of time with zero flow (247, 241, 242 days respectively for the scenario B1, A2, A1B) compared to current conditions (173 days). These analyses indicate more prolonged drought in the catchment.

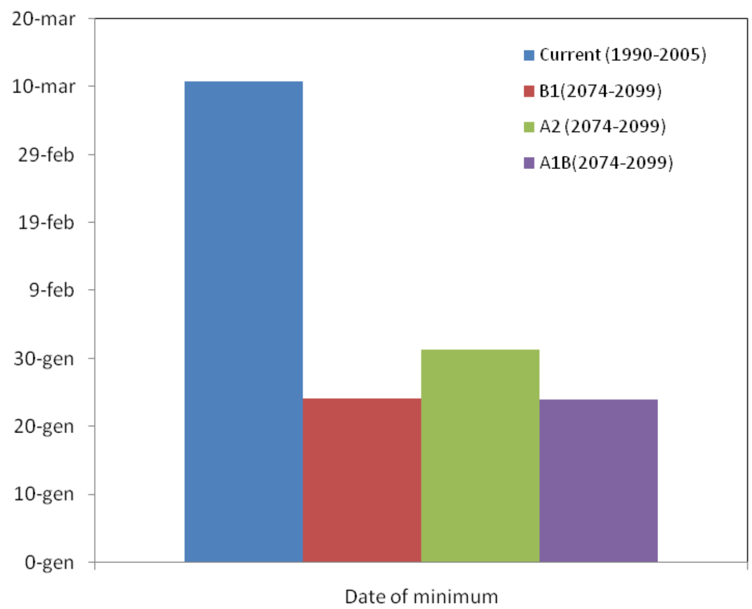

Figure 5.22 Timing of the 1-day minimum for the Merguellil River, using simulated flows under current climate and downscaled GCM-predicted stream flows.

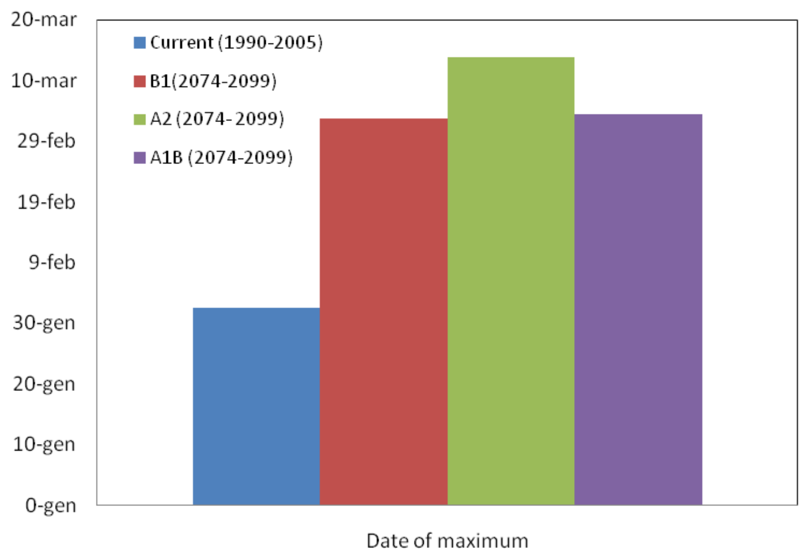

Figure 5.23 Timing of the 1-day maximum for the Merguellil River, using simulated flows under current climate and downscaled GCM-predicted stream flows.

There were significant changes in the magnitude of the 1-, 3-, 7-, 30- and 90-day maxima under predicted future climate compared to modeled current conditions (Figure 5.24). On average, the magnitude and duration of yearly floods under future climatic scenarios is expected to decrease comparing to current conditions. However, the magnitude of the 1-, 3-, 7-, 30- and 90-day minima were all much lower under predicted future climatic scenarios than under current conditions. This suggests that, on average, the lowest water flows will be lower and the river bed will even dry completely. In addition, low water periods will last longer under predicted future climatic scenarios.

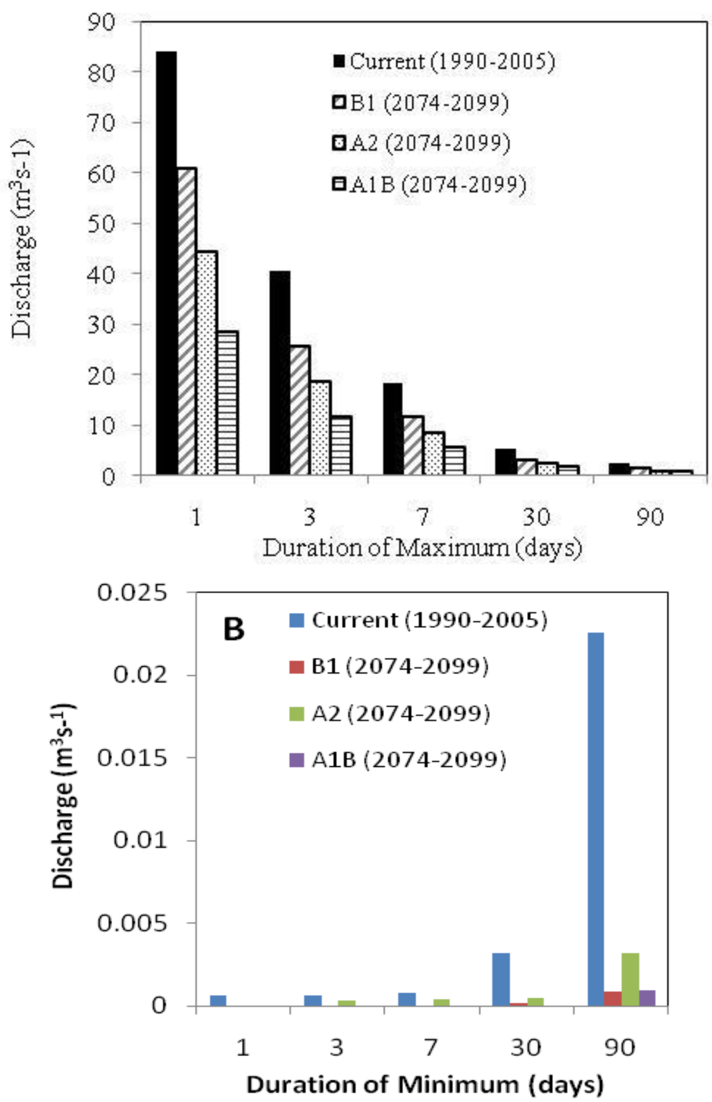

Figure 5.24 One-, 3-, 7-, 30- and 90-day maxima flows (A) and minimum flows (B) for the Merguellil River, using simulated flows under current climate and downscaled GCM-predicted stream flows.

We assessed the variability by calculating the coefficient of variation of mean monthly discharge over the simulated data for current and future climate. Thus, the coefficient of variation is a measure of inter-annual variation. For the most part, the predicted future coefficient of variation was greater than the current coefficient of variation (Figure 5.25). The exception was in March where the coefficient of variation was a little bit higher under current climate.

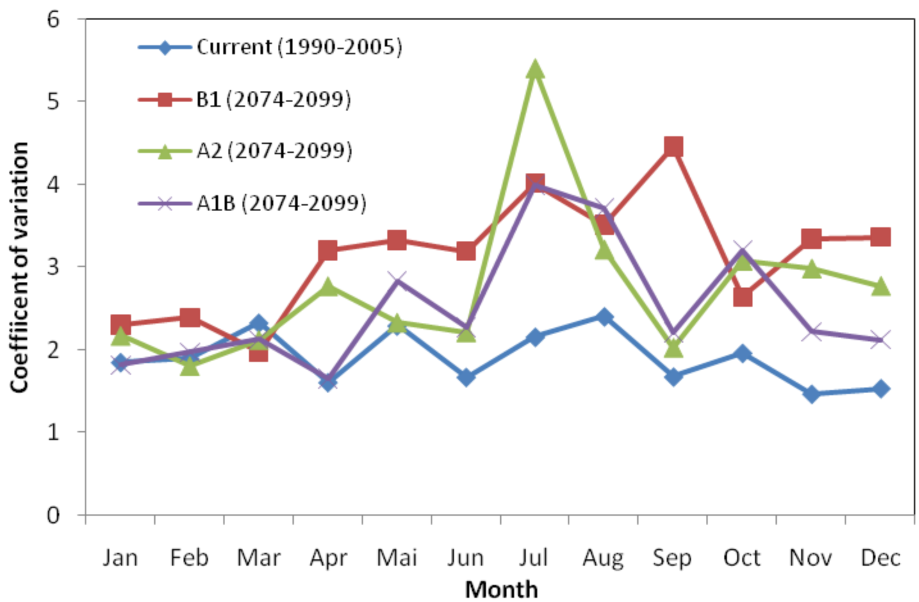

Figure 5.25 Coefficient of variation for mean monthly flow of the Merguellil River using simulated flows under current climate and downscaled GCM-generated stream flow.

In such a vulnerable situation of water resources availability, it can be expected that self-sufficiency in terms of wheat production will become even more difficult in the future, and the looming impact of climate change will further worsen the situation. All the more, it is of great importance to balance water budgets in water-scarce regions and to improve the efficiency of water resources utilization.

CONCLUSION 3

In this study, the CGCM data were statistically downscaled using the non linear model based on fourth degree regression on monthly basis. This downscaling showed an increase temperature for all scenarios in near and far future. This decrease concerns also precipitation expect in November in A2 and B1 where we note an increase of about 0.6mm day^{-1}. When looking on long-term average changes to climate (2070-2099), the results pointed out that the seasonal distribution of rainfall and temperature would be affected differently from season to another. All seasons will experience an increase of temperature and a decrease in precipitation. Change in temperature and precipitation would intensify summer droughts. In winter, the decrease in precipitation would affect more the ecosystem of this already small water resource region.

The combination of increased temperature and reduced rainfall would have a significant effect on water resources in the Merguellil catchment. On near and far future the decrease in precipitation would lead to decease on the TWY. Potential evapotranspiration is also expected to increase due to rise in temperature. Since the amount of water resources in expected to decrease in all scenarios, the actual evapotranspiration would also experience a reduction.

Different spatial responses to climate change were observed in the catchment for near future simulations. Higher altitude regions would experience an increase of the total water yield, while a reduction is foreseen for lower parts. For far future, a noticeable decrease would affect water resources in all part of the catchment.

The objective of the last part in this work aimed to examine the potential impacts of future climate scenarios on river flow regime at the catchment scale. Monthly flows decreased considerably compared to current conditions. These analyses indicate more prolonged drought in the catchment. On average, the magnitude and duration of yearly floods under future climatic scenarios is expected to decrease. The lowest water flows will be lower and the river bed will even dry completely. In addition, low water periods will last longer under predicted future climatic scenarios. A probable consequence of these changes could be a trend towards increased irregularity in river flow regimes.

It should be highlighted that prediction of future land-use/land cover is an important but difficult problem in climate change studies. One limitation of this study is that we that assumed that the land cover in the future will stay the same as the simulation period.

Both drought and extreme rainfall could result in worsened water quality and can increase the total microbial loads. A changing climate also may alter chemical processes in the soil, including chemical weathering, thus will change quality of waters. A rise in water temperature will affect the rate of operation of biogeochemical processes which determine water quality. Changes in flow volumes will alter residence times and dilution. Increased atmospheric CO2 will affect the rate at which CO2 is dissolved in water, and hence the rate of operation of many processes. Changes in inputs of chemicals to the catchment – perhaps due to the effects of climate change on agriculture – will alter stream water chemistry. Soil erosion is already large in the Merguellil catchment, area with larger amounts of rainfall are expected to have even larger soil erosion affecting crop yield, sedimentation in reservoirs, and river water quality.

CONCLUSION

The fundamental goal of this study was to setup a hydrological model to estimate runoff generation within the study catchment and provide a basis for planners and decision makers to plan future land developments and assess their impacts on water resources. This objective was achieved through the setting up and calibration of the SWAT model to adequately reproduce the recorded streamflow. This also achieved the specific objective of assessing and modeling runoff generation at a daily time scale which is the most relevant to all water users in the area and also for operational purposes.

In the process of setting up SWAT, a number of useful datasets and files of potential great use to other studies in the area were created. These include a digital elevation model derived from 10m contours lines, the new land use map with the updated crop in the study area, soils database of soil profile data in the area from hardcopies of the same and shape files which were created by adding soils profile data to the existing land type files. This is particularly important for other related projects.

Sensitivity analysis helped in identifying the important parameters that were used in the calibration exercise. These important parameters included CN2, ESCO, SOL_AWC and GWQMN as defined in the preceding chapter. Calibration was successful as evidenced by reasonable match between observed and simulated streamflows. The set of the optimized parameters along with the other parameters that were used can therefore be accepted as the representative set of parameters for the system. These best parameter values were applied in the Merguellil catchment which has similar biophysical properties, thereby enabling prediction in the ungauged catchment.

The model is also capable of adequately characterizing the relative effects of different land cover conditions. SWAT simulates sediment loadings from Durum wheat, to be about 30% of total basin loadings. This is due to the high surface runoff (27.21mm/year). Land-cover, where relatively high quantity of mineral and organic nitrogen are produced, is principally durum wheat and urban (7.17 kg/ha and 10.17 kg/ha respectively). Without more quantitative data from the area, assessing the accuracy of simulated sediment loads from different land-covers cannot be assumed. Acquiring such data would most certainly allow fine tuning of the model and as a result improve basin-wide sediment yield simulations.

The simulation results have clearly shown that contour ridges (considered as pothole in this study) within the watershed have an important role of the retention of sediment; whereas, they showed to have an impact on the hydrologic regime in the catchment by reducing the surface runoff by 32 %. In addition, planting the Olive tree between the contour ridges has shown an increase of the olive yield.

A better use of the fertilizer, such as not over-applying it, could substantially reduce the amount of nutrients flowing down river without compromising crop yields. The results of this analysis will make good discussions on the impact of nitrogen control policies and will be of interest to government, farmers, fertilizer producers and environmental stakeholders.

This work has also shown how a modeling tool can be used to study the response of hydrology and crop productivity to change in climate factors. The modeling results indicate that, in this Mediterranean region, the watershed's water resources are highly vulnerable to change in rainfall and temperature, which affect the hydrologic regime of the catchment. We provide an overview of the impact of climate change on various hydrologic components for the Merguellil catchment.

These analyses could be very useful in strategic planning of water resources management and crop production for the future years. As different parts of the catchment are affected differently, a number of management options could be considered in order to alleviate the climate change impact on this catchment. The result will contribute to the scientific community's understanding of climate change impact on water resources and provide information to support future water resources planning and management in the Merguellil and other catchments with the same climatic conditions.

The results from the modeling and scenarios undertaken in this research represent the important contributions made by this PhD to the knowledge of Mediterranean hydrological modeling.

REFERENCES

- Abbaspour, K. C., Faramarzi, M., Ghasemi, S. S., and Yang, H. (2009). Assessing the impact of climate change on water resources in Iran, Water Resour. Res., 45, W10434, doi: 10.1029/2008WR007615.

- Abdulla, F. A., Lettenmaier, D. P. and Liang, X. (1999). Estimation of the ARNO model baseflow parameters using daily streamflow data, J. Hydrol., 222, pp. 37-54.

- Aber, J.D., Ollinger, S.V., Federer, C.A., Reich, P.B., Goulden, M.L., Kicklighter, D.W., Melillo, J.M., Lathrop Jr., R.G. (1995). Predicting the effects of climate change on water yield and forest production in the northeastern United States. Climate Research 5, 207–222.

- Achour M., ViertmannW. (1984). Les aménagements anti-érosifs recommandés par le projet TU.81/14, leurs caractéristiques et les possibilités de leur application. Kairouan, 65p.

- Albergel J., Rejeb N. (1997) - Les lacs collinaires en Tunisie : Enjeux, contraintes et perspectives. C.R. Acad.Agric. Fr., 1997, 83, n°2, pp.77-88.

- Allen R.G., Pereira L.S., Raes D., Smith M. (1998). Crop Evapotranspiration Guidelines for computing crop water requirements, Rome, FAO Irrigation and drainage paper 56, 1998, 300

- Anderson, M.G. and Burt, T.P. (1985). Modelling strategies. In Anderson, M. G. and Burt, T.P. (eds.), Hydrological forecasting, John Wiley & Sons, New York, pp. 1- 13.

- Anderson, M. G. and Bates, P. D., eds. (2001). Validation in hydrological modelling, John Wiley & Sons, New York, pp. 500.

- Arnold, J.G., Williams, J.R., Srinivasan, R., King, K.W., Griggs, R.H. (1994). SWAT - Soil and Water Assessment Tool, USDA, Agricultural Research Service, Grassland, Temple, TX 76502.

- Arnold, J.G., Srinivasan, R., Muttiah, R.S., Williams, J.R. (1998). Large area hydrologic modeling and assessment part I: model development. J. Am. Water Resour. Assoc. 34 (1), 73–89.

- Arnold, J. G., R. Srinivasan, R. S. Muttiah, P. M. Allen, and C. Walker. 1999a. Continental-scale simulation of the hydrologic balance. J. American Water Resour. Assoc. 35(5): 1037-1052.

- Arnold, J. G., and N. Fohrer. 2005. SWAT2000: Current capabilities and research opportunities in applied watershed modeling. Hydrol. Process. 19(3): 563-572.

- AVFA. (2007). Agriculture Ministry of Tunisia, Agence de Vulgarization et Formation Agricole. Ghirassate a zaytoun (Olive cultivation) pp 1-32.

- Baker, D. B., Richards, R. P., Loftus, T. T., and Kramer, J. W. (2004). A new flashiness index: characteristics and applications to Midwestern rivers and streams. Journal of the American Water Resources Association. Paper n. 03095: 503-522.

- Band, L., Mackay, D., Creed, I., Semkin, R., and Jeffries, D. (1996). Ecosystem processes at the watershed scale: sensitivity to potential climate change. Limnol Oceanogr 41(5):928–938.

- Barbery, J., Mohdi, M. (1987). Carte des ressources en sols de la Tunisie (1/200.000), feuille de Kairouan. DCES, Ministère de l’Agriculture. Tunis, Tunisie, 49p.

- Barraque, B. (1998) Groundwater management in Europe: regulatory, organisational and institutional change.

- Bastidas, L. A,, Gupta, H. V., Sorooshian, S., Shuttleworth, W., and Yang, Z .L. (1999). Sensitivity analysis of a land surface scheme using multicriteria methods. J. of Geophys. Rex, 104(D16), 19481-19490.

- Beck, M. B. (1981). A procedure for modeling. In Orlob, G.T. (ed.) Mathematical modeling of water quality: Streams, lakes, and reservoirs. John Wiley & Sons, 11-41.

- Benabdellah, S. (2007). The Water Resources and Water Management Regimes in Tunisia. Proceedings of a Workshop in Tunisia.Strengthening science-based decision making in developing Countries agricultural Water Management. Science and Technology for Sustainability Program Policy and Global Affairs. Pp 81-87the National Academies Press. Washington, D.C.

- Ben MansourH., Frigui L. (1994). Lacs collinaires dans le gouverneras de Siliana. Tunis, 98 p.

- Beven, K., (1989), Changing ideas in hydrology—the case of physically-based models. Journal of hydrology 105, 157–172.

- Beven, K. J. (1993). Prophecy, reality and uncertainty in distributed hydrological modelling. Adv. In Water Resourc., 16, 41–51.

- Beven, K. J. (2000). Rainfall-runoff modeling: The primer. John Wiley and Sons, Chichester, U.K, pp. 360.

- Binley, A. M. and Beven, K. J. (1989). A physically based model of heterogeneous hillslopes. 2: Effective hydraulic conductivities. Water Resour. Res., 25(6) 1227–33.

- Boers, T. M. (1994). Rainwater harvesting in arid and semi-arid zones, Publication 55, ILRI, Wageningen, The Netherlands.

- Bolle, H-J. (2003). Climate, climate variability, and Impacts in the Mediterranean Area: an Overview. Ed, In Mediterranean Climate. Variability and trends. Pcm, Regional Climate studies. ISBN 3-540-43838-6. Springer-Verlag berlin Heidelberg New York. PP, 5-76.

- Borah, D. K., Yagow, G. Saleh, A. Barnes, P. L. Rosenthal, W. Krug, E. C., and Hauck, L. M. (2006). Sediment and nutrient modeling for TMDL development and implementation. Trans. ASABE 49(4): 967-986.

- Bouzid M. (1998). Entre la construction et l'exploitation des lacs collinaires, un déséquilibre à soulever. Ministère de l'Agriculture, journal d'Essabeh, Tunis.

- Box, G.E.P., Jenkins, G.M., (1976), Time Series Analysis: Forecasting and Control. Holden-Day, Son-Fransisco, 588 pp.

- Boyle, D. P., H. V. Gupta, and S. Sorooshian (2000). Toward improved calibration of hydrological models: Combining the strengths of manual and automatic methods. Water Resource Research, 36(12), 3663–3674.

- CEAP. 2007. Conservation Effects Assessment Project. Washington, D.C.: USDA Natural Resources Conservation Service. Available at: www.nrcs.usda.gov/technical/NRI/ceap/. Accessed 14 February 2007.

- CES. (1986). Aménagement intégré du bassin versant de l'oued Merguellil. Tunis, 50 p.

- CES. (1995). Guide de conservation des eaux et du sol. Tunis, p 273.

- Chaplot, V. (2007). Water and soil resources response to rising levels of atmospheric CO_2 concentration and to changes in precipitation and air temperature. Journal of Hydrology 337 (1–2), 159–171.

- Chen, E. and Mackay, D.S. (2004). Effects of distribution-based parameter aggregation on a spatially distributed agricultural nonpoint source pollution model. J. Hydrology, 295:211-224.

- Clarke, R.T. (1973). Mathematical Models in Hydrology. Irrigation and Drainage Paper 19, FAO, Rome, Italy.

- Crawford, N. H. and Linsley, R. K. (1966). Digital simulation in hydrology: the StanfordWatershed Model IV, Tech. Report no. 39, Stanford University, California.

- Critchley, W and Klaus, S. (1991). A Manual for the Design and Construction of Water Harvesting Schemes for Plant Production. Rome: Food and Agriculture Organization of the United Nations, 1991.

- Dagan, G. (1986). Statistical theory of groundwater flow and transport: pore to laboratory; laboratory to formation and formation to regional scale. Water Resour. Res., 22, 120–35.

- Daget, P. (1980). Un element actuel de la caracterisation du monde mediterraneen: le climat, in Colloque de la Fondation L. Emberger sur) 'La Mise en Place, L'Evolution et La Caracterisation de la Flore et de la Vegetation Circummediterraneennes.' Naturalia Monspelliensia, No Hors Serie, 101–126.

- Dawdy, D.R. and ODonnell, T. (1965). Mathematical models of catchment behaviour. J. of the HydraulicDivision, ASCE, 91(HY4), pp. 123-137.

- De Girolamo A.M, Lo Porto A, Abouabdillah A., De Luca D., Santese G. (2008). Evaluation of flow regime in the Mediterranean streams using flashiness index. In: 21st Century Watershed Tecnology: Improving Water Quality and Environment. UNIVERSITY OF CONCEPCION, CHILE, March 2 - April 3, 2008, ISBN/ISSN: 701P0208cd.

- DGF and GTZ. (1994). Restauration, réhabilitation des terres dégradées des zones arides et semi-arides. Congrès international, Tunisie, 48 p.

- Diaz-Nieto and Wilby, R.L (2005). A comparison of statistical downscaling and climate change factor methods: impacts on low flows in the River Thames, United Kingdom, Climatic Change 69 (2005), pp. 245–268.

- Dibike, Y.B., and Coulibaly. P. (2005) Hydrologic impact of climate change in the Saguenay watershed: comparison of downscaling methods and hydrologic models. J. of Hydrol., 307: 145–63.

- Dridi, B., 2000. Impact des aménagements sur la disponibilité des eaux de surface dans le bassin versant du Merguellil (Tunisie centrale). PhD thesis, Université Louis Pasteur, Strasbourg, 194 p.

- Du, B., Arnold, J. G., Saleh, A., Jaynes, D. B. (2005). Development and application of SWAT to landscape with Tiles and Potholes. Transactions of the ASAE. Vol. 48(3): 1121-1133.

- Duan, Q., Sorooshian, S. and Gupta, V. K. (1994). Optimal use of the SCE-UA global optimization method for calibrating watershed models. J. Hydrol., 158, pp. 265- 284.

- Duan, Q. (2003): Global Optimization for Watershed Model Calibration, in Calibration of Watershed Models, Water Science Application Series (6), edited by Duan, Q. et al., AGU, Washington, DC, 89–104.

- EAWAG. (2005). Proc. 3rd International SWAT Conference. Zurich, Switzerland: Swiss Federal Institute for Environmental Science and Technology. Available at: www.brc.tamus.edu/swat/3rdswatconf/SWAT%20Book%203rd%20Conference.pdf. Accessed 14 February 2007.

- EEA, European Environment Agency (2000). Europe's environment: the third assessment. Copenhagen.

- El Amami, S. (1984). Les aménagements hydrauliques traditionnels en Tunisie, Centre de Recherche en Génie Rural, Tunis, Tunisia, 1984.

- Emberger, L. 1955. Une classification biogdographique des climats. Rec. Trav. lab. Bot. G6ol. Zool. Fac. Sc. de Montpellier 7: 3-43.

- European Climate Support Network. (1995). Climate of Europe. KNM. de Bilt, Nl.

- Fontaine, T.A., Klassen, J.F., Hotchkiss, R.H. (2001). Hydrological response to climate change in the Black Hills of South Dakota, USA. Hydrological Sciences 46 (1), 27–40.

- Fornes JM, de la Hera A, Llamas MR (2005). The silent revolution in groundwater intensive use and its influence in Spain. Water Policy 10:1–16.

- Freer, J., Beven, K., and Abroise, B. (1996). Bayesian uncertainty in runoff prediction and the value of data: an application of the GLUE approach. Water Resour. Res., 32, 2163–73.

- Freeze, R. A. and Harlan, R. L. (1969). Blueprint for a physically based, digitally simulated hydrologic response model. J. Hydrol., 9, 237–58.

- Freeze, R. A. (1972). Role of subsurface flow in generating surface runoff. 2: Upstream source areas. Water Resour. Res., 8(5) 1272–83.

- Garrido A, Llamas MR (eds) (2006). Water policy in Spain, Resources for the Future, Washington, DC (in press).

- Garrote L, Flores F, Iglesias A. (2005). Linking drought indicators to policy. The case of the Tagus basin drought plan. Water Resour Manag (in press).

- Gershenfeld, N. (1999). The nature of mathematical modelling. Cambridge University Press, Cambridge, UK.

- Ghola H., 1993 - Gestion des lacs collinaires. Tunis, 105 p.

- Gibson C. A., Meyer J. L., Poff, N. L. Hay L. E. And Georgakakos. A. (2005). flow regime alterations under changing climate in two river basins: implications for freshwater ecosystems. River Research and Applications River Res. Applic. 21: 849–864 (2005).

- Giorgi F. (2006). Climate change hot-spots. Geophysical Research Letters 33: L08707.

- Grenon, M. and M. Batisse (eds) (1989). Futures for the Mediterranean Basin: The Blue Plan. Oxford University Press, Oxford.

- Gupta, V. K., Sorooshian, S. and Yapo, P. O. (1998). Towards improved calibration of hydrological models: multiple and noncomensurable measures of information. Water Resources Research, 34, 751–763.

- Gupta, H. V., K. J. Beven, and T. Wagener (2005). Model calibration and uncertainty estimation. In: Anderson, M. G. and McDonnell, J. (Eds.), Encyclopedia of Hydrologic Sciences, Wiley, Chichester, UK.

- Hargreaves, G.L., Hargreaves, G.H. and Riley, J.P. (1985). Agricultural benefits for Sengel River Basin. Journal of Irrigation and Drainage Engineering. 108(3):225-230.

- Hellegers P, van Ierland E. (2003). Policy instruments for groundwater management in The Netherlands. Environ Resour Econ 26:163–172.

- Henriksen, H. J., Troldorg, L., Nyegaard, P., Sonnenborg, T.O., Refsgaard, J.C. and Madsen, B. (2003). Methodology for construction, calibration and validation of a national hydrological model for Denmark. Journal of Hydrology. 280: 52-71.

- Huntingford, G. Gash, J., and Giacomello, G.M. (2006). Climate change and hydrology: next steps for climate models. Hydrol. Process. 20: 2085–87.

- Iglesias A, Moneo M (eds) (2005). Drought preparedness and mitigation in the Mediterranean: Analysis of the Organizations and Institutions. Opions Méditerranéenness, CIHEAM, Centre international de Hautes Etudes Agronomiques Méditerranéennes, Paris. 200.

- IGNF. (1957). Carte d'Etat Major de la Tunisie, 1/50 000. Feuilles de Makthar (L III), de Djebel Serdj (L IV), de Djebel Barbrou - Rohia (L XI), de Haffouz (L XII), de Sbiba (L X IX), de Trozza (L XX) et de Pavillier (L X XI). Edition I. Office de la Topographie et de la Cartographie (OTC). El Menzah, Tunis, Tunisie.

- Institute of Hydrology (1999). Flood Estimation Handbook. Wallingford: Institute of Hydrology.

- Intergovernmental Panel on Climate Change (IPCC) (2001). Climate Change 2001: Impacts, Adaptation, and Vulnerability Contribution of Working Group II to the Third Assessment Report of the Intergovernmental Panel on Climate Change. Cambridge University Press, Cambridge.

- IPCC: Intergovernmental Panel on Climate Change. (2002). Climate Change 2001: Impacts, Adaptation, and Vulnerability, McCarthy J, Canziani O, Leary N, Dokken D, White K (eds). Cambridge University Press: Cambridge.

- IPCC. (2007). Climate Change 2007: The Physical Science Basis. Contribution of Working Group I to the Fourth Assessment Report of the Intergovernmental Panel on Climate Change. Cambridge University Press, Cambridge, United Kingdom and New York, NY, USA.

- IRD, CES. (1998). Annuaire hydrologique des lacs collinaires 1996/97.

- Jha, M., J. G. Arnold, P. W. Gassman, F. Giorgi, and R. Gu. (2006). Climate change sensitivity assessment on upper Mississippi river basin steamflows using SWAT. J. American Water Resour. Assoc. 42(4): 997-1015.

- Kallel M.R., Bouzaiane S., Ghorbel A., Eoche-Duval J.M., Claude J., Gouyet R.C., Lamachère J.M. (1975). Etude hydrologique préliminaire des Oueds Zeroud et Merguellil. Direction des resources en Eau et en Sols, Institut de la recherché pour le developpment.

- Kalnay, E., Cai, M. (2003). Impact of urbanization and land-use change on climate. Nature 423, 528–531.

- Kamga, F.M. (2001). Impact of greenhouse gas induced climate change on the runoff of the Upper Benue River (Cameroon). Journal of Hydrology 252, 145–156.

- Karr JR. (1991). Biological integrity: a long-neglected aspect of water resource management. Ecological Applications 1: 66–84.

- Kingumbi. A. (1999). Bilan et modélisation de la retenue du barrage d'El Houareb, Mémoire de Diplôme d'études Approfondies de l'Ecole Nationale des Ingénieurs de Tunis. Laboratoire d'Hydraulique, 105 p. + annexes.

- Kingumbi, A., Bargaoui, Z., Ledoux, E., Besbes, M., Hubert, P. (2007). Modélisation hydrologique stochastique d’un bassin affecté par des changements d’occupation: cas du Merguellil en Tunisie centrale. Hydrological Sciences–Journal–des Sciences Hydrologiques, 52(6) décembre 2007.

- Kleissen, F. M., Beck, M. B., and Wheater, H. S. (1990). Identifiability of conceptual hydrochemical models. Water Resour. Res., 26(2), 2979– 92.

- Klemes, V. (1986). Operational testing of hydrological simulation models. Hydrological Sciences J., 3 1 (I), pp. 13-24.

- Köppen, W. (1936). Das geographishe System der Klimate. In Koppen and Geiger Eds, Handbuch der Klimatologie 3. Gebrueder Borntraeger, Berlin, 46 pp.

- Kosmas, C., N. Danalatos, L. H. Cammeraat, M. Chabart, J. Diamantopoulos, R. Farand, L. Gutierrez, A. Jacob, H. Marques, J. Martinez-Fernandez, A. Mizara, N. Moustakas, J. M. Nicolau, C. Oliveros, G. Pinna, Lange, J., and A. K. Singh. (2003). Water Resources Assessment in Dry Catchments by Hydrological Modelling adopted to limited data availability. River Anas; India. Geophysical. Research Abstracts, Vol. 5, 02521, 2003. European Geophysical Society.

- Krause, P., Boyle, D. P., Bäse, B. (2005). Comparison of different efficiency criteria for hydrological model assessment, Advances in Geosciences **5** (2005), pp. 89–97

- Labat, D., Godderis, Y., Probst, J.L., Guyot, J.L. (2004). Evidence for global runoff increase related to climate warming. Advances in Water Resources 27 (6), 631– 642.

- Lange, J., Singh, A.K. (2003). Water Resources Assessment in Dry Catchments by Hydrological Modelling adapted to limited data availability. River Anas; India. Geophysical. Research Abstracts, Vol. 5, 02521, 2003. European Geophysical Society.

- Leavesley. (1983). Precipitation-Runoff Modeling System: User’s Manual. US Geological Survey, Denver, CO, USA.

- Leduc, C., Ben Ammar, S., Favreau, G., Beji, R., Virrion, R., Lacombe, G., Tarhouni, J., Aouadi, C., Zenati Chelli, B., Jebnoun, N., Oi, M., Michelot, J.L., Zouari, K. (2007). Impacts of hydrological changes in the Mediterranean zone: environmental modifications and rural development in the Merguellil catchment, central Tunisia. Hydrological Sciences Journal, 52(6): 1162-1178.

- Lees, M. J. andWagener, T. (1999). A Monte Carlo Analysis Toolbox (MCAT) for Matlab. User manual. Imperial College, London.

- Legates, D. R. and McCabe Jr., G. J. (1999). Evaluating the use of "goodness-of-fit" measures in hydrologic and hydroclimatic model validation. Water Resour. Res., 35(I), pp. 233-241.

- Legesse, D., Vallet-Coulomb, C., Gasse, F. (2003). Hydrological response of a catchment to climate and land use changes in Tropical Africa: case study South Central Ethiopia. Journal of Hydrology 275 (1–2), 67–85.

- Lettenmaier, D., Gan, T. (1990). Hydrologic sensitivities of the Sacramento-San Joaquin River basin, California, to global warming. Water Resources Research 26, 69–86.

- Liden, R., and Harlin, J. (2001). Analysis of conceptual rainfall-runoff modeling performance in different climates. Journal of Hydrology 238, 231-247.

- Lo presti, R., Barca, E., Passarella, G. (2010). A methodology for treating missing data applied to daily rainfall data in the Candelaro River Basin (Italy). Environ Monit Assess (2010) 160 : 1-22.

- Masden, H. (2000). Automatic calibration of a conceptual rainfall-runoff model using multiple objectives. Journal of hydrology 235, 276-288.

- Mausbach, M. J., and A. R. Dedrick. (2004). The length we go: Measuring environmental benefits of conservation practices. J. Soil Water Cons. 59(5): 96A-103A.

- McIntyre, N., Lees, M. J. and Wheater, H. S. (2002). Estimation and propagation of parametric uncertainty in environmental models. J. of Hydroinfomtics, in Review.

- McMahon, T. A. 1979. Hydrological characteristics of arid zones. Proc. Symposium on the Hydrology of Areas of Low Precipitation, Canberra, IAHS. Publ. No. 128, 105–23.

- Medlyn, B.E., Barton, C.V.M., Broadmeadow, M.S.J., Ceulemans, R., De Angelis, P., Forstreuter, M., Freeman, M., Jackson, S.B., Kellomaki, S., Laitat, E., Rey, A., Roberntz, P., Sigurdsson, B.D., Strassemeyer, J., Wang, K., Curtis, P.S., Jarvis, P.G. (2001). Stomatal conductance of forest species after long-term exposure to elevated CO2 concentrations: a synthesis. New Phytologist 149, 247–264.

- Melching, C. S., Yen, B. C. and Wenzel, H. G., Jr. (1990). A reliability estimation in modeling watershed runoff with uncertainties. Water Resour. Rex, 26, pp.

- Melching, C. S. (1995). Reliability estimation. In Singh, V.P. (ed.) Computer models of watershed hydrology. Water Resources Publishers, USA, pp. 69- 1 18.

- Micale, F., Genovese, G. (2004). Methodologiy of the MARS Crop Yield Forcasting System. Vol 1: Meteorological Data Collection, Processing and Analysis. ISBN 92-894-8130-3-EUR 21291/EN/1.

- Mizouri M., Barbery J., Willaine P. (1990). Carte des ressources en sols de la Tunisie (1/200.000) : nouvelle approche méthodologique, feuille de Makthar. DCES, Ministère de l'Agriculture, Tunis, Tunisie.

- Monat F. (2000). Mise en place d'un Système d'Information Géographique sur la partie amont du bassin versant du Merguellil. AGRO Montpellier – IRD Tunis, Tunisie.

- Monteith, J.L. (1977). Climate and the efficiency of crop production in Britain. Phil. Trans. Res. Soc. London Ser. B 281:277-329.

- Moradkhani, H., S. Sorooshian, H. V. Gupta, and P. R. Houser (2005): Dual state-parameter estimation of hydrological models using ensemble Kalman filter. Advanced Water Resource, 28(2), 135–147.

- Moriasi, D. N. (2007). Model Evaluation Guidelines for Systematic Quantification of Accuracy in Watershed Simulations," Transactions of the ASABE, 50:(3), 885–900.

- Moustafa, A. T. A. 1994. Agricultural development in the northwestern zones of Egypt. In: Water harvesting for improved agricultural production. Proceedings of the FAO Expert Consultation, Cairo, Egypt, Nov 1993. Rome, Italy: FAO.

- Mroczkowski, M., Raper, G. P. and Kuczera, G. (1997). The quest for more powerful validation of conceptual catchment models. Water Resour. Res., 33(10), pp. 2325- 2335.

- Mtimet A., Dérouiche C. (1996). Evaluation des paramètres physico-hydriques de la sensibilité des sols à l'érosion hydrique. Tunis, p l00.

- Mtimet A. Dérouiche C. Louati M. (1997). Etude de l'érosion en Tunisie. Tunis. 120 p.

- Mtimet, A. (1999). Atlas des sols tunisiens.

- Mtimet. A. (2000). Soils of Tunisia. Options Méditerranéennes, Série B, vol. 34.

- Nash, J. E. and Sutcliffe, J.V. (1970). River flow forecasting through conceptual models part I - A discussion of principles. J. Hydrol., 10, pp. 282-290.

- Nash, L.L., Gleick, P.H. (1991). Sensitivity of streamflow in the Colorado Basin to climatic changes. Journal of Hydrology 125 (3–4), 221–241.

- Nasri, S., M. Laaroussi, and H. Habaieb. (2006). Impacts hydrologiques des banquettes antiérosives sur un versant semi-aride en Tunisie centrale. In: M. Sabir (Editor), 14th International Soil Conservation Organization Conference. Water Management and Soil Conservation in Semi-Arid Environments. ISCO, Marrakech, Morocco, pp. 5-12.

- Nasri, S. (2007). Caractéristiques et impacts hydrologiques de banquettes en cascade sur un versant semi-aride en Tunisie centrale. Hydrological Sciences, Journal des sciences hydrologiques, Special edition: Dry land Hydrology in Mediterranean Regions, 52 (6) pp 1134-1145.

- Neitsch, S. L., Arnold, J. G., Kiniry, J. R. and Williams, J. R. (2001). Soil and Water Assessment Tool, Theoretical Documentation and Users Manual, Temple, Texas, United States Department of Agriculture.

- Neitsch, S.L., Arnold, J.G., and Srinivasan, R. (2002). Pesticides Fate and Transport Predicted by the Soil and Water Assessment Tool (SWAT): Atrazine, Metolachlor and Trifluralin in the Sugar Creek Watershed Submitted to Office of Pesticide Programs Environmental Protection Agency February 27, 2002.

- Nemec, J. and Rodier, J. A. (1979). Streamflow characteristics in areas of low precipitation. Proc. Symposium on the Hydrology of Areas of Low Precipitation. Canberra: IAHS Publ. No. 128, 125–40.

- NERC. Natural Environment Research Council (1975). Flood Studies Report, 5 vols. Wallingford, UK: NERC.

- Oreskes, N., Shrader-Frechette, K. and Belitz, K. (1994). Verification, validation, and confirmation of numerical models in the earth sciences. Science, 263, pp. 641-646.

- Osidele, O. O. and Beck, M. B. (2001). Identification of model structure for aquatic ecosystems using regionalized sensitivity analysis. Water Science and Technology, 43(7), pp. 271-278.

- Oweis, T., A. Hachum, and J. Kijne. (1999). Water harvesting and supplementary irrigation for improved water use efficiency in dry areas. SWIM Paper 7. Colombo, Sri Lanka: International Water Management Institute.

- Oweis, T., A. Hachum, and A. Bruggeman. (2004). Indigenous water harvesting in West Asia and North Africa, ICARDA, Aleppo, Syria, 2004.

- Papadopoulos I. (1995) Present and perspective use of wastewater for irrigation in the Mediterranean basin. In 2nd Int. Symposium on Wastewater Reclamation and Reuse, eds. A. N. Angelakis et al., October, Vol. 2, pp. 735–746. IAWQ, Iraklio, Greece.

- Pilgrim, D. H., Chapman, T. G., and Doran, D. G. (1988). Problems of rainfallrunoff modelling in arid and semi-arid regions. Hydrol. Sci. J., 33(4), 379– 400.

- Piñol, J., M. J. Lledó, and A. Escarré. (1991). Hydrological balance of two Mediterranean forested catchments (Prades, northeast Spain), Hydrological Science Journal. 36 (1991) (2), pp. 95–107.

- Plan Bleu. (2000). Vision méditerranéenne sur l'eau, la population et l'environnement au XXIème siècle Mediterranean vision on water, population and the environment for the 21st century MARGAT Jean, VALLEE Domitille Sophia Antipolis :Plan bleu, 62.

- Poesen, J. and Lavee, H. (1994). Rock fragments in top soils: significance and processes. Catena 23: 1-28.

- Poff NL, Allan JD, Bain MB, Karr JR, Prestegaard KL, Richter BD, Sparks RE, Stromberg JC. (1997). The natural flow regime: a paradigm for river conservation and restoration. BioScience 47: 769–784.

- Popper, K. (2000). The logic of scientific discovery. First published 1959 by Hutchinson education, Routledge, London, UK.

- Potter, T. D., Colman, B.R. (2003). Handbook of weather, climate, and water: chemistry, hydrology, and societal impacts. Section 2: Hydrology. Hydrology Overview. Soroosh Sorooshian and Martha P. L. Whitaker. pp 415-430.

- Pritchard, S.G., Rogers, H.H., Prior, S.A., Peterson, C.M. (1999). Elevated CO2 and plant structure: a review. Global Change Biology 5, 807–837.

- Raspic. V. (1999). Projet MERGUSIE, Synthèse du transport solide et de r érosion hydrique sur le bassin versant du Merguellil. Rapport de stage à 1TRD. Institut des Sciences de l'Ingénieur de Montpellier, Département des Sciences et Technologies de l'eau, France.

- Richter, B.D., Baumgartner, J.V., Powell, J., and Braun, D.P. (1996). A method for assessing hydrologic alteration within ecosystems. Conservation Biology. 10: 1163–1174.

- Rind, D., Goldberg, R., Hansen, J., Rosenzweig, C., Ruedy, R. (1990). Potential evapotranspiration and the likelihood of future drought. Journal of Geophysical Research 95 (D7), 9983–10004.

- Saxe, H., Ellsworth, D.S., Heath, J. (1998). Trees and forest functioning in an enriched CO2 atmosphere. New Phytologist 139, 395–436.

- Saxton, K. E., and Rowls, W.J. (2006). Soil water characteristic estimates by texture and organic matter for hydrologic solutions. Soil Sci. Sco. Am. J. 70, 1569-1578.

- Seibert, J. (1999). Conceptual runoff models - fiction or representation of reality? Ph.D. Thesis, University of Uppsala, S.

- Selmi S., Talineau J-L., 1995. - Diversité et problématique de la gestion collective des lacs collinaires tunisiens. Tunis, 11 p.

- Singh, V. P. & Woolhiser, D. A., (2002). Mathemathical Modelling of Watershed Hydrology. Journal of Hydrologic Engineering. Pgs 270-292. American Society of Civil Engineers, 150th Anniversary Paper.

- Shahin, M. (2007). Water Resources and Hydrometeorology of the Arab Region. Water Science and Technology Library. Springer Netherlands. Volume 59. 223-277.

- Shuttleworth, W. J., Evaporation, in D. R. Maidment (Ed.) (1993). Handbook of Hydrology, McGraw- Hill, New York, Chapter 4.

- Spear, R. C. and Hornberger, G. M. (1980). Eutrophication in Peel inlet, II: Identification of critical uncertainties via generalised sensitivity analysis. Water Resour. Res., 14, 43–9.

- Soil Conservation Services (1972). Section 4: Hydrology In National Engineering Handbook. SCS.

- Sorooshian S. and V. K. Gupta (1995). Model calibration. In: Singh, V. P. (Ed.), Computer Models of Watershed Hydrology, Water Resources Publications, Highlands Ranch, CO, pp. 23–67.

- Sorooshian, S., Hsu, K. L., Coppola, E., Tamassetti, B., Verdecchia, M., and Visconti, G. (2008). General Review of Rainfall-Runoff Modeling: Model Calibration, Data Assimilation, and Uncertainty Analysis. Eds, in Hydrological Modelling And The Water Cycle. Coupling the Atmospheric and Hydrological Models. VOLUME 63, pp 1-25. Moradkhani, H., Sorooshian, S. 2008. Water Science and Technology Library.

- Stone, M., Hotchkiss, R., Hubbard, C., Fontaine, T., Mearns, L., and Arnold, J. (2001). Impacts of climate change on Missouri River Basin water yield. J Am Water Resour Assoc 37(5):1119–1128.

- Thiemann, M., M. Trosset, H. Gupta, and S. Sorooshian (2001). Bayesian recursive parameter estimation for hydrological models. Water Resource Research, 37(10), 2521–2535.
- Thornes, J. B., J. X. Shao, E. Diaz, A. Roldan, M. McMahon, and J. C. Hawkes. (1996). Testing the MEDALUS hillslope model. Catena, 26, 137-160.

- UN Population Division (1994). World Population Prospects (Sustaining Water: An Update). The 1994 Revision. TheUN, New York.

- USEPA (2004) Global Warming Site. [Online] Available: http://yosemite.epa.gov/oar/globalwarming.nsf/content/index.html.

- USGS, the water balance. http://ga.water.usgs.gov/edu/watercycle.html.

- Van Griensven, A., Meixner, T., Grunwald, S., Bishop, T., Diluzio, M., and Srinivasan, R., (2006). A global sensitivity analysis tool for the parameters of multi-variable catchment models. Journal of Hydrology, 324, 10–23.

- Van Liew, M.W., Arnold, J.G., Bosch, D.D. (2005). Problems and potential of autocalibrating a hydrologic model. Trans. Am. Soc. Agric. 48(3), 1025-1040.

- Viessman, W., & Lewis, G. L. (2003). Introduction to Hydrology. 5th Ed. Upper Saddle River, N. J. Prentice Hall. ISBN 067399337X. x11, 612p. Chapter 12, pgs 453-536.

- Wand, S.J.E., Midgley, G.F., Jones, M.H., Curtis, P.S. (1999). Responses of wild C4 and C3 grass (Poaceae) species to elevated atmospheric CO2 concentrations: a metaanalytic test of current theories and perceptions. Global Change Biology 5, 723– 741.

- Wagener, T. (1998). Developing a prototype knowledge based system to support rainfallrunoff modelling. Unpublished M.Sc. Thesis, Delft University of Technology, Delft, NL.

- Wagener, T., Lees, M. J., and Wheater, H. S. (1999). A Rainfall-Runoff Modelling Toolbox (RRMT) for Matlab. User manual. Imperial College, London.

- Wagener, T., Wheater, H.S. and Gupta, H.V. (2003). Identification and evaluation of conceptual rainfall-runoff models. In Duan, Q., Sorooshian, S., Gupta, H.V., Rousseau, A. and Turcotte, R. (eds.) Advances in calibration of watershed models. AGU Monograph Series, USA, pp. 29-47.

- Wainwright, J., and Thornes, J.B. (2004). Water resources. Ed, In Environmental Issues in the Mediterranean. John Wainwright and John B. Thornes.

- Ward, A.D. and W.J. Elliot. (1995). Environmental hydrology. Lewis Publishers, CRC Press, Inc., Boca Raton, FL.

- Wheater, H. S., A. J. Jakeman, and K. J. Beven. (1993). Progress and directions in rainfall-runoff modeling. In: Jakeman, A. J., Beck, M. B., and McAleer, M. J. (Eds.), Modleing change in environmental systems. John Wiley & Sons, Chichester, UK, pp. 101–132.

- Wheater, H.S., Sorooshian, S., Sharma, K.D., Hsu, K.L., Imam, B., Hong, Y., Hughes, D.S., Croke, B.F.W., Jakeman, A.J., Semmens, D.J., Goodrich, D.C., Unkrich, C.L., Smith, R.E., Woolhiser, D.A., Miller, S.N., Leavesley, G.H., Markstrom, S.L., Viger, R.J., Hay, L.E., Wagener, T., McIntyre, N., Young, P.C., Singh, R.D., Ahmed, S., Maréchal, J.C., Ledoux, E., De Marsily, G. (2007). Hydrological Modelling in Arid and Semi-Arid Areas. Series: International Hydrology Series. ISBN-13: 9780511372810.

- Wheater, H.S., Sorooshian, S., and Sharma, K.D. (2007). Hydrological Modelling in Arid and Semi-Arid Areas. Series: International Hydrology Series. ISBN-13: 9780511372810.

- Wilby, R L., Hassan, H., and Hanaki, K. (1998). Statistical downscaling of hydrometeological variables using general circulation model output. J. Hydrol, 205 (1-2), 1-19

- Wilby, R.L., Dawson, C.W. and Barrow, E.M. (2001). SDSM User Manual- A Decision SupportTool for the Assessment of Regional Climate Change Impacts. http://wwwstaff.lboro.ac.uk/~cocwd/sdsm.html.

- Wilby, R.l., and Harris, I. (2006). A framework for assessing uncertainties in climate change impacts: low flow scenarios for the River Thames, UK, Water Resources Research **42** (2006), p. W02419.

- Williams, J.R. (1975). Sediment routing for agricultural watersheds. Water Resour. Bull. 11(5):965-974.

- WMO. (1999). Annual review of the world climate research programme and report of the twentieth session of the joint research committee. Procedding of the the 2nd seminar for homegenisation of surface climatological data. Budapest, 9-13 Nov. 1998, WCDMP-No, 41, WMO-TD No, 962, 214 pages.

- Woolhiser, D. A. (1971). Deterministic approach to watershed modelling. Nordic Hydrol. 11, 146–66.

- Wullschleger, S.D., Gunderson, C.A., Hanson, P.J., Wilson, K.B., Norby, R.J. (2002). Sensitivity of stomatal and canopy conductance to elevated CO2 concentrationinteracting variables and perspectives of scale. New Phytologist 153, 319–331.

- Yates, D.N. (1996). WatBal: an integrated water balance model for climate impact assessment of river basin runoff. International Journal of Water Resources Development 2, 121–139.

- Zoppou, C. (2001). Review of urban storm water models. Journal of Environmental Modelling and Software 16 (2001)195-231.

APPENDICES

Appendix 1 Soil profiles (Direction des sols 1963-1982)

SOL PEU EVOLUE NON CLIMATIQUE D'APPORT HYDROMORPHE

A. MORI - Profil N. 73 dans étude 225 C

Situation géomorphologique : Plaine alluviale
Topographie : Zone de diffluence et d'inondation de l'Oued Mellah.
Végétation : Phallaris.
Régime agronomique : cultures annuelles sur billons
Matériau originel : alluvions fines de l'Oued Mellah

Description du profil

0 - 40 cm : Argilo-limoneux - olive - motteux - horizon de culture remanié par l'aménagement de billons - calcaire - conductivité = 2,2 mmhos/cm - Cl = 0,5 %.

40 - 80 cm : Argilo-limoneux - olive - structure en gros blocs de consistance et de compacité très fortes - calcaires - conductivité = 4,5 mmhos/cm - Cl = 1,2 %

80 - 120 cm : Argilo-limoneux - brun-olive - structure à éléments continus, plastiques amas et nodules salins - des taches d'hydromorphie rougeâtres sont visibles par endroits - calcaire - conductivité = 10,3 mmhos/cm - Cl = 2,4 %

120 - 160 cm : Argilo-sableux - brun-olive - structure à éléments continus - rares taches d'hydromorphie - calcaire - conductvité = 9,5 mmhos/cm - Cl = 2,6 %

Profondeur	A	L	STF	SF	SG	Chlore en mg%	Satur. pâte%	Cond. mmhos/cm
0 - 40cm	37	40	22,0	1,0	trac.	0,53	56,0	2,2
40 - 80cm	42	36	17,5	3,0	0.5	1,15	58,0	4,5
80 - 120cm	46	31	10,5	6.5	2,5	2,4	60,0	10,3
120 - 160cm	28	16	11,5	23,0	21,5	2,57	46,0	9,5

SOL PEU EVOLUE NON CLIMATIQUE D'APPORT HYDROMORPHE

E. ELIZECHEA - Profil N. 28 dans étude 269

Coordonnées X = 538,100 Y = 298,600 H - 14 m
Topographie : pente 3 %
Roche-mère : alluvions-colluvions
Cultures : blé tendre - Florence aurore.

Description du profil :

9 - 10 cm : Sable argileux - brun-foncé à brun jaune foncé (0 YR 4/3,5) - sec - structure nuciforme - porosité bonne - cohésiin faible - horizon de labour - racines nombreuses - peu calcaire.

10 - 40 cm : Argile sableuse - brun jaune (10 YR 5/4) - sec - structure polyédrique fine bonne porosité - cohésion moyenne - galeries de vers-grains de silice - peu calcaire - pH 8,4 - capacité de rétention : 19 % - racines nombreuses.

40 - 70 cm : Argilo-limoneux - brun jaune (10 YR 5/4] - sec - structure cubique - porosité moyenne - nombreux nodules de torba - grains de silice - calcaire 28,3 % de calcaire total) - 0,60 % de matière organique - pH 8,9 - conductivité 0,97 mmhos cm - racines peu nombreuses.

70 - 115 cm : Argilo-limoneux - brun jaune claire (10 YR 6/4) - frais structure cubique à tendance prismatique - quelques radicelles - non poreux - cohésion forte - compact - légers coatings - taches calcaires - calcaires (20,4 % de calcaire total) - 0,24 % de matière organique - pH 8,8 - conductivité : 3,0 mmhos/cm.

15 - 145 cm : Argilo-sableux - humide - structure à tendance polyédrique fine - non poreux - couleur marmorisée - taches de pseudogley et taches rouilles de fer - 15 % de calcaire total - conductivité : 7,5 mmhos/cm - pH : 8,5.

45 - 200 cm : Sable argileux - brun vif (7,5 YR 5/6) - humide - structure polyédrique - taches de pseudogley et de fer grains de silice - 2,9 % de calcaire total - conductivité : 16 mmhos/cm - pH : 8,3.

Résultats d'analyses

Profondeur en cm	A %	L %	STF %	SF %	SG %	pH 1/2,5	CO3Ca total %	SO4Ca 2H20	Mat. Org.	Sat. de la pâte %	C. mmhos/em 25 %	Cap. de rétention
10 - 40 cm	28	17	6,5	20,5	28	8,4						19 %
40 - 70 cm	38	22	5,5	16,0	18,5	8,9	28,3	0,60		46,8	0,93	25
70 - 115 cm	13	23	6	15,5	12,5	8,8	20,4	0,24		62	3	28
115 - 145 cm	28	15	6,5	24,5	25,5	8,5	15,0	0,16		49,6	7,5	
145 - 200 cm	17	11	5	36	29	8,3	2,9	0,16		36,8	16	

Profondeur en cm	Extrait de saturation (me/l)				
	Cl	CO3H	Ca	Mg	Na
40 - 70 cm	6				
70 - 115 cm	17,5	2,5	2,5	2,7	30
115 - 145 cm	8				
145- 200 cm	11,25	2,25	49,1	37,9	120

SOL PEU EVOLUE NON CLIMATIQUE
D'APPORT VERTIQUE

14

A. MORI - Profil N. 104 dans étude 225 A.

Situation morphologique : bourrelet de l'Oued Kloufi - Plaine alluviale de l'Oued Tine.
Topographie : Plane.
Cultures : Céréales
Matériau originel : Alluvions de texture fine.

Description du profil :

0 - 10 cm : Argilo-limoneux, brun olive, structure élément polyédrique 3 à 4 cm, cohésion et consistance fortes, calcaires.

10 - 50 cm : Argilo-limoneux - brun olive - structure continue avec fentes de retrait délimitant des blocs (10 cm) à cohésion et consistance élevées - racines très fines jusqu'à 45 cm - calcaire.

50 - 90 cm : Argileux - brun olive - structure identique - calcaire.

90 - 120 cm : Argileux - brun olive clair - structure à éléments continus - cohésion consistance et compacité très élevées - calcaire.

20 - 170 cm : Argileux - brun olive clair - structure à éléments continus - consistance moins élevée - compacité forte - pas de fente de retrait - calcaire. Conductivité : 8 mmhos/cm.

N.B. — Profil observé humide.

Résultats d'analyses

profondeur	Granulométrie %					pH	CO3Ca total %	SO4 %	Gypse %	Mat. Org. %	Carbone %	Sat. %	Cond. mmhos /cm	Cl me/l	Ca me/l	pM l\em	Na me/l	SO4 me/l	SAR	Na/T %
	A	L	STF	SF	SG															
0 - 10	36	49	10,5	4,0	0,5	8,3	25,4	0,25	0,44	1,76	1,03	56,8	1,3	10						
0 - 50	46	38	1,5	10,0	0,5	8,3	25,8	0,29	0,51	1,19	0,69	54,8	1,15	10						
50 - 90	52	33	6,0	4,9	1,0	8,4	16,2	0,29	0,51	1,19	0,69	59,2	2,13	15	3,5	4,5	8,75	—	4,35	5
90 - 120	—	—	—	—	—	—	—	—	—	—	—	—	—	—	—	—	—	—	—	—
120 - 170									1,09	—	—	58,4	8,2	40	27,5	22,5	35,0	38	7	8

145

35

SOL BRUN CALCAIRE HUMIFERE

P. DIMANCHE - Etude d'Oum Djeddour N. 302

Situation morphologique : Butte témoin
Topographie : Pente faible
Végétation : Association du Pin d'Alep.

Description du Profil N. 72 :

0 - 15 cm : Brun jaune foncé, humifère, texture limono-argileuse, structure particulaire à grumeleuse faiblement développée, moyennement nuciforme, friable, cailloux et racines abondants, calcaire.

15 - 40 cm : Brun jaune foncé, assez humifère, texture limono-argileuse, structure finement grumeleuse et moyennement nuciforme bien développée, cohérent, meuble, racines assez abondantes - cailloux abondants.

40 - 80 cm : Jaune pâle, texture limono-argileuse, encroûtement très calcaire, sans structure (poussiéreux), peu de racines, cailloux abondants.

80 - 130 cm : Jaune pâle, colluvions argilo-limoneuses caillouteuses, encroûtées, structure polyèdrique à nuciforme bien développées, racines peu abondantes.

30 - 170 cm : Brun très pâle, cailloutis avec limon argileux calcaire, quelques racines.

sultats d'analyses

Profondeur	Granulométrie %					pH	CO3Ca total	CO3Ca actif	Mat. Org.	C
	A	L	STF	SF	SG					
0 - 5	22	21	15,5	20,5	7	7,8	53,2 %	19 %	7,44 %	1
15 - 15	34	22	16	16	7	7,8	64,3	25,5	2,58	1
15 - 40	25	25	14,5	19,5	9,5	7,8	76,6	28,5	1,55	1
40 - 80	35	25	14	18,5	4,5	8,7	62,2	25		
80 - 130	26,5	27	19,5	14,5	6	8,2	54,9	17,5		
130 - 170	36,5	24	15	15,5	6	8,7	46,3	16		

mus %

Profondeur	MHT	AH	AF	MHT / HT	AH / MHT
0 - 5	5,60	2,97	2,63	7,5	53
5 - 15	3	1,80	1,20	11,6	59,8
15 - 55	1,74	0,92	0,82	11,2	53

150

31

RENDZINE HUMIFERE DE MONTAGNE

P. DIMANCHE - Etude d'Oum Djeddour N. 302

Situation morphologique : glacis
Topographie : Pente moyenne
Végétation naturelle . Chêne vert - Erinacéa anthyllis

Description du profil :

0 - 15 cm : Brun foncé, texture équilibrée, structure finement granulaire (micropolyèdres accolés), calcaire, abondants fragments d'encroûtement calcaire, racines et radicelles très abondantes.

15 - 45 cm : Blanc, encroûtement calcaire à très abondants cailloux, très calcaire, sans structure, consistant.

45 - 85 cm : Brun pâle, encroûtement calcaire à cailloutis et pseudomycélium calcaire, très calcaire.

85 - 125 cm : Marnes en voie d'encroûtement par larges plages de torba, sans structure, très consistant.

125 cm et plus Marnes altérées se divisant en plaquettes ou en boules.

Résultats d'analyse

Profondeur	Ganulométrie %						CO3Ca total %	CO3Ca actif	Mat. Org. %	C/N
	A	L	STF	SF	SG	pH				
0 - 15	16	14	14,5	14,1	21,4	8,5	77,8	27 o/o	4,8	16
15 - 45	14	18	19	25,5	15,5	8,8	85,2	20,5	0,82	12,3
45 - 85	18	21	14	25,5	12	8,8	82,3	17,5	—	—

Humus %

MHT	HA	AF	MHT / HT	HA / THM
8,28	4,35	3,93	10,6	52,3

12

15 α **SOL PEU EVOLUE NON CLIMATIQUE D'APPORT MODAL (CALCIMORPHE)**

SOGETHA - (A. CALO) - Profil 407 dans étude N. 305

Situation morphologique :
Topographie :
Végétation :
Matériau originel : Colluvions de sol calcimorphe descendues du Djebel Rebia.

Description du profil :

0 - 25 cm : Limon argileux, poreux, frais, calcaire-brun foncé, polyèdrique moyen, à fin bien développé plus ou moins émoussé quelques petits cailloux calcaires, racines.

25 - 65 cm : Argilo-limoneux, poreux, frais, calcaire, brun, polyèdrique moyen très bien développé, racines, vague tendance à une structure prismatique grossière.

65 - 115 cm : Humide nette, argilo-limoneux, peu poreux, frais, calcaire plus ou moins, brun gris sombre, structure prismatique moyenne se débitant en prismatico-cubique fine, racines.

115 - 150 cm : Argilo-limoneux, peu poreux, frais, calcaire, brun gris plus clair que le précédent, lissage des agrégats, cubique à prismatique moyen bien développé, nombreux pseudomycéliums calcaires, quelques amas.

Résultats d'analyses

Profondeur	Granulométrie %					pH	Calcaire	Matière Organique
	A	L	STF	SF	SG			
0 - 25	28	32	11	19	11	8,1	18 %	2,28 %
25 - 65	34	30	11	19	6	8,4	27	1,34
65 - 115	41	27	7	13	9	8.3	14	1,66
115 - 150	36	32	4	15	10	8,3	10	1.48

RENDZINE SUR CROUTE 10

A. FOURNET - Profil S-8 - Ousseltia

Situation morphologique : Glacis sur cône alluvial ancien
Topographie : Pente faible à moyenne régulière
Régime agronomique : Culture en sec des céréales
Matériau originel : Limon quaternaire.

Description du profil :

) - 30 cm : Brun foncé, texture équilibrée, structure nuciforme à grumeleuse, sans cohésion, calcaire, bonne porosité, bien colonisé par les radicelles.

0 - 60 cm : Beige rosé, texture sablo-limoneuse, structure polyèdrique fine émoussée, calcaire, bien colonisé par les racines, emballe une croûte calcaire beige rosée à pellicule zonaire disloquée en miches soulevées.

) cm et plus Encroûtement calcaire feuilleté au sommet, diffus à la base, beige rosé, texture sablo-limoneuse..

Résultats d'analyses

Profondeur	Granulométrie %					CO3Ca total %	M. O. %
	A	L	STF	SF	SG		
0 - 30	23	19	13	28	13	48	3,6
30 - 60	10	9	12	30	35	72,8	3,5
60 et plus	7	8	7	41	34	86,4	1,0

SOL BRUN CALCAIRE ENCROUTE 36

A. FOURNET - Profil N. 58 - Oued Zit

Situation morphologique : glacis
Topographie : Pente régulière, faible
Régime agronomique . Céréales
Matériau originel : Limon quaternaire.

Description du profil :

\- 30 cm : Brun (10 YR 5/3), texture équilibrée, structure polyèdrique émoussée dans une surstructure en grands éléments peu développés de 10 cm de diamètre, calcaire fort, meuble, poreux.

\- 70 cm : Jaune brun (10 YR 7/6), limoneux, structure prismatique se défaisant en plaquettes cubiques de 1 cm d'épaisseur, très calcaire, bonne macroporosité.

\- 120 cm : Jaune brun (10 YR 5/6), argilo-limoneux, structure prismatique cubique fine, agrégats révêtus d'argile, taches calcaires blcnches de 1 cm de diamètre, piquetures ferro-manganiques, calcaire, compact, trè.s peu poreux.

cm et plus Jaune-rouge, argileux, structure en gros prismes cubiques déformés, faces horizontales des agrégats lisses, brillantes à slikensides, revêtement en nappe de calcaire sur les faces verticales des agrégats, calcaire.

Résultats d'analyses

Profondeur	Granulométrie					CO3Ca %	pH	M. O. %	Conductivité mmhos/cm
	A	L	STF	SF	SG				
0 - 30	23,5	11	9	35	19	18,8	8,4	1,19	0,82
30 - 70	34,5	29	8	19	7	34,8	8,3	1,03	2,13
70 - 120	37	30	22	16	4	40,9	8,5	0,21	—
120 et plus	46	15	15	21	3	48,8	8,7	0,21	

SOL PEU EVOLUE NON CLIMATIQUE D'APPORT MODAL (STEPPIQUE)

J. LE FLOCH - Profil N. 29 étude N. 253

Situation géomorphologique : glacis quaternaire
Topographie : Mi-pente
Cultures . Céréales - localement plantations arbustives - oliviers
Matériau originel : Alluvions colluvions remaniant des apports éoliens, gypseux.

Description du profil :

- 40 cm : Texture équilibrée, couleur brun-jaune, structure à tendance polyèdrique moyenne, horizon humifère, calcaire, 20 % CO_3Ca, pH 8,5.
- 60 cm : Argilo-limoneux, couleur brun jaune, structure à tendance cubique, cohésion moyenne à forte, quelques taches plus calcaires humifères, calcaire.
- 200 cm : Sablo-argileux, couleur beige jaune, structure massive-fentes de retrait étroites profondes délimitant de grands prismes, compacité moyenne à forte.

s d'analyses

deur	Granulométrie					pH	CO3Ca %	Mat Org. %	Sat p %	Cl mmhos	CL me/L
	A	L	STF	SF	SG						
40	30	11	16,0	38,5	3,0	8,5	20,0	0,88	—	—	—
80	42	11	13,0	26,5	4,5	8,5	30,4	0,83	42	1,5	3

SOL CALCAIRE HYDROMORPHE CULTIVE

A. FOURNET - Etude pédologique de l'U.R.D. de Béja

Situation morphologique : versant marneux colluvionné
Topographie : Pente moyenne à forte
Régime agronomique : Céréales
Matériau originel : Grès argileux du miocène inférieur

Description du Profil N. 16 :

0 - 35 cm : Brun foncé, argilo-sableux, à sable fin, structure motteuse, grossièrement nuciforme, calcaire, compacité moyenne, bonne porosité radiculaire.

35 - 95 cm : Brun jaune à beige jaune, argilo-sableux à sable fin, surstructure en prismes de 5 à 10 cm de diamètre tendant à se pulvériser au sommet et à la base de l'horizon sous forme de petits prismes irréguliers, structure en petits polyèdres, calcaire, compacité moyenne, bonne porosité. Présence de taches calcaires à partir de 35 cm, groupées en essaims nombreux à partir de 65 cm.

95 - 135 cm : Ocre jaune, sableux à sable grossier, sans structure, quelques blocs de grès argileux burdigalien.

135 - 200 cm : Substrat jaune grise de gley, marne vindobonienne altérée et remaniée à surstructure prismatique et structure en éclats à cassure conchoïdale. Accumulation d'amas calcaires pulvérulents au sommet de la couche.

33

SOL BRUN CALCAIRE ENCROUTE

A. FOURNET - Profil N. 75 bis - Oued Zarga

Situation morphologique : Glacis résiduel ancien
Topographie : Pente forte .
égétation naturelle : Association végétale à Pinus halépensis et Rosmarinus officinalis, forme dégradée à Stipa tenacissima.
Mctériou originel : Limon quatemaire.

Description du profil :

0 - 20 cm : Couleur brune 7,5 YR 5 4, texture équilibrée, structure nuciforme moyenne à fine, faiblement calcaire (horizon A1).

20 - 50 cm : Couleur brun 7,5 YR 5/4, texture équilibrée structure nuciforme moyenne à fine, calcaire, pseudomycélium calcaire tubulaire et sur les faces d'agrégats.

50 - 90 cm : Couleur brun très pâle 10 YR 7/4, texture équilibrée, structure polyèdrique émoussée au sommet en éclats à la base, fortement calcaire, (horizon B.).

90 cm et plus Couleur brun très pâle 10 YR 7/4, texture limono-sableuse, structure en éclats, fortement calcaire, (horizon C).

Résultats d'analyses

Profondeur	Granulométrie %					pH	CO3Ca total %	M. O. %	C/N
	A	L	STF	SF	SG				
0 - 20	18,5	17,5	12,0	23,0	27	7,9	27,5	3,36	11,1
20 - 50	22,0	19,5	13,0	22,0	23	8,05	37,5	1,08	10,0
50 - 50	20,0	20,5	14,0	20,0	23	8,10	48,0	—	—
90 et plus	14,5	24,5	13,0	19,0	29	8,15	50,0		

RENDZINE SUR CROUTE

A. FOURNET - Profil 75 a - Béja

Situation morphologique : Glacis de piedmont ancien
Topographie : Zone plane à pente moyenne
Végétation naturelle : Absente
Régime agronomique : Culture de céréales
Matériau originel, grès oligocène

Description du profil :

0 - 30 cm : Couleur brun rouge foncé 5 YR 3/3, texture équilibrée, structure motteuse, sous structure finement nuciforme, calcaire (korizon A1).

30 - 50 cm : Couleur blanc jaunâtre 5 YR 8/2, texture sablo-argileuse, structure fondue, encroûtement calcaire (Horizon B).

50 cm et plus Couleur blanc jaunâtre 5 YR 8/2, texture sablo argileuse, structure feuilletée, encroûtement calcaire (horizon Cca).

Résultats d'analyses

Profondeur	Granulométrie %					pH	CO3 Ca Total %	M.O. %	C/N
	A	L	STF	SF	SG				
0 - 30 cm	29	15	12	16	25	8,0	26,4	3,05	9
30 - 50 cm	19	8	9	18	42	—	87,3	—	—
50 et plus	13	11	10	17	44	—	89,3	—	—

SOL PEU EVOLUE NON CLIMATIQUE D'APPORT VERTIQUE

L. GUYOT - Profil N. 123 dans étude N. 173

Coordonnées : 39G64 9G32
Topographie : Pente faible et régulière
Régime agronomique : Quelques oliviers médiocres isolés et céréales

Description du profil :

0 - 50 cm : Marron-limono-argileux à argilo-limoneux sur structure prismatique très grossière à très larges fentes. La structure est cubique moyenne (4 cm) - très cohérent, non poreux. Lissage de quelques faces horizontales. Un léger gauchissement, peu calcaire.

50 - 100 cm : Idem, mais plus massif - le lissage est plus important, le gauchissement un peu plus accentué. Aucune porosité-calcaire.

00 - 160 cm : Marron sombre - limono-argileux - la structure prismatique moyenne se défait en polyèdres moyens bien développés - très cohérent.

60 - 180 cm : Brun sombre - argilo-sableux - peu calcaire.

SOL BRUN CALCAIRE SUR LIMON A NODULES CALCAIRES

A. FOURNET - Ousseltia

Situation morphologique : Ravinement de glacis remblayé
Topographie : Pente faible autour d'une petite dépression
Régime agronomique : Céréales
Matériau originel : Limon quaternaire

Description du profil S-17 :

0 - 35 cm : Brun foncé limono-argileux, structure nuciforme à granulaire, calcaire, cohérent, porosité moyenne radiculaire.

35 - 70 cm : Ocre-rosé, limono-argileux, structure polyèdrique émoussée à faible tendance prismatique, calcaire, compacité moyenne, porosité faible.

70 - 135 cm : **Ocre-rosé**, limono-argileux, structure polyédrique émossee, calcaire, présence croissante en profondeur de nodules bosselés, indurés de couleur rosé, très compact porosité nulle.

Résultats d'analyses

Profondeur	Granulométrie %					CO3Ca total %	Mat. Org. %
	A	L	STF	SF	SG		
0 - 35	25	27	12,5	23,5	9	19	1,84
85 - 70	23	30	13	23	8,5	34,7	0,62
70 - 135	24	29	10	24	11	26	—

35

SOL BRUN CALCAIRE A ACCUMULATION CALCAIRE

A. FOURNET - Profil - P 11 - Ousseltia

(Non publié)

Situation morphologique : Vallon alluvial ancien
Topographie : Plane régulière à pente faible
Régime agronomique : Céréales
Matériau originel : Limon quaternaire

Description du profil :

35 cm : Couleur brun foncé, texture limono-argileuse, structure nuciforme à faible cohésion, calcaire, porosité radiculaire, bien colonisé par les radicelles.

55 cm : Couleur brune, texture limon-argileuse, structure polyèdrique émoussée à faible cohésion, compacité nette, calcaire avec léger pseudomycélium calcaire, porosité radiculaire, bien colonisé par les radicelles.

100 cm : Couleur beige rosée, texture équilibrée, structure polyèdrique émoussée fine à cohésion moyenne, encroûtement calcaire.

200 cm : Couleur rosée beige, texture limono-sableuse, structure polyèdrique émoussée fine à cohésion moyenne avec agrégats enrobés de calcaire.

Résultats d'analyses

Profondeur	Granulométrie %					CO3Ca total %	CO3Ca actif %	M. O. %
	A	L	STF	SF	SG			
0 - 35	30	28	8,5	22,5	9,5	34,2	20,0	2,24
35 - 55	32	33	3,5	20,0	9,0	46,2	35,5	1,29
55 - 100	27	20	13,5	28,5	10,0	65,8	48,5	0,65
100 - 200	14	22	10,5	34,0	20,5	59,6	33,5	—

37-39-40

SOL ISOHUMIQUE

Sol isohumique subtropical chatain modal

R. GADDAS - Profil 493 - Etude 245

Topographie : Pente comprise entre 3 et 7 =
Végétation : Hypéricum crispum - Carlino corymbosa - Cichorium Mentibus - Asteriscus aquaticus - Linaria Langera - Rhapuncticum Acaule - Convolvulus althaeoides.

Description du profil :

0 - 30 cm : Brun-rouge, texture limoneuse, structure nuciforme, friable, effervescence forte, riche en matière organique. Racines nombreuses, pH : 8,3.

0 - 70 cm : Rouge-brun, texture limono-argileuse, structure nuciforme à polyèdrique. Effervescence forte. Faces lissées, quelques petits grains de silice.

70 cm : Rouge-brun, texture argilo-limoneuse, structure polyèdrique à prismatique, porosité faible, très compact, très riche en nodules et taches calcaires friables.

ses :

ofondeur	Granulométrie %					CO3 Ca %	Mat. Org. %	pH	Fer libre %	Fer total %	Fer l. Fer t.
	A	L	STF	SF	SG						
— 30 cm	18	31	11	26	14	10	2,9	8,3	0,42	3,5	0,12
— 70 cm	29	28	8	22	14	12	1,1	8,5	0,34	3,5	0,09
— 70 cm	41	23	8	16	14	27	0,6	8,9	0,56	3,5	0,16

SOL ISOHUMIQUE

Sol isohumique subtropical brun modal ✓

K. BELKHODJA - Profil 44 - Etude N. 272

Situation géomorphologique : En bas d'une colline dont le sommet est encroûté.
Matériau originel : Sable et argiles du Miopliocène
Régime agronomique : Non cultivé.

Description du profil :

0 - 25 cm : Frais brun, limono-sableux, structure nuciforme, friable, nombreux pores, racines et radicelles, petits granules calcaires.

25 - 70 cm : Brun beige clair, limono-sableux, structure massive se débite en éclats polyèdriques, porosité moyenne, nombreux nodules calcaires de diamètre variable, certains friables crayeux d'autres durcis. Consistance et cohésion moyenne.

70 - 160 cm : Beige jaune, limono-sableux, structure massive se débite en éclats polyèdriques, porosité moyenne, nombreux mycéliums calcaires et nodules blancs friables de 0,5 à 2 cm de diamètre, certains arrondis d'autres allongés avec des apophyses.

Résultats d'analyses

Profondeur	Granulométrie %					CO3 Ca %	M.O. %
	A	L	STF	SF	SG		
0 — 25 cm	19	11	8	43	19	12	1,2
25 — 50 cm	15	10	7	44	23	15	0,8
50 — 70 cm	19	7	5	46	22	10	0,5
70 — 100 cm	16	11	5	45	22	21,6	0,05

SOL ISOHUMIQUE

Sol isohumique subtropical chatain-rouge

P. MARTINI - Ph. GRAFFIN - Profil N. - Cheylus

(Non publié)

Situation géomorphologique : Glacis aux pieds d'une barre calcaire

Topographie : Pente faible

Matériau originel : Marnes grises du crétacé inférieur

Végétation :

Régime agronomique . Céréales.

Description du profil :

0 - 15 cm : Brun 7,5 YR 4/4 argilo-limoneux, structure grumeleuse à nuciforme, porosité moyenne, consistance et cohésion faible, calcaire faible, quelques petits cailloux calcaires, assez nombreuses racines.

15 - 40 cm : Brun 7,5 YR 4/4, argilo-limoneux, structure nuciforme porosité moyenne à assez forte, cohésion et consistance moyenne, quelques petits cailloux (plus rares que dans l'horizon précédent), calcaire moyen, bon enracinement.

40 - 65 cm : Brun rouge, 5 YR 4/4, argileux, structure polyèdrique grossière (5 cm) se défaisant en polyèdres fins, quelques faces luisantes, porosité tubulaire moyenne à faible, cohésion moyenne à forte, consistance forte, quelques petites taches calcaires arrondies (0,5 cm), calcaire, racines.

65 - 95 cm : Brun rouge, 5 YR 4/4, argileux, structure prismatique moyenne (10 cm) se défaisant en cube à faces subhorizontales lissées puis en polyèdres fins, porosité tubulaire moyenne à faible, cohésion et consistance fortes, quelques petits granules et taches calcaires, calcaire, racines peu nombreuses.

95 - 115 cm : Brun rouge, 5 YR 4/4, argileux, structure cubique, quelques plaquettes à faces lissées, miroirs de glissement, petits granules et taches calcaires, calcaire moyen à fort, quelques racines.

115 - 150 cm : Brun rouge 5 YR 4/4 panachures grises et plages blanches (calcaire), argilo-limoneux, structure polyèdrique moyenne bien individualisée, porosité faible, consistance et cohésion forte, amas calcaires pulvérulents plus ou moins consolidés concrétions moyennes (1 à 2 cm) très peu de racines, calcaire fort.

150 - 175 cm : Gris à taches brun rougeâtre et quelques taches bleutées (couleur de l'altération de la marne), limono-argileux, structure polyèdrique mal définie, on retrouve le litage de la marne, filons de calcite, petites taches noires ferro-manganeuses, calcaire fort, peu de racines.

175 et plus Gris, horizon d'altération de la marne, fragmentation en éléments de forme polyèdrique vaguement arrondie par pellicules de desquamation, cassure plus ou moins conchoïdale.

173

PROFIL N° 11

- Région de Kairouan - plaine de Merguellil

Etage bioclimatique :
semi-aride supérieur à hiver tempéré

Régime hydrique du sol :
aridique
Régime de température du sol :
thermique

Géomorphologie :
plaine alluviale

Occupation du sol :
cultures annuelles, blé

Classification française :
sols salés à alcali à caractère vertique

Soil taxonomy :
haplic natrargids

Classification F.A.O. :
solonetz orthiques.

TABLEAU D'ANALYSES

Profon. cm	pH	GRANULOMETRIE					CE mmhos cm	M.O. %	Carb. %	Azote %	CaCo3 tot.act %	p.F. 4,2 %
		A %	L.F. %	L.G. %	S.F. %	S.G. %						
0-15	8,6	27,27	32	14	19	7	2,1				29/13	
15-45	8,3	35	26	12	20	6	9,1				29/13	
45-85	8,5	23	19	21	34	2	10				32/11	
85-120	8,2	41	38	14	4	6	10,1				29/14	
120-160	8,5	S a b l e u x					7,5					

52

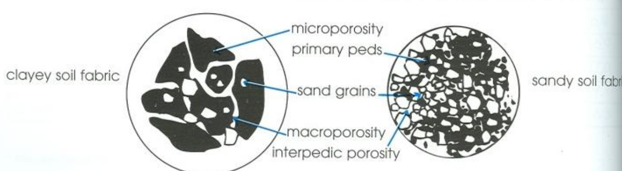

Modèle morphologique de la structure du sol *(Brewer, 1964)*

PROFIL N° 11 :

deux sols l'un sur l'autre, tous deux salés

Description :

1er Sol

0 à 15 : Ap
Frais : 10 YR 5/3 texture limono-argileuse - meuble - peu poreux - quelques racines fines pénétrant les agrégats, - activité biologique peu abondante - calcaire - structure polyédrique subangulaire.

15 à 45 :
Sec, 10 YR 5/2 - texture argilo-limoneuse- poreux-cohérent - très peu de racines très fines - activité biologique peu abondante,- effervescence calcaire - structure cubique - présence de faces de glissement.

2ème Sol

45 à 85:
Sec, 10 YR 5/4 - texture limono-argileuse - cohérent - peu poreux - très peu de racines très fines, - activité biologique peu abondante,- effervescence calcaire - structure lamellaire.

85 à 120 :
Sec, 10 YR 4/4 - texture argilo-limoneuse - cohérent - poreux, - pas de racines - activité biologique peu abondante - effervescence calcaire - structure prismatique - présence de faces de glissement.

120 à 160 :
Sec, 10 YR 7/3 - texture sableuse - non poreux, - pas de racines ni d'activité biologique - effervescence calcaire faible - structure particulaire.

(décrit par Mohdi, Novembre 1973)

53

Appendix 2a Point Analysis for soil samples (Dridi, 2000)

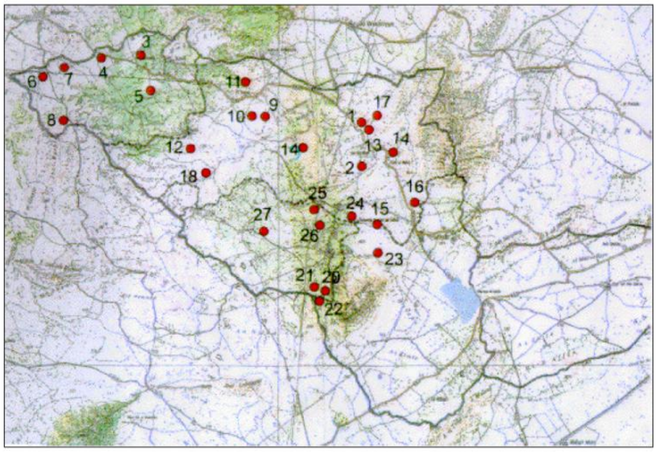

Appendix 2b Analysis result for soil characteristics (Dridi 2000)

Tableau 16 : Caractéristiques texturales des sites de simulation

Numéro des sites	Nom des sites	Usages	Textures
1	Oued Hajar	Labour	12 % Ag +37% SG+51% (L+SF)
2	Fidh Ali	Labour	25% Ag +16% SG+59% (L+SF)
3	El Hammam	Labour	33% Ag +5% SG+62% (L+SF)
4	Tella	Jachère	30% Ag +10% SG+60% (L+SF)
5	Kesra Forêt	Parcours-litière	13% Ag +5% SG+82% (L+SF)
6	Tella	Labour	24% Ag +18% SG+58% (L+SF)
7	Tella	Parcours	39% Ag +3% SG+57% (L+SF)
8	Kesra	Parcours	29% Ag +7% SG+64% (L+SF)
9	Garia Janoubia	Parcours	15% Ag +15% SG+70% (L+SF)
10	Garia Janoubia	Labour	15% Ag +18% SG+67% (L+SF)
11	Garia Chamalia	Parcours	25% Ag +10% SG+65% (L+SF)
12	El Fdhoul	Labour	24% Ag +10% SG+66% (L+SF)
13	O. Ettiour	Parcours	34% Ag +11% SG+55% (L+SF)
14	Khit El Oued	Labour	9% Ag +15% SG+76% (L+SF)
15	Awlad Isawy	Labour	32% Ag +15% SG+53% (L+SF)
16	Oued Hoshas	Parcours	16% Ag +42% SG+42% (L+SF)
17	Forêt 7 Nov	Parcours	40% Ag +14% SG+46% (L+SF)
18	Oued Morra	Labour	26% Ag +13% SG+61% (L+SF)
19	Moazil	Labour	29% Ag +15% SG+56% (L+SF)
20	Trozza	Parcours	3% Ag +51% SG+46% (L+SF)
21	Trozza	Labour	5% Ag +31% SG+64% (L+SF)
22	Trozza	Jachère	7% Ag +46% SG+47% (L+SF)
23	Oued Zebbes	Parcours	7% Ag +62% SG+31% (L+SF)
24	El Msaid	Parcours	5% Ag +54% SG+41% (L+SF)
25	Awlad Amor	Parcours	10% Ag +45% SG+45% (L+SF)
26	Awlad Amor	Jachère	12% Ag +40% SG+48% (L+SF)
27	Missouita	Labour	7% Ag +50% SG+43% (L+SF)

Appendix 3 Soil profiles characteristics in the Merguellil catchment

Soil Name: S1
Soil Hydrologic Group: C
Maximum rooting depth(m) : 2000.00
Porosity fraction from which anions are excluded: 0.500
Crack volume potential of soil: 0.500
Texture 1 : SANDY CLAY LOAM

Depth [mm]:	400.00	600.00	2000.00
Bulk Density Moist [g/cc]:	1.56	1.48	1.57
Ave. AW Incl. Rock Frag :	0.10	0.12	0.11
Ksat. (est.) [mm/hr]:	4.95	0.74	11.54
Organic Carbon [weight %]:	1.52	1.43	1.00
Clay [weight %]:	30.50	43.00	21.27
Silt [weight %]:	11.50	12.00	27.30
Sand [weight %]:	58.00	45.00	51.43
Rock Fragments [vol. %]:	10.00	10.00	10.00
Soil Albedo (Moist) :	0.17	0.17	0.17
Erosion K :	0.09	0.10	0.14
Salinity (EC, Form 5) :	0.00	0.00	0.00

Soil Name: S2
Soil Hydrologic Group: C
Maximum rooting depth(m) : 1600.00
Porosity fraction from which anions are excluded: 0.500
Crack volume potential of soil: 0.500
Texture 1 : CLAY LOAM

Depth [mm]:	150.00	450.00	850.00	1200.00	1600.00
Bulk Density Moist [g/cc]:	1.48	1.45	1.52	1.35	1.49
Ave. AW Incl. Rock Frag :	0.15	0.14	0.14	0.15	0.04
Ksat. (est.) [mm/hr]:	4.43	2.69	6.94	2.42	140.74
Organic Carbon [weight %]:	1.52	0.58	1.00	1.00	1.00
Clay [weight %]:	28.00	35.00	24.00	40.00	3.00
Silt [weight %]:	46.00	38.00	40.00	50.00	3.00
Sand [weight %]:	26.00	27.00	36.00	10.00	94.00
Rock Fragments [vol. %]:	10.00	10.00	10.00	10.00	10.00
Soil Albedo (Moist) :	0.17	0.17	0.17	0.17	0.17
Erosion K :	0.09	0.17	0.16	0.18	0.11
Salinity (EC, Form 5) :	0.00	0.00	0.00	0.00	0.00

Soil Name: S3
Soil Hydrologic Group: C
Maximum rooting depth(m) : 1500.00
Porosity fraction from which anions are excluded: 0.500
Crack volume potential of soil: 0.500
Texture 1 : CLAY LOAM

Depth [mm]:	250.00	650.00	1150.00	1500.00
Bulk Density Moist [g/cc]:	1.44	1.46	1.40	1.42
Ave. AW Incl. Rock Frag :	0.13	0.13	0.13	0.13
Ksat. (est.) [mm/hr]:	7.42	3.25	1.74	2.66
Organic Carbon [weight %]:	3.93	2.31	2.86	2.55
Clay [weight %]:	28.00	34.00	42.00	37.00
Silt [weight %]:	32.00	30.00	28.00	33.00
Sand [weight %]:	40.00	36.00	30.00	30.00
Rock Fragments [vol. %]:	10.00	10.00	10.00	10.00
Soil Albedo (Moist) :	0.17	0.17	0.17	0.17
Erosion K :	0.12	0.12	0.12	0.12
Salinity (EC, Form 5) :	0.00	0.00	0.00	0.00

Soil Name: S5
Soil Hydrologic Group: C
Maximum rooting depth(m) : 2000.00
Porosity fraction from which anions are excluded: 0.500
Crack volume potential of soil: 0.500
Texture 1 : SANDY CLAY LOAM

Depth [mm]:	400.00	700.00	1150.00	1450.00	2000.00
Bulk Density Moist [g/cc]:	1.47	1.43	1.40	1.52	1.57
Ave. AW Incl. Rock Frag :	0.11	0.12	0.13	0.10	0.08
Ksat. (est.) [mm/hr]:	8.30	2.57	1.45	16.32	22.92
Organic Carbon [weight %]:	5.00	4.31	3.45	2.59	2.05
Clay [weight %]:	28.00	38.00	43.00	28.00	18.00
Silt [weight %]:	17.00	22.00	23.00	15.00	12.00
Sand [weight %]:	55.00	40.00	34.00	57.00	70.00
Rock Fragments [vol. %]:	10.00	10.00	10.00	10.00	10.00
Soil Albedo (Moist) :	0.17	0.17	0.17	0.17	0.17
Erosion K :	0.10	0.11	0.11	0.09	0.09
Salinity (EC, Form 5) :	0.00	0.00	0.00	0.00	0.00

Soil Name: S6
Soil Hydrologic Group: C
Maximum rooting depth(m) : 1000.00
Porosity fraction from which anions are excluded: 0.500
Crack volume potential of soil: 0.500
Texture 1 : CLAY LOAM

Depth [mm]:	350.00	550.00	1000.00
Bulk Density Moist [g/cc]:	1.45	1.46	1.57
Ave. AW Incl. Rock Frag :	0.13	0.14	0.11
Ksat. (est.) [mm/hr]:	6.56	3.54	6.29
Organic Carbon [weight %]:	3.86	2.22	1.12
Clay [weight %]:	30.00	33.00	27.00
Silt [weight %]:	29.00	34.00	21.00
Sand [weight %]:	41.00	33.00	52.00
Rock Fragments [vol. %]:	10.00	10.00	10.00
Soil Albedo (Moist) :	0.17	0.17	0.17
Erosion K :	0.12	0.12	0.12
Salinity (EC, Form 5) :	0.00	0.00	0.00

Soil Name: S7
Soil Hydrologic Group: C
Maximum rooting depth(m) : 2000.00
Porosity fraction from which anions are excluded: 0.500
Crack volume potential of soil: 0.500
Texture 1 : SANDY LOAM

Depth [mm]:	200.00	500.00	900.00	2000.00
Bulk Density Moist [g/cc]:	1.44	1.56	1.56	1.56
Ave. AW Incl. Rock Frag :	0.10	0.10	0.10	0.10
Ksat. (est.) [mm/hr]:	24.26	12.51	13.80	25.39
Organic Carbon [weight %]:	5.79	1.86	0.05	0.05
Clay [weight %]:	19.00	22.00	20.50	14.50
Silt [weight %]:	18.00	20.00	21.50	24.50
Sand [weight %]:	63.00	58.00	58.00	61.00
Rock Fragments [vol. %]:	10.00	10.00	10.00	10.00
Soil Albedo (Moist) :	0.17	0.17	0.17	0.17
Erosion K :	0.10	0.10	0.14	0.15
Salinity (EC, Form 5) :	0.00	0.00	0.00	0.00

Soil Name: S8
Soil Hydrologic Group: C
Maximum rooting depth(m) : 1000.00
Porosity fraction from which anions are excluded: 0.500
Crack volume potential of soil: 0.500
Texture 1 : CLAY LOAM

Depth [mm]:	350.00	550.00	1000.00
Bulk Density Moist [g/cc]:	1.45	1.46	1.57
Ave. AW Incl. Rock Frag :	0.13	0.14	0.11
Ksat. (est.) [mm/hr]:	6.56	3.54	6.29
Organic Carbon [weight %]:	3.86	2.22	1.12
Clay [weight %]:	30.00	33.00	27.00
Silt [weight %]:	29.00	34.00	21.00
Sand [weight %]:	41.00	33.00	52.00
Rock Fragments [vol. %]:	10.00	10.00	10.00
Soil Albedo (Moist) :	0.17	0.17	0.17
Erosion K :	0.12	0.12	0.12
Salinity (EC, Form 5) :	0.00	0.00	0.00

Soil Name: S9
Soil Hydrologic Group: C
Maximum rooting depth(m) : 2000.00
Porosity fraction from which anions are excluded: 0.500
Crack volume potential of soil: 0.500
Texture 1 : SANDY CLAY LOAM

Depth [mm]:	300.00	700.00	1200.00	2000.00
Bulk Density Moist [g/cc]:	1.57	1.47	1.52	1.45
Ave. AW Incl. Rock Frag :	0.09	0.13	0.12	0.12
Ksat. (est.) [mm/hr]:	11.13	2.71	2.40	0.50
Organic Carbon [weight %]:	2.05	1.78	0.36	0.36
Clay [weight %]:	24.00	35.00	34.00	46.00
Silt [weight %]:	12.00	30.00	27.00	15.00
Sand [weight %]:	64.00	35.00	39.00	39.00
Rock Fragments [vol. %]:	10.00	10.00	10.00	10.00
Soil Albedo (Moist) :	0.17	0.17	0.17	0.17
Erosion K :	0.09	0.12	0.15	0.14
Salinity (EC, Form 5) :	0.00	0.00	0.00	0.00

Soil Name: S10
Soil Hydrologic Group: C
Maximum rooting depth(m) : 1000.00
Porosity fraction from which anions are excluded: 0.500
Crack volume potential of soil: 0.500
Texture 1 : SANDY LOAM

Depth [mm]:	250.00	500.00	700.00	1000.00
Bulk Density Moist [g/cc]:	1.57	1.59	1.61	1.63
Ave. AW Incl. Rock Frag :	0.08	0.07	0.07	0.07
Ksat. (est.) [mm/hr]:	20.75	31.71	20.48	25.98
Organic Carbon [weight %]:	2.07	1.38	0.86	0.09
Clay [weight %]:	19.00	15.00	19.00	16.00
Silt [weight %]:	11.00	11.00	8.00	12.00
Sand [weight %]:	70.00	74.00	73.00	72.00
Rock Fragments [vol. %]:	10.00	10.00	10.00	10.00
Soil Albedo (Moist) :	0.17	0.17	0.17	0.17
Erosion K :	0.09	0.09	0.10	0.12
Salinity (EC, Form 5) :	0.00	0.00	0.00	0.00

Soil Name: S12
Soil Hydrologic Group: C
Maximum rooting depth(m) : 1600.00
Porosity fraction from which anions are excluded: 0.500
Crack volume potential of soil: 0.500
Texture 1 : SILTY LOAM

Depth [mm]:	1600.00
Bulk Density Moist [g/cc]:	1.40
Ave. AW Incl. Rock Frag :	0.19
Ksat. (est.) [mm/hr]:	5.50
Organic Carbon [weight %]:	0.05
Clay [weight %]:	25.00
Silt [weight %]:	65.00
Sand [weight %]:	10.00
Rock Fragments [vol. %]:	10.00
Soil Albedo (Moist) :	0.17
Erosion K :	0.22
Salinity (EC, Form 5) :	0.00

Soil Name: S14
Soil Hydrologic Group: C
Maximum rooting depth(m) : 1600.00
Porosity fraction from which anions are excluded: 0.500
Crack volume potential of soil: 0.500
Texture 1 : SILTY CLAY LOAM

Depth [mm]:	1600.00
Bulk Density Moist [g/cc]:	1.40
Ave. AW Incl. Rock Frag :	0.17
Ksat. (est.) [mm/hr]:	4.86
Organic Carbon [weight %]:	0.05
Clay [weight %]:	29.00
Silt [weight %]:	56.00
Sand [weight %]:	15.00
Rock Fragments [vol. %]:	10.00
Soil Albedo (Moist) :	0.17
Erosion K :	0.20
Salinity (EC, Form 5) :	0.00

Soil Name: S8
Soil Hydrologic Group: C
Maximum rooting depth(m) : 1000.00
Porosity fraction from which anions are excluded: 0.500
Crack volume potential of soil: 0.500
Texture 1 : CLAY LOAM

Depth [mm]:	350.00	550.00	1000.00
Bulk Density Moist [g/cc]:	1.45	1.46	1.57
Ave. AW Incl. Rock Frag :	0.13	0.14	0.11
Ksat. (est.) [mm/hr]:	6.56	3.54	6.29
Organic Carbon [weight %]:	3.86	2.22	1.12
Clay [weight %]:	30.00	33.00	27.00
Silt [weight %]:	29.00	34.00	21.00
Sand [weight %]:	41.00	33.00	52.00
Rock Fragments [vol. %]:	10.00	10.00	10.00
Soil Albedo (Moist) :	0.17	0.17	0.17
Erosion K :	0.12	0.12	0.12
Salinity (EC, Form 5) :	0.00	0.00	0.00

Soil Name: S10
Soil Hydrologic Group: C
Maximum rooting depth(m) : 1000.00
Porosity fraction from which anions are excluded: 0.500
Crack volume potential of soil: 0.500
Texture 1 : SANDY LOAM

Depth [mm]:	250.00	500.00	700.00	1000.00
Bulk Density Moist [g/cc]:	1.57	1.59	1.61	1.63
Ave. AW Incl. Rock Frag :	0.08	0.07	0.07	0.07
Ksat. (est.) [mm/hr]:	20.75	31.71	20.48	25.98
Organic Carbon [weight %]:	2.07	1.38	0.86	0.09
Clay [weight %]:	19.00	15.00	19.00	16.00
Silt [weight %]:	11.00	11.00	8.00	12.00
Sand [weight %]:	70.00	74.00	73.00	72.00
Rock Fragments [vol. %]:	10.00	10.00	10.00	10.00
Soil Albedo (Moist) :	0.17	0.17	0.17	0.17
Erosion K :	0.09	0.09	0.10	0.12
Salinity (EC, Form 5) :	0.00	0.00	0.00	0.00

Soil Name: S11
Soil Hydrologic Group: B
Maximum rooting depth(m) : 1200.00
Porosity fraction from which anions are excluded: 0.500
Crack volume potential of soil: 0.500
Texture 1 : SANDY LOAM

Depth [mm]:	200.00	400.00	600.00	950.00	1200.00
Bulk Density Moist [g/cc]:	1.47	1.54	1.56	1.58	1.56
Ave. AW Incl. Rock Frag :	0.05	0.05	0.05	0.05	0.04
Ksat. (est.) [mm/hr]:	90.53	59.24	63.66	46.70	79.38
Organic Carbon [weight %]:	3.62	2.24	1.55	1.55	0.86
Clay [weight %]:	7.00	11.00	10.00	13.00	8.00
Silt [weight %]:	4.00	2.00	3.00	2.00	2.00
Sand [weight %]:	89.00	87.00	87.00	85.00	90.00
Rock Fragments [vol. %]:	10.00	10.00	10.00	10.00	0.00
Soil Albedo (Moist) :	0.17	0.17	0.17	0.17	0.17
Erosion K :	0.07	0.05	0.05	0.05	0.07
Salinity (EC, Form 5) :	0.00	0.00	0.00	0.00	0.00

```
Soil Name: S13
Soil Hydrologic Group: B
Maximum rooting depth(m) : 1600.00
Porosity fraction from which anions are excluded: 0.500
Crack volume potential of soil: 0.500
Texture 1                 : SILTY LOAM
Depth                [mm]:     1600.00
Bulk Density Moist [g/cc]:        1.51
Ave. AW Incl. Rock Frag  :        0.15
Ksat. (est.)      [mm/hr]:       21.96
Organic Carbon [weight %]:        0.05
Clay           [weight %]:       12.00
Silt           [weight %]:       51.00
Sand           [weight %]:       37.00
Rock Fragments   [vol. %]:       10.00
Soil Albedo (Moist)      :        0.17
Erosion K                :        0.23
Salinity (EC, Form 5)    :        0.00

Soil Name: S15
Soil Hydrologic Group: B
Maximum rooting depth(m) : 1600.00
Porosity fraction from which anions are excluded: 0.500
Crack volume potential of soil: 0.500
Texture 1                 : SANDY LOAM
Depth                [mm]:     1600.00
Bulk Density Moist [g/cc]:        1.52
Ave. AW Incl. Rock Frag  :        0.10
Ksat. (est.)      [mm/hr]:       54.62
Organic Carbon [weight %]:        0.05
Clay           [weight %]:        7.00
Silt           [weight %]:       31.00
Sand           [weight %]:       62.00
Rock Fragments   [vol. %]:       10.00
Soil Albedo (Moist)      :        0.17
Erosion K                :        0.21
Salinity (EC, Form 5)    :        0.00
```

```
Soil Name: S16
Soil Hydrologic Group: C
Maximum rooting depth(m) : 1600.00
Porosity fraction from which anions are excluded: 0.500
Crack volume potential of soil: 0.500
Texture 1                : SILTY CLAY
Depth                [mm]:      1600.00
Bulk Density Moist [g/cc]:         1.34
Ave. AW Incl. Rock Frag  :         0.15
Ksat. (est.)      [mm/hr]:         2.89
Organic Carbon [weight %]:         0.05
Clay           [weight %]:        40.00
Silt           [weight %]:        46.00
Sand           [weight %]:        14.00
Rock Fragments   [vol. %]:        10.00
Soil Albedo (Moist)      :         0.17
Erosion K                :         0.19
Salinity (EC, Form 5)    :         0.00
```

```
Soil Name: S17
Soil Hydrologic Group: C
Maximum rooting depth(m) : 1600.00
Porosity fraction from which anions are excluded: 0.500
Crack volume potential of soil: 0.500
Texture 1                : SILTY CLAY LOAM
Depth                [mm]:      1600.00
Bulk Density Moist [g/cc]:         1.38
Ave. AW Incl. Rock Frag  :         0.16
Ksat. (est.)      [mm/hr]:         4.21
Organic Carbon [weight %]:         1.55
Clay           [weight %]:        32.00
Silt           [weight %]:        53.00
Sand           [weight %]:        15.00
Rock Fragments   [vol. %]:        10.00
Soil Albedo (Moist)      :         0.17
Erosion K                :         0.19
Salinity (EC, Form 5)    :         0.00
```

```
Soil Name: S18
Soil Hydrologic Group: C
Maximum rooting depth(m) : 1600.00
Porosity fraction from which anions are excluded: 0.500
Crack volume potential of soil: 0.500
Texture 1                : SILTY LOAM
Depth               [mm]:     1600.00
Bulk Density Moist [g/cc]:       1.41
Ave. AW Incl. Rock Frag  :       0.19
Ksat. (est.)      [mm/hr]:       5.71
Organic Carbon [weight %]:       0.05
Clay           [weight %]:      24.00
Silt           [weight %]:      66.00
Sand           [weight %]:      10.00
Rock Fragments   [vol. %]:      10.00
Soil Albedo (Moist)      :       0.17
Erosion K                :       0.23
Salinity (EC, Form 5)    :       0.00
```

```
Soil Name: S19
Soil Hydrologic Group: C
Maximum rooting depth(m) : 1600.00
Porosity fraction from which anions are excluded: 0.500
Crack volume potential of soil: 0.500
Texture 1                : SILTY CLAY LOAM
Depth               [mm]:     1600.00
Bulk Density Moist [g/cc]:       1.37
Ave. AW Incl. Rock Frag  :       0.18
Ksat. (est.)      [mm/hr]:       4.64
Organic Carbon [weight %]:       0.05
Clay           [weight %]:      29.00
Silt           [weight %]:      64.00
Sand           [weight %]:       7.00
Rock Fragments   [vol. %]:      10.00
Soil Albedo (Moist)      :       0.17
Erosion K                :       0.21
Salinity (EC, Form 5)    :       0.00
```

```
Soil Name: S20
Soil Hydrologic Group: B
Maximum rooting depth(m) : 1600.00
Porosity fraction from which anions are excluded: 0.500
Crack volume potential of soil: 0.500
Texture 1                : SANDY LOAM
Depth               [mm]:     1600.00
Bulk Density Moist [g/cc]:       1.51
Ave. AW Incl. Rock Frag  :       0.13
Ksat. (est.)      [mm/hr]:      61.61
Organic Carbon [weight %]:       0.05
Clay           [weight %]:       3.00
Silt           [weight %]:      46.00
Sand           [weight %]:      51.00
Rock Fragments   [vol. %]:      10.00
Soil Albedo (Moist)      :       0.17
Erosion K                :       0.32
Salinity (EC, Form 5)    :       0.00
```

```
Soil Name: S21
Soil Hydrologic Group: B
Maximum rooting depth(m) : 1600.00
Porosity fraction from which anions are excluded: 0.500
Crack volume potential of soil: 0.500
Texture 1                : SILTY LOAM
Depth               [mm]:     1600.00
Bulk Density Moist [g/cc]:       1.45
Ave. AW Incl. Rock Frag  :       0.23
Ksat. (est.)      [mm/hr]:       7.59
Organic Carbon [weight %]:       0.05
Clay           [weight %]:      13.00
Silt           [weight %]:      82.00
Sand           [weight %]:       5.00
Rock Fragments   [vol. %]:      10.00
Soil Albedo (Moist)      :       0.17
Erosion K                :       0.36
Salinity (EC, Form 5)    :       0.00
```

```
Soil Name: S22
Soil Hydrologic Group: C
Maximum rooting depth(m) : 1600.00
Porosity fraction from which anions are excluded: 0.500
Crack volume potential of soil: 0.500
Texture 1                : SILTY LOAM
Depth                [mm]:     1600.00
Bulk Density Moist [g/cc]:        1.40
Ave. AW Incl. Rock Frag  :        0.20
Ksat. (est.)      [mm/hr]:        5.43
Organic Carbon [weight %]:        0.05
Clay           [weight %]:       33.00
Silt           [weight %]:       62.00
Sand           [weight %]:        5.00
Rock Fragments   [vol. %]:       10.00
Soil Albedo (Moist)      :        0.17
Erosion K                :        0.21
Salinity (EC, Form 5)    :        0.00

Soil Name: S24
Soil Hydrologic Group: C
Maximum rooting depth(m) : 1600.00
Porosity fraction from which anions are excluded: 0.500
Crack volume potential of soil: 0.500
Texture 1                : SILTY LOAM
Depth                [mm]:     1600.00
Bulk Density Moist [g/cc]:        1.41
Ave. AW Incl. Rock Frag  :        0.18
Ksat. (est.)      [mm/hr]:        5.48
Organic Carbon [weight %]:        3.97
Clay           [weight %]:       26.00
Silt           [weight %]:       61.00
Sand           [weight %]:       13.00
Rock Fragments   [vol. %]:       10.00
Soil Albedo (Moist)      :        0.17
Erosion K                :        0.21
Salinity (EC, Form 5)    :        0.00
```

```
Soil Name: S25
Soil Hydrologic Group: B
Maximum rooting depth(m) : 1600.00
Porosity fraction from which anions are excluded: 0.500
Crack volume potential of soil: 0.500
Texture 1                : SANDY LOAM
Depth              [mm]:     1600.00
Bulk Density Moist [g/cc]:      1.52
Ave. AW Incl. Rock Frag  :      0.14
Ksat. (est.)      [mm/hr]:     38.19
Organic Carbon [weight %]:      1.55
Clay           [weight %]:      7.00
Silt           [weight %]:     47.00
Sand           [weight %]:     46.00
Rock Fragments   [vol. %]:     10.00
Soil Albedo (Moist)      :      0.17
Erosion K                :      0.26
Salinity (EC, Form 5)    :      0.00
```

```
Soil Name: S26
Soil Hydrologic Group: B
Maximum rooting depth(m) : 1600.00
Porosity fraction from which anions are excluded: 0.500
Crack volume potential of soil: 0.500
Texture 1                : SILTY LOAM
Depth              [mm]:     1600.00
Bulk Density Moist [g/cc]:      1.46
Ave. AW Incl. Rock Frag  :      0.20
Ksat. (est.)      [mm/hr]:      9.57
Organic Carbon [weight %]:      3.97
Clay           [weight %]:     15.00
Silt           [weight %]:     70.00
Sand           [weight %]:     15.00
Rock Fragments   [vol. %]:     10.00
Soil Albedo (Moist)      :      0.17
Erosion K                :      0.28
Salinity (EC, Form 5)    :      0.00
```

```
Soil Name: S27
Soil Hydrologic Group: B
Maximum rooting depth(m) : 1600.00
Porosity fraction from which anions are excluded: 0.500
Crack volume potential of soil: 0.500
Texture 1                 : SANDY LOAM
Depth               [mm]:     1600.00
Bulk Density Moist [g/cc]:       1.52
Ave. AW Incl. Rock Frag  :       0.14
Ksat. (est.)      [mm/hr]:      38.19
Organic Carbon [weight %]:       1.55
Clay           [weight %]:       7.00
Silt           [weight %]:      47.00
Sand           [weight %]:      46.00
Rock Fragments   [vol. %]:      10.00
Soil Albedo (Moist)      :       0.17
Erosion K                :       0.26
Salinity (EC, Form 5)    :       0.00
```

```
Soil Name: S28
Soil Hydrologic Group: B
Maximum rooting depth(m) : 1600.00
Porosity fraction from which anions are excluded: 0.500
Crack volume potential of soil: 0.500
Texture 1                 : SILTY LOAM
Depth               [mm]:     1600.00
Bulk Density Moist [g/cc]:       1.51
Ave. AW Incl. Rock Frag  :       0.15
Ksat. (est.)      [mm/hr]:      22.36
Organic Carbon [weight %]:       1.55
Clay           [weight %]:      12.00
Silt           [weight %]:      48.00
Sand           [weight %]:      40.00
Rock Fragments   [vol. %]:      10.00
Soil Albedo (Moist)      :       0.17
Erosion K                :       0.22
Salinity (EC, Form 5)    :       0.00
```

```
Soil Name: S30
Soil Hydrologic Group: C
Maximum rooting depth(m) : 1600.00
Porosity fraction from which anions are excluded: 0.500
Crack volume potential of soil: 0.500
Texture 1                 : SILTY CLAY
Depth                 [mm]:     1600.00
Bulk Density Moist [g/cc]:        1.29
Ave. AW Incl. Rock Frag  :        0.16
Ksat. (est.)       [mm/hr]:       3.61
Organic Carbon [weight %]:        8.28
Clay           [weight %]:       40.00
Silt           [weight %]:       57.00
Sand           [weight %]:        3.00
Rock Fragments   [vol. %]:       10.00
Soil Albedo (Moist)       :        0.17
Erosion K                 :        0.20
Salinity (EC, Form 5)     :        0.00
```

```
Soil Name: S31
Soil Hydrologic Group: B
Maximum rooting depth(m) : 1600.00
Porosity fraction from which anions are excluded: 0.500
Crack volume potential of soil: 0.500
Texture 1                 : LOAM
Depth                 [mm]:     1600.00
Bulk Density Moist [g/cc]:        1.51
Ave. AW Incl. Rock Frag  :        0.14
Ksat. (est.)       [mm/hr]:      17.24
Organic Carbon [weight %]:        8.28
Clay           [weight %]:       16.00
Silt           [weight %]:       42.00
Sand           [weight %]:       42.00
Rock Fragments   [vol. %]:       10.00
Soil Albedo (Moist)       :        0.17
Erosion K                 :        0.19
Salinity (EC, Form 5)     :        0.00
```

Appendix 4 Textural triangle

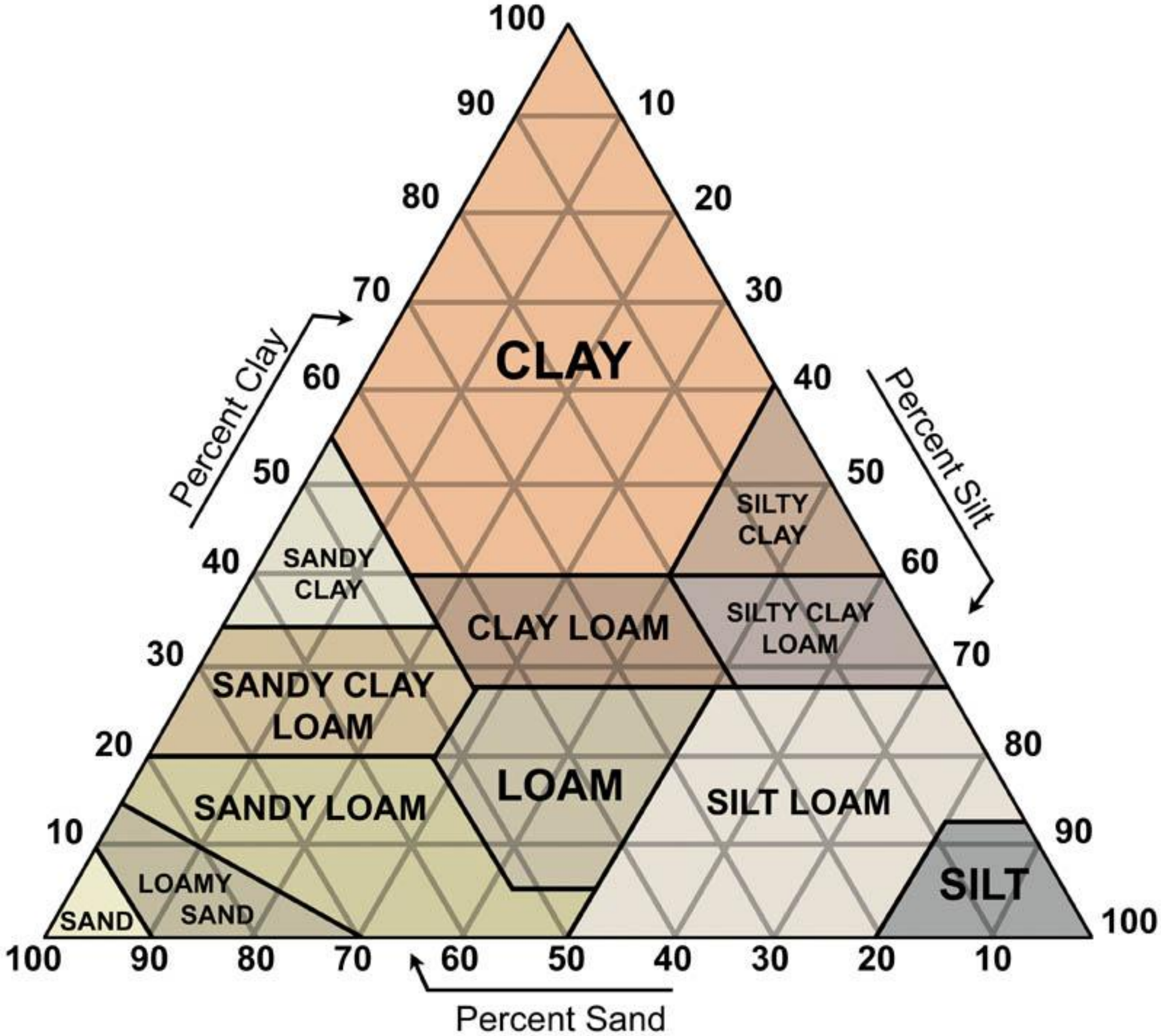

Appendix 5 Ponds characteristics

Données concernant les lacs exécutés dans le cadre du projet Marguellil à Siliana

	Anné Prog	Nom	déleg.	Secteur	S.BV (ha)	Cap. (M^3)	Sup (ha) Lac Nor	Sup (ha) Lac Max	Vol.(M3) Lac Nor act	Vol.(M3) Lac Max.act	Vol.(M3) Initial	Concent Initial	Concent Normale	Conductiv Hydraul	Phosph	Azote
1	1967 SILIANA	Skhira 3	Makthar	Soualem	211	38000	1	1,5	0	2000	38000					
2	1968 SILIANA	Skhira 1	Makthar	Soualem	150	52000	1,5	2,5	20000	23000	52000	0,007				
3	1969 SILIANA	Skhira 2	Makthar	Soualem	157	79000	1	1,5	50000	54000	79000	0,007				
4	1970 SILIANA	Skhira 18	Makthar	Soualem	183	160000	3	4	100000	110000	160000	0,007				
5	1971 SILIANA	Skhira 12	Makthar	Soualem	148	60000	2	3	40000	43000	60000	0,007				
6	1972 SILIANA	Skhira 4	Makthar	Soualem	474	181000	3	4,5	80000	94000	181000	0,007				
7	1968 SILIANA	Garia 1	Kessra	Garia	172	18000	1	1,5	0	1000	18000					
8	1968 SILIANA	Garia 3	Kessra	Garia	114	28000	1	1,5	0	2000	28000					
9	1968 SILIANA	Garia 2	Kessra	Garia	64	19000	1,5	2,5	0	1000	19000					
10	1968 SILIANA	Skira 22	Makthar	Soualem	175	90000	3	4,5	30000	40000	90000	0,007				
11	1968 SILIANA	Skira 27	Makthar	Soualem	113	16000	2	2,5	0	2000	16000	0,007				
13	1968 SILIANA	Skira 5	Makthar	Soualem	266	120000	3	3,5	60000	70000	120000	0,007				
36	1990 SILIANA	O.Tella	Makthar	Bez	125	60000	2	3	40000	50000	60000					
37	1990 SILIANA	O.Jannet	Makthar	Bez	565	105000	3	4	0	5000	105000					
56	1992 SILIANA	Fidh El Ghaba	Bourouis	Tricha	230	146000	1,5	2	80000	94000	146000					
64	1993 SILIANA	O. El Haffar	Kessra	Garia N	50	30000	1	1,5	10000	12000	30000					
65	1993 SILIANA	O. El Ajmi	Makthar	Ras El oued	250	92000	2	3	60000	68000	92000					
75	1994 SILIANA	O. El Hablane	Rouhia	Hmaima	230	51000	2	3	0	4000	51000					
77	1994 SILIANA	O. Jetta	Siliana Sud	El Gantra	200	85000	1,5	2	50000	60000	85000	0,007				
83	1995 SILIANA	O. Essarg	Makthar	beni Hazem	50	75000	1	1,5	40000	45000	75000					

Donnée Spéciphique des lacs collinaires réalisé dans le bassin versant de Marguellil Gouvernorat de Kairouan

N°	Nom du Lac	Délégation	annee d'execution	% de sediment	Surface en Ha		Volume en m3		Cond.Hyd
					R,Normale	R,Maximale	R,Normale	R,Maximale	
1	Absa 1	El Ala	1992	100	0,9	1,1	35000	40000	moyenne
2	Abda	Haffouz	1970	100	3,2	3,4	37000	43000	faible
3	Smili1	Oueslatia	1994	40	4,5	5,4	130000	166000	moyenne
4	Ben Houria	Haffouz	1970	100	0,8	1,0	17000	21000	moyenne
5	Selem Theber	Haffouz	1973	60	3,15	3,5	63000	68000	moyenne
6	Dhahbi	Haffouz	1980	100	1,8	2,1	26000	29000	moyenne
7	Sidi Sofiène	Oueslatia	[illegible]	30	1,3	1,6	40000	55000	moyenne
8	Bou Ksab	Haffouz	1985	20	2,3	2,6	55000	69000	faible
9	El Maiz	Haffouz	1986	40	13	17,0	500000	580000	faible
10	El Hoshas	Haffouz	1989	5	2,5	2,9	130000	144000	forte
11	O. fidh B.Nasser	Haffouz	1990	30	1,2	1,4	100000	118000	moyenne
12	O. fidh Ali	Haffouz	1991	70	3	3,3	127000	133000	moyenne
13	O Gualar	Oueslatia	1992	30	5	6,0	160000	195000	faibla
14	O.El Habsa	El Ala	1994	100	1,5	2,0	50000	64000	moyenne
15	O.fich Mbarek	Haffouz	1992	30	2	2,9	53000	70000	moyenne
16	Ben Zitoun	Haffouz	1993	20	2,5	4,0	50000	80000	faible
17	Ain Faouar	Haffouz	1994	25	2	2,9	66000	118000	forte
18	El Ghtatis	Oueslatia	1995	15	2,8	3,6	1060000	160000	faible
19	Smili 2	Oueslatia	1996	20	1,5	2,0	35000	45000	moyenne
20	Gassaa	Oueslatia	1996	30		2,8	104800	120000	faible
21	Choâba Hamra	Haffouz	1996	20	5,4	8,7	160000	318000	moyenne
22	El Assa	Oueslatia	2003	20	2	2,7	69000	90000	fable

رئيس دائرة المحافظة على المياه والتربة بالقيروان
المجاهد بالطيبي

REMARQUE : pour la concentration des sediments et la concentration organique nous n'avons pas d'informtion car il n'y a pas eu ce relevé pour ces deux données.

Appendix 6 Potholes characteristics

Pothole HRUs						Hru drain (contribute to HRU_pothole)			
Subbasin Number	Hru_Pothole	Hru number	crop_soil_slope	Pot Fractio	Pot_max Volume m (mm)	HRU drain	hru number	Pot Fraction-drain	crop soil slope_HRU drain
1	4	4	DWHT/S7/0-7	0.8	200	0	0	0	0
2	4	13	DWHT/S30/0-7	0.2	70	0	0	0	0
3	0	0	0	0	0	0	0	0	0
4	4	28	DWHT/S2/0-9	0.9	100	1	25	0.5	DWHT/S12/7-99
5	5	38	dwht/s9/0-7	1	70	0	0	0	0
7	5	58	dwht/s3/0-7	1	100	0	0	0	0
8	1	63	DWHT/S14/0-7	0.3	70	4	66	0.3	DWHT/S3/07
9	5	77	OLIV_/S1/07	1	80	4	76	0.7	DWHT/S9/0-7
10	4	85	DWHT/S16/0-7	1	200	14	95	0.9	frst/s16/7-99
11	5	101	dwht/s3/0-7	1	60	12	108	0.5	swrn/s5/0-7
12	1	109	dwht/s18/0-7	0.4	89	3	111	0.5	swrn/S18/7-99
13	7	122	swrn/s3/0-7	0.3	100	0	0	0	0
14	1	130	dwht/s18/0-7	0.9	200	9	138	0.7	swrn/s18/0-7
						4	145	1	oliv/s10/0-7
15	7	148	oliv /s28/0-7	1	90	6	147	0.9	soliv/s25/7-99
						4	152	0.9	swrn/S1/0-7
16	3	151	Olive/s1/0-7	1	100	6	154	0.9	swrn/s25/0-7
						5	153	1	swrn/s2/0-7
17	6	160	swrn/s1/0-7	1	100	7	161	0.9	swrn/s16/0-7
18	3	170	swrn/s1/0-7	0.9	60	1	168	0.1	dwht/s1/0-7
20	4	189	oliv/s17/0-7	0.9	70	3	188	0.9	oliv/s1/0-7
21	3	197	dwht/s31/0-7	0.6	100	0	0	0	0
22	10	213	swRn/s31/0-7	0.7	80	0	0	0	0
24	10	230	oliv/s6/0-7	0.9	100	15	235	0.2	swrn/s20/0-7
						3	239	0.1	oliv/s2770-7
25	12	248	orcd/S6/0-7	1	100	4	240	1	oliv/S6/0-7
						11	247	0.8	orcd/s27/0-7
26	3	251	swrn/s11/0-7	0.1	100	0	0	0	0
						2	261	0.4	dwht/s20/7-99
27	3	262	dwht/s20/0-7	0.5	80	4	263	1	Olive/s10/0-7
						5	264	1	oliv/s20/0-7
						6	265	1	oliv/s6/0-7
28	10	275	swrn/s1/0-7	0.9	150	3	268	0.3	dwht/s27/0-7
						4	269	0.1	DWHT/S6/0-7
29	8	286	orcd/s170-7	0.5	150	7	285	0.4	oliv/s2/0-7
30	5	292	Olive/s270-7	0.6	100	0	0	0	0

Appendix 7 Land management practice data procured from interviews.
(The interviewer is a Master student from INAT “Mr. Aymen Lazrek”).

Agriculture N°1					
Nom :	Henchir El Mrabet				
Emplacement :	Hoffia Sud				
Surface Total (Ha) :	50 Ha				
Types de cultures	Pluvial (surface Ha)		Irriguées (surfaces Ha)		
	30		20		
Travail du sol		**Irrigation**			
Action	**Types de culture**	**Source**	**Type**	**Quantité**	
Binage profond Désherbage manuelle Taille Fumage	Arbo légumes Arbo Arbo	PPI Puit	Surface Gouttes à gouttes	5-6 milles/ha 2 l/s	

Agriculture N°2					
Nom :	Hedi Elmeskini				
Emplacement :	CHRICHIRA				
Surface Total (Ha) :	50 Ha				
Types de cultures	Pluvial surface Ha)		Irriguées (surfaces Ha)		
	50				
Types de cultures	**Genre**	**Date de semis (1)**	**les engrais Kg/Ha**	**Date d’application**	**Les pesticides**
Arbo en sec (20 ha)	Olive Amandiers		100Amm (50kg/ha) 250 DAP		Insecticides
Céréales (30ha)	Blé dur	Nov.	250 Amm	JAN	Herbicides
	Orge	Nov.	100Amm 100DAP	Nov. Fev.	
	Blé tendre	Nov.	200 Amm	Jan.	

Agriculture N°4

Nom :	Brahim Essidi	
Emplacement :	CHRICHIRA	
Surface Total (Ha) :	50 Ha	
Types de cultures	Pluvial surface Ha)	Irriguées (surfaces Ha)
	50	

Types de cultures	Genre	Date de semis (1)	les engrais Kg/Ha	Date d'application	Les pesticides
Arbo en sec (20 ha)	Olive Amandiers		100Amm (50kg/ha)		Insecticides
			250 DAP		
Céréales (30ha)	Blé dur	Nov.	250 Amm	JAN	Herbicides
	Orge	Nov.	100Amm 100DAP	Nov. Fev.	
	Blé tendre	Nov.	200 Amm	Jan.	

Agriculture N°5		
Nom :	Mabrouk El Jabnouni	
Emplacement :	Khit el wad	
Surface Total (Ha) :	2 Ha	
Types de cultures	Pluvial surface Ha)	Irriguées (surfaces Ha)
		2

Types de cultures	Genre	Date de semis (1)	les engrais Kg/Ha	Date d'application	Les pesticides
					Insecticides
			100Amm	MARS	
Arbo en irriguée (2 ha)	Olive P		Fumier (30T/ha)	JAN.	OTEX

Travail du sol	Irrigation

Action	Types de culture	Source	Type	Quantité
Binage profond Désherbage manuelle Taille Fumage	Arbo	PPI	Surface	5-6 milles/ha

Agriculture N°6		
Nom :	Chrif el Jabnouni	
Emplacement :	Khit el wad	
Surface Total (Ha) :	5 Ha	
Types de cultures	Pluvial surface Ha)	Irriguées (surfaces Ha)
		5

Types de cultures	Genre	Date de semis (1)	les engrais Kg/Ha	Date d'application	Les pesticides
Arbo en irriguée (5 ha)	Olive 10% Abricots 80% Pommiers 10%		100Amm Fumier (30T/ha)	MARS JAN	Insecticides OTEX

Travail du sol		Irrigation		
Action	Types de culture	Source	Type	Quantité
Binage profond Désherbage manuel Taille Fumage	Arbo	PPI	Surface	5-6 milles/ha

Appendix 8 Crop management operations

DURUM WHEAT

Operation	Time	Other information
Tillage	1-November	Harrow 10 Barr tine 36 Ft
Plant	6 November	
Fertilizer application	10 January	DAP 25kg/ha
Fertilizer application	19 Mars	Nitrate Ammonium
Harvest and kill operation	15 June	

OLIVE NON IRRIGATED

Operation	Time	Other information
Fertilizer application	20 January	08-12-24 500 kg
Plant	10 April	
Fertilizer application	15 April	26-13-00 170 kg/ha
Fertilizer application	1 May	Sheep-Fresh Manure 330 kg/ha
Harvest only	1 November	

OLIVE IRRIGATED

Operation	Time	Other Information
Fertilizer Application	January 20	08-12-24 500 Kg
Plant	10 April	
Irrigation	11 April	30 Mm
Fertilizer Application	15	26-13-00 170 Kg/Ha
Irrigation	20april	30 Mm
Fertilizer Application	1 May	Sheep-Fresh Manure 330 Kg/Ha
Irrigation	10 May	30 Mm
Irrigation	20 May	30 Mm
Irrigation	15 June	30 Mm
Irrigation	30 June	30 Mm
Irrigation	10 July	30 Mm
Irrigation	20 July	30 Mm
Irrigation	1 August	30 Mm
Irrigation	20 August	30 Mm
Irrigation	1 September	30 Mm
Irrigation	10 September	30 Mm
Irrigation	20 September	30 Mm
Irrigation	1 October	30 Mm
Irrigation	10 October	30 Mm
Irrigation	20 October	30 Mm
Harvest Only	1 November	

Appendix 9 Database for the Olive tree plant growth

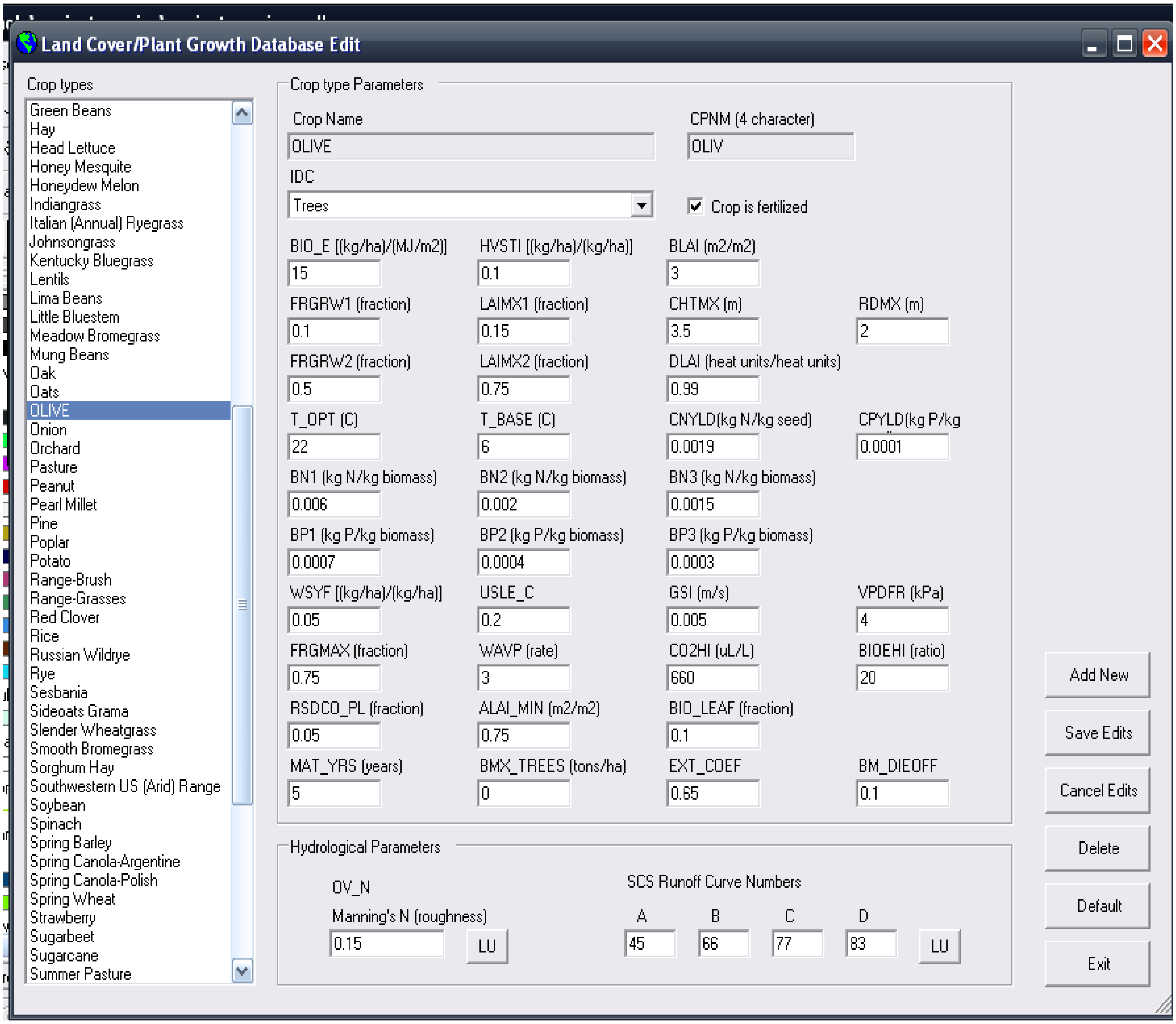

Appendix 10 Runoff curve number for cultivated agriculture lands.

Table 20-1: Runoff curve numbers for cultivated agricultural lands

Land Use	Treatment or practice	Hydrologic condition	A	B	C	D
Fallow	Bare soil	- - - -	77	86	91	94
	Crop residue cover*	Poor	76	85	90	93
		Good	74	83	88	90
Row crops	Straight row	Poor	72	81	88	91
		Good	67	78	85	89
	Straight row w/ residue	Poor	71	80	87	90
		Good	64	75	82	85
	Contoured	Poor	70	79	84	88
		Good	65	75	82	86
	Contoured w/ residue	Poor	69	78	83	87
		Good	64	74	81	85
	Contoured & terraced	Poor	66	74	80	82
		Good	62	71	78	81
	Contoured & terraced w/ residue	Poor	65	73	79	81
		Good	61	70	77	80
Small grains	Straight row	Poor	65	76	84	88
		Good	63	75	83	87
	Straight row w/ residue	Poor	64	75	83	86
		Good	60	72	80	84
	Contoured	Poor	63	74	82	85
		Good	61	73	81	84
	Contoured w/ residue	Poor	62	73	81	84
		Good	60	72	80	83
	Contoured & terraced	Poor	61	72	79	82
		Good	59	70	78	81
	Contoured & terraced w/ residue	Poor	60	71	78	81
		Good	58	69	77	80
Close-seeded or broadcast legumes or rotation	Straight row	Poor	66	77	85	89
		Good	58	72	81	85
	Contoured	Poor	64	75	83	85
		Good	55	69	78	83
	Contoured & terraced	Poor	63	73	80	83
		Good	51	67	76	80

Table 20-2: Runoff curve numbers for other agricultural lands

Cover Type	Hydrologic condition	A	B	C	D
Pasture, grassland, or range—continuous forage for grazing[1]	Poor	68	79	86	89
	Fair	49	69	79	84
	Good	39	61	74	80
Meadow—continuous grass, protected from grazing and generally mowed for hay	- - - -	30	58	71	78
Brush—brush-weed-grass mixture with brush the major element[2]	Poor	48	67	77	83
	Fair	35	56	70	77
	Good	30	48	65	73
Woods—grass combination (orchard or tree farm)	Poor	57	73	82	86
	Fair	43	65	76	82
	Good	32	58	72	79
Woods[3]	Poor	45	66	77	83
	Fair	36	60	73	79
	Good	30	55	70	77
Farmsteads—buildings, lanes, driveways, and surrounding lots.	- - - -	59	74	82	86

Appendix 11 Linear and non linear regression.

Linear model: $Y = \text{a0\_lm} + \text{a1\_lm}\,X$

Non linear model: $Y = \text{a0\_nlm}_4 + \text{a1\_nlm}_4\,X + \text{a2\_nlm}_4\,X^2 + \text{a3\_nlm}_4\,X^3 + \text{a4\_nlm}_4 X^4$

Station 1 Tmax

month	R2_lm	a0_lm	a1_lm	R2_nlm4	a0_nlm4	a1_nlm4	a2_nlm4	a3_nlm4	a4_nlm4
Apr	0.994271846	8.048484548	0.62735143	0.99790899	-0.7921782	2.530006009	-0.1387083	0.0041326	-4.30E-05
Aug	0.957040121	13.13473634	0.63111166	0.99034765	-75.3189195	13.18566933	-0.62490452	0.01308891	-9.81E-05
Dec	0.952672331	5.264181602	1.16176423	0.99516067	7.53959231	0.715920708	-0.0070751	0.00171589	8.78E-05
Feb	0.986593134	6.077383366	0.8381639	0.9941815	4.52192643	1.427584362	-0.08132069	0.0048519	-0.00010289
Jan	0.989369528	6.447285206	0.77877114	0.99478391	5.89562224	1.159564423	-0.06020143	0.00299246	-3.43E-05
Jul	0.962495084	14.2848845	0.58868796	0.99603429	-99.5318596	13.89502706	-0.55479886	0.00974846	-6.05E-05
Jun	0.98806339	7.976211691	0.72666203	0.99634492	-77.9552683	11.58673921	-0.49456329	0.0096381	-6.79E-05
Mar	0.984470632	9.16685373	0.57158877	0.99638066	5.56170398	1.251554443	-0.04079328	0.00099972	-9.54E-06
May	0.991914457	7.207577302	0.7255381	0.99619895	-1.36353527	1.884517347	-0.04856595	0.00063397	1.30E-07
Nov	0.981602037	7.54923131	0.94534168	0.9967082	12.4769345	-1.681668005	0.39703853	-0.02259963	0.00042902
Oct	0.991739386	12.66734226	0.61736255	0.99309373	13.668938	0.168432288	0.0509472	-0.00212922	2.95E-05
Sep	0.985099901	10.65863665	0.70550696	0.99502079	0.26711658	3.031617744	-0.1611709	0.0043984	-4.11E-05

Station 1 Tmin

month	R2_lm	a0_lm	a1_lm	R2_nlm4	a0_nlm4	a1_nlm4	a2_nlm4	a3_nlm4	a4_nlm4
Apr	0.99294257	3.91682646	0.83223391	0.99662331	4.0693828	0.69712818	0.01811907	-0.00047349	-6.3858E-07
Aug	0.96151527	9.82272733	0.66299382	0.98349836	-17.6488624	8.97876544	-0.8820849	0.03926479	-0.00062297
Dec	0.9890097	3.6513351	0.9096438	0.99706907	3.47655771	0.82042938	0.02893793	0.00252937	-0.00033554
Feb	0.98383894	2.46647721	0.9264629	0.99197404	2.34692258	0.88601032	0.02101662	-0.00102679	3.8817E-05
Jan	0.97714546	2.81082638	0.99423619	0.9893155	2.67536526	0.84925607	0.02921569	0.00632037	-0.0004885
Jul	0.99348099	7.93279452	0.69730025	0.99537244	3.05177979	2.3746613	-0.19225711	0.00898012	-0.00014657
Jun	0.98772163	7.3429827	0.6975847	0.99649807	7.65426451	1.11280045	-0.09665453	0.0064235	-0.00013009
Mar	0.98668161	2.86318141	0.86415066	0.99653352	2.87508352	0.74325819	0.01467788	0.00221911	-0.00018495
May	0.99022096	5.61585606	0.80853023	0.99426533	6.09511796	0.56195484	0.03692979	-0.00246757	6.7001E-05
Nov	0.99189251	5.25629855	0.98401688	0.99718768	5.33164335	0.97832617	-0.01201363	-0.00179792	0.00046868
Oct	0.98602182	7.93331163	0.80301193	0.99531115	8.39482535	0.72659592	-0.033785	0.00550682	-0.00017857
Sep	0.97562041	8.35023953	0.86198661	0.99125684	9.55349771	0.26291296	0.13681035	-0.01347889	0.0004503

Station 2 Tmax

month	R2_lm	a0_lm	a1_lm	R2_nlm4	a0_nlm4	a1_nlm4	a2_nlm4	a3_nlm4	a4_nlm4
Apr	0.990709617	11.27980602	0.60745572	0.993345994	3.45853761	2.3144253	-0.12775162	0.00394864	-4.30E-05
Aug	0.94094005	15.08809191	0.64896119	0.981627921	-86.1618098	14.6747869	-0.68319448	0.01401333	-0.00010279
Dec	0.968132087	8.805381136	1.12622418	0.987484055	10.2810504	0.72744758	0.03455373	-0.00324011	0.00021008
Feb	0.985311247	9.344041913	0.80856188	0.987040405	9.18965372	0.80993017	0.00078006	0.00019086	-1.12E-05
Jan	0.971003807	9.349800753	0.80464378	0.983739267	7.99539236	1.62796952	-0.12943418	0.00699818	-0.00010935
Jul	0.941435953	17.3607117	0.5675656	0.987469631	-3.4744656	2.18257067	-0.01175575	-0.00130007	2.26E-05
Jun	0.963127119	11.08134141	0.70549818	0.990644279	-108.125595	15.6214246	-0.66761081	0.01267725	-8.61E-05
Mar	0.969768966	11.86146592	0.57388814	0.989894638	8.44001094	1.14941324	-0.03020628	0.00069303	-7.78E-06
May	0.97771173	10.21460717	0.70588993	0.99080575	-2.15069083	2.24881765	-0.05414114	0.0002953	7.84E-06
Nov	0.98133945	10.83682742	0.92043515	0.99011555	14.6600302	-1.14423265	0.31617493	-0.01826934	0.00035295
Oct	0.98903766	15.24165393	0.62641136	0.990863885	15.4205579	0.37218324	0.03667075	-0.00173697	2.62E-05
Sep	0.97292546	13.85562084	0.67498144	0.989862334	-12.4664207	5.35000437	-0.28152804	0.0069272	-5.92E-05

Station 2 Tmin

month	R2_lm	a0_lm	a1_lm	R2_nlm4	a0_nlm4	a1_nlm4	a2_nlm4	a3_nlm4	a4_nlm4
Apr	0.97810451	7.64390742	0.71227324	0.98386368	7.58124145	0.64175045	0.02114561	-0.000751727	-4.39E-05
Aug	0.96273277	14.5344978	0.57550891	0.97212616	13.6812876	1.42221588	-0.1379114	0.007789171	-0.00014312
Dec	0.98583653	6.86765125	0.90972236	0.98735754	6.81057075	0.89210997	0.00446724	7.13E-05	0.0001193
Feb	0.96853162	5.62318311	0.93264298	0.97636352	5.46066133	0.88255768	0.03220616	-0.000656366	-0.00019906
Jan	0.97502831	5.93757384	1.00493881	0.98653555	5.6178646	0.93877538	0.07594174	0.002694329	-0.00171544
Jul	0.97191506	12.4539041	0.60823842	0.97269307	7.02002831	2.0345864	-0.1329919	0.005269399	-7.54E-05
Jun	0.95839523	11.2925588	0.62744065	0.9827885	12.8697056	0.54473371	-0.02041456	0.001466904	-1.83E-05
Mar	0.97082559	6.52674307	0.7761437	0.98155776	6.52618255	0.73768571	-0.00094623	0.002656501	-0.00018653
May	0.98397875	9.70715712	0.68270773	0.98441539	9.65480237	0.62161236	0.02325144	-0.002259033	6.47E-05
Nov	0.98559109	8.61559426	0.97252496	0.98839187	8.62146238	0.89280775	0.00737851	0.000995668	-1.89E-05
Oct	0.9833399	11.5618414	0.75991335	0.98540086	11.682411	0.85407371	-0.04467626	0.00474291	-0.00013635
Sep	0.97068923	13.1477799	0.71151266	0.97492524	13.3300763	0.81373289	-0.02617472	0.001381999	-5.84E-06

Station PCP 1

	month	R2_lm	a0_lm	a1_lm	R2_nlm4	a0_nlm4	a1_nlm4	a2_nlm4	a3_nlm4	a4_nlm4
1	Apr	0.605710654	-0.76728767	0.97773792	0.97531423	-0.15328139	0.8790447	-0.54087846	0.08116392	-0.00269664
2	Aug	0.45641258	-0.66843815	1.04182068	0.9263892	-0.06919403	0.77608593	-0.49411127	0.07697692	-0.00245493
3	Dec	0.791099185	-1.11007467	1.21474307	0.95956832	0.334436	-0.92703594	0.31234194	-0.01007509	4.08E-05
4	Feb	0.461399004	-0.57462995	0.33464935	0.96285117	-0.10057954	0.28074832	-0.10655455	0.01016849	-0.00020375
5	Jan	0.805221212	-1.28795902	1.66083811	0.9813169	0.2303632	-0.95591172	0.41984755	-0.01949647	0.00033498
6	Jul	0.058233242	-0.00047005	0.00046487	0.34399231	0.00031375	-0.00257759	0.00152063	-0.00024319	1.11E-05
7	Jun	0.385783777	-0.3062501	0.25401019	0.93215516	0.05114	-0.27851035	0.09838388	-0.00959968	0.00027238
8	Mar	0.492064632	-1.67751823	1.51126247	0.93073061	0.68441711	-2.1257231	0.79149383	-0.06968594	0.00198025
9	May	0.657504417	-0.57507349	0.89119228	0.95975205	0.06542553	-0.37708207	0.08442297	0.01143207	-0.00057997
10	Nov	0.685816192	-1.35767873	1.61533051	0.98822029	0.10201489	-0.3337173	0.05452093	0.02174872	-0.00087468
11	Oct	0.851280596	-0.90653465	1.40589929	0.95241713	0.16182015	-1.16516106	0.64024746	-0.04136763	0.00077063
12	Sep	0.83939349	-0.95185141	1.74901019	0.98712823	0.14298601	-0.8232213	0.30605226	0.01043876	-0.00117315

Station PCP3

month	R2_lm	a0_lm	a1_lm	R2_nlm4	a0_nlm4	a1_nlm4	a2_nlm4	a3_nlm4	a4_nlm4
Apr	0.72845856	-0.98889456	1.36975853	0.98828374	-0.04248732	0.28969785	-0.22901836	0.04987305	-0.00171995
Aug	0.50159208	-0.48491818	0.82647541	0.83073622	0.03195383	-0.26684549	0.09624802	-0.00298888	0.00036108
Dec	0.762914	-1.54008218	1.56524808	0.9393009	0.23349081	-0.57372015	0.16582778	0.00556162	-0.00033276
Feb	0.51925691	-1.29173656	0.78865436	0.97020559	0.08162939	-0.14814116	0.02268287	0.0013538	1.88E-05
Jan	0.87157381	-1.4101141	2.02916679	0.98750143	0.28483415	-1.49440328	0.8966484	-0.07855287	0.00231804
Jul	0.29057409	-0.10749293	0.10940225	0.96810044	0.02445872	-0.2139874	0.13420082	-0.02301608	0.00113958
Jun	0.67379187	-0.4873811	0.53316564	0.89959601	0.15979907	-0.87635679	0.27628115	-0.01864191	0.0004031
Mar	0.7969867	-1.34481391	1.42484847	0.98620574	0.29244924	-1.07542201	0.44646445	-0.02658765	0.00056864
May	0.8314381	-0.49987802	0.98533379	0.98164408	0.08968408	-0.7330271	0.35445669	-0.01709373	0.00013772
Nov	0.8093155	-1.2320482	1.6621166	0.99099931	0.10836447	-0.58646607	0.30677668	-0.00293906	-0.00032951
Oct	0.91019824	-0.73294242	1.36045759	0.98156812	0.02731748	-0.61730685	0.50358862	-0.03057792	0.00052854
Sep	0.90818726	-1.08245903	2.32128643	0.9894821	0.07660792	-0.76755434	0.65249103	-0.04405412	0.00110881

Station PCP4

month	R2_lm	a0_lm	a1_lm	R2_nlm4	a0_nlm4	a1_nlm4	a2_nlm4	a3_nlm4	a4_nlm4
Apr	0.74843632	-1.01232642	1.46576489	0.98413088	-0.01943594	0.05336254	-0.01964597	0.0201449	-0.00059741
Aug	0.66856373	-0.509975	0.9205624	0.98104696	0.00500287	-0.0016794	-0.07156921	0.02907303	-0.00113567
Dec	0.76067488	-1.47384611	1.453367	0.99475318	0.01986719	-0.07433294	0.01336798	0.012514	-0.0003793
Feb	0.60366342	-1.85328789	1.1826193	0.98178911	0.22224677	-0.48689301	0.1209295	-0.00339542	1.09E-04
Jan	0.85561901	-2.43396796	3.38179856	0.98092507	0.54310654	-2.58820143	1.38019222	-0.10644369	0.00283404
Jul	0.25899529	-0.12423851	0.12567325	0.94204066	0.035424	-0.30638442	0.18971898	-0.03200831	0.00155073
Jun	0.56726225	-0.43407841	0.48978315	0.83769603	0.21712369	-1.24520262	0.42366399	-0.03357139	0.00077848
Mar	0.75908222	-2.40548541	2.50852595	0.99368852	0.3595186	-1.44222376	0.66879448	-0.04358481	0.00108517
May	0.80918154	-0.82370266	1.55313377	0.9795735	0.07696442	-0.67446021	0.34545812	-0.00720866	-0.00022023
Nov	0.78901334	-1.28728397	1.71557194	0.97118827	0.12804298	-0.72474783	0.40311937	-0.01905462	0.00034612
Oct	0.91543364	-1.17805848	1.89226064	0.95094471	-0.16389494	-0.09227868	0.38538361	-0.02194379	0.00038375
Sep	0.90235859	-0.84556941	1.90889378	0.98387733	-0.08694931	0.30382859	0.15475337	0.00668974	-0.00048398

Appendix 12 Calibration and validation of downscaled CGCM